ACKNOWLEDGMENTS

Looking back for the previous five years, there were several people and institutions to which I express my greatest gratitude, for their support and love was essential.

In first place, I would like to thank both Prof. Rui Reis and Prof. Margarida Casal, co-supervisors of my PhD, for their trust in me and their scientific and personal dedication to the orientation of my doctorate. To Prof Rui: my deep thanks for all the opportunities you have provided me, that changed my life and opened in me new horizons. The city of Braga and our country have much to thank him for the excellence he has help created in the 3B's Research Group. To Prof. Margarida: my deep gratitude for her great dedication, friendliness and advices. Our time working together was always inspiring, uplifting and of great support.

To Prof. Heinz Redl and Prof. Martijn my sincere gratitude for receiving me at the LBI group, in Vienna, and for many scientific discussions and your big support. Thanks Prof. Redl for your enthusiasm and for all your inspiring advices. And thanks Prof. Martijn for all your kindness and friendliness. To both of you, I am very grateful for the permanent trust, input, constant assistance and friendship you have provided. My life in Vienna and at the LBI was surely one full of enthusiasm. Ich möchte mich hiermit ganz besonders bei Prof. Redl and Prof. Martijn für ihre Unterstützung bedanken!

I am very grateful to my family, both my mother, my father and my brother, and my both grandmothers, to which I would like to dedicate this thesis. To my mother, for her compassion, understanding, love and care; to my father for all words of strength, courage and wisdom. To both of you, my greatest thank you. Estou muito grato a vós!

To my eternal companion and love, Pami, my infinite and heartfelt thanks, for your ever present support, understanding, care and love. I will always be immensely grateful for your words of strength, compassion and peace. And may our path ahead shine with the light of our highest dreams and aspirations. Obrigado pelo teu apoio, do fundo do meu coração!

To a long list of people in both the 3B's Research Group and in the Department of Biology, I also express my sincere and great gratitude. Many of them directly helped in a part of the work developed in this thesis. First, my great thanks to Rita and Raul for help with learning the

molecular procedures described here. A particular thank you to Raul, for your important support with collaborating in the work of elastin, the last experimental chapter of the thesis. Thanks also for Jorge, Neide, Susana and Isabel João. My dears, you were all more than colleagues, you were great friends always providing support, companionship and joy!

In the 3B's Research Group, I express my words of gratitude to the following people, for their friendship, support and input: Pirraco, Adriano, Bruno Ferreira, Ricardo Silva; Miguel, Rui Pereira, Tommaso, Simone, Elizabeth, João, Patrícia, Johan, Mariana Cerqueira, Marina, Belinha, Sílvia Gomes, Tírcia, Xana, Helena Azevedo, Manuela, Gabriela, Tó, Catarina, Ana Martins, Isa, Sofia Caridade, Paula, Helena Lima, Víctor and many others. A special thanks to you Elizabeth for our work together in Vienna with the silk (thank you for everything, all the input and work together; our positive discussions); to Pirraco, Adriano, Mariana e Tommaso for the cell culture work; to Helena, Simone, Miguel, Belinha e Sílvia, for our experimentation with possible delivery systems for BMPs (Helena for chitosan membranes, Simone for soy membranes and composites, Miguel with the dendrimers, Belinha e Sílvia with biomimetic coatings). Also thanks to the support of the MT management team and our lab technician Liliana Gomes. And last but not the least, special thanks for the football team, in both the 3B's and Biology for your friendship and after-work good times!!

In Vienna, I express my greatest gratitude to the whole MolBio group, especially Georg, Ara, David and Khristina, for their friendship and support. You are great colleagues; it's a pleasure to work in the MolBio! Thanks for the good moments. Remember Braunschweig?! I would also like to acknowledge the friendliness of many other colleagues, such as Andreas, Katharina Schöbitz, Anna, Pierre, Cathy, Sylvia, Burkhard, Daniela and Asmita, Peter for support with size exclusion chromatography, Joachim, Sabine and Gerald for *in vivo* work, and certainly to many of you in the LBI group. My greatest gratitude for your friendliness and sympathy. I would also thank Magda Graça for providing gene sequencing, Sr. Adelino and Manela for making our life in the Biology Dept. corridors full of amusing moments, Elsa Ribeiro for SEM analysis and the Sanger Institute for free genetic materials. Still not ending, my heartfelt thanks to Johan, Simone, Isabel João, Belinha, Prof. João Mano and Prof. Nuno Neves for the support and the critical input with the review papers.

Finally, a word of special thanks to the many friends with whom I have shared plenty of unique moments: Hélder for our adventures together, for your great care and friendship, Marta, Hugo Rafael, Joana Branco, and the chemical sisters (Sónia, Sara, Magda and Isabel) with whom I

spend very happy moments in the past few years, Pirraco and friends for inspiring moments and great times spent together, Sara, Ana Sofia, for their great friendship, Ricjo, Simão, Abel and Zeph with whom I shared unforgettable moments, Sr. Barroso for his kindly service and friendship, Amaro, for our hiking and beautiful trips, and the “Hippos!” pela vossa amizade e hospitabilidade! You are all in my heart! A great hug to you all.

I hereby acknowledge with much gratitude the Fundação para a Ciência e Tecnologia, for the financial support (PhD grant SFRH/BD/17049/2004), project ElastM (POCI/CTM/57177/2004) supported by FEDER and FCT, European NoE EXPERTISSUES (NMP3-CT-2004-500283) and EU-funded project HIPPOCRATES (NMP3-CT-2003-505758), and Marie Curie Alea Jacta EST short-term grant (MEST-CT-2004-8104). This work was carried out under the scope of the European NoE EXPERTISSUES (NMP3-CT-2004-500283).

Aos meus pais Fátima e César e ao meu amor Pami

Novel Biodegradable Drug Delivery Systems for the Controlled Release of Growth Factors in Bone Healing and Tissue Engineering

ABSTRACT

Tissue engineering has emerged recently as a promising alternative in cases of tissue loss or organ failure by overcoming the problems of rejection and donor scarcity. Tissue engineering attempts to mimetize the body mechanisms of healing. By combining cells from the patient, growth factors and supportive scaffolds, it seeks to achieve the total regeneration of tissues.
Bone morphogenetic proteins (BMPs) are cytokines with important roles during embryogenesis, and with strong ability to induce formation of new bone and cartilage. These growth factors have been used as powerful osteoinductive components in several tissue engineering products for bone grafting.

In this context, the main objectives proposed for this thesis were:
i. To develop a strategy to produce, purify and characterize high amounts of recombinant BMPs.
ii. To evaluate the potential of new natural-origin biodegradable polymers for delivery of BMPs.

Currently, most BMPs are obtained from mammalian cell cultures in low yields or from bacteria inclusion bodies after time-consuming refolding steps. Aiming to circumvent the disadvantages of the previously reported methods, we have developed a novel approach for the production of high amounts of pure recombinant BMPs. The mature domains of human BMPs were cloned in pET-25b vector in *Escherichia coli*. This vector contained a leader sequence for secretion of the recombinant protein into the periplasm, where conditions are more adequate for the formation of the dimer conformation of BMPs. The method was applied for producing human BMP-2, BMP-4, BMP-9, BMP-10, BMP-11 and BMP-14. Overexpression of the BMPs was achieved and scaled-up in a bioreactor. The BMPs were purified with affinity chromatography by tagging the protein with an histidine tag, resulting in significantly large amounts of pure protein. In murine myoblast C2C12 cells and in primary cultures of human fat-derived adult stem cells, these growth factors showed bioactivity. This was observed by the induction of alkaline phosphatase activity and the upregulation of the

expression of different genes, stimulated during osteogenic differentiation. No cytotoxicity was observed as inferred by cell viability assays.
Different materials have been proposed as carriers for BMPs. Carriers are used to increase the lifetime, stability and bioactivity of the BMPs and release these growth factors in both timely and site-specific ways. Silk fibroin and an elastin-like polypeptide were investigated as potential microparticle systems for the sustained delivery of different recombinant BMPs.

Silk fibroin microparticles were produced by dropwise addition of ethanol. BMP-2, BMP-9 or BMP-14 were loaded into the particles and could be released in a sustained way in a period of two weeks, as evaluated by ELISA and quantitative dot-blot. The fibroin particles did not show any significant *in vitro* cytotoxicity. The fibroin particles loaded with BMP-2 were able to induce high levels of ALP activity and osteogenic mineralization in C2C12 cells. In rats, the BMP-2 loaded particles were implanted subcutaneously and ectopic bone formation was observed by live microCT and histology, four weeks post-implantation.

Elastin-like nanoparticles, created by thermoresponsive self-assembly, were also explored for a combined release of BMP-2 and BMP-14. Both growth factors were encapsulated with a high efficiency, and could be delivered in a combined and sustained way, retaining their bioactivity, as observed in C2C12 cells.

The results obtained in the thesis demonstrate that the methodologies that were developed may result in novel therapeutical applications in the biomaterial and regenerative medicine fields.

Novos Sistemas Biodegradáveis para Libertação Controlada de Factores de Crescimento em Medicina Regenerativa e Engenharia de Tecidos do Osso

RESUMO

A Engenharia de Tecidos emergiu recentemente como uma alternativa promissora nos casos de perda ou falha da função de um órgão ou tecido, ultrapassando os problemas de rejeição imunitária e da escassez de dadores. Através da combinação do uso de células do paciente, de factores de crescimento e de estruturas de suporte, espera-se a total regeneração dos tecidos. As proteínas morfogenéticas do osso (BMPs) são citocinas com funções importantes durante a embriogénese, possuindo uma forte capacidade de induzir a formação e regeneração de osso e de cartilagem. Estes factores de crescimento têm sido usados como potentes componentes osteoinductores de diversos produtos de engenharia de tecidos para aplicações ósseas.

Neste contexto, os objectivos principais propostos nesta tese são:
i. Desenvolver uma estratégia para produzir, purificar e caracterizar quantidades significativas de BMPs recombinantes.
ii. Avaliar o potential de novos sistemas naturais de polímeros biodegradáveis para a libertação de BMPs.

De momento, a maioria das BMPs são obtidas a partir de culturas de células de mamífero, produzidas em pequenas quantidades, ou ainda a partir de corpos de inclusão em bactéria, após protocolos morosos de renaturação. Com o objectivo de ultrapassar estas desvantagens, foi desenvolvida uma nova metodologia para a produção de largas quantidades de BMPs puras. O domínio funcional das BMPs humanas foi clonado no vector pET-25b em *Escherichia coli*. Este vector contém uma sequência sinal que permite a secreção da proteína recombinante para o periplasma, onde o ambiente favorece a formação dos dímeros de BMPs. Este método foi aplicado para a produção de BMP-2, BMP-4, BMP-9, BMP-10, BMP-11 e BMP-14 humanas. A sobreexpressão de BMPs foi atingida e aplicada à larga escala, em bioreactor. As BMPs foram purificadas por cromatografia de afinidade para uma cauda de histidinas, resultando em quantidades significativamente elevadas de proteína pura. Estes factores de crescimento demonstraram bioactividade em células mioblásticas C2C12 e em culturas primárias de células estaminais adultas obtidas de tecido adiposo, observada através da indução da actividade da fosfatase alcalina e da expressão de genes relacionados com a

diferenciação osteogénica. Não foi observada citotoxicidade, como demonstraram testes de viabilidade celular.

Diferentes materials têm sido propostos como suportes de libertação de BMPs. Estes auxiliam o aumento da estabilidade e bioactividade das BMPs, libertando estes factores de crescimento de maneira específica espacial e temporalmente. A fibroína da seda e um polipéptido baseado em elastina foram investigados como sistemas microparticulados para libertação controlada de diferentes BMPs recombinantes.

Micropartículas de fibroína da seda foram produzidas por adição gota-a-gota com etanol. BMP-2, BMP-9 ou BMP-14 foram imobilizadas nas partículas e poderam ser libertadas de modo contínuo durante um período de duas semanas, como demonstrou a análise por ELISA e dot-blot semi-quantitativo. As partículas de fibroína não demonstraram citotoxicidade *in vitro*. Partículas carregadas com BMP-2 foram capazes de induzir elevados níveis de actividade de ALP e mineralização osteogénica na linha celular C2C12. Em ratos, as partículas com BMP-2 foram implantadas subcutaneamente e foi observada formação ectópica de osso, através de microCT e análise histológica, quatro semanas após implantação.

Nanopartículas baseadas em elastina foram também estudadas para a libertação combinada de BMP-2 e BMP-14, criadas por auto-organização termosensível. Ambos os factores de crescimento foram encapsulados com eficiências elevadas, e poderam ser libertados de maneira controlada, retendo a sua bioactividade, como observado em células C2C12.

Os resultados descritos nesta tese demonstram que as metodologias que foram desenvolvidas podem resultar em novas aplicações terapéuticas nas áreas dos biomateriais e da medicina regenerativa.

TABLE OF CONTENTS

	Page
Acknowledgments	I
Abstract	V
Resumo	VII
Table of Contents	IX
List of Abbreviations	XVII
List of Figures	XIX
List of Tables	XXVI
Short *Curriculum Vitae*	XXIX
List of Publications	XXXI
Introduction to the Thesis Format	XXXV

SECTION 1

CHAPTER I

General introduction. Bone morphogenetic proteins in tissue engineering: the road from laboratory to the clinic – Part A. Basic concepts **3**

Abstract	4
1. Body morphogenetic proteins	4
2. Members of the BMP family	5
2.1. Subgroups within the BMP family	6
3. The structure of BMPs	8
3.1. Wrist and knuckle epitopes	9
3.2. N-terminal of BMP	10
3.3 BMP antagonists	10
4. BMP signaling – from cell receptor to gene activation	11
4.1. BMP/ Smad signaling	12
4.2. BMP/ MAPK signaling	13
4.3. BMP gene modulation	14
4.4 Cross-talk with other pathways	15

5. Recombinant BMPs for tissue engineering 16
5.1 From manufacture of BMPs to tissue-engineering products 18
References 22

CHAPTER II

General Introduction. Bone morphogenetic proteins in tissue engineering: the road from laboratory to the clinic – Part B. BMP delivery **31**

Abstract 32
1. Introduction 32
2. Delivering BMPs 33
2.1. BMP carriers– from bench to clinical approval 33
2.2. BMP retention at the orthopedic site 34
2.3. Pharmacokinetic profiles of released BMP 34
3. Carriers for BMPs 35
3.1. Synthetic polymers 35
3.2. Collagen 38
3.3. Natural origin polymers 39
3.4. Ceramics 47
3.5. Nanoparticles and microparticles for BMP delivery 49
4. Human clinics and the future of bone tissue engineering 51
4.1. Spinal fusion 52
4.2. Long bone fractures 53
4.3. Dental Tissue Engineering 53
4.4. Future challenges, a global perspective 54
References 56

SECTION 2

CHAPTER III

Materials and methods **69**

1. Recombinant technology for cloning and expression of proteins 70
1.1. BL21 DE3 strain *Escherichia coli* expression system 70

1.2. pET-25b expression system 70
2. Cloning of bone morphogenetic proteins 71
2.1 Obtaining bone morphogenetic cDNA (BMP mature domain) 71
2.2. Molecular biology tools used for cloning of BMPs 73
2.2.1. Designing primers for bone morphogenetic protein cloning 73
2.2.2. Cloning of BMP cDNA by polymerase chain reaction (PCR) 73
2.2.3. Restriction of DNA and ligation into expression vector 74
2.2.4. Transformation of XL1BLUE and BL21DE3 *Escherichia coli* strains 83 74
3. Expression, folding and purification of bone morphogenetic proteins 75
3.1 Expression of rhBMPs 75
3.1.1. Expression of BMPs in BL21DE3 *Escherichia coli* strain 75
3.1.2. Analysis of protein expression using SDS-PAGE 75
3.1.3. Analysis of protein expression using Western-blot 76
3.1.4. Optimization of protein expression levels 76
3.1.5. Bioreactor scale-up protein production 78
3.2 Recovery of rhBMPs 78
3.2.1. Protein folding and solubilization 78
3.2.2. Recovery of rhBMP-2 from periplasm 80
3.3 Purification of rhBMPs 80
3.3.1. Purification by nickel affinity chromatography 80
3.3.2. Buffer exchange and storage 81
3.4 Stability of rhBMPs 82
4. Assessing the bioactivity of BMPs 82
4.1. Bone differentiation and BMPs 82
4.2. Human adult stem cells 83
4.3. C2C12 cell line 83
4.4. MTS cell viability assay 84
4.5. Alkaline phosphatase enzymatic activity 84
4.6. RNA extraction and RT-PCR analysis of osteoblastic markers 85
4.7.Mineralization assay: Alizarin Red staining 85
5. Production of silk fibroin and elastin particles for BMP delivery 86
5.1. Development of silk fibroin particles 86
5.1.1. Isolation of silk fibroin 86
5.1.2. Microparticle preparation and loading of BMPs 86
5.2. Development of elastin-like nanoparticles 87

5.2.1. Nanoparticle preparation 87
5.2.2. Loading of BMPs 87
5.3. Physical characterization of the particles 88
5.3.1. Morphological characterization 88
5.3.2. Size distribution 88
5.3.3. Water uptake 88
5.4. Release of BMPs 88
5.4.1. Determination of loading capacity and encapsulation efficiency 88
5.4.2. *In vitro* release 89
5.4.3. Quantification of released BMPs 89
5.4.4. Release kinetics models 89
5.5. *In vitro* bioactivity 90
5.6. *In vivo* bioactivity (silk fibroin particles) 90
5.6.1. Rat ectopic bone formation model 90
5.6.2. *In vivo* microCT 91
5.6.3. Histological analysis 91
6. Statistical analysis 91
References 92

SECTION 3

CHAPTER IV

Osteoinduction in human fat-derived stem cells by recombinant human BMP-2 (bone morphogenetic protein-2) produced in Escherichia coli **97**

Abstract 98
1. Introduction 98
2. Materials and methods 99
2.1. Cloning of rhBMP-2 99
2.2. Expression of rhBMP-2 in *E. coli* in bioreactor 99
2.3. Purification of rhBMP-2 101
2.4. Analytical detection of rhBMP-2 by reducing and non-reducing SDS-PAGE and Western-blot 101
2.5. Bioactivity tests 101

3. Results 103
3.1. Cloning, expression and purification of rhBMP-2 103
3.2. Biological activity in C2C12 cells 104
3.3. Biological activity in mesenchymal stem cells 105
4. Discussion 106
References 107

CHAPTER V

Expression, purification and osteogenic bioactivity of recombinant human BMP-4, -9, -10, -11 and -14 **109**

Abstract 110
1. Introduction 110
2. Materials and methods 111
2.1. Cloning and expression of rhBMP-4, -9, -10, -11 and -14 111
2.2. Purification of rhBMPs 112
2.3. Western-blot detection of rhBMPs 113
2.4. Bioactivity tests 113
2.5. Statistical analysis 114
3. Results 114
3.1. Cloning, expression and purification of rhBMPs 114
3.2. Cytotoxicity of rhBMPs 115
3.3. Expression of osteogenic markers induced by rhBMPs 116
4. Discussion 120
References 122

SECTION 4

CHAPTER VI

Silk fibroin microparticles as carriers for the controlled release of human recombinant BMPs. Physical characterization and drug release **127**

Abstract 128
1. Introduction 128

2. Materials and methods 129
2.1. Materials 129
2.2. Methods 130
2.2.1. Preparation of BMP-loaded silk fibroin microparticles 130
2.2.2. Physical characterization 130
2.2.3. *In vitro* release studies 131
2.2.4. Statistical analysis 133
3. Results 133
3.1. Morphology, size distribution and encapsulation efficiency 133
3.2. Water uptake and degradation studies 136
3.3. *In vitro* release studies 136
4. Discussion 140
References 142

CHAPTER VII

Silk fibroin microparticles as carriers for the controlled release of human recombinant BMP-2. In vitro and in vivo bioactivity **145**

Abstract 146
1. Introduction 146
2. Materials and methods 147
2.1. Materials 147
2.2. Methods 147
2.2.1. Bioactivity in C2C12 cells 147
2.2.2. MTS cell viability assay 148
2.2.3. Rat ectopic bone formation model 148
2.2.4. *In vivo* μCT 149
2.2.5. Histology 149
2.2.6. Statistical analysis 150
3.Results 150
3.1. Alkaline phosphatase activity in C2C12 cells 150
3.2. Cell viability 150
3.3. *In vivo* μCT 150
3.4. Histology 155
4. Discussion 155

References 159

CHAPTER VIII

Thermoresponsive self-assembled elastin-based nanoparticles for delivery of BMPs **161**

Abstract 162
1. Introduction 162
2. Materials and methods 164
2.1. Materials 164
2.2. Methods 164
2.2.1. Production of elastin-like nanoparticles 164
2.2.2. Physical characterization 164
2.2.3. *In vitro* delivery studies 165
2.2.4. Biological activity of released BMP 167
2.2.5. Statistical analysis 168
3.Results 168
3.1. Physical characterization 168
3.2. Loading and release of BMP-2 and BMP-14 171
3.3. *In vitro* bioactivity 172
4. Discussion 176
References 179

SECTION 5

CHAPTER IX

General Conclusions and Final Remarks **183**

General conclusions 184
1. A method for the production of recombinant BMPs 185
2. Innovative microparticulate delivery systems for BMPs 187
Future directions 189

ATTACH I

Supplementary data **191**

Refolding studies with recombinant BMPs 192

A stepwise optimization of BMP refolding 192

Bioactivity of BMPs refolded by the new method 194

Stability of bioactive BMP-2 196

Correct refolding *versus* misfolding 198

Different variables are known to affect refolding 199

References 202

LIST OF ABBREVIATIONS

AEC (3-amino-9-ethylcarbazole)

ALP (Alkaline phosphatase)

BMP (Bone morphogenetic protein)

BSA (Bovine serum albumin)

BSP (Bone sialoprotein)

BW (Body weight)

Ca-P (Calcium phosphate)

CHO (Chinese Hamster Ovary)

C2C12 (Mouse myoblast cell line)

DNA (Desoxyribonucleic Acid)

cDNA (complementary DNA)

Dlx5 (Distal-less homeobox 5)

DLS (Dynamic light scattering)

DMEM (Dulbecco's modified Eagle's medium)

E. coli (*Escherichia coli*)

E.E. (Encapsulation efficiency)

ELISA (Enzyme Linked Immunosorbent Assay)

ELPs (Elastin-like polymers)

FDA (Food and Drug Administration)

GDF (Growth and differentiation factor)

H & E (Hematoxylin and eosin)

HA (Hydroxyapatite)

HRP (Horseradish peroxidase)

HSV (Herpes simplex virus)

IPTG (Isopropyl-1-thio-β-galactopyranoside)

ITT (Inverse Temperature Transition)

LB (Luria-Bertani broth)

L.C. (Loading capacity)

MTS(3-(4,5)-dimethylthiazol-2-yl)-5-(3-carboxy-methoxyphenyl)-2-(4-sulfophenyl)-2H-tetrazolium)

MTT (3-(4,5-dimethylthiazol-2-yl)-2,5-diphenyltetrazolium bromide)

Mw (Molecular weight)

MwCO (Mw cut-off, in membrane dialysis)

n (release exponent of Korsmeyer model of kinetics)

OC (Osteocalcin)

OP-1 (Osteogenic protein-1)

OSX (Osterix)

p (Probability value, in statistic significance tests)

PBS (Phosphate buffer saline)

PCR (Polymerase chain reaction)

pI (Isoelectric point)

PLA (Polylactic acid)

PLA-DX-PEG (Polylactic acid p-dioxanone polyethylene glycol)

PLGA (Polylactic-co-glycolic acid)

PEG (Polyethylene glycol)

PGA (Polyglycolic acid)

POLII (Polymerase II)

PVDF (Polyvinylidene Fluoride)

R (Released percentage)

r^2 (Correlation value)

rhBMP (Recombinant human bone morphogenetic protein)

RNA (Ribonucleic Acid)

mRNA (Messenger RNA)

rpm (Rotations per minute)

RT-PCR (Reverse transcription polymerase chain reaction)

Runx2/Cbfa1 (Runt-related transcription factor 2/ core binding factor alpha-1)

SaOS-2 (Human osteosarcoma cell line)

SD (Standard deviation)

SDS-PAGE (Sodium dodecyl sulphate polyacrylamide gel electrophoresis)

SEM (Scanning electron microscopy)

SOC (Super Optimal broth with Catabolite repression) (added glucose)

T_t (Transition temperature) (of elastin-like polypeptides)

TGF-β (Transforming growth factor β)

UR (Unreleased percentage)

v/v (Volume per volume)

w/v (Weight per volume)

W_d (Dry weight)

W_w (Wet weight)

WU (Water uptake)

μCT (Micro computer tomography)

LIST OF FIGURES

Page

SECTION 1

CHAPTER I

General introduction. Bone morphogenetic proteins in tissue engineering: the road from laboratory to the clinic – Part A. Basic concepts

Figure 1. BMP signaling pathways: schematic representation of Smad-dependent and independent pathways and their main mechanisms of modulation **15**

SECTION 2

CHAPTER III

Materials and methods

Figure 1. Vector pET-25b was used for the expression of different human BMPs in *E. coli*. In the representation above, the vector restriction sites (A) and multiple cloning site (coding strand transcribed by T7 RNA polymerase) (B), are shown. **72**

Figure 2. Schematic representation of cloning of human BMP-2 in pET-25b vector, showing the N-terminal histidine tag of vector, and peIB signal sequence for secretion into periplasm. Signal sequence is proteolytically cleaved in periplasm of *Escherichia coli*. The (natural-occurring) heparin binding domain of BMP-2 is indicated in dark green color. The same methodology was performed for cloning of human BMP-4, BMP-9, BMP-10, BMP-11/GDF-11 and BMP-14/GDF-5. *Bam*HI and *Xho*I restriction sites, used for cloning, are indicated. **73**

Figure 3. SDS-PAGE of samples of crude lysates (pellet fraction) with different temperature used for expression of rhBMP-2. Respectively, A-G correspond to the negative control, BMP-2 variant I (25ºC), BMP-2 variant II (25ºC), BMP-2 variant I (18ºC), BMP-2 variant II (18ºC), BMP-2 variant I (4ºC), BMP-2 variant II (4ºC). BMP-2 monomer and dimer are marked (18 kDa, 36 kDa). Marker: 116 kDa, 97 kDa, 66 kDa, 45 kDa, 22 kDa and 14 kDa. Expression of BMP-2 was significantly higher at 25ºC. Expression was performed for 24 h. Please refer to section 3.2.5. for rhBMP-2 variants. **77**

Figure 4. SDS-PAGE of samples of crude lysates (pellet fraction) with different time periods for expression of rhBMP-2. Respectively, A-H correspond to the following times of production: A (0h), B (4h), C (8h), D (16h), E (22h), F (24h), G (2 days) and H (4 days). Temperature of expression was 25ºC. BMP-2

monomer and dimer are marked (18 kDa, 36 kDa). Marker: 200 kDa, 116 kDa, 97 kDa, 66 kDa, 45 kDa, 22 kDa and 14 kDa. Expression of BMP-2 peaked after 24 -48 h. **77**

Figure 5. SDS-PAGE of samples of crude lysates (pellet fraction) with rhBMP-2 produced with native gene sequence (1), codon usage optimized sequence (2) and a negative control (C). Codon usage optimized sequence does not result in significant changes in the expression of rhBMP-2. **77**

Figure 6. Use of a bioreactor allowed producing large-scale amounts of recombinant BMPs. **78**

Figure 7. Nickel affinity chromatography was used for the purification of histidine-tagged recombinant human BMPs. **81**

Figure 8. Silver stained SDS-PAGE showing the stability of BMP-2 in phosphate buffer, at different pH. The protein was stored for a period of two weeks at 4°C. The figure shows proteins present before and after centrifugation to remove precipitates. Lanes: A) protein stored in pH 5.0; B) protein stored in pH 7.0; C) protein stored in pH 9.0; D) protein stored in pH 11.0. BMP-2 seems to be more stable and soluble when stored at pH 7.0-9.0, in phosphate buffer (B and C). **82**

Figure 9. Silk fibroin microparticles, for loading and delivery of rhBMPs, were formed after dropwise addition of ethanol and overnight incubation at - 20 ºC. **87**

SECTION 3

CHAPTER IV

Osteoinduction in human fat-derived stem cells by recombinant human BMP-2 (bone morphogenetic protein-2) produced in Escherichia coli

Figure 1. Strategy used for cloning the mature domain of human bone morphogenetic protein-2. A) BMP-2 gene contains three exons represented by boxes and two introns corresponding to the lines. Coding region is represented by black boxes located in exon 2 and 3. The mature domain of human BMP-2 protein is entirely located on exons 3 correspondent to amino acids 283 to 396. B) Construction of vector pET-25b/rhBMP-2 for expression of human BMP-2 in *E. coli*. The mature BMP-2 was cloned into the vector pET-25b together with its own leader sequence and 6-histidine tag for purification. **100**

Figure 2. A) Coomassie-blue stained SDS-PAGE of crude lysates, pellet fraction, from batch cultivation of transformed *E. coli*. Lanes 1) pET-25b clone; 2) rhBMP-2/pET-25b clone. Monomer appears as a well-defined band around 17 kDa. Molecular weight is in kDa (Broad Range, BioRad). B) rhBMP-2 purified by affinity chromatography: 1) Silver stained reduced SDS-PAGE, showing the monomer of BMP-2 with significant purity; 2) Western-blot using anti-his tag antibody; 3) Western-blot using anti-BMP-2 antibody. BMP-2 is visible in monomer, dimer and polymer. **103**

Figure 3. RT-PCR for genes involved during osteoblast differentiation of C2C12 cells after 5 days of culture with purified rhBMP-2 and commercial mammalian rhBMP-2 as control. Gene expression was analyzed with ChemiImage 4400 AlphaEase FC Image Analysis Software (Alpha Innotech) and

standardized with Polymerase II expression. OSX: osterix; OC: osteocalcin; ALP: alkaline phosphatase. Conditions used: 1) No rhBMP-2; 2) 250 ng/ml; 3) 500 ng/ml; 4) 1000 ng/ml; 5) 250 ng/ml commercial preparation; 6) 500 ng/ml commercial preparation; 7) 1000 ng/ml commercial preparation. Data presented are mean values of two independent experiments. (* bioassay was not performed) **104**

Figure 4. A) Tetrazolium salt (MTS) test performed in fat tissue derived human stem cells as a function of rhBMP-2 concentration, after 3, 7 and 14 days of cell culture. Cell viability is expressed in percentage. B) Bioactivity of rhBMP-2 as measured by the induction of alkaline phosphatase activity in fat tissue derived human stem cells. ALP activity levels are expressed in µmol ALP per mg of total protein. **105**

Figure 5. Cell morphology of fat derived human stem cells after 10 days of cell culture with A) no growth factor (control) and B) with 500 ng/ml purified rhBMP-2 (replacement of growth factor and culture media every two days). x400. Fibroblast-like (f) and osteoblast-like (o) morphologies were observed when rhBMP-2 was used on the mesenchymal stem cell primary culture. **105**

CHAPTER V

Expression, purification and osteogenic bioactivity of recombinant human BMP-4, -9, -10, -11 and -14

Figure 1. Western-blot of purified rhBMP-4, -9, -10, -11 and -14 and a negative control (respectively 1-6) using an anti 6-His tag antibody. The BMPs are visible in monomer, dimer and polymer. **114**

Figure 2. Tetrazolium salt (MTS) test performed in C2C12 cells as a function of the concentration of the different rhBMPs, after 3 days of cell culture. Cell viability is expressed in percentage (mean ± S.D., n=3, * $p < 0.05$). **116**

Figure 3. mRNA expression of signaling molecules and transcription factors (A) and osteogenic-specific markers (B) induced by BMPs, measured by semi-quantitative RT-PCR after 5 days of cell culture in C2C12 cell line. Bars represent mean values ± SD of gene expression fold variation of at least three independent determinations (* $p < 0.05$). Smad-1 and Smad-5 were induced mostly for BMP-4, -9 and -14, Osterix for BMP-4 and -9, Runx2 was induced for all BMPs but higher for BMP-9. Bone sialoprotein was induced mostly for BMP-4 and -11; ALP was induced 1.5 to 2-fold for all BMPs except BMP-11; osteopontin was induced mainly for BMP-9, BMP-10 and BMP-14. **118**

Figure 4. Cell morphology of C2C12 cells after 5 days of cell culture with A) no growth factor (control), B) 500 ng/ml rhBMP-4, C) 500 ng/ml rhBMP-9, D) 500 ng/ml rhBMP-10, E) 500 ng/ml rhBMP-11, and F) 500 ng/ml rhBMP-14. Purified BMP was used. x400. Osteoblast-like morphology (o) was observed in C2C12 cells stimulated with BMP-4, BMP-9 and BMP-14 and myoblast-like morphology (m) in control and cells stimulated with BMP-10. **119**

Figure 5. mRNA expression of early markers of osteogenic differentiation induced by BMPs, measured by semi-quantitative RT-PCR after 3 days of human adult stem cell cultures. Bars represent mean values ± SD of gene expression fold variation of at least three independent determinations (* $p < 0.05$). The

expression of osteogenic markers was induced mainly with BMP-4. BMP-9 induced runx2 and ALP (2-fold) and BMP-14 induced solely ALP (5-fold) and bone sialoprotein (3-fold). **120**

SECTION 4

CHAPTER VI

Silk fibroin microparticles as carriers for delivery of human recombinant BMPs. Physical characterization and drug release

Figure 1. SEM micrographs of unloaded fibroin microparticles, produced with different ethanol : silk solution ratios: A) 1:2 ratio, B) 1:3 ratio, and C) 1:4 ratio. Magnification 10.000 x. Scale 5 μm. **134**

Figure 2. Size distribution of unloaded silk fibroin particles. Almost all particles showed sizes ranging between 1.5 and 3.0 μm, with a mean diameter of 2.7 ± 0.3 μm. Size refers to particle diameter (nanometers). **135**

Figure 3. Evolution of water uptake behavior of unloaded silk fibroin microparticles in phosphate buffer saline as a function of immersion time (t). (mean ± S.D., *n*=3). Water uptake increased significantly up to 5 days, peaked after 8 days, and then slightly declined (non-significantly). * $p < 0.01$ related to the difference between consecutive time measurements. **136**

Figure 4. Evolution of weight loss of unloaded fibroin particles in phosphate buffer saline as a function of immersion time (t). (mean ± SD, n = 3). The remaining mass decreased to 97.1 ± 1.5 % after day 5, 95.4 ± 2.5 % after day 14, and 93.5 ± 3.3 % after day 30. **137**

Figure 5. Release kinetics of BMP-2, BMP-9 and BMP-14 immobilized in fibroin particles. ELISA was used for BMP-2 quantification and dot-blot for BMP-9 and BMP-14 quantification (Mean ± SD, n= 3). A) Release from particles loaded with 0.5 μg of BMP per mg of fibroin; B) release from particles loaded with 5.0 μg of BMP per mg of fibroin. Cumulative release is expressed in percentage of loaded protein. **138**

CHAPTER VII

Silk fibroin microparticles as carriers for delivery of human recombinant BMP-2. In vitro and in vivo bioactivity

Figure 1. Alkaline phosphatase activity of C2C12 cell line after 5 days of culture. A-C) BMP-2 soluble protein, positive control, 0.1, 0.5 and 1.0 μg/ml; D) control cells (no growth factor or particles added); E and F) unloaded particles; G) particles with loaded BMP-2 (0.5 μg), H) fibroin particles with loaded BMP-2 (2.5 μg), I-J) fibroin particles with adsorbed BMP-2. ALP activity is reported in nmol /min /mg of total protein (Mean ± SD, *n* = 3), * $p < 0.01$ relative to negative control cells (D). **151**

Figure 2. Alizarin red mineralization staining of showing sites of calcium-phosphate deposits (orange color) in C2C12 cell line differentiated into osteoblast after 14 days of culture with particles loaded with 0.5 µg BMP-2 (A), and 0.5 µg/ml BMP-2 added to culture medium (B). Unloaded fibroin particles did not show any mineralization (C). **152**

Figure 3. Cell viability tetrazolium salt (MTS) test performed in SaOS-2 cells as a function of the time of cells culture with 0.5 mg/ml silk fibroin microparticles. DMEM and Latex were used as a negative and a positive control for cell death, respectively. (mean ± SD, *n* = 3) **152**

Figure 4. Live microCT analysis of ectopic bone formation induced by fibroin particles + 2.5 µg BMP-2 after 2 weeks (A) and 4 weeks (B), and fibroin particles + 12.5 µg BMP-2 after 4 weeks (C). Scale is 5 mm. **153**

Figure 5. Detailed live microCT analysis of ectopic bone formation induced by fibroin particles + 2.5 µg BMP-2 after 2 weeks (A and B) and 4 weeks (C and D), and fibroin particles + 12.5 µg BMP-2 after 4 weeks (E). Background signal in A and B is due to a lower threshold used for bone visualization. Scale is 1 mm. **154**

Figure 6. H&E staining for animals implanted with fibroin particles + 5 µg BMP-2 (group II) at 4 weeks post-implantation (A). Newly formed bone was indicated by the presence of a mineralized extracellular matrix (E.M.) which was stained with Alizarin Red (B), osteocytes (O.C.), and osteoblasts (O.B.) which were stained by osteocalcin immunostaining (C). **158**

CHAPTER VIII

Thermoresponsive self-assembled elastin-based nanoparticles for delivery of BMPs

Figure 1. SEM micrographs of unloaded elastin nanoparticles. Magnification 50.000 x. Scale is 1 µm. **169**

Figure 2. Size distribution of unloaded elastin-like particles, obtained by Dynamic Light Scattering (DLS). Almost all particles showed sizes ranging between 190 nm and 295 nm, with a mean diameter of 237.5 ± 3.0 nm. Size refers to particle diameter (nanometers). **169**

Figure 3. Evolution of water uptake behavior of unloaded elastin particles in phosphate buffer saline as a function of immersion time (t). (mean ± SD, *n* = 3). Water uptake increased significantly up to 24 hours, and then stabilized. * $p < 0.05$ is relative to the difference between consecutive time measurements. **170**

Figure 4. Evolution of weight loss of unloaded elastin particles in phosphate buffer saline as a function of immersion time (t). (mean ± SD, *n* = 3). The remaining mass decreased to 97.1 ± 3.1 % after day 5, 88.9 ± 6.3 % after day 14, and to 64.5 ± 12.5 % after day 30. **170**

Figure 5. Release kinetics of BMP-2 and BMP-14 loaded in the elastin nanoparticles. ELISA was used for BMP-2 quantification and dot-blot for BMP-14 quantification (Mean ± SD, *n* = 3). Cumulative release is expressed in percentage of loaded protein. **171**

Figure 6. Release kinetics of encapsulated BMP-2. First order (log cumulative percent drug remaining *vs*. time), Higuchi kinetics (cumulative percent drug released *vs*. square root of time) and Korsmeyer kinetics (log cumulative percent drug released *vs*. log time), with correlation values (r^2). **172**

Figure 7. Release kinetics of encapsulated BMP-14. First order (log cumulative percent drug remaining *vs*. time), Higuchi kinetics (cumulative percent drug released *vs*. square root of time) and Korsmeyer kinetics (log cumulative percent drug released *vs*. log time), with correlation values (r^2). **173**

Figure 8. Cell viability tetrazolium salt (MTT) test performed in C2C12 cells, after 5 days of cell culture, with 10 or 100 µg/ml unloaded elastin-like nanoparticles. DMEM was used as a positive control for cell viability. Cell viability is expressed as a percentage of the control (scored as 100% viability) as mean ± SD (n = 3). * $p < 0.05$ is relative to differences to the control. **173**

Figure 9. Alkaline phosphatase activity of C2C12 cell line after 5 days of culture, incubated with loaded and unloaded elastin nanoparticles: A) negative control with no added particles or growth factor; Elastin particles were loaded with: B-E) BMP-2 (0.1, 0.25, 0.5, 2.5 µg); F-I) BMP-2 and BMP-14 (0.1, 0.25, 0.5, 2.5 µg each); N-Q) BMP-14 (0.1, 0.25, 0.5, 2.5 µg); J-M) BMP-2 added to culture medium (0.1, 0.25, 0.5, 2.5 µg) as positive control; R-U) BMP-14 added to culture medium (0.1, 0.25, 0.5, 2.5 µg) as positive control. ALP activity is reported in nmol /min /mg of total protein (Mean ± SD, n = 3). * $p < 0.05$ and ** $p < 0.01$ are relative to the differences indicated. **174**

Figure 10. Alizarin Red mineralization staining of showing sites of calcium-phosphate deposits (orange color) in C2C12 cell line differentiated into osteoblast after 14 days of culture with particles loaded with BMP-2 (A), BMP-2 and BMP-14 (B), and the positive controls of BMP-2 (C) and BMP-2 + BMP-14 (D) added to culture media, at 2.5 µg/ml. Unloaded particles did not showed any mineralization (E). Unstained cells treated with particles loaded with BMP-2 + BMP-14 showed osteoblast morphology (F). **175**

ATTACH I

Supplementary data

Figure 1. ALP activity in C2C12 cells after 5 days of culture with refolded BMP-2 (blue), BMP-4 (green) and positive BMP-2 control (red), at 25 to 1000 ng/ml. (mean ± S.D., n=3, * $p < 0.05$ relative to negative control) **195**

Figure 2. Morphology of C2C12 cells after 4 days of culture with refolded BMP-2 and BMP-4, positive BMP-2 control (mammalian-derived, Wyeth, UK), at 1000 ng/ml, and negative control (no growth factor). Osteoblast-like morphology is observed in all conditions except in negative control. **195**

Figure 3. Alizarin Red staining of C2C12 cells treated with refolded BMP-2 and BMP-4, at 1000 ng/ml, in comparison with the positive control (mammalian-derived, Wyeth, UK), at 1000 ng/ml, and negative control (no growth factor), after 15 days of culture. Mineralized extracellular matrix is stained in cells treated with refolded BMP-2, BMP-4 and positive BMP-2 control. **196**

Figure 4. ALP activity in C2C12 cells after 5 days of culture of refolded BMP-2 stored at different pH conditions, added at 150 ng/ml, and a negative control with no growth factor (C). Loss of ALP activity is observed at pH 3.0 and pH 11.0. Activity is retained between pH 4.5 and pH 9.0. **197**

Figure 5. ALP activity in C2C12 cells after 5 days of culture of refolded BMP-2 stored at different ionic strength buffer conditions (phosphate buffer, pH 7.4), added at 150 ng/ml, and a negative control with no growth factor (C). Loss of ALP activity is observed at buffer conditions below 10 mM phosphate. Activity is retained in 10 mM to 1 M phosphate buffer. **197**

Figure 6. Western-blot showing unfolded and reduced inclusion bodies, prior to refolding (A); renaturation of BMP-2 inclusion bodies with formation of dimer, after 3 days of reaction at 4ºC (B); purification of refolded BMP-2 and isolation of dimer (C) by heparin affinity chromatography, with separation of monomer (2-4) and dimer (5). **198**

Figure 7. Simplified model of correct folding versus misfolding and aggregation. The correct protein folding pathway (1) often competes with misfolding (2) and aggregation (3), depending in several variables. Disulfide knot proteins, such as BMPs, can easily form misfolded products, due to the complicate nature of intra- and intermolecular disulfide bridges. These misfolded dimers would have the correct molecular weight but no bioactivity. **199**

LIST OF TABLES

Page

SECTION 1

CHAPTER I

General introduction. Bone morphogenetic proteins in tissue engineering: the road from laboratory to the clinic – Part A. Basic concepts

Table 1. BMP members in humans and their main physiological roles. BMPs known to induce complete bone morphogenesis are underlined. **7**

Table 2. Suggested subgroups within BMP family (grouped by similarity to BMP-7 / OP-1). **8**

Table 3. Selected works reporting the production of recombinant BMPs in diverse expression systems. **18**

Table 4. Chemical or genetic engineering modifications for improving particular characteristics of BMPs for use in tissue engineering applications. **21**

CHAPTER II

General Introduction. Bone morphogenetic proteins in tissue engineering: the road from laboratory to the clinic – Part B. BMP delivery

Table 1. Synthetic-polymer-based matrices/scaffolds for drug delivery of BMPs for tissue engineering applications. **37**

Table 2. Natural origin polymer based matrices for delivery of BMPs for tissue engineering applications. Please refer to table 3 for micro and nanoparticles formulations. **45**

Table 3. Micro and nanoscale drug delivery systems based on synthetic and natural-origin polymers. The average size or size range of the particles is noted on the formulation. **49**

SECTION 2

CHAPTER III

Materials and methods

Table 1. Effect of different L-arginine concentrations on the recovery of total protein of crude extracts, from which rhBMP-2 is a main fraction. Similar conditions of dilution of protein and pH 8.5 were used for these recovery assays. Protein was quantified using the Bradford method. **79**

Table 2. Effect of different pH on the recovery of total protein of crude extracts, from which rhBMP-2 is a main fraction. Similar conditions of dilution of protein and a fixed concentration of 0.5 M L-arginine were used for these recovery assays. Protein was quantified using the Bradford method. **79**

SECTION 3

CHAPTER IV

Osteoinduction in human fat-derived stem cells by recombinant human BMP-2 (bone morphogenetic protein-2) produced in Escherichia coli

Table 1. Oligonucleotide primers for semi-quantitative RT-PCR analysis in murine C2C12 cells. **102**

CHAPTER V

Expression, purification and osteogenic bioactivity of recombinant human BMP-4, -9, -10, -11 and -14

Table 1. Oligonucleotide primers for cloning of human BMP-4, -9, -10, -11 and -14. The nucleotides for restriction by *BamH*I and *Xho*I are underlined in the forward and reverse primers, respectively. The codons representing the beginning and the end of BMP sequences are represented in bold. **112**

Table 2. Purification of recombinant human BMP-4, BMP-9, BMP-10, BMP-11 (GDF-11) and BMP-14 (GDF-5). **115**

SECTION 4

CHAPTER VI

Silk fibroin microparticles as carriers for delivery of human recombinant BMPs.
Physical characterization and drug release

Table 1. Loading and encapsulation efficiencies of BMP loaded fibroin microparticles (mean ± S.D., *n*=3) **135**

Table 2. Release kinetics of BMPs immobilized in fibroin particles. First order (log cumulative percent drug remaining *vs*. time), Higuchi kinetics (cumulative percent drug released *vs*. square root of time) and Korsmeyer kinetics (log cumulative percent drug released *vs*. log time), with correlation values (r^2). **139**

CHAPTER VII

Silk fibroin microparticles as carriers for delivery of human recombinant BMP-2.

In vitro and in vivo bioactivity

Table 1. Analysis of *in vivo* µCT data, showing bone size, surface area, volume and mean density. Group II (fibroin particles + 5 µg BMP-2), group III (fibroin particles + 12.5 µg BMP-2). (mean ± standard error, *n* = 2) **155**

SHORT *CURRICULUM VITAE*

Paulo C. Bessa was born in 1981 in Porto, Portugal. He presently lives in Vienna, Austria and works, as a researcher, in the 3B's Research Group (Biomaterials, Biodegradables and Biomimetics), under the supervision of Prof. Rui L. Reis, in the Ludwig Boltzmann Institute for Experimental and Clinical Traumatology, in Vienna Austria, under the supervision of Prof. Heinz Redl and of Prof. Martijn van Griensven, and in the Center for Molecular and Environmental Biology (CMBA), under the supervision of Prof. Margarida Casal.

His background includes a four-year graduation in Applied Biology, by the School of Sciences, University of Minho. He has just submitted his PhD thesis entitled "Novel Biodegradable Drug Delivery Systems for the Controlled Release of Growth Factors in Bone Healing and Tissue Engineering" to the University of Minho, which was prepared in cooperation with the Ludwig Boltzmann Institute for Experimental and Clinical Traumatology, in Vienna, Austria.
During the last year of his graduation, Paulo C. Bessa worked in neurobiology and molecular biology fields, in Leiden, The Netherlands. This work was the subject of his senior research project.

In 2004 he joined the 3B's Research Group, where he has been working ever since on the production of recombinant growth factors and in the development of new drug delivery systems, for both controlled release and tissue engineering applications. During this phase he worked for different time periods at the Ludwig Boltzmann Institute for Experimental and Clinical Traumatology, in Vienna, Austria, under the supervision of Prof. Heinz Redl and of Prof. Martijn van Griensven, under the same scope of study.

As a researcher of the 3B's Research Group he has been involved in the preparation of several grant proposals, both at the National (Portuguese Foundation for Science and Technology) and European levels (frameworks VI and VII), including the only Tissue Engineering Network of Excellence of Europe, EXPERTISSUES and the EU-funded project HIPPOCRATES.

Paulo C. Bessa has been also involved in the organization of some meetings and conferences such as in the first meeting of the SPCE-TC (Sociedade Portuguesa de Células Estaminais e Terapia Celular) in 2005, Lisboa, Portugal, and in the ESF-EMBO Symposium on "Stem Cells in Tissue Engineering: Isolation, Culture, Characterization and Applications", in 2006, in Sant Feliu

de Guixols, Spain. In the group of Prof. Margarida Casal, he has also been involved in assisting in several practical classes of both Genetics and Genetic Engineering (Applied Biology BsC) and in the Master in Biotechnology, during 2004, 2005 and 2008. Finally, he has also assisted in the invited peer-revision of several manuscripts in the field.

As a result of his research work he attended several important international and national meetings in the present field of research. Presently he is the author of 7 papers in international peer-reviewed journals (4 published, 3 submitted), 1 published book chapter and 11 abstracts published in international conferences.

LIST OF PUBLICATIONS

The work performed during this PhD resulted in the following publications:

- PAPERS IN REFEREED JOURNALS

Bessa PC, Pedro AJ, Klösch B, Nobre A, van Griensven M, Reis RL and Casal M, 2008, Osteoinduction in human fat derived stem cells by recombinant human bone morphogenetic protein-2 produced in *Escherichia coli*, Biotechnology Letters **30**, 15-21

Bessa PC, Casal M and Reis RL, 2008, Bone morphogenetic proteins in tissue engineering: the road from laboratory to the clinic, part I, basic concepts, Journal of Tissue Engineering and Regenerative Medicine **2**, 1-13

Bessa PC, Casal M and Reis RL, 2008, Bone morphogenetic proteins in tissue engineering: the road from laboratory to the clinic, part II, BMP delivery, Journal of Tissue Engineering and Regenerative Medicine **2**, 81-96.

Bessa PC, Cerqueira MT, Rada T, Gomes ME, Neves NM, Nobre A, Reis RL and Casal M, 2009, Expression, purification and osteogenic bioactivity of recombinant human BMP-4, -9, -10, -11 and -14, Protein Expression and Purification **63**, 89-94.

Bessa PC, Balmayor ER, Azevedo HS, Nürnberger S, Casal M, van Griensven M, Reis RL, Redl H, 2009, Silk fibroin microparticles as carriers for delivery of human recombinant BMPs. Physical characterization and drug release, Journal of Tissue Engineering and Regenerative Medicine, *submitted.*

Bessa PC, Balmayor ER, Hartinger J, Zanoni G, Dopler D, Meinl A, Banerjee A, Casal M, Redl H, Reis RL, van Griensven M, 2009, Silk fibroin microparticles as carriers for delivery of human recombinant BMP-2. *In vitro* and *in vivo* bioactivity, Tissue Engineering, Part C - Methods, *submitted.*

Bessa PC, Machado R, Nürnberger S, Dopler D, Meinl A, Banerjee A, Cunha AM, Rodríguez-Cabello JC, Redl H, van Griensven M, Reis RL, Casal M, 2009, Thermoresponsive self-assembled elastin-based nanoparticles for delivery of BMPs, Journal of Controlled Release, *submitted.*

- BOOK CHAPTERS

Leonor IB, Gomes S, **Bessa PC**, Casal M, Mano JF and Reis RL, 2008, New biomineralization strategies on natural-based polymeric materials for bone tissue engineering approaches, In Handbook of Natural-based Polymers for Biomedical Applications, eds. Reis RL, Neves NM, Mano JF, Gomes ME, Marques AP, Azevedo HS, Woodhead Publishing Limited, Cambridge, United Kingdom, 193-230.

- CONFERENCES PROCEEDINGS IN SCIENTIFIC JOURNALS:

Bessa PC, Pedro AJ, Casal M and Reis RL, 2005, Production of biologically active recombinant human BMP-2 for Tissue Engineering applications, International Journal of Artificial Organs **28**, 866-900

Balmayor ER, **Bessa PC**, Tuzlakoglu K, Azevedo HS, Casal M and Reis RL, 2008, Novel Biodegradable Polymeric Microparticles for the Localized Delivery of Differentiation Agents in Bone Tissue Engineering Applications, Tissue Engineering: Part A **14**, 762-763.

Bessa PC, Balmayor ER, Cerqueira MT , Rada T, Gomes ME, Neves NM, Azevedo HS, Casal M and Reis RL, 2008, Silk nanoparticles for delivery of human BMP-2 in bone regenerative medicine applications, Tissue Engineering: Part A **14**, 776-777.

Bessa PC, Cerqueira MT, Rada T, Gomes ME, Neves NM, Reis RL and Casal M, 2008, Expression, purification and bioactivity of recombinant human bone morphogenetic protein-4, -9, -10, -11 and -14, Tissue Engineering: Part A **14**, 852.

- COMMUNICATIONS IN NATIONAL AND INTERNATIONAL CONFERENCES:

Bessa PC, Pedro AJ, Casal M and Reis RL, Production of biologically active recombinant human BMP-2 for Tissue Engineering applications, European Society for Artificial Organs Congress (ESAO2005), Bologna, Italy, October 2005, oral

Bessa PC, Pedro AJ, Reis RL and Casal M, Production of recombinant human BMP-2 for bone biomedical applications, Congresso Nacional Micro'05 e Biotec'05, Póvoa de Varzim, Portugal, November 2005, poster

Bessa PC, Pedro AJ, Nobre A, Dung P, Klösch B, Redl H, Casal M and Reis RL, A novel approach for the production of human recombinant BMP-2 for bone tissue engineering applications, 6th European Symposium on Biochemical Engineering Science (ESBES2006), Salzburg, Austria, August 2006, poster

Bessa PC, Pedro AJ, Nobre A, Dung P, Banerje A, Dople D, Klösch B, Redl H, Casal M and Reis RL, Expression, purification and *in vitro* biological activity from human recombinant BMP-2 produced by a novel approach, ESF-EMBO Symposium - Stem Cells in Tissue Engineering: Isolation, Culture, Characterisation and Applications, Sant Feliu de Guixols, Spain, October 2006, poster

Bessa PC, Pedro AJ, Nobre A, Dung P, Banerje A, Dople D, Klösch B, Redl H, Casal M and Reis RL, A novel system for producing human recombinant BMP-2 and study of the growth factor stabilizing conditions, 6th International Conference on Bone Morphogenetic Proteins, Dubrovnik, Croatia, October 2006, poster

Bessa PC, Pedro AJ, Nobre A, Dung P, Banerje A, Dople D, Klösch B, Redl H, Casal M and Reis RL, Expression, purification and *in vitro* biological activity from human recombinant BMP-2 produced by a novel approach, National Congress of Biochemistry, Aveiro, Portugal, December 2006, poster

Bessa PC, Gomes S, Leonor IB, Klösch B, Redl H, Casal M and Reis RL, Natural origin biomimetic scaffolds for the delivery of human bone morphogenetic protein-2 produced by recombinant technology, InVents 4th Marie Curie Cutting Edge Conference (Biocompatibility evaluation and biological behaviour of polymeric biomaterials), Algarve, Portugal, October 2007, oral

Bessa PC, Gomes S, Leonor IB, Klösch B, Redl H, Reis RL and Casal M, Osteoinduction of human fat derived stem cells and murine C2C12 cell line by recombinant human bone morphogenetic protein-2, Congresso Nacional Microbiotec'07, Lisboa, Portugal, December 2007, oral

Balmayor ER, **Bessa PC**, Tuzlakoglu K, Azevedo HS, Casal M and Reis RL, Novel biodegradable polymeric microparticles for the localized delivery of differentiation agents in bone tissue engineering applications, TERMIS-EU 2008 Annual meeting , Porto, Portugal, June 2008, oral

Bessa PC, Balmayor ER, Cerqueira MT , Rada T, Gomes ME, Neves NM, Azevedo HS, Casal M and Reis RL, Silk nanoparticles for delivery of human BMP-2 in bone regenerative medicine applications, TERMIS-EU 2008 Annual meeting, Porto, Portugal, June 2008, oral

Bessa PC, Cerqueira MT, Rada T, Gomes ME, Neves NM, Casal M and Reis RL, Expression, purification and bioactivity of recombinant human bone morphogenetic protein-4, -9, -10, -11 and -14 produced in *Escherichia coli* for Tissue Engineering applications, TERMIS-EU 2008 Annual meeting, Porto, Portugal, June 2008, poster

INTRODUCTION TO THE THESIS FORMAT

This thesis is divided in five sections containing nine different chapters, with five of them being experimental research. The contents of each are summarized bellow.

Section 1 (*Chapter I, II*) presents an extensive overview on the several aspects behind the field of bone morphogenetic proteins and their importance for the research in bone regenerative medicine. Chapter I starts by presenting an historical background on the discovery and main advances with the use of BMPs in the biomedical field, revealing the importance of these growth factors in inducing new bone and cartilage formation. At the same time, the progress with the expression of recombinant BMPs is discussed. Chapter II introduces the emerging challenges of drug delivery and biomaterial science, from bench to clinical approval. It covers the literature with the use of synthetic polymers, natural polymers, microparticle systems, and ceramics for a controlled release of BMPs, and main clinical applications in bone healing. **Section 2** (*Chapter III*) presents in detail the materials and experimental procedures used for cloning, expression, purification and bioactivity characterization of the proposed BMPs, and for the fabrication of a silk fibroin microparticle delivery system. In **Section 3** (*Chapters IV, V*) different studies are described that explore the use of recombinant technology in bacteria for the production of human BMPs and their bioactive potential in selected cell lines and in primary cultures of human adult stem cells. In Chapter IV, a novel methodology was proposed for the production of human recombinant BMP-2 that showed bioactivity in human adult stem cells. In Chapter V the same methodology was used for the production of human BMP-4, -9, -10, -11 and -14. In **Section 4** (*Chapter VI, VII, VIII*) novel particulate-based delivery carriers are proposed for the controlled release of human BMPs. In Chapter VI, the silk microparticles were characterized using SEM, DLS, swelling ability, and the release profile of BMP-2, -9 and -14. In Chapter VII the particles were studied for the bioactivity of released BMP-2, using C2C12 cell line, and a rat ectopic bone formation model. In Chapter VIII, elastin-like nanoparticles were produced by thermoresponsive self-assembly, for a combined delivery of BMP-2 and BMP-14. **Section 5** (*Chapter IX*) contains the general conclusions regarding the overall work carried out under the scope of this thesis, as well as some final remarks and future directions. In the end, Attach I provides supplementary data on the refolding and bioactivity of recombinant BMPs.

Pedras no Caminho?

Guardo todas, um dia vou construir um castelo.

Fernando Pessoa (1888-1935)

SECTION 1

Chapter I

General Introduction

Bone morphogenetic proteins in tissue engineering: the road from the laboratory to the clinic, part I (basic concepts)

This Chapter is based on the following publication:

Bessa PC, Casal M and Reis RL, 2008, Bone morphogenetic proteins in tissue engineering: the road from laboratory to the clinic, part I, basic concepts, Journal of Tissue Engineering and Regenerative Medicine **2**, 1-13

Chapter I

General Introduction

Bone morphogenetic proteins in tissue engineering: the road from the laboratory to the clinic, part I (basic concepts)

Abstract

Discovered in 1965, bone morphogenetic proteins (BMPs) are a group of cytokines from the transforming growth factor-*β* (TGF-β) superfamily with significant roles in bone and cartilage formation. BMPs are used as powerful osteoinductive components of diverse tissue engineering products for the healing of bone. Several BMPs with different physiological roles have been identified in humans. The purpose of this review is to cover the biological function of the main members of BMP family, the latest research on BMPs signaling pathways and advances in the production of recombinant BMPs for tissue engineering purposes.

1. Body morphogenetic proteins

Research on bone regeneration began decades ago as a result of intensive studies on bone growth and healing. Bone has been recognized, among the many tissues in human body, as one with the highest potential for regeneration. As early as 1889 Senn noticed that decalcified bone could induce healing of bone defects (Senn, 1889). Later Lavender provided the first evidence of ectopic bone formation after injecting bone crude extracts into muscle (Levander, 1934, 1938). In 1965 the pioneering work by Urist marked a landmark on the research in bone regeneration. Urist discovered that the active compound responsible for bone regeneration was a mix of proteins and named these as *bone morphogenetic proteins* (BMPs; Urist, 1965). In the years that followed Sampath and Reddi created a crude but highly reproducible bioassay for BMP for ectopic bone formation (Sampath and Reddi, 1981). The assay was based on the activity of the enzyme alkaline phosphatase enzyme and the content of calcium in the newly formed bone. Reddi proposed that BMPs are responsible for the initiation of a cascade of developmental events, in which progenitor cells in the bone marrow were induced by these factors to produce bone cells leading to bone regeneration (Reddi and Huggins, 1972; Reddi, 1981).

During the decades of 80s and 90s the BMP genes were cloned and the recombinant proteins were shown to be biologically potent (Wozney *et al.*, 1988). Much work followed with

the use of recombinant BMPs (rhBMPs) for clinical applications such as spinal fusion, fracture healing and dental tissue engineering (Nakashima and Reddi, 2003; Seeherman and Wozney, 2005). Human BMPs are now produced in larger amounts by recombinant technology. In 2002 FDA gave approval of two products containing rhBMP-2 and rhBMP-7 in absorbable collagen carriers for spinal fusion and long bone non-unions (McKay *et al.*, 2007; White *et al.*, 2007). In a recent review Reddi proposed naming BMPs also as *body morphogenetic proteins*, due to their extensive roles in various tissues and organs beyond the bone (Reddi, 2005).

2. Members of the BMP family

In humans several members are under the designation of BMPs, from BMP-2 to BMP-18 (**Table 1**). BMP-1 is not a member of the BMP family. It is a misidentified protein with chordinase and procollagen proteinase activities, implicated in embryonic patterning (Kessler *et al.*, 1996). In fact, since BMPs were named by homology-based cDNA cloning, there is confusion over BMP designations and there is a need to develop a more appropriate nomenclature for the BMP family.

The biological functions of BMPs are mainly related to bone and cartilage formation (Reddi, 2005), although BMP-8b, -10 and -15 do not have known roles in bone or cartilage. BMP-10 is involved in cardiac development and BMP-15 in ovarian physiology (Chen *et al.*, 2004; Knight and Glister, 2006). BMP-8b is involved in reproductive cells (Zhao *et al.*, 1996). Usually only BMP-2 to BMP- 11 are considered to be BMPs. BMP-12, -13 and -14 are named cartilage-derived morphogenetic proteins (CDMPs), as these induce chondrogenic phenotypes rather than osteogenesis (Reddi, 2003). BMPs are also involved in embryonic patterning (Kishigami and Mishina, 2005), in skeletal formation (Tsumaki and Yoshikawa, 2005) and in organogenesis of other tissues behind bone. For example, BMP-2 plays a role in heart morphogenesis (Callis *et al.*, 2005) and in neural stem cells (White *et al.*, 2001), BMP-7 in kidney formation (Simic and Vukicevic, 2005) and diverse BMPs have unique roles in reproductive organs (Shimasaki *et al.*, 2004; Tsumaki and Yoshikawa, 2005). During the events of early embryogenesis, BMPs are involved in the dorsal–ventral patterning with different roles, e.g. BMP-2 and -4 induce embryo ventral differentiation, while BMP-3 and -3b oppose the ventralizing effect by inducing tail and head formation, respectively (Hino *et al.*, 2004). During gastrulation a BMP gradient in signaling established by BMP antagonists is responsible for directing cells into forming organs such as bone, cartilage, kidney or heart, depending on the levels of BMP activity and of other cytokines (Yamamoto and Oelgeschlager, 2004). The pleiotropic effect of the different BMPs is of important consideration for tissue engineering. For instance, besides being used for

differentiation of cartilage and bone BMP-4 is being studied for a role in keeping the undifferentiated state in embryonic stem cells (Qi *et al.*, 2004). BMPs clearly possess pivotal roles in controlling the proliferation and differentiation fates of cells. In bone formation a clear bone-inducing role is observed for BMP-2, -4, -6, -7 and -9. These BMPs have been shown to induce bone mineralization and increase in osteocalcin levels in C2C12 cells (Chen *et al.*, 2003) and orthotopic ossification in mice (Kang *et al.*, 2004). BMP-3 and -3b are possibly inhibitors or negative regulators of osteogenesis, as these downregulate the expression of ALP in bone cells (Hino *et al.*, 2004). During fracture healing different BMPs follow specific defined temporal sequences. BMP-2 appears to be an early factor peaking at day 1 after fracture while BMP-14 peaks at day 7 during cartilage formation and BMP-3, -4, -7 and -8 are expressed mainly after 2 weeks (Cho *et al.*, 2002). In analogy different BMPs are also expressed in site-specific patterns during the formation of bone (Zoricic *et al.*, 2003).

2.1. Subgroups within the BMP family

BMPs belong to TGF-β superfamily, which includes several other growth factors, such as activins, inhibins or TGF-βs. The members of the BMP family may be subdivided into different subgroups based in their gene homology and similarity in protein structure (Wozney and Rosen, 1998; Kishigami and Mishina, 2005; Reddi, 2005; **see Table 2**). The proteins within the BMP-2/4 group, osteogenic protein-1 (OP-1) group, BMP-9/10 group and BMP-12/13/14 group share sequence similarities of more than 50%. BMP-11 and BMP-15 are more distant members, similar to growth differentiation factors -8 and -9, respectively. Interestingly, the morphogens named as growth and differentiation factors (GDFs) have similarity to some BMPs and could therefore be included in the BMP family. However, these are not described in this review since their biological roles are beyond bone induction, except for GDF-3 a BMP inhibitor, and GDF-8, a negative regulator of bone and muscle mass (Levine and Brivanlou, 2006; Hamrick *et al.*, 2007). Additionally, under the term BMP are BMP-16 to -18. These were given disclosure in patent applications (Celeste and Murray, 1999, 2000). BMP-16 is a human homologue to murine Nodal and BMP-17/18 are related to Lefty. Both have important roles during embryonic patterning, mainly by antagonizing the effect of BMP signaling in mesoderm formation (Nodal) or for the establishment of left-right embryonic asymmetry (Lefty) (Meno *et al.*, 1997; Thisse *et al.*, 2000). Since BMP-16 to -18 are more distantly related to BMPs than to other TGF-β superfamily members these should conceivably form a different group in the TGF-β superfamily, distinct from BMPs.

Table 1. BMP members in humans and their main physiological roles. BMPs known to induce complete bone morphogenesis are underlined.

BMP	Nomenclature	Main physiological roles	References
Bone morphogenetic proteins			
BMP-2	BMP-2a	Cartilage and bone morphogenesis / heart formation	(Wang *et al.*, 1990a; Kang *et al.*, 2004; Callis *et al.*, 2005)
BMP-3	Osteogenin	Negative regulator of bone morphogenesis	(Hino *et al.*, 2004)
BMP-3b	GDF-10	Negative regulator of bone morphogenesis	(Hino *et al.*, 2004)
BMP-4	BMP-2b	Cartilage and bone morphogenesis / kidney formation	(Luyten *et al.*, 1994; Kubler *et al.*, 1998a; Oxburgh *et al.*, 2005)
BMP-5	-	Limb development / Cartilage and bone morphogenesis	(Cho *et al.,* 2002; Zuzarte-Luis *et al.,* 2004 ; Feldman *et al.* 2007; Mailhot *et al.* 2008)
BMP-6	Vrg1, Dvr6	Hypertrophy of cartilage / Bone morphogenesis / estrogen mediation	(Gitelman *et al.,* 1994; Rickard *et al.,* 1998; Kang *et al.,* 2004)
BMP-7	OP-1	Cartilage and bone morphogenesis / kidney formation	(Reddi, 1998; Kang *et al.*, 2004; Simic and Vukicevic, 2005)
BMP-8	OP-2	Bone morphogenesis ? / spermatogenesis	(Ozkaynak *et al.,* 1992; Zhao *et al.,* 1996; Cho *et al.,* 2002)
BMP-9	GDF-2	Bone morphogenesis / Development of cholinergic neurons / glucose metabolism	(Chen *et al.,* 2003; Kang *et al.,* 2004; Lopez-Coviella *et al.,* 2006)
BMP-11	GDF-11	Axial skeleton patterning / eye development / pancreas development / kidney formation	(Esquela and Lee, 2003; Harmon *et al.*, 2004; Kim *et al.*, 2005; Andersson *et al.*, 2006)
Cartilage derived morphogenetic proteins			
BMP-12	CDMP-3, GDF-7	Ligament and tendon development / Development of sensory neurons	(Reddi, 2003; Lo *et al.*, 2005)
BMP-13	CDMP-2, GDF-6	Cartilage development and hypertrophy	(Reddi, 2003)
BMP-14	CDMP-1, GDF-5	Chondrogenesis / Angiogenesis	(Yamashita *et al.*, 1997; Reddi, 2003; Zeng *et al.*, 2007)

Others			
BMP-8b	OP-3	Spertmatogenesis	(Zhao *et al.*, 1996)
BMP-10	-	Heart morphogenesis	(Chen *et al.*, 2004)
BMP-15	GDF-9b	Ovary physiology	(Knight and Glister, 2006)
BMP-16	Nodal	Embryonic patterning	(Celeste and Murray, 1999)
BMP-17	Lefty	Embryonic patterning	(Celeste and Murray, 2000)
BMP-18	Lefty	Embryonic patterning	(Celeste and Murray, 2000)

Table 2. Suggested subgroups within BMP family (grouped by similarity to OP-1)

Subgroup	Members of TGF-β superfamily
OP-1 (BMP-7)	BMP-5, -6, -7, -8, -8b
BMP-2/4	BMP-2, -4
CDMP1/2/3	BMP-12, -13, -14 (GDF-5, 6, 7)
BMP-9/10	BMP-9 (GDF-2), BMP-10
BMP-3/3b	BMP-3, BMP-3b (GDF-10)
BMP-11/GDF-8	BMP-11 (GDF-11), GDF-8
BMP-15/GDF-9	BMP-15 (GDF-9b), GDF-9

3. The structure of BMPs

BMPs as all members of the TGF-β superfamily, are homo or heterodimers linked via disulphide bridges. These proteins are expressed as large precursor polypeptide chains containing a hydrophobic signal sequence, a long and poorly conserved N-terminal pro-region sequence, a mature domain with a highly conserved C-terminal region and an N-terminal region that varies among the different BMPs.

BMPs are biologically active in homodimer and heterodimer conformation (Israel *et al.*, 1996). BMPs form a conserved motif of seven cysteines, which is involved in the formation of six intrachain disulphide bonds and a single interchain bond, necessary to dimer formation. Heterodimers in cell cultures have been observed to induce much higher yields of osteogenic marker alkaline phosphatase (ALP) (Aono *et al.*, 1995) than homodimeric BMP. Moreover, BMP-4/7 heterodimers have also been reported for their very potent mesoderm inducing activity in *Xenopus* (Suzuki *et al.*, 1997). A role has been attributed to heterodimers of BMP-

4/8b in primordial germ cell formation (Ying *et al.*, 2001). In humans, there is evidence that BMP heterodimers may be also involved in specific biological processes (Butler and Dodd, 2003), challenging researchers to look for working with heterodimers besides the widely documented investigation with BMP homodimers.

Intracellularly BMPs are produced as precursors that dissociate after proteolytical cleavage by subtilisin-like proprotein convertases to form mature proteins (Ge *et al.*, 2005). However, in some cases the pro-region remains associated after secretion to the extracellular space, inhibiting the binding of BMPs to cell receptors. Importantly, propeptide forms of mature BMPs have been linked to specific physiological roles, such as in synovial rheumatoid arthritis for proBMP-2 and proBMP-6 (Lories *et al.*, 2007), and in the stabilisation of BMPs in the cases of proBMP-4 (Degnin *et al.*, 2004) and proBMP-9 (Brown *et al.*, 2005). It is possible that the half-life of mature BMPs may be influenced by the identity of their prosequences, and that prodomains serve for other cellular effects (Gregory *et al.*, 2005) which by itself is an important consideration for tissue-engineering approaches involving the use of these morphogens.

3.1. Wrist and knuckle epitopes

During the last years crystallographic studies have provided insights into the structure of BMPs and their interaction with receptors upon binding. Crystallographic studies have been reported for BMP-7 (Griffith *et al.*, 1996), BMP-2 (Scheufler *et al.*, 1999) BMP-9 (Scheufler *et al.*, 1999), BMP-9 (Brown *et al.*, 2005) and BMP-14 (Schreuder *et al.*, 2005). These studies have revealed a common polypeptide core for BMPs and TGF-β. The differences in hydrophobic core amongst these BMPs explain the different affinities for the various cell receptors and possibly for its different physiological roles (Allendorph *et al.*, 2006). In BMP-2 two symmetrical pairs of juxtaposed epitopes were described: the wrist epitope, with affinity to BMP receptor I (BmprI), containing residues from both monomers; and the knuckle epitope, which includes residues from only one monomer, with low affinity for BMP receptor II (BmprII; Nickel *et al.*, 2001). Mutations in epitope II lead to loss of activation of both BMP/Smad pathway and induction of ALP, or even complete inhibition of its function (Kirsch *et al.*, 2000). Variants with antagonistic properties are exclusively generated by mutations in the knuckle epitope of BMP-2. A synthetic knuckle peptide alone was also sufficient to induce ALP, osteocalcin and ectopic bone formation in a rat model (Saito *et al.*, 2003). Alterations in epitope I lead only to a reduction of ALP activity while activation of the BMP–Smad pathway is maintained (Knaus and Sebald, 2001). From these findings it was possible to conclude that the activation of the BMP–Smad pathway and the induction of early osteogenic marker ALP were triggered by distinct

BMP–receptor complexes. Different pathways are probably triggered in consequence to the interaction between the different epitopes of BMPs and cell receptors (Hassel *et al.*, 2003).

3.2. N-terminal of BMP

Another particular feature of the structure of BMP-2 is a heparin-binding domain in the N-terminal region of the mature polypeptide, which modifies its biological activity (Ruppert *et al.*, 1996). Ruppert and colleagues demonstrated that the presence of the N-terminus of BMP-2 reduced its specific activity by interacting with heparinic sites in the extracellular matrix. A variant of recombinant BMP-2 was produced without this domain (EHBMP-2), and biological activity increased five-fold in a limb bud assay when compared to normal BMP-2 and was not affected by the presence of heparin. However, other studies have demonstrated that the presence of heparin binding site increased region increased retention times at the site of injury, and that this was necessary for higher osteoinductive effects (Wurzler *et al.*, 2004). In a recent work a basic core of only three amino acids in the N-terminal region of BMP-4 was demonstrated to be required for its site restriction to the non-neural ectoderm (Ohkawara *et al.*, 2002). The authors suggested that heparan sulphate proteoglycans bind to this basic core and thus play a role in trapping BMP-4. This study was the first to identify a critical domain responsible for the interaction between the BMP and the extracellular environment that restricts its diffusion *in vivo*. Interestingly, heparan sulphates were also observed to be required for BMP-7 signaling (Irie *et al.*, 2003) and recently these have been observed to greatly influence the chondrogenic activity of BMPs (Fisher *et al.*, 2006) and the transcription of several osteogenic genes in response to BMP (Manton *et al.*, 2007). For these reasons heparin has been included in several different tissue engineering constructs using BMPs (Jeon *et al.*, 2007; Lin *et al.*, 2008).

3.3. BMP antagonists

There are diverse BMP-binding proteins that act as modulators of BMP activity or as antagonists, such as Noggin (Zimmerman *et al.*, 1996), Chordin (Blader *et al.*, 1997), Follistatin (Fainsod *et al.*, 1997) and Gremlin (Hsu *et al.*, 1998). These are extracellular regulator proteins that prevent the BMP assembly to cell receptors and in this way modulate the effect of BMP signaling during the formation of tissues. Crystallographic studies showed that the binding of antagonists, such as Noggin, to BMPs inhibited its signaling through blocking the binding of BMP epitopes for type I and type II receptors to which BMPs bind (Groppe *et al.*, 2002). Recently, two new cofactors that regulate BMP signaling, Betaglycan and crypto, were described (Dale *et al.*, 2004). Betaglycan formed a complex with inhibins which binds to activin

type II receptors, thus preventing BMP signaling (Wiater and Vale, 2003). Because of the association of these proteins with various diseases and with additional biological roles, the generation of antagonists of TGF-β superfamily members might generate potent tools for basic research and therapeutic approaches (Gazzerro and Canalis, 2006).

4. BMP signaling – from cell receptor to gene activation

BMPs, and all members of the TGF-β superfamily, bind to serine–threonine kinase receptors on the cell surface, triggering specific intracellular pathways that activate and influence gene transcription, having precise effects in cell proliferation and differentiation (**Figure 1**). There are types I, II and III receptors for TGF-β superfamily members. Only types I and II appear to play significant roles in BMP binding and signaling, both of which are required for signal transduction (Heldin *et al.*, 1997; Shi and Massague, 2003). For the BMP family, significantly more ligands than receptors are known. To the best of our knowledge the main receptors to which most BMPs bind are type I receptors activin receptor Ia (ActR-I or Alk2), BmprIa (Alk3) and BmprIb (Alk6) and the type II receptors BMP receptor II (BmprII), activin type II receptor (ActR-II) and activin type IIB receptor (ActR-IIB) (Derynck and Zhang, 2003). However, type III TGF-β receptors have been shown to serve as cell receptors for BMP signaling, mediating epithelial to mesenchymal cell conversion (Kirkbride *et al.* 2008).

Upon BMP binding low-affinity type II receptors are constitutively activated and type I receptors are activated by the transphosphorylation of the glycine–serine (GS)-rich domain of these receptors (Heldin *et al.*, 1997). Therefore, the specificity of intracellular signals is mainly determined by type I receptors (Miyazono *et al.*, 2005). BMP2-binding to preformed receptor complexes induces the SMAD pathway whereas signaling complexes sequentially assembled by BMP2 result in the activation of p38-mitogen-activated protein kinase (MAPK; Hassel *et al.*, 2003). Different combinations of type I and type II receptors are the key to providing different and specific signals which result in different cell effects (Sebald *et al.*, 2004). In fact, a recent study showed that Alk3 (type Ia) and Alk6 (type Ib) BMP receptors may transmit different signals during the specification and differentiation of mesenchymal lineages (Kaps *et al.*, 2004). BMP-2 and BMP-4 bind preferentially to Alk3 and Alk6, whereas the BMP-7 group binds more to Alk2 and Alk6. BMP-14 (GDF5) binds to Alk6, but not efficiently to other receptors (Miyazono and Miyazawa, 2002), and the same is noted for BMP-15 (Shimasaki *et al.*, 2004; Tsumaki and Yoshikawa, 2005). BMP-13 (GDF6) binds to Alk3 (Kishigami and Mishina, 2005). All these BMPs activate Smad-1, -5 and -8 signaling, whereas for TGF-β, Nodal and activins, Smad-2 and -3 are mainly involved (Shimasaki *et al.*, 2004; Tsumaki and Yoshikawa, 2005). Differently,

BMP-11 binds to Alk4, -5 and -7 to activate Smad-3 signaling (Andersson *et al.*, 2006). It has been shown that BMP-3 binds to Alk4 type I receptor and that it may block BMP signaling by competing with ActR-IIB and reducing Smad-1, -5, -8 or Smad-2, -3 phosphorylation (Gamer *et al.*, 2005). Finally, activin receptor-like kinase 1 (Alk1) was identified as a potential receptor for BMP-9 (Brown *et al.*, 2005) acting through Smad-1 and -5 signaling (Lopez-Coviella *et al.*, 2006). Mutations in the BMP receptors have been described to cause diseases. Mutations in the *BmprII* gene have been found in patients with primary pulmonary hypertension (PPH; Lane *et al.*, 2000); those in the *BmprIA* gene have been found in some patients with juvenile polyposis (Howe *et al.*, 2001). Furthermore, proteomic studies have revealed that the C-terminal tail of BMP receptors type II is also involved in the regulation of cytoskeletal proteins (Hassel *et al.*, 2004). Targeting BMP cell receptors may then be an alternative way to mediate bone-inducing stimuli in tissue-engineering approaches.

4.1. BMP/Smad signaling

Smads are the main signal transducers of serine–threonine receptors (Derynck and Zhang, 2003). Upon BMP binding, type I receptors phosphorylate receptor-regulated Smads (R-Smads). Different R-Smads were identified in mammals: Smad1, Smad5, Smad8 and possibly Smad9 (Xu *et al.*, 2003). Activated RSmads form a complex with common-partner Smad (Co-Smad((Xu *et al.*, 2003)). There is only one described Co-Smad, Smad4. Two phosphorylated R-Smads form a heterotrimeric complex with one Co-Smad, which is translocated into the nucleus and modulates gene transcription with cooperation with other transcription factors (Massague and Wotton, 2000; Derynck and Zhang, 2003; Vincent *et al.*, 2003). All R-Smads are activated by BMP-2 or -4, whereas BMP-6, -7 and -9 only efficiently induce Smad1 and -5 but not Smad8 (Aoki *et al.*, 2001; Brown *et al.*, 2005). Negative regulation of BMP-induced Smad signal transduction is modulated by inhibitory Smads (ISmads). I-Smads act by inhibiting the activation of type I receptors upon BMP binding (Hanyu *et al.*, 2001). Smad6 and -7 act as I-Smads. Smad6 preferentially inhibits BMP signaling while Smad7 inhibits both TGF-β –activin and BMP signaling. I-Smads also interact with R-Smads, preventing the formation of the complex with Smad4 (Murakami *et al.*, 2003) inhibiting the transcription of specific genes (Edlund *et al.*, 2003). BMP signaling is also modulated by ubiquitin-dependent protein degradation. Smad ubiquitin regulatory factors (Smurfs) induce the ubiquitination and degradation of Smads thus controlling the signal of BMP. Smurfs form a complex with inhibitory Smad7, which associates with type I receptors, promoting the ubiquitination and degradation of these receptors (Murakami *et al.*, 2003). Interestingly, Smurfs also enhance the responsiveness to Smad2, which mediates TGF-β signaling and has as opposite effect to that of

BMPs (Zhu *et al.*, 1999; Zhang *et al.*, 2001). The Smad signaling pathway has been also investigated in cancer treatment (Leivonen and Kahari, 2007; ten Dijke and Arthur, 2007; Katoh, 2007). By controlling the different Smad signaling and thus specific cell responses, researchers could in the near future not only achieve a better knowledge of how BMPs but also modulate the subtle biological roles inherent to the diverse TGF-β and BMP members (Schmierer and Hill, 2007).

4.2. BMP/MAPK signaling

Mitogen-activated protein kinase (MAPK) pathways are alternative pathways that are also implicated in the signal transduction of BMPs (Derynck and Zhang, 2003; Massague, 2003). There are three characterized MAPK pathways in mammalian cells: the extracellular signal regulated kinases (ERKs); the c-Jun-NH2-terminal kinases (JNKs); and the p38 MAPK pathways. These pathways are triggered either by cytokines such as BMPs or by environmental stress (Tibbles and Woodgett, 1999). Thus it may be of importance for biomedical purposes that MAPK pathways are considered since these are connected to a wide range of cellular responses. Cooperative interactions have been reported between Smads and transcription factors activated by MAPK pathways. The X-linked inhibitor of apoptosis links the BMP receptor signaling to TGF-β1-activated tyrosine kinase 1 (TAK1) and activates p38 and JNK kinases and nuclear factor-kappaB (NF-*κ*B) (Silverman *et al.*, 2003; Takaesu *et al.*, 2003). In osteoprogenitor cells TAK1 interacts with Smads, thus interfering with the BMP signals and osteogenic differentiation (Hoffmann *et al.*, 2005). MAPK pathways interact with other pathways mediated by different cytokines such as epithelial growth factor (EGF), insulin-like growth factor (IGF) or fibroblast growth factor (FGF) (Massague, 2003). These act by extracellular signal-regulated kinases which inhibit the BMP–Smad signaling through Ras/Raf/Mek (Aubin *et al.*, 2004). It was reported that during embryonic differentiation activation of these pathways inhibit the BMP signaling thus favoring neural differentiation (Pera *et al.*, 2003). It appears that MAPK pathways modulate BMP–Smad signaling through interaction with two conserved globular domains present in Smads, the MH1 and MH2 domains. The MH1 domain is involved in DNA binding and the MH2 domain in binding to cytoplasmic retention factors, activated receptors, nucleoporins in the nuclear pore, and DNA-binding cofactors, coactivators and corepressors in the nucleus (Yamamoto *et al.*, 2003). Recently, it has been shown that MAPK pathways promoted the termination of Smad mediated BMP signaling, in *Xenopus* (Fuentealba *et al.*, 2007). The simultaneously application of BMPs and other cytokines in therapeutical situations may therefore have specific

antagonistic or synergistic effects depending on the interactions occurring between the signaling pathways triggered by each growth factor.

4.3. BMP gene modulation

When translocated to the nucleus, Smads regulate gene transcription by interacting and binding to specific DNA sequences and DNA-binding proteins, such as transcriptional factors (Miyazono *et al.*, 2000). BMP activated Smads bind preferentially to the GCCGnCGC sequence of target genes and only weakly to AGAC or GTCT gene sequences, which are preferentially bound by TGF-β- or activin-activated Smads (Kusanagi *et al.*, 2000). Smads also interact with transcriptional factors and transcriptional coactivators and corepressors.

Runt-related transcription Factor (Runx) is one the most studied transcription factors for BMP signaling, regulating processes such as bone formation and haematopoiesis (Ito and Miyazono, 2003). Three isoforms have been identified in mammals: Runx1, Runx2 (also known as Cbfa1, core binding factor A1) and Runx3. The three are reported to interact with R-Smads. Runx2 cooperatively regulates transcription of genes leading to the differentiation of mesenchymal progenitor cells into osteoblasts (Zhang *et al.*, 2000; Miyazono *et al.*, 2004), and for this reason is widely screened as a marker for commitment of cells into the osteochondral lineage and differentiation into bone. Expression levels of Runx2 are low in mesenchymal cells and are induced upon BMP signaling (Maeda *et al.*, 2004). The induction of Runx2 is mediated by a balance between two transcription factors, Dlx5 andMsx2 that responding to BMP signaling, triggering the activation of Runx2 (Miyama *et al.*, 1999; Lee *et al.*, 2003, 2005). Diverse osteogenic markers are then induced by Runx2, such as ALP, osteocalcin, osteopontin and others (Kumar *et al.*, 2005; Takahashi *et al.*, 2005), which are closely related to the process of endochondral calcification.

Osterix (OSX) is another transcription factor that is mediated by BMP/Smad signals and probably by MAPK signaling and other pathways (Celil *et al.*, 2005). Osterix, together with Runx2, are the most studied transcription factors specific for BMP signaling, involved in the differentiation of mesenchymal stem cells into bone cells (Satija *et al.*, 2007). Smad signaling also interacts with other proteins such as ATF4, TAZ, and NFATc1 transcriptional factors (Deng *et al*, 2008), Hoxc-8 (Shi *et al.*, 1999), MyoD (Liu *et al.*, 2001), OAZ (Hata *et al.*, 2000), Msx1 (Yamamoto *et al.*, 2000), and SIP1 (Verschueren *et al.*, 1999). Menin is another required factor that regulates Runx2-induced transcription of genes during the early commitment phase of osteoblast differentiation (Sowa *et al.*, 2004). Among the several BMP target genes, Id (inhibitor of differentiation or inhibitor of DNA binding) proteins are some of the most important ones (Ogata *et al.*, 1993). Id proteins function as negative regulators of cell

differentiation and as positive regulators of cell proliferation (Yokota, 2001). Recent advances in microarray analysis enable the identification of many BMP target genes in diverse cell types (Clancy *et al.*, 2003; Garcia *et al.*, 2002; Korchynskyi *et al.*, 2003; Kowanetz *et al.*, 2004) and allow a better understanding of the physiological effects of BMPs.

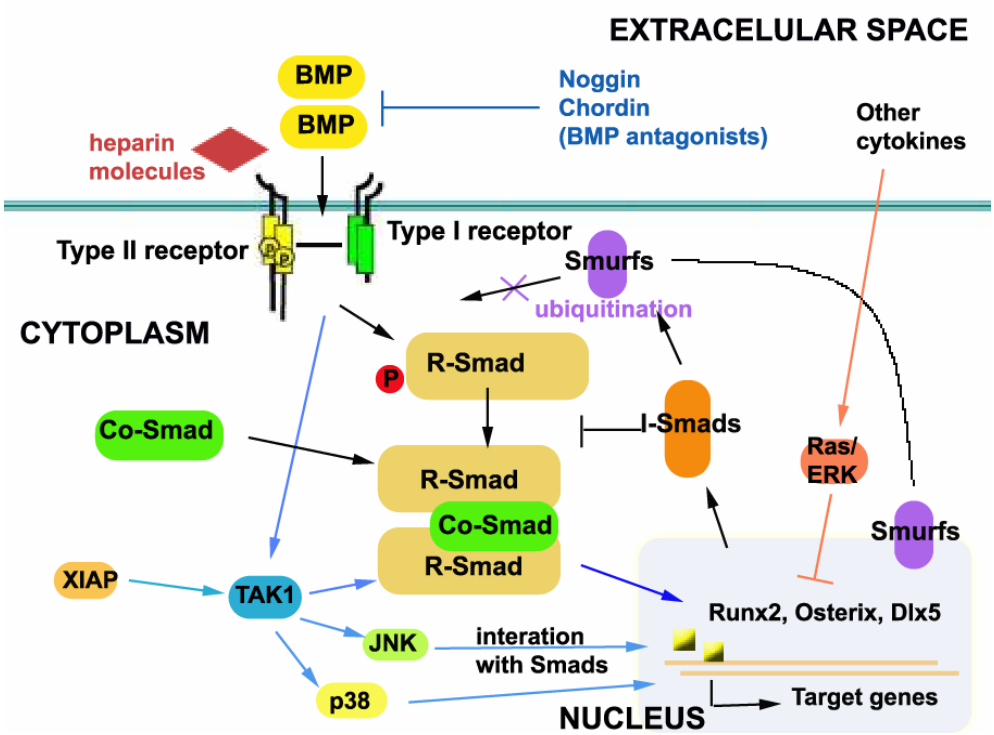

Figure 1. BMP signaling pathways: schematic representation of Smad-dependent and -independent pathways and their main mechanisms of modulation

4.4. Cross-talk with other pathways

BMP signaling is modulated by cross-talk with several other pathways in a very elaborate network of interacting molecules. BMP and TGF-β –activin pathways compete with each other, as they share similar signaling molecules, such as Smad-4 (Candia *et al.*, 1997). Inhibitory Smads are also modulated by several other cytokines and the presence of shear stress in cells (Miyazono *et al.*, 2000). Expression of endogenous TGF-β in preosteoblastic differentiation cells induces I-Smads, which regulate a faster or slower BMP-induced differentiating effect (Maeda *et al.*, 2004). The BMP–Smad pathway was also observed to interact in either synergistic or antagonistic ways with other signaling pathways, such as the Notch pathway (Dahlqvist *et al.*, 2003), the EGF pathway (Kretzschmar *et al.*, 1997), the STAT/LIF pathway (Nakashima *et al.*, 1999), the Wnt pathway (Nishita *et al.*, 2000), IGF and FGF signaling (Pera *et al.*, 2003) and in convergence/antagonistic effect with the MAP kinase pathway (Aubin *et al.*, 2004). MAPK pathway has also been shown to enhance BMP signaling in response to collagen

stimulus through activation of the Ras–ERK pathway (Suzawa *et al.*, 2002). These molecular pathways have been involved in modulating BMP signaling in diverse cellular effects and processes, such as osteoblast maturation (Zamurovic *et al.*, 2004), migration of endothelial cells (Itoh *et al.*, 2004), epithelial-to-mesenchymal cell transition (Zavadil *et al.*, 2004) and inhibition of myogenic differentiation (Dahlqvist *et al.*, 2003).

5. Recombinant BMPs for tissue engineering

After Urist's pioneering experiments in 1965, BMPs were extracted and purified from bone of several different species including rabbit (Urist *et al.*, 1979), cow (Wang *et al.*, 1988) and human (Urist *et al.*, 1983). Isolation of native BMP from bone results in very low yields around 1–2 µg/kg cortical bone. The need for obtaining larger quantities of BMPs for tissue engineering prompted researchers to produce and purify these growth factors by DNA recombinant technology (**Table 3**).

Nowadays, recombinant BMPs are produced mainly by two expression systems: in mammalian cells or in bacteria. With mammalian cells the recombinant protein is obtained active but yields are usually very low. With bacteria the protein is obtained in much larger yields but usually in non-soluble inactive inclusion bodies which are later solubilized and refolded to yield bioactive protein. A common disadvantage is that the protein is not glycosylated as is normal in the human body and thus may present reduced stability or biological activity.

Recombinant human BMP-2 was first obtained in mammalian cell cultures from Chinese hamster ovary (CHO) cells (Wang *et al.*, 1990a). The rhBMP-2 induced ectopic bone and cartilage formation when implanted in rats after 2 weeks. Characterization of rhBMP-2 produced in CHO cells led to the conclusion that the protein was secreted in three forms, a propeptide of 40–45 kDa, a mature homodimer of 30 kDa and a small portion of uncleaved precursor of 60 kDa (Israel *et al.*, 1992). The mature peptide possessed N-glycosylation. Sampath *et al.* confirmed the bioactivity of rhBMP-7 from CHO cells by analysis of bone formation and specific osteogenic markers, such as osteocalcin (Sampath *et al.*, 1992). Koenig *et al.* (1994) noticed a strong tendency of recombinant BMP-2 to adhere non-specifically to culture dishes or to the negatively charged extracellular matrix via its positively charged N-terminal. They modified the BMP by a mild trypsin digestion, removing the first seven to nine residues, and named it digit-removed BMP-2, that still binds to the BMP receptor. Nowadays, commercial recombinant human BMP-2 lack this N-terminal heparin binding end, since the region decreases the specific bioactivity of the BMP (Ruppert *et al.*, 1996).

In 1996, various combinations of rhBMPs were coexpressed in CHO cells to test for possible heterodimers formation (Israel *et al.*, 1996). Transient co-expression between the different rhBMPs resulted in more bioactivity than expression of any single rhBMP. The rhBMP-2/7 heterodimer yielded 20-fold higher activity in the *in vivo* ALP assay. In 1998 Kubler and colleagues produced rhBMP-2 and -4 in *Escherichia coli* and rhBMPs were tested in a collagen carrier and induced bone formation in rats after 4 weeks. Recombinant human BMP-6 was later expressed and purified in *E. coli* (Yang *et al.*, 2003), using pET-15b vector. The protein was obtained in inclusion bodies, refolded and induced ALP activity in C3H10T1/2 cells and other osteogenic markers, as observed by RT–PCR.

During the last years, Vallejo and colleagues reported interesting works regarding the production of rhBMP-2 in inclusion bodies, with optimized protein refolding procedures (Vallejo *et al.*, 2002; Vallejo and Rinas, 2004). The group found that refolding of BMP-2 was particularly sensitive to pH, temperature and concentration, but not so much to ionic strength or redox conditions. The rhBMP-2 was refolded in buffer with L-arginine or CHES at pH 8.5 to a yield of 750 mg dimer per litre of bacteria growing media.

In 2005, mature rhBMP-2, unprocessed rhBMP-2 and propeptide of rhBMP-2 were produced in *E. coli* (Hillger *et al.*, 2005), using a pET-11a expression vector. This group reported bioactivity from both the propeptide and an N-terminal truncated BMP-2 form. Curiously, in 2004, Wurzler and co-workers used mutants of rhBMP-2 with enhanced heparin binding sites (in the N-terminus) and a variant with no heparin binding site. The variant with no binding site showed great reduction in osteoinduction, while the mutants with additional heparin binding sites led to enhanced bone formation, due to longer retention times of the BMP-2 in the extracellular matrix (Wurzler *et al.*, 2004; Depprich *et al.*, 2005). This fact could be of great interest for drug-delivery approaches providing recombinant proteins with increased affinity for binding to the extracellular matrix itself *in vivo*. In 2005, rat BMP-4 has been expressed and purified as inclusion bodies in *Escherichia coli* that are stable in a physiological compatible buffer showing bioactivity in MC3T3-E1 cells (Klösch *et al.*, 2005).

A report on the production of rhBMP-2 was published in 2006, using pET-21a in *E. coli*. The protein, obtained in inclusion bodies, was refolded in different folding buffers (Long *et al.*, 2006). RhBMP-2 was best refolded at low concentrations (0.1 mg/ml), 4 ºC and in the presence of L-arginine. Recently, soluble rhBMP-2 was obtained upon production with the use of pET25b *E. coli* vector. The rhBMP-2 showed bioactivity in primary cultures of human fat-derived stem cells and an increase in levels of osteogenic markers Runx2, Osterix and Smad-1 and -5 in the C2C12 cell line (Bessa *et al.*, 2008).

Table 3. Selected works reporting the production of recombinant BMPs in diverse expression systems.

BMP	Expression system	Novelty	References
BMP2	CHO cells	Bone formation, characterization of expressed BMP-2	(Wang *et al.*, 1990b; Israel *et al.*, 1992)
BMP-2	Insect cells	Alternative expression system	(Maruoka *et al.,* 1995)
BMP2	*E. coli*	The heparin binding domain reduces ALP and specific *in vitro* biological activity	(Ruppert *et al.,* 1996)
BMP2	*E. coli*	High density expression in bacteria	(Li *et al.,* 1998)
BMP2	*E. coli*, pCYTEXP3	Optimization of refolding conditions for BMP-2	(Vallejo *et al.*, 2002; Vallejo and Rinas, 2004)
BMP2	*E. coli*	Additional heparin binding domains enhance *in vivo* bone formation	(Wurzler *et al.,* 2004).
BMP2	*E. coli*, pET-11a	Comparison with BMP-2 propeptide	(Hillger *et al.,* 2005)
BMP2	*E. coli*, pET-21a	Use of different refolding buffers	(Long *et al.,* 2006)
BMP2	*E. coli*, pET-25b	Bioactivity in human stem cells	(Bessa *et al.,* 2007)
BMP4	*E. coli*	Bone formation in mice	(Kubler *et al.*, 1998a)
BMP4	*E. coli*, pET-11a	Stability in physiological buffer	(Klösch *et al.,* 2005)
BMP6	*E. coli,* pET-15b	Induction of several osteogenic markers	(Yang *et al.,* 2003)
BMP7	CHO cells	Bioactivity in rats	(Sampath *et al.,* 1992)
BMP2/7, 4/7	CHO cells	Heterodimer expression	(Israel *et al.,* 1996)

5.1. From manufacture of BMPs to tissue-engineering products

Since their discovery in 1965, BMPs have revealed a promising future in the field of tissue engineering as powerful components of biomedical products for the regeneration of body parts of human patients, namely bone and cartilage. At present, the state of the art of regenerative medicine envisages the use of growth factors, loaded into scaffolding materials and using precursor or stem cells, possibly from the patient him/herself. It is expected that future advances in fundamental biology will allow researchers to design novel tissue engineering strategies that make use of combinations of different BMPs and other growth factors. The use of these growth factor cocktails will certainly present a challenging approach

in tissue engineering since much is still poorly understood about the orchestration of molecular cascades underlying the regeneration of tissues.

Currently, there are two products approved by the Food and Drug Administration (FDA) consisting of recombinant BMP-2 and BMP-7 loaded into absorbable collagen sponges for clinical use for fusion of spinal vertebrae and treatment of long bone fractures (McKay *et al.*, 2007; White *et al.*, 2007). However, a whole set of other less understood BMPs will probably make its way into the clinic, such as with the case of cartilage derived morphogenetic proteins (BMP-12, -13 and -14) for cartilage or tendon reconstruction, or BMP-9 that has stronger osteogenic potencies compared to other BMPs (Kang *et al.* 2004). Recombinant BMPs used in clinics are derived from mammalian expression cells, which elevates much of the cost of clinical products containing rhBMPs. It is expected that advances in recombinant technology namely those involving the large-scale production of BMPs in bacteria will allow researchers to obtain and use these proteins at a much lower cost.

At present, recombinant technology is also a useful tool to achieve molecular modifications of BMPs to improve their bioactivity, stability and affinity to both the tissue-engineering scaffold or the extracellular matrix and cells (see **Table 4**). For example, by adding additional heparin binding domains, there is a significantly different bioactivity and bioavailability of the rhBMP, decreasing its specific activity *in vitro* but increasing bone formation *in vivo* (Depprich *et al.*, 2005). Currently, most recombinant BMP-2 and BMP-7 are produced with no heparin binding domain and thus may present reduced bioactivity when used for clinical uses. Another approach may consist of producing recombinant peptides containing only the binding sites to the cell receptors thus achieving specific biological effects with no problems derived from loss of bioactivity or stability which occur during the incorporation into the scaffold (Suzuki *et al.*, 2000; Saito *et al.*, 2003, 2004, 2005, 2006). Designing chimeric proteins is a further powerful approach which may include the addition of other domains of biological importance such as immune modulatory agents, RGD for increased cell attachment, GFP for *in vivo* localization, or domains for specific binding to biomaterials such as for example to collagen (Han *et al.*, 2002) or to fibrin (Schmoekel *et al.*, 2005). Naturally, the chimeric rhBMPs would have different refolding characteristics as compared to native proteins. These could have altered stability, solubility, surface binding and bioactivity/biospecificity thus making an appealing approach of producing specific tissue target proteins and with increased bioactivity (Oppermann *et al.*, 2005). Chemical modification also improves binding, stability, bioactivity and bioavailability of BMPs (Luginbuehl *et al.*, 2004). Thus, by chemically or recombinantly modifying the isoelectric point of the BMP the affinity of the BMPs to the delivery matrices could be greatly enhanced that allows the achievement of a

desired release profile. Chemically modified rhBMP-2 with enhanced affinity to carriers has been reported by succinylation (Hollinger *et al.*, 1998), acetylation (Uludag *et al.*, 2000) and biotinylation (Uludag *et al.*, 1999b). Finally, the expression of recombinant BMP heterodimers is another way of obtaining these growth factors with much increased bioactivity (Aono *et al.*, 1995; Israel *et al.*, 1996).

Despite being promising recombinant technology is still at as early stage, since there is a need to bypass some fundamental limitations, such as optimizing the stability and bioactivity of recombinant BMPs, obtaining glycosylation patterns identical to that of native BMP, and reducing the possibility of triggering immunogenic responses when used in clinical situations. In the next years, the combination of advances of the BMP field with that of biomaterial science (Mano *et al.*, 2007) will surely herald a revealing future for the use of these morphogens for biomedical and tissue-engineering applications.

Table 4. Chemical or genetic engineering modifications for improving particular characteristics of BMPs for use in tissue engineering applications.

Modification process	Advantages	References
Enzymatic cleavage of BMP heparin binding domain	Reduces non-specific interactions with extracellular matrix, leading to increased bioactivity *in vitro*	(Koenig *et al.,* 1994; Uludag *et al.,* 2001)
Plasmin enzymatic cleavage of BMP	Reduces non-specific interactions with extracellular matrix, leading to increased bioactivity *in vitro*	(Israel *et al.,* 1992; Hollinger *et al.,* 1998)
Adding additional heparin binding domains	Increases retention to extracellular matrix or affinity to biomaterial, leading to increased activity *in vivo*	(Wurzler *et al.,* 2004; Depprich *et al.,* 2005)
Immobilization of synthetic peptides of partial BMP sequences	Improves the stability and specific activity of the BMP and reduces the initial burst release	(Suzuki *et al.*, 2000; Saito *et al.*, 2003, 2004, 2005; Saito *et al.*, 2006; Seol *et al.*, 2006; Bergeron *et al.*, 2007; Park *et al.*, 2007)
Fusion protein BMP with domain to bind a specific biomaterial	Increases the retention of BMP on carrier, accelerating tissue regeneration; increases stability and activity of the BMP	(Han *et al.,* 2002; Schmoekel *et al.,* 2005)
Fusion protein BMP with RGD for enhanced cell attachment or domain for other specific biological function	Enhances attachment of cells, tissue regeneration and possibly the biocompatibility of the material	Not yet reported
Chemical modification of BMP such as with succinylation, acetylation or biotinylation, changes the isoelectric point	Enhances the affinity for binding to the biomaterial by changing the peptide solubility, to suit a desired release profile	(Hollinger *et al.*, 1998; Uludag *et al.*, 1999a; Uludag *et al.*, 1999b; Uludag *et al.*, 2000; Uludag *et al.*, 2001)
Formation of heterodimers between different BMPs	The increased bioactivity of BMP heterodimers leads to lower dose	(Aono *et al.,* 1995; Israel *et al.,* 1996; Zhu *et al.* 2006)

References

Andersson O, Reissmann E, Ibanez CF. 2006; Growth differentiation factor 11 signals through the transforming growth factor-beta receptor ALK5 to regionalize the anterior-posterior axis. EMBO Rep 7: 831-837.

Aoki H, Fujii M, Imamura T, *et al.* 2001; Synergistic effects of different bone morphogenetic protein type I receptors on alkaline phosphatase induction. J Cell Sci 114: 1483-1489.

Aono A, Hazama M, Notoya K, *et al.* 1995; Potent ectopic bone-inducing activity of bone morphogenetic protein-4/7 heterodimer. Biochem Biophys Res Commun 210: 670-677.

Aubin J, Davy A, Soriano P. 2004; *In vivo* convergence of BMP and MAPK signaling pathways: impact of differential Smad1 phosphorylation on development and homeostasis. Genes Dev 18: 1482-1494.

Bergeron E, Marquis ME, Chretien I, *et al.* 2007; Differentiation of preosteoblasts using a delivery system with BMPs and bioactive glass microspheres. J Mater Sci Mater Med 18: 255-263.

Bessa PC, Pedro AJ, Klösch B, *et al.* 2008; Osteoinduction in human fat-derived stem cells by recombinant human bone morphogenetic protein-2 produced in *Escherichia coli*, Biotechnol Lett , 30: 15-21.

Blader P, Rastegar S, Fischer N, *et al.* 1997; Cleavage of the BMP-4 antagonist chordin by zebrafish tolloid. Science 278: 1937-1940.

Brown MA, Zhao Q, Baker KA, *et al.* 2005; Crystal structure of BMP-9 and functional interactions with pro-region and receptors. J Biol Chem 280: 25111-25118.

Butler SJ, Dodd J. 2003; A role for BMP heterodimers in roof plate-mediated repulsion of commissural axons. Neuron 38: 389-401.

Callis TE, Cao D, Wang DZ. 2005; Bone morphogenetic protein signaling modulates myocardin transactivation of cardiac genes. Circ Res 97: 992-1000.

Candia AF, Watabe T, Hawley SH, *et al.* 1997; Cellular interpretation of multiple TGF signals: intracellular antagonism between activin/BVg1 and BMP-2/4 signaling mediated by Smads. Development 124: 4467-4480.

Celeste AJ, Murray BL. 1999; Nucleic acids encoding bone morphogenic protein-16 (BMP-16). US Patent No. 596503.

Celeste AJ, Murray BL. 2000; Bone morphogenetic protein (BMP)-17 and BMP-18 compositions. US Patent No. 6027917.

Celil AB, Hollinger JO, Campbell PG. 2005; Osx transcriptional regulation is mediated by additional pathways to BMP2/Smad signaling. J Cell Biochem 95: 518-528.

Chen C, Grzegorzewski KJ, Barash S, *et al.* 2003; An integrated functional genomics screening program reveals a role for BMP-9 in glucose homeostasis. Nat Biotechnol 21: 294-301.

Chen H, Shi S, Acosta L, *et al.* 2004; BMP10 is essential for maintaining cardiac growth during murine cardiogenesis. Development 131: 2219-2231.

Cho TJ, Gerstenfeld LC, Einhorn TA. 2002; Differential temporal expression of members of the transforming growth factor beta superfamily during murine fracture healing. J Bone Miner Res 17: 513-520.

Clancy BM, Johnson JD, Lambert AJ, *et al.* 2003; A gene expression profile for endochondral bone formation: oligonucleotide microarrays establish novel connections between known genes and BMP-2-induced bone formation in mouse quadriceps. Bone 33: 46-63.

Dahlqvist C, Blokzijl A, Chapman G, *et al.* 2003; Functional Notch signaling is required for BMP4-induced inhibition of myogenic differentiation. Development 130: 6089-6099.

Dale RA, Harrison JS, Redding SW. 2004; Oral complications in cancer chemotherapy, cancer incidence, and mortality in the US. Gen Dent 52: 64-71; quiz, 72.

Degnin C, Jean F, Thomas G, *et al.* 2004; Cleavages within the prodomain direct intracellular trafficking and degradation of mature bone morphogenetic protein-4. Mol Biol Cell 15: 5012-5020.

Depprich R, Handschel J, Sebald W, *et al.* 2005; [Comparison of the osteogenic activity of bone morphogenetic protein (BMP) mutants]. Mund Kiefer Gesichtschir 9: 363-368 [in German].

Derynck R, Zhang YE. 2003; Smad-dependent and Smad-independent pathways in TGF family signalling. Nature 425: 577-584.

Edlund S, Bu S, Schuster N, *et al.* 2003; Transforming growth factor-beta1 (TGF)-induced apoptosis of prostate cancer cells involves Smad7-dependent activation of p38 by TGF-activated kinase 1 and mitogen-activated protein kinase kinase 3. Mol Biol Cell 14: 529-544.

Esquela AF, Lee SJ. 2003; Regulation of metanephric kidney development by growth/differentiation factor 11. Dev Biol 257: 356-370.

Fainsod A, Deissler K, Yelin R, *et al.* 1997; The dorsalizing and neural inducing gene follistatin is an antagonist of BMP-4. Mech Dev 63: 39-50.

Fisher MC, Li Y, Seghatoleslami MR, *et al.* 2006; Heparan sulfate proteoglycans including syndecan-3 modulate BMP activity during limb cartilage differentiation. Matrix Biol 25: 27-39.

Gamer LW, Nove J, Levin M, *et al.* 2005; BMP-3 is a novel inhibitor of both activin and BMP-4 signaling in Xenopus embryos. Dev Biol 285: 156-168.

Ge G, Hopkins DR, Ho WB, *et al.* 2005; GDF11 forms a bone morphogenetic protein 1-activated latent complex that can modulate nerve growth factor-induced differentiation of PC12 cells. Mol Cell Biol 25: 5846-5858.

Gitelman SE, Kobrin MS, Ye JQ, *et al.* 1994; Recombinant Vgr-1/BMP-6-expressing tumors induce fibrosis and endochondral bone formation *in vivo*. J Cell Biol 126: 1595-1609.

Gregory KE, Ono RN, Charbonneau NL, *et al.* 2005; The prodomain of BMP-7 targets the BMP-7 complex to the extracellular matrix. J Biol Chem 280: 27970-27980.

Griffith DL, Keck PC, Sampath TK, *et al.* 1996; Three-dimensional structure of recombinant human osteogenic protein 1: structural paradigm for the transforming growth factor beta superfamily. Proc Natl Acad Sci USA 93: 878-883.

Groppe J, Greenwald J, Wiater E, *et al.* 2002; Structural basis of BMP signalling inhibition by the cystine knot protein Noggin. Nature 420: 636-642.

Hamrick MW, Shi X, Zhang W, *et al.* 2007; Loss of myostatin (GDF8) function increases osteogenic differentiation of bone marrow-derived mesenchymal stem cells but the osteogenic effect is ablated with unloading. Bone 40: 1544-1553.

Han B, Perelman N, Tang B, *et al.* 2002; Collagen-targeted BMP3 fusion proteins arrayed on collagen matrices or porous ceramics impregnated with type I collagen enhance osteogenesis in a rat cranial defect model. J Orthop Res 20: 747-755.

Hanyu A, Ishidou Y, Ebisawa T, *et al.* 2001; The N domain of Smad7 is essential for specific inhibition of transforming growth factor-beta signaling. J Cell Biol 155: 1017-1027.

Harmon EB, Apelqvist AA, Smart NG, *et al.* 2004; GDF11 modulates NGN3+ islet progenitor cell number and promotes cell differentiation in pancreas development. Development 131: 6163-6174.

Hassel S, Eichner A, Yakymovych M, *et al.* 2004; Proteins associated with type II bone morphogenetic protein receptor (BMPR-II) and identified by two-dimensional gel electrophoresis and mass spectrometry. Proteomics 4: 1346-1358.

Hassel S, Schmitt S, Hartung A, *et al.* 2003; Initiation of Smad-dependent and Smad-independent signaling via distinct BMP-receptor complexes. J Bone Joint Surg Am 85A(suppl 3): 44-51.

Hata A, Seoane J, Lagna G, *et al.* 2000; OAZ uses distinct DNA- and protein-binding zinc fingers in separate BMP-Smad and Olf signaling pathways. Cell 100: 229-240.

Heldin CH, Miyazono K, ten Dijke P. 1997; TGF signalling from cell membrane to nucleus through SMAD proteins. Nature 390: 465-471.

Hillger F, Herr G, Rudolph R, *et al.* 2005; Biophysical comparison of BMP-2, ProBMP-2, and the free pro-peptide reveals stabilization of the pro-peptide by the mature growth factor. J Biol Chem 280: 14974-14980.

Hino J, Kangawa K, Matsuo H, *et al.* 2004; Bone morphogenetic protein-3 family members and their biological functions. Front Biosci 9: 1520-1529.

Hoffmann A, Preobrazhenska O, Wodarczyk C, *et al.* 2005; Transforming growth factor-beta-activated kinase-1 (TAK1), a MAP3K, interacts with Smad proteins and interferes with osteogenesis in murine mesenchymal progenitors. J Biol Chem 280: 27271-27283.

Hollinger JO, Uludag H, Winn SR. 1998; Sustained release emphasizing recombinant human bone morphogenetic protein-2. Adv Drug Deliv Rev 31: 303-318.

Howe JR, Bair JL, Sayed MG, *et al.* 2001; Germline mutations of the gene encoding bone morphogenetic protein receptor 1A in juvenile polyposis. Nat Genet 28: 184-187.

Hsu DR, Economides AN, Wang X, *et al.* 1998; The Xenopus dorsalizing factor Gremlin identifies a novel family of secreted proteins that antagonize BMP activities. Mol Cell 1: 673-683.

Irie A, Habuchi H, Kimata K, *et al.* 2003; Heparan sulfate is required for bone morphogenetic protein-7 signaling. Biochem Biophys Res Commun 308: 858-865.

Israel DI, Nove J, Kerns KM, *et al.* 1996; Heterodimeric bone morphogenetic proteins show enhanced activity *in vitro and in vivo*. Growth Factors 13: 291-300.

Israel DI, Nove J, Kerns KM, *et al.* 1992; Expression and characterization of bone morphogenetic protein-2 in Chinese hamster ovary cells. Growth Factors 7: 139-150.

Ito Y, Miyazono K. 2003; RUNX transcription factors as key targets of TGF superfamily signaling. Curr Opin Genet Dev 13: 43-47.

Itoh F, Itoh S, Goumans MJ, *et al.* 2004; Synergy and antagonism between Notch and BMP receptor signaling pathways in endothelial cells. EMBO J 23: 541-551.

Kang Q, Sun MH, Cheng H, *et al.* 2004; Characterization of the distinct orthotopic bone-forming activity of 14 BMPs using recombinant adenovirus-mediated gene delivery. Gene Ther 11: 1312-1320.

Kaps C, Hoffmann A, Zilberman Y, *et al.* 2004; Distinct roles of BMP receptors type IA and IB in osteo-/chondrogenic differentiation in mesenchymal progenitors (C3H10T1/2). Biofactors 20: 71-84.

Kessler E, Takahara K, Biniaminov L, *et al.* 1996; Bone morphogenetic protein-1: the type I procollagen C-proteinase. Science 271: 360-362.

Kim J, Wu HH, Lander AD, *et al.* 2005; GDF11 controls the timing of progenitor cell competence in developing retina. Science 308: 1927-1930.

Kirsch T, Nickel J, Sebald W. 2000; BMP-2 antagonists emerge from alterations in the low-affinity binding epitope for receptor BMPR-II. EMBO J 19: 3314-3324.

Kishigami S, Mishina Y. 2005; BMP signaling and early embryonic patterning. Cytokine Growth Factor Rev 16: 265-278.

Klösch B, Furst W, Kneidinger R, *et al.* 2005; Expression and purification of biologically active rat bone morphogenetic protein-4 produced as inclusion bodies in recombinant *Escherichia coli*. Biotechnol Lett 27: 1559-1564.

Knaus P, Sebald W. 2001; Cooperativity of binding epitopes and receptor chains in the BMP/TGF superfamily. Biol Chem 382: 1189-1195.

Knight PG, Glister C. 2006; TGF superfamily members and ovarian follicle development. Reproduction 132: 191-206.

Koenig BB, Cook JS, Wolsing DH, *et al.* 1994; Characterization and cloning of a receptor for BMP-2 and BMP-4 from NIH 3T3 cells. Mol Cell Biol 14: 5961-5974.

Korchynskyi O, Dechering KJ, Sijbers AM, *et al.* 2003; Gene array analysis of bone morphogenetic protein type I receptor-induced osteoblast differentiation. J Bone Miner Res 18: 1177-1185.

Kowanetz M, Valcourt U, Bergstrom R, *et al.* 2004; Id2 and Id3 define the potency of cell proliferation and differentiation responses to transforming growth factor beta and bone morphogenetic protein. Mol Cell Biol 24: 4241-4254.

Kretzschmar M, Doody J, Massague J. 1997; Opposing BMP and EGF signalling pathways converge on the TGF family mediator Smad1. Nature 389: 618-622.

Kubler NR, Moser M, Berr K, *et al.* 1998a; [Biological activity of *E. coli* expressed BMP-4]. Mund Kiefer Gesichtschir 2(suppl 1): S149-152.

Kubler NR, Reuther JF, Faller G, *et al.* 1998b; Inductive properties of recombinant human BMP-2 produced in a bacterial expression system. Int J Oral Maxillofac Surg 27: 305-309.

Kumar S, Mahendra G, Ponnazhagan S. 2005; Determination of osteoprogenitor-specific promoter activity in mouse mesenchymal stem cells by recombinant adeno-associated virus transduction. Biochim Biophys Acta 1731: 95-103.

Kusanagi K, Inoue H, Ishidou Y, *et al.* 2000; Characterization of a bone morphogenetic protein-responsive Smad-binding element. Mol Biol Cell 11: 555-565.

Lane KB, Machado RD, Pauciulo MW, *et al.* 2000; Heterozygous germline mutations in BMPR2, encoding a TGF receptor, cause familial primary pulmonary hypertension. The International PPH Consortium. Nat Genet 26: 81-84.

Lee MH, Kim YJ, Kim HJ, *et al.* 2003; BMP-2-induced Runx2 expression is mediated by Dlx5, and TGF1 opposes the BMP-2-induced osteoblast differentiation by suppression of Dlx5 expression. J Biol Chem 278: 34387-34394.

Lee MH, Kim YJ, Yoon WJ, *et al.* 2005; Dlx5 specifically regulates Runx2 type II expression by binding to homeodomain-response elements in the Runx2 distal promoter. J Biol Chem 280: 35579-35587.

Levander G. 1934; On the formation of new bone in bone transplantation. Acta Chir Scand 74: 425-426.

Levander G. 1938; A study of bone regeneration. Surg Gynecol Obstet 67: 705-714.

Levine AJ, Brivanlou AH. 2006; GDF3, a BMP inhibitor, regulates cell fate in stem cells and early embryos. Development 133: 209-216.

Li M, Chen C, Pu Q, *et al.* 1998; Production of human recombinant bone morphogenetic protein-2A by high density culture of *Escherichia coli* with stationary dissolved oxygen fed-batch condition. Chin J Biotechnol 14: 157-163.

Liu D, Black BL, Derynck R. 2001; TGF inhibits muscle differentiation through functional repression of myogenic transcription factors by Smad3. Genes Dev 15: 2950-2966.

Lo L, Dormand EL, Anderson DJ. 2005; Late-emigrating neural crest cells in the roof plate are restricted to a sensory fate by GDF7. Proc Natl Acad Sci USA 102: 7192-7197.

Long L, MacLean MR, Jeffery TK, *et al.* 2006; Serotonin increases susceptibility to pulmonary hypertension in BMPR2-deficient mice. Circ Res 98: 818-827.

Lopez-Coviella I, Mellott TM, Kovacheva VP, *et al.* 2006; Developmental pattern of expression of BMP receptors and Smads and activation of Smad1 and Smad5 by BMP9 in mouse basal forebrain. Brain Res 1088: 49-56.

Lories RJ, Derese I, de Bari C, *et al.* 2007; Evidence for uncoupling of inflammation and joint remodeling in a mouse model of spondylarthritis. Arthrit Rheum 56: 489-497.

Luginbuehl V, Meinel L, Merkle HP, *et al.* 2004; Localized delivery of growth factors for bone repair. Eur J Pharm Biopharm 58: 197-208.

Luyten FP, Chen P, Paralkar V, *et al.* 1994; Recombinant bone morphogenetic protein-4, transforming growth factor-beta 1, and activin A enhance the cartilage phenotype of articular chondrocytes *in vitro*. Exp Cell Res 210: 224-229.

Maeda S, Hayashi M, Komiya S, *et al.* 2004; Endogenous TGF signaling suppresses maturation of osteoblastic mesenchymal cells. EMBO J 23: 552-563.

Mano JF, Silva GA, Azevedo HS, *et al.* 2007; Natural origin biodegradable systems in tissue engineering and regenerative medicine: present status and some moving trends. J R Soc Interface 4: 999-1030.

Maruoka Y, Oida S, Iimura T, *et al.* 1995; Production of functional human bone morphogenetic protein-2 using a Baculovirus system. J Dent Res 74: 568-568.

Massague J. 2003; Integration of Smad and MAPK pathways: a link and a linker revisited. Genes Dev 17: 2993-2997.

Massague J, Wotton D. 2000; Transcriptional control by the TGF/Smad signaling system. EMBO J 19: 1745-1754.

Meno C, Ito Y, Saijoh Y, *et al.* 1997; Two closely-related left-right asymmetrically expressed genes, lefty-1 and lefty-2: their distinct expression domains, chromosomal linkage and direct neuralizing activity in Xenopus embryos. Genes Cells 2: 513-524.

Miyama K, Yamada G, Yamamoto TS, *et al.* 1999; A BMP-inducible gene, dlx5, regulates osteoblast differentiation and mesoderm induction. Dev Biol 208: 123-133.

Miyazono K, Maeda S, Imamura T. 2004; Coordinate regulation of cell growth and differentiation by TGF superfamily and Runx proteins. Oncogene 23: 4232-4237.

Miyazono K, Maeda S, Imamura T. 2005; BMP receptor signaling: transcriptional targets, regulation of signals, and signaling cross-talk. Cytokine Growth Factor Rev 16: 251-263.

Miyazono K and Miyazawa K. 2002; Id: a target of BMP signaling. Science signaling , 2002: PE40.

Miyazono K, ten Dijke P, Heldin CH. 2000; TGF signaling by Smad proteins. Adv Immunol 75: 115-157.

Murakami G, Watabe T, Takaoka K, *et al.* 2003; Cooperative inhibition of bone morphogenetic protein signaling by Smurf1 and inhibitory Smads. Mol Biol Cell 14: 2809-2817.

Nakashima K, Yanagisawa M, Arakawa H, *et al.* 1999; Synergistic signaling in fetal brain by STAT3-Smad1 complex bridged by p300. Science 284: 479-482.

Nakashima M, Reddi AH. 2003; The application of bone morphogenetic proteins to dental tissue engineering. Nat Biotechnol 21: 1025-1032.

Nickel J, Dreyer MK, Kirsch T, *et al.* 2001; The crystal structure of the BMP-2:BMPR-IA complex and the generation of BMP-2 antagonists. J Bone Joint Surg Am 83A(suppl 1): S7-14.

Nishita M, Hashimoto MK, Ogata S, *et al.* 2000; Interaction between Wnt and TGF signalling pathways during formation of Spemann's organizer. Nature 403: 781-785.

Ogata T, Wozney JM, Benezra R, *et al.* 1993; Bone morphogenetic protein-2 transiently enhances expression of a gene, Id (inhibitor of differentiation), encoding a helix-loop-helix molecule in osteoblast-like cells. Proc Natl Acad Sci USA 90: 9219-9222.

Ohkawara B, Iemura S, ten Dijke P, *et al.* 2002; Action range of BMP is defined by its N-terminal basic amino acid core. Curr Biol 12: 205-209.

Oppermann H, Tai M, McCartney J. 2005; Modified proteins of the TGF superfamily, including morphogenic proteins/US Patent No. 6846906.

Oxburgh L, Dudley AT, Godin RE, *et al.* 2005; BMP4 substitutes for loss of BMP7 during kidney development. Dev Biol 286: 637-646.

Ozkaynak E, Schnegelsberg PN, Jin DF, *et al.* 1992; Osteogenic protein-2. A new member of the transforming growth factor-beta superfamily expressed early in embryogenesis. J Biol Chem 267: 25220-25227.

Park JB, Lee JY, Park HN, *et al.* 2007; Osteopromotion with synthetic oligopeptide-coated bovine bone mineral *in vivo*. J Periodontol 78: 157-163.

Pera EM, Ikeda A, Eivers E, *et al.* 2003; Integration of IGF, FGF, and anti-BMP signals via Smad1 phosphorylation in neural induction. Genes Dev 17: 3023-3028.

Qi X, Li TG, Hao J, *et al.* 2004; BMP4 supports self-renewal of embryonic stem cells by inhibiting mitogen-activated protein kinase pathways. Proc Natl Acad Sci USA 101: 6027-6032.

Reddi AH. 1981; Cell biology and biochemistry of endochondral bone development. Coll Relat Res 1: 209-226.

Reddi AH. 1998; Cartilage-derived morphogenetic proteins and cartilage morphogenesis. Microsc Res Technol 43: 131-136.

Reddi AH. 2003; Cartilage morphogenetic proteins: role in joint development, homoeostasis, and regeneration. Ann Rheum Dis 62(suppl 2): ii73-78.

Reddi AH. 2005; BMPs: from bone morphogenetic proteins to body morphogenetic proteins. Cytokine Growth Factor Rev 16: 249-250.

Reddi AH, Huggins C. 1972; Biochemical sequences in the transformation of normal fibroblasts in adolescent rats. Proc Natl Acad Sci USA 69: 1601-1605.

Rickard DJ, Hofbauer LC, Bonde SK, *et al.* 1998; Bone morphogenetic protein-6 production in human osteoblastic cell lines. Selective regulation by oestrogen. J Clin Invest 101: 413-422.

Ruppert R, Hoffmann E, Sebald W. 1996; Human bone morphogenetic protein 2 contains a heparin-binding site which modifies its biological activity. Eur J Biochem 237: 295-302.

Saito A, Suzuki Y, Kitamura M, *et al.* 2006; Repair of 20 mm long rabbit radial bone defects using BMP-derived peptide combined with an -tricalcium phosphate scaffold. J Biomed Mater Res A 77: 700-706.

Saito A, Suzuki Y, Ogata S, *et al.* 2003; Activation of osteo-progenitor cells by a novel synthetic peptide derived from the bone morphogenetic protein-2 knuckle epitope. Biochim Biophys Acta 1651: 60-67.

Saito A, Suzuki Y, Ogata S, *et al.* 2004; Prolonged ectopic calcification induced by BMP-2-derived synthetic peptide. J Biomed Mater Res A 70: 115-121.

Saito A, Suzuki Y, Ogata S, *et al.* 2005; Accelerated bone repair with the use of a synthetic BMP-2-derived peptide and bone-marrow stromal cells. J Biomed Mater Res A 72: 77-82.

Sampath TK, Maliakal JC, Hauschka PV, *et al.* 1992; Recombinant human osteogenic protein-1 (hOP-1) induces new bone formation *in vivo* with a specific activity comparable with natural bovine osteogenic protein and stimulates osteoblast proliferation and differentiation *in vitro*. J Biol Chem 267: 20352-20362.

Sampath TK, Reddi AH. 1981; Dissociative extraction and reconstitution of extracellular matrix components involved in local bone differentiation. Proc Natl Acad Sci USA 78: 7599-7603.

Satija NK, Gurudutta GU, Sharma S, *et al.* 2007; Mesenchymal stem cells: molecular targets for tissue engineering. Stem Cells Dev 16: 7-23.

Scheufler C, Sebald W, Hulsmeyer M. 1999; Crystal structure of human bone morphogenetic protein-2 at 2.7 A resolution. J Mol Biol 287: 103-115.

Schmoekel HG, Weber FE, Schense JC, *et al.* 2005; Bone repair with a form of BMP-2 engineered for incorporation into fibrin cell ingrowth matrices. Biotechnol Bioeng 89: 253-262.

Schreuder H, Liesum A, Pohl J, *et al.* 2005; Crystal structure of recombinant human growth and differentiation factor 5: evidence for interaction of the type I and type II receptor-binding sites. Biochem Biophys Res Commun 329: 1076-1086.

Sebald W, Nickel J, Zhang JL, *et al.* 2004; Molecular recognition in bone morphogenetic protein (BMP)/receptor interaction. Biol Chem 385: 697-710.

Seeherman H, Wozney JM. 2005; Delivery of bone morphogenetic proteins for orthopedic tissue regeneration. Cytokine Growth Factor Rev 16: 329-345.

Senn N. 1889; On the healing of aseptic bone cavities by implantation of antiseptic decalcified bone. Am J Med Sci 98: 219-243.

Seol YJ, Park YJ, Lee SC, *et al.* 2006; Enhanced osteogenic promotion around dental implants with synthetic binding motif mimicking bone morphogenetic protein (BMP)-2. J Biomed Mater Res A 77: 599-607.

Shi X, Yang X, Chen D, *et al.* 1999; Smad1 interacts with homeobox DNA-binding proteins in bone morphogenetic protein signaling. J Biol Chem 274: 13711-13717.

Shi Y, Massague J. 2003; Mechanisms of TGF signaling from cell membrane to the nucleus. Cell 113: 685-700.

Shimasaki S, Moore RK, Otsuka F, *et al.* 2004; The bone morphogenetic protein system in mammalian reproduction. Endocr Rev 25: 72-101.

Silverman N, Zhou R, Erlich RL, *et al.* 2003; Immune activation of NF-B and JNK requires Drosophila TAK1. J Biol Chem 278: 48928-48934.

Simic P, Vukicevic S. 2005; Bone morphogenetic proteins in development and homeostasis of kidney. Cytokine Growth Factor Rev 16: 299-308.

Sowa H, Kaji H, Hendy GN, *et al.* 2004; Menin is required for bone morphogenetic protein 2- and transforming growth factor beta-regulated osteoblastic differentiation through interaction with Smads and Runx2. J Biol Chem 279: 40267-40275.

Suzawa M, Tamura Y, Fukumoto S, *et al.* 2002; Stimulation of Smad1 transcriptional activity by Ras-extracellular signal-regulated kinase pathway: a possible mechanism for collagen-dependent osteoblastic differentiation. J Bone Miner Res 17: 240-248.

Suzuki A, Kaneko E, Maeda J, *et al.* 1997; Mesoderm induction by BMP-4 and -7 heterodimers. Biochem Biophys Res Commun 232: 153-156.

Suzuki Y, Tanihara M, Suzuki K, *et al.* 2000; Alginate hydrogel linked with synthetic oligopeptide derived from BMP-2 allows ectopic osteoinduction *in vivo*. J Biomed Mater Res 50: 405-409.

Takaesu G, Surabhi RM, Park KJ, *et al.* 2003; TAK1 is critical for IB kinase-mediated activation of the NF-B pathway. J Mol Biol 326: 105-115.

Takahashi T, Kato S, Suzuki N, *et al.* 2005; Autoregulatory mechanism of Runx2 through the expression of transcription factors and bone matrix proteins in multipotential mesenchymal cell line, ROB-C26. J Oral Sci 47: 199-207.

Thisse B, Wright CV, Thisse C. 2000; Activin- and Nodal-related factors control antero-posterior patterning of the zebrafish embryo. Nature 403: 425-428.

Tibbles LA, Woodgett JR. 1999; The stress-activated protein kinase pathways. Cell Mol Life Sci 55: 1230-1254.

Tsumaki N, Yoshikawa H. 2005; The role of bone morphogenetic proteins in endochondral bone formation. Cytokine Growth Factor Rev 16: 279-285.

Uludag H, D'Augusta D, Golden J, *et al.* 2000; Implantation of recombinant human bone morphogenetic proteins with biomaterial carriers: a correlation between protein pharmacokinetics and osteoinduction in the rat ectopic model. J Biomed Mater Res 50: 227-238.

Uludag H, Friess W, Williams D, *et al.* 1999a; rhBMP-collagen sponges as osteoinductive devices: effects of *in vitro* sponge characteristics and protein pI on *in vivo* rhBMP pharmacokinetics. Ann N Y Acad Sci 875: 369-378.

Uludag H, Gao T, Porter TJ, *et al.* 2001; Delivery systems for BMPs: factors contributing to protein retention at an application site. J Bone Joint Surg Am 83-A(suppl 1): S128-135.

Uludag H, Golden J, Palmer R, *et al.* 1999b; Biotinated bone morphogenetic protein-2: *in vivo* and *in vitro* activity. Biotechnol Bioeng 65: 668-672.

Urist MR. 1965; Bone: formation by autoinduction. Science 150: 893-899.

Urist MR, Mikulski A, Lietze A. 1979; Solubilized and insolubilized bone morphogenetic protein. Proc Natl Acad Sci USA 76: 1828-1832.

Urist MR, Sato K, *et al.* 1983; Human bone morphogenetic protein (hBMP). Proc Soc Exp Biol Med 173: 194-199.

Vallejo LF, Brokelmann M, Marten S, *et al.* 2002; Renaturation and purification of bone morphogenetic protein-2 produced as inclusion bodies in high-cell-density cultures of recombinant *Escherichia coli*. J Biotechnol 94: 185-194.

Vallejo LF, Rinas U. 2004; Optimized procedure for renaturation of recombinant human bone morphogenetic protein-2 at high protein concentration. Biotechnol Bioeng 85: 601-609.

Verschueren K, Remacle JE, Collart C, *et al.* 1999; SIP1, a novel zinc finger/homeodomain repressor, interacts with Smad proteins and binds to 5-CACCT sequences in candidate target genes. J Biol Chem 274: 20489-20498.

Vincent SD, Dunn NR, Hayashi S, *et al.* 2003; Cell fate decisions within the mouse organizer are governed by graded Nodal signals. Genes Dev 17: 1646-1662.

Wang EA, Rosen V, Cordes P, *et al.* 1988; Purification and characterization of other distinct bone-inducing factors. Proc Natl Acad Sci USA 85: 9484-9488.

Wang EA, Rosen V, D'Alessandro JS, *et al.* 1990a; Recombinant human bone morphogenetic protein induces bone formation. Proc Natl Acad Sci USA 87: 2220-2224.

Wang EA, Rosen V, Dalessandro JS, *et al.* 1990b; Recombinant human bone morphogenetic protein induces bone formation. Proc Natl Acad Sci USA 87: 2220-2224.

White PM, Morrison SJ, Orimoto K, *et al.* 2001; Neural crest stem cells undergo cell-intrinsic developmental changes in sensitivity to instructive differentiation signals. Neuron 29: 57-71.

Wiater E, Vale W. 2003; Inhibin is an antagonist of bone morphogenetic protein signaling. J Biol Chem 278: 7934-7941.

Wozney JM and Rosen V. 1998; Bone morphogenetic protein and bone morphogenetic protein gene family in bone formation and repair, Clin Orthop Relat Res , 346: 26-37.

Wozney JM, Rosen V, Celeste AJ, *et al.* 1988; Novel regulators of bone formation: molecular clones and activities. Science 242: 1528-1534.

Wurzler KK, Emmert J, Eichelsbacher F, *et al.* 2004; [Evaluation of the osteoinductive potential of genetically modified BMP-2 variants]. Mund Kiefer Gesichtschir 8: 83-92 [in German].

Xu XL, Dai KR, Tang TT. 2003; [The role of Smads and related transcription factors in the signal transduction of bone morphogenetic protein inducing bone formation]. Zhongguo Xiu Fu Chong Jian Wai Ke Za Zhi 17: 359-362 [in Chinese].

Yamamoto M, Takahashi Y, Tabata Y. 2003; Controlled release by biodegradable hydrogyels enhances the ectopic bone formation of bone morphogenetic protein. Biomaterials 24: 4375-4383.

Yamamoto TS, Takagi C, Ueno N. 2000; Requirement of Xmsx-1 in the BMP-triggered ventralization of Xenopus embryos. Mech Dev 91: 131-141.

Yamamoto Y, Oelgeschlager M. 2004; Regulation of bone morphogenetic proteins in early embryonic development. Naturwissenschaften 91: 519-534.

Yamashita H, Shimizu A, Kato M, *et al.* 1997; Growth/differentiation factor-5 induces angiogenesis *in vivo*. Exp Cell Res 235: 218-226.

Yang JH, Zhao L, Yang S, *et al.* 2003; [Expression of recombinant human BMP-6 in *Escherichia coli* and its purification and bioassay *in vitro*]. Sheng Wu Gong Cheng Xue Bao 19: 556-560 [in Chinese].

Ying Y, Qi X, Zhao GQ. 2001; Induction of primordial germ cells from murine epiblasts by synergistic action of BMP4 and BMP8B signaling pathways. Proc Natl Acad Sci USA 98: 7858-7862.

Yokota Y. 2001; Id and development. Oncogene 20: 8290-8298.

Zamurovic N, Cappellen D, Rohner D, *et al.* 2004; Coordinated activation of notch, Wnt, and transforming growth factor-beta signaling pathways in bone morphogenic protein 2-induced osteogenesis. Notch target gene Hey1 inhibits mineralization and Runx2 transcriptional activity. J Biol Chem 279: 37704-37715.

Zavadil J, Cermak L, Soto-Nieves N, *et al.* 2004; Integration of TGF/Smad and Jagged1/Notch signalling in epithelial-to-mesenchymal transition. EMBO J 23: 1155-1165.

Zeng Q, Li X, Beck G, *et al.* 2007; Growth and differentiation factor-5 (GDF-5) stimulates osteogenic differentiation and increases vascular endothelial growth factor (VEGF) levels in fat-derived stromal cells *in vitro*. Bone 40: 374-381.

Zhang Y, Chang C, Gehling DJ, *et al.* 2001; Regulation of Smad degradation and activity by Smurf2, an E3 ubiquitin ligase. Proc Natl Acad Sci USA 98: 974-979.

Zhang YW, Yasui N, Ito K, *et al.* 2000; A RUNX2/PEBP2 A/CBFA1 mutation displaying impaired transactivation and Smad interaction in cleidocranial dysplasia. Proc Natl Acad Sci USA 97: 10549-10554.

Zhao GQ, Deng K, Labosky PA, *et al.* 1996; The gene encoding bone morphogenetic protein 8B is required for the initiation and maintenance of spermatogenesis in the mouse. Genes Dev 10: 1657-1669.

Zhu H, Kavsak P, Abdollah S, *et al.* 1999; A SMAD ubiquitin ligase targets the BMP pathway and affects embryonic pattern formation. Nature 400: 687-693.

Zimmerman LB, De Jesus-Escobar JM, Harland RM. 1996; The Spemann organizer signal noggin binds and inactivates bone morphogenetic protein 4. Cell 86: 599-606.

Zoricic S, Maric I, Bobinac D, *et al.* 2003; Expression of bone morphogenetic proteins and cartilage-derived morphogenetic proteins during osteophyte formation in humans. J Anat 202: 269-277.

Zuzarte-Luis V, Montero JA, Rodriguez-Leon J, *et al.* 2004; A new role for BMP5 during limb development acting through the synergic activation of Smad and MAPK pathways. Dev Biol 272: 39-52.

Chapter II

General Introduction

Bone morphogenetic proteins in tissue engineering: the road from the laboratory to the clinic, part II (BMP delivery)

This Chapter is based on the following publication:

Bessa PC, Casal M and Reis RL, 2008, Bone morphogenetic proteins in tissue engineering: the road from laboratory to the clinic, part II, BMP delivery, Journal of Tissue Engineering and Regenerative Medicine **2**, 81-96.

Chapter II

General Introduction

Bone morphogenetic proteins in tissue engineering: the road from the laboratory to the clinic, part II (BMP delivery)

Abstract

Bone morphogenetic proteins (BMPs) are cytokines with a strong effect on bone and cartilage growth and with important roles during embryonic patterning and early skeletal forming. BMPs have promising potential for clinical bone and cartilage repair, working as powerful bone-inducing components in diverse tissue engineering products. Synthetic polymers, natural origin polymers, inorganic materials and composites may be used as carriers for delivery of BMPs. Carriers range from nanoparticles to complex 3D scaffolds, membranes for tissue-guided regeneration, biomimetic surfaces and smart thermo-sensitive hydrogels. Current clinical uses include spinal fusion, healing of long bone defects, craniofacial and periodontal applications, amongst others. BMP-2 and BMP-7 have recently received approval by Food and Drug Administration (FDA) for specific clinical cases, delivered in absorbable collagen sponges. Considering the expanding number of publications in the field of BMPs, there are prospects of a brilliant future in the field of regenerative medicine of bone and cartilage with the use of BMPs.

1. Introduction

Every year millions of surgical operations are performed for the healing or repair of an organ. In the past two decades, tissue engineering has emerged as a very promising alternative that circumvents several of the limitations of the existing options of autografting and allografting for the treatment of a malfunctioning or lost body part. Tissue engineering combines precursor cells from the patient with scaffolding matrices and the stimulus of growth factors. Since the advent of tissue engineering, bone has received particular interest since it is one of the tissues with most regenerative abilities in the human body.

Bone morphogenetic proteins (BMPs) are probably the most important growth factors in bone formation and healing (Reddi, 1998, 2005). These cytokines have been extensively studied during the past decades and, nowadays, recombinant human BMPs (rhBMPs) are widely used several tissue engineering products that might serve for the complete

regeneration of bone or cartilage. Current applications include loaded rhBMPs in delivery systems made of synthetic or natural polymers and the differentiation of transplanted stem cells from the patient with rhBMPs for later body implantation. The purpose of this review is to cover the latest developments in the research for a BMP delivery carrier involving the use of biomaterials science, particularly with the use of natural origin polymers, to the recent preclinical trials and approved products for clinical applications.

2. Delivering BMPs

2.1. BMP carriers– from bench to clinical approval

The main role of a delivery system for BMPs is to retain these growth factors at the site of injury for a prolonged time frame, providing an initial support for cells to attach and form regenerated tissue (Seeherman and Wozney, 2005). The carrier should provoke optimal inflammatory responses, be biodegradable to allow the formation of an interface with the surrounding biological tissue or complete biodegradability for complete invasion of healed tissues, it should present adequate porosity to allow the infiltration of cells and formation of blood vessels at the new bone. Furthermore, the carrier should protect the BMPs from degradation and maintain its bioactivity whilst releasing the protein on a time and space-controlled way for promoting the formation of new bone at the treatment site. Finally, carriers should be conveniently sterilized, easy to handle, stable over time with well-defined storage procedures, as well as suitable for commercial production, allowing scale-up production and approval by regulatory agencies. Having in consideration, the type of tissue to be regenerated is also of critical importance as different mechanical requirements differ for repair of bone, cartilage or tendon. For example, bone carriers are simplified by the fact that, upon fracture, bone is immobilized but carriers should allow vascular ingrowth due to the highly vascularised nature of bone. In cartilage, defects are subject to high compressive and shear stresses thus making healing more challenging. In tendon the regenerative ability appears to be intermediate to those of bone and cartilage, so tendons are very difficult to immobilize, needing a carrier that is able to withstand considerable tensile forces. The geometry of the carrier also affects significantly the biophysical process of osteoinduction and capillary penetration (Jin *et al.,* 2000). All this in consideration, a research may have to keep in mind that the carrier is evidently aimed for common usage by surgeons and physicians.

2.2. BMP retention at the orthopedic site

The delivery of BMP shall last for a sufficient period of time to induce a specific amount of bone mass to treat the defect. Retention of BMP at the orthopedic site of injury is affected by many parameters such as interaction between the biomaterial and the BMP, influence of pH, temperature, porosity, influence of salts, concentration. Evidently, retention of the growth factor depends on whether the BMP is immobilized on the carrier during its manufacture or absorbed into the surface of the device.

Immobilization of the BMPs in a delivery system may be performed by different methodologies: via adsorption, entrapment or immobilization or by covalent binding (Luginbuehl *et al.*, 2004). In case of adsorption, impregnation of the delivery matrix with the BMP is simpler but conformational changes might occur and the release of the protein is less sustained. Furthermore, delivery by adsorbed growth factors often results in initial burst release. With entrapment methodology, hydrophobic polymeric matrices are well known and described to immobilize and release bioactive agents over extended period of times (Langer and Folkman, 1976). However, difficulty arises over the fact that during processing of certain materials into carriers, pH conditions or temperature conditions often result in denaturation of the protein. Much research nowadays aims to develop specific methods of producing delivery carriers for BMPs that do not cause their loss of activity. Lastly, the BMP may become immobilized by covalent binding to the carrier. This may be performed by production of a fusion BMP protein with a domain of specific binding to a biomaterial (Suzuki *et al.,* 2000). In this regard, recombinant technology offers great versatility for expression of a BMP capable of binding to most natural polymers. Other interesting approaches include exploring the strong affinity of BMPs to the extracellular matrix heparan sulfate/heparin proteoglycans (Blanquaert *et al.,* 1999), ion-complexation by binding to charged polymers such as the cases of chitosan, alginate, hyaluronans or synthetic polyelectrolytes (Yamamoto *et al.,* 1998) and crystallization of growth factors (Jen *et al.,* 2002).

2.3. Pharmacokinetic profiles of released BMP

It is crucial to consider that release may preferably be sustained over time. Extremes in release profiles such as long low-amount release of BMP or initial burst of BMP are known for not being beneficial to bone healing. A delicate balance in concentration of BMPs helps to prevent either insufficient binding to carrier due to low concentration or to precipitation due to high BMP concentration. The time of release may be dependent on the type of fracture or the application in question. It is clear that there is more than one desirable pharmacokinetic profile. The pharmacokinetic profile varies according to the material in consideration, its

formulation, and the type and amount of BMP in use. By chemical modification of the carrier or the BMP, we may achieve a specific release profile, which is of interest since different BMPs may present different release profiles due to their different amino acid sequence, different species have different optimal release profiles (Li and Wozney, 2001) and chances are that the optimal profile may be also site-specific. Depending on the site of injury or on a particular application, various formulations of delivery systems may be designed, from simple nano/microparticles to scaffolds of increased 3D complexicity, such as those that mimic the physical properties of the extracellular matrix or hydrogels that respond to physiological shifts such as pH or temperature.

3. Carriers for BMPs

3.1. Synthetic biodegradable polymers

Synthetic polymers have been widely used in tissue engineering applications (Saito and Takaoka, 2003) (**Table 1**). Initially, poly(lactic acid) (PLA) was investigated as a carrier for BMP delivery (Miyamoto *et al.,* 1992) but the material was considered ineffective due the release of acidic degradation sub-products. However, novel biodegradable synthetic polymers have attracted attention since these are free of the risk of disease transmission that occurs with other materials used for bone applications such as collagen. Biodegradable polymers like polylactic acid p-dioxanone polyethylene glycol (PLA-DX-PEG) allow percutaneous injection after heating, for use as a scaffold and a delivery carrier for BMPs, due to its versatile temperature-dependent liquid–semisolid transition. This plasticity allows synchronizing the biodegradation of the polymer with the induction of new bone by BMP (Saito *et al.,* 2001) and this type of injectable polymeric delivery system, polymerizing *in situ*, enables a less invasive approach to bone surgeries (Saito *et al.*, 2003b). These scaffolds were tested, as carriers for BMPs, in a variety of models, such as a canine spinal fusion model and in the formation of artificial joint (Saito *et al.*, 2005b), for long bone defects in rabbits (Yoneda *et al.,* 2005) and in dogs (Murakami *et al.,* 2003), and in healing of rat cranial defects (Suzuki *et al.,* 2006). These works showed that PLA-DX-PEG delivered rhBMP-2 successfully, inducing the repair of bone defects several weeks after implantation. In other reports, composites of PLA-DX-PEG with calcium phosphate were shown to require less rhBMP to induce new bone formation in mice (Matsushita *et al.,* 2004) and in healing femur defects of rabbits (Matsushita *et al.,* 2006). Composites of PLA-PEG with hydroxyapatite were also evaluated for articular cartilage repair in rabbits (Tamai *et al.,* 2005) and in a rabbit radii model (Kaito *et al.*, 2005), showing enhanced tissue repair in the animals treated with rhBMP-2 and hydroxyapatite composites.

Poly (lactic-co-glycolic acid) (PLGA) combines the adsorptive stability of PLA with the mechanical strength of polyglycolic acid (PGA) and has received particular attention (Winet and Hollinger, 1993). Biodegradation of the synthetic composite is achieved by varying the proportion of each of the two component materials (Miller *et al.,* 1977; Grayson *et al.,* 2004). PLGA as a carrier for rhBMP-2 delivery was reported in alveolar cleft repair on dogs (Mayer *et al.,* 1996), in gelatin sponge composites in a rabbit ulna model (Kokubo *et al.,* 2003) and in tooth defects of dogs (Kawamoto *et al.,* 2003), and in combination with bone marrow cells in a rabbit segmental bone defect model (Hu *et al.,* 2005). These studies confirm the good results that are usually obtained with PLGA scaffolds; bone formation was observed successfully when the scaffolds delivered rhBMP, as compared to controls. The dosage of rhBMP was also observed to significant affect the repair of bone defects. Recently, PLGA scaffolds have been also tested in rats (Shimazu *et al.,* 2006), a canine model (Jones *et al.,* 2006) and sheep (Zheng *et al.,* 2006), showing that delivered BMP induced much higher bone formation than the scaffold alone, over the several weeks following implantation. Another report, which involved a PLGA scaffold conjugated to heparin, showed that a much longer sustained release of rhBMP-2 and significantly increased *in vivo* new formation of bone were achieved (Jeon *et al.*, 2007), indicating the promising potential that heparin has as a stabilizing agent for BMP bioactivity.

Synthetic polymers have been also formulated as hydrogels for delivery of BMPs. Since hydrogels contain large amounts of water, they are interesting devices for the delivery of therapeutic proteins. Lutolf and colleagues reported using synthetic PEG-based hydrogels that mimic the invasive characteristics of extracellular matrices, with integrin-binding sites for cell attachment and substrates for matrix metalloproteinases (Lutolf *et al.*, 2003a; Lutolf *et al.*, 2003b), in a rat model, for rhBMP-2 delivery. The authors demonstrated that cells were able to fully penetrate the hydrogels and bone tissue was formed within 3-4 weeks in the gels that delivered rhBMP-2. Similarly, PEG-based hydrogels were reported by Pratt and co-workers showing that cells were able to fully invade the gel networks that were conjugated with peptides that mimic characteristics from extracellular matrix such as plasmin and a heparin molecule to improve the rhBMP-2 stability (Pratt *et al.,* 2004). In another work, Fisher and colleagues evaluated thermoreversible hydrogels of poly(propylene fumarate-co-ethylene glycol), that mimicked properties of cartilage matrix hydrophilic proteoglycans, for cartilage tissue engineering, using rhBMP-7 (Fisher *et al.*, 2004). The solutions of this polymer were aqueous at 25 ºC but readily polymerized into gel above 35 ºC. The group proposed the use of these hydrogels for articular cartilage repair. Identically, Gao and Uludag also reported using rhBMP-2 in N-isopropylacrylamide-based thermoreversible hydrogels in a rat model (Gao and

Uludag, 2001). The authors studied the effect of different hydrogel compositions on the *in vivo* retention of rhBMP and conclude that these polymers were much versatile for delivering proteins such as BMPs in more effective and controlled ways. A major disadvantage of the use of synthetic polymers is the risk of inflammatory response due to acidic sub-products of degradation (Winet and Hollinger, 1993), which may be also detrimental to the stability of the incorporated BMPs. This has lead researchers to look forward to other materials such as collagen and other natural polymers, as alternatives for BMP delivery.

Table 1. Synthetic-polymer-based matrices/scaffolds for drug delivery of BMPs for tissue engineering applications.

Polymer(s)/Carrier/ scaffold structure	Formulation	Biological model	References
PLA	Scaffolds	Rabbit ulna	(He *et al.,* 2003)
	Scaffolds	*In vitro* differentiation of chondrocytes	(Yang *et al.,* 2006)
	Scaffolds	Rat ectopic bone formation	(Chang *et al.,* 2007)
PLA-collagen	Membrane	Rabbit ectopic bone formation	(Tian *et al.,* 2004)
PLA-collagen-HA	Composites	Radius defects in dogs	(Hu *et al.,* 2003)
	Composites	Mice ectopic bone formation	(Zhang *et al.,* 2005)
PLA-PEG-HA	Composites	Rabbit radius model	(Kaito *et al.,* 2005)
	Composites	Articular cartilage repair rabbits	(Tamai *et al.,* 2005)
PLA-DX-PEG	Scaffolds	Femoral canine model	(Murakami *et al.,* 2003)
	Scaffolds	Rat cranial defects	(Suzuki *et al.,* 2006)
	Scaffolds	Mice ectopic bone formation	(Kato *et al.*, 2006)
PLA-DX-PEG-CaP	Composites	Ectopic bone formation in mice	(Matsushita *et al.,* 2004)
	Composites	Spinal fusion in rabbits	(Namikawa *et al.,* 2005)
	Composites	Femur defects in rabbits	(Yoneda *et al.,* 2005)
	Composites	Femur defects in rabbits	(Matsushita *et al.,* 2006)

PGA	Membrane	Periodontal repair in dogs	(Wikesjo *et al.,* 2003)
	Scaffolds	*In vitro* cartilage formation	(Blunk *et al.,* 2003)
	Scaffolds	Cervical spinal fusion in goats	(Lippman *et al.,* 2004)
PLGA	Scaffolds	Alveolar cleft repair in dogs	(Mayer *et al.,* 1996)
	Scaffolds	Rabbit radius defects	(Hu *et al.,* 2005)
	Scaffolds	Alveolar ridge defects in rats	(Shimazu *et al.,* 2006)
	Scaffolds	Canine mandible defects	(Jones *et al.,* 2006)
	Scaffolds	Reconstruction of orbital floor defects in sheep	(Zheng *et al.,* 2006)
PLGA-heparin	Composite	Rat ectopic model	(Jeon *et al.,* 2007)
PLGA-gelatin	Composites	Rabbit ulna defects	(Kokubo *et al.,* 2003)
	Composites	Tooth defects in dogs	(Kawamoto *et al.,* 2003)
	Composites	Tibia defects in dogs	(Kokubo *et al.,* 2004)
PEG-based	Hydrogels	Rat cranial defects	(Lutolf *et al.*, 2003a; Lutolf *et al.*, 2003b)
PEG-based, heparin	Hydrogels	Rat critical size calvarial defects	(Pratt *et al.,* 2004)
PEG-based	Hydrogels	Rat critical size calvarial defects	(Rizzi *et al.*, 2006)
Polypropylene fumarate	Hydrogels	Proliferation of chondrocytes	(Fisher *et al.,* 2004)
Isopropylacrylamide	Hydrogels	Ectopic bone formation	(Gao and Uludag, 2001)

3.2. Collagen

Collagen is the major non-mineral component of bone and also the most abundant protein in connective tissues of mammals. Collagen has received lots of attention due to having good biocompatibility, degrading into physiological compatible products and being suitable for interaction with cells and other macromolecules. The large variety of collagen formulations includes collagen gels, demineralized bone matrix, fibril collagen, collagen strips, membranes, absorbable collagen sponges and composites (Kirker-Head, 2000; Geiger *et al.*, 2003). Another advantage is that collagen can be processed in aqueous form. Collagen has also a favorable influence on cell infiltration and wound healing. During the last years, most researchers have

focused on the use of absorbable collagen sponges although several other formulations have been investigated (Kirker-Head, 2000). Collagen sponges are very versatile, easily manipulated and wettable. Manufacture of collagen sponge carrier depends in several factors that include sponge mass, cross-linking methods, sterilization methods, soaking time, protein concentration and buffer composition (Geiger *et al.,* 2003). These steps impact the interaction of the BMP with the collagen carrier and therefore the profile and the efficacy of released protein. For collagen sponges, binding of rhBMP is highly dependent on the pH. Studies using modified versions of recombinant BMP led to conclude that modification of the isoelectric point could bring up to 100-fold differences in the retention of protein to the collagen carrier (Uludag *et al.*, 1999b). Binding of rhBMP-2 is therefore dependable on the isoelectric point of the two proteins and other factors such as ionic strength. Collagen sponges have since then been tested and evaluated in several animal models and clinical trials for cases of fracture repair, critical size defects, spinal fusion and dental and craniofacial reconstruction (Geiger *et al.,* 2003). The collagen sponge consists of lyophilized rhBMP which is reconstituted with water prior to injection and impregnates the collagen sponge for several minutes before implantation. Two models using collagen sponges delivering recombinant human BMP-2 or BMP-7 were approved by FDA for human use as an alternative to bone grafts, for spinal fusion and long bone fractures, after many pre-clinical trials that have been recently reviewed (Gautschi *et al.,* 2007). The collagen sponge holds the BMP and releases it just in the local environment where the surgery was performed, eliminating the need to harvest autologous bone which causes post-operative pain. Based on the extensive preclinical and clinical trials, the use of collagen sponges delivering BMPs has revealed to be a safer and superior alternative to autogenous bone graft. However, although showing success, collagen sponges pose risks of immunogenic reactions since the collagen used on these applications is derived from animal tissues, creating concerns on the risks of transmission of infectious agents and of immunological reactions. For this reason, the development of a superior carrier material for BMP delivery based on other natural polymers is currently being investigated. Alternatively, other sources of collagen, namely from recombinant origin, provides means of obtaining reliable and chemically defined sources of purified human collagens that are free of animal components (Yang *et al.,* 2004).

3.3. Natural origin polymers

The materials for tissue engineering applications should ideally mimic the natural environment of tissues and, in this regard, natural polymers can send signals to guide cells at the various stages of their development and thus accelerate healing (Mano and Reis, 2007).

There are several natural polymers that may be used as carriers for BMP delivery. These may include collagen, starch-based polymers, chitin and chitosan, hyaluronans, alginate, silk, agarose, soy and algae derived materials, and poly(hydroxyalkanoates) (Mano *et al.*, 2007) (**Table 2**). Several of these polymers are derived from occurring substances in bone, cartilage or in the extracellular matrix. For this reason, these materials often present excellent properties for use in regenerative medicine applications, such as being biodegradable, bioresorbable and versatile, as these may be processed into different formulations (Malafaya *et al.*, 2003; Gomes *et al.*, 2004). Natural polymers may present risks of immunogenic reactions and disease transmission, and disadvantages such as the sourcing and processing of the materials. Nevertheless, researchers have been looking for materials from plant origin and produced by microorganisms and/or from recombinant technology which may overcome these concerns.

Alginate is a generally safe polysaccharide, known to support the proliferation of chondrocytes *in vitro* (Park *et al.*, 2005b) Very interesting work has been developed by Saito and colleagues with small synthetic peptides corresponding to BMP-2 regions binding to cell receptors, incorporated in cross-linked alginate gels, showing *in vitro* osteogenic differentiation and success in repairing bone defects in rats (Saito *et al.*, 2003a, 2004, 2005a) and in rabbit radial bone defects (Saito *et al.,* 2006). The use of alginate seems to be particularly appealing for cartilage tissue engineering applications since alginate is a major component of cartilage tissue. Alginate hydrogels were also reported for delivery of rhBMP-2 in rats (Simmons *et al.,* 2004) with use of bone marrow cells with RGD peptide for improving cell adhesion.

Chitosan is another natural degradable polymer, obtained by alkaline deacetylation of chitin, extracted from the exoskeletons of arthoropods. Chitosan has been formulated in many forms, such as hydrogels (Baran *et al.,* 2004) and fiber meshes (Tuzlakoglu *et al.,* 2004), that showed potential for use in osteochondral tissue engineering, making it suitable for BMP delivery (Prabaharan and Mano, 2005). Several works have reported the use of chitosan for delivering BMPs, particularly in composites with synthetic polymers or with other natural polymers. A chitosan-alginate composite gel, loaded with mesenchymal stem cells and rhBMP-2, was evaluated as an injectable tissue engineering construct in mice and induced new trabecular bone formation over a period of 12 weeks (Park *et al.*, 2005a). Liang and colleagues described a chitosan-gelatin scaffold with incorporated rhBMP-2 (Liang *et al.,* 2005) which demonstrated increased expression of bone-marker osteocalcin in osteoblast and myoblast cell lines. In another report, a chitosan blend with PGA was studied as a novel delivery carrier for rhBMP-2 (Hsieh *et al.,* 2006). Derivates of chitosan are also reported. Chemical

modifications of chitosan may enhance certain bioactive properties and increase its solubility in water, thus aiding in the incorporation of rhBMPs, such as in the case of carboxymethyl chitosan. Mattioli-Belmonte and co-workers reported the use of N,N-dicarboxymethyl chitosan, with delivery of rhBMP, for enhancing cell proliferation and healing in articular cartilage lesions (Mattioli-Belmonte *et al.*, 1999a). Recently, rhBMP-2 was immobilized directly on a guided bone-regenerative membrane surface made of chitosan nanofibers that functioned as a bioactive surface to enhance bone-healing (Park *et al.,* 2006). The BMP-2 conjugated membrane surface retained bioactivity for up to 4 weeks of incubation, as well as holding over 50% of the initial BMP-2 attached, promoting cell attachment, proliferation, ALP activity and calcification, when compared with BMP-2 absorbed to the membrane. In two other works, dextran/gelatin based microspheres, containing rhBMP-2, were adhered to chitosan films for guided-tissue regeneration (Chen *et al.*, 2005a) and chitosan membranes activated with BMP-2 were also reported to successfully differentiate C2C12 cells (Lopez-Lacomba *et al.*, 2006b).

Fibrin is derived from blood cots and can be formulated into an adhesive glue-like delivery system (Hattori, 1990). Fibrin has been used as a delivery system for BMPs in a variety of animal models, that includes the use of a fibrin-fibronectin sealing system for rat calvarial defects as a carrier for rhBMP-4 (Han *et al.,* 2005) and for rhBMP-2 (Hong *et al.,* 2006), and a fibrin sealant with rhBMP-2 in the healing of dental pulp of dogs (Ren *et al.,* 2000). In these reports, bone formation was much higher when the fibrin carrier was loaded with the rhBMP, as compared to controls. Fibrin glue might be also a great aid in limiting the diffusion of BMPs into surrounding tissues which could cause undesirable biological effects. In a rat spinal model, fibrin glue significantly limited the diffusion of rhBMP-2 that was loaded into a collagen sponge, preventing the BMP from inducing bone growth in the surrounding spinal cord and nerves (Patel *et al.*, 2006a). Interesting research has been developed by the group of Hubbell with the use of fibrin matrices for the delivery of rhBMPs (Schmoekel *et al.*, 2004; Schmoekel *et al.*, 2005a; Schmoekel *et al.*, 2005b). The group studied the influence of a non-glycosylated form of rhBMP-2 (Schmoekel *et al.,* 2004) in fibrin. Since non-glycosylated rhBMP-2 is less soluble, retention into the fibrin scaffold was enhanced. The fibrin matrices were used to treat critical-size defects and non-unions in rats, dogs and cats. In these studies, bridging of bone defects showed more successful percentages of tissue healing when compared to controls. The group has also reported the use of a fusion BMP protein with an affinity domain to fibrin to increase binding to the carrier (Schmoekel *et al.*, 2005b). Recently, a work using fibrin constructs to deliver rhBMP-2, vascular endothelial growth factor (VEGF) and fibroblast growth factor-2 (FGF-2), combined with hyaluronic acid or collagen, dramatically improved the ability

of blood vessels to directly invade the fibrin-based scaffolds (Smith *et al.,* 2007). Finally, a human trial was reported showing partial reconstruction of a frontal bone defect using heparin together with bovine collagen, hyaluronic acid, and fibrin as vehicles for rhBMP-2 (Arnander *et al.,* 2006). Altogether, fibrin glue certainly seems to be a very useful addition to a bone tissue engineering scaffold using BMPs, having in consideration that aids in promoting osteoinduction (Schwarz *et al.*, 1993) and retention of growth factors (Hubbell, 2006).

Hyaluronans are present in extracellular matrix and can be formulated into gels, sponges and pads. Hyaluronans have been used in a variety of trials as a delivery vehicle for rhBMPs including in sponge form in the treatment of alveolar ridge defects in dogs (Hunt *et al.,* 2001), periodontal repair in dogs (Wikesjo *et al.,* 2003), in tibial defects of rabbits (Eckardt *et al.,* 2005), in sheep in combination with hydroxyapatite (Aebli *et al.,* 2005), in the healing of critical size defect in rats in composites with polylactic acid (Vogelin *et al.,* 2005) and in gel and paste forms in non human primates (Seeherman *et al.,* 2004). Kim and Valentini evaluated the kinetics of hyaluronic acid as a delivery system for rhBMP-2 *in vitro* and demonstrated that hyaluronans-based carriers retained more BMP than collagen gels (Kim and Valentini, 2002). In two other studies, hyaluronic acid was used to deliver BMPS for treating mandibular defects of rats (Arosarena and Collins, 2005a; Arosarena and Collins, 2005b). Significantly more bone was formed in presence of rhBMP-2 and, although not significant, the volumes of new bone were larger for the hyaluronic acid carrier. Recently, a acrylated hyaluronic acid hydrogel was used with human mesenchymal stem cells and rhBMP-2, for healing of rat calvarial defects (Kim *et al.,* 2007). Higher levels of osteocalcin expression and bone formation occurred when the BMP-2 and stem cells were tested. Diverse hydrogel formulations of hyaluronic acid were also evaluated by Bulppit and Aeschlimann, showing excellent cell infiltration and osteochondral differentiation when loaded with BMP-2, in combination with either insulin growth factor-1 or transforming growth factor beta, implanted into rats (Bulpitt and Aeschlimann, 1999). Hyaluronans are observed to interfere positively with BMP cascade (Zou *et al.*, 2004) and since these are part of the extracellular matrix, these may well be priority choices as scaffolds for delivery of BMPs in regenerative medicine of bone.

Gelatin has been used mostly in form of hydrogels for delivery of BMPs. Gelatin is an irreversibly hydrolyzed form derived from collagen that is usually cross-linked or hardened through thermal treatment to reduce its high water solubility and enhance the retention of protein to achieve a long-term release. Gelatin hydrogels delivering rhBMP-2 were studied in rabbit skulls (Hong *et al.,* 1998), in mice (Yamamoto *et al.*, 2003b) and recently in skull of non-human primates (Takahashi *et al.,* 2007). Gelatin hydrogels delivering rhBMP-2 were observed to show higher levels of ALP and osteocalcin in comparison with rhBMP-2 delivered

in collagen sponges (Yamamoto *et al.*, 2003a). Recently, thermomechanical hydrogels based on methacrylated dextran in combination with gelatin have been reported by Chen and colleagues (Chen *et al.*, 2007a; Chen *et al.*, 2007b). The group used rhBMP-2 encapsulated in microspheres of same materials, loaded into the hydrogels, which delivered the growth factor over a period of 18 to 28 days. Their work will be discussed later on the section referring to nanoparticles.

Dextran is another natural polysaccharide, synthesized by some bacteria, that has attracted attention for use as a BMP delivery system, because of its excellent hydrophilic nature and biocompatibility. Dextran has been particularly used in form of nanospheres for delivery of rhBMPs that will be detailed in a later chapter. Dextran hydrogels has been evaluated for rhBMP-2 delivery both *in vitro* and *in vivo*, in a rat ectopic model, showing formation of new bone (Maire *et al.,* 2005). The possibility of using natural polymers for designing intelligent hydrogel systems for BMP delivery, is also an interesting and very attractive option. However, no studies have been reported with the use of these systems.

Starch based polymers are another interesting alternative for delivering BMPs, that was proposed by Reis as materials with high potential for tissue engineering of bone and cartilage due to their interesting mechanical properties (Malafaya *et al.,* 2001; Elvira *et al.,* 2002). These starch based polymers are used in composites with different synthetic polymers and have been formulated into a variety of forms such as hydrogels (Pereira *et al.,* 1998), nanofibbers (Tuzlakoglu *et al.,* 2005), microparticles (Silva *et al.*, 2004b), or 3D scaffolds (Gomes *et al.,* 2002). The wide variety of formulations and compositions make these polymers suitable scaffolds for bone tissue engineering and controlled release of BMPs. In general, composites of natural polymers with synthetic polymers may become the future option of choice for tissue engineering of bone, since these combine the own specificities of synthetic and natural polymers to produce superior materials.

Silk fibroin is a protein derived from cocoons made by the larvae of silkworms. Silk has been proposed and widely investigated as a delivery carrier for BMPs in some contributions reported by the group of Kaplan. In one work, rhBMP-2 was directly immobilized on silk fibroin films and the effect of the delivery system studied in human bone marrow stromal cells and in critical sized cranial defects in mice (Karageorgiou *et al.,* 2004). The rhBMP retained its biological activity. In another report, silk scaffolds fibers, prepared by electrospining, were used to deliver rhBMP-2 and hydroxyapatite nanoparticles, for *in vitro* bone formation (Li *et al.,* 2006). The rhBMP-2 survived the aqueous-based electrospinning process in bioactive form and induced osteogenesis in cultures of human mesenchymal stem cells. The group also tested BMP-2 delivered via silk fibroin scaffolds in critical size defects in mice (Karageorgiou *et al.,*

2006). In both works, the delivered rhBMP-2 increased levels of ALP activity, calcium deposition, and transcript levels for bone sialoprotein, osteopontin, osteocalcin, and runx2. In the last years, Meinel and co-workers evaluated the use of silk for tissue engineering constructs with silk-RGD covalently bound matrices, in human mesenchymal cells (Meinel *et al.,* 2004) but not with use of BMPs. In 2006, Meinel and colleagues tested human stem cells loaded in silk fibroin scaffolds, in combination with rhBMP-2, and compared stem cells transfected with BMP-2 via an adenovirus with exogenous protein (Meinel *et al.,* 2006). The expression of osteogenic markers was induced but the BMP was not studied when delivered directly on the silk scaffolds. Recently, rhBMP-2 delivered via silk fibroin scaffolds, in combination with human mesenchymal stem cells, was reported with promising results, in the healing of critical size defects of femurs in rats (Kirker-Head *et al.*, 2007). Compared with other protein-based materials such as collagen, silks have distinguishable mechanical properties, presenting slower degradation times thus allowing adequate time for proper bone remodelling. For this reason, silk is a feasible and potential option as a carrier for controlled delivery of BMPs and, in general, for generating diverse bone tissue engineering constructs for clinical applications (Meinel *et al.*, 2005). Other possible sources of natural polymers for BMP delivery include soy, casein, polyhydroxyalkanoate, polyhydroxybutyrate, corals, carrageenan, gellan gum, agarose and other fibrous proteins such as keratin and elastin (Kirker-Head *et al.*, 2007)

Table 2. Natural origin polymer based matrices for delivery of BMPs for tissue engineering applications. Please refer to Table 3 for micro and nanoparticles formulations.

Polymer(s)/Carrier	Formulation	Biological model	References
Alginate	Hydrogels	Ectopic bone formation in mice	(Simmons *et al.,* 2004)
	Gels, synthetic BMP-2 oligopeptides	Ectopic bone formation and tibial defects in rats	(Suzuki *et al.*, 2000; Saito *et al.*, 2003a, 2004, 2005a)
	Gels	Rabbit radial bone defects	(Saito *et al.,* 2006)
Carboxymethylchitosan	-	*In vivo* cartilage formation	(Mattioli-Belmonte *et al.*, 1999b)
Chitosan	Nanofibre membranes	Differentiation of osteoblast cells	(Park *et al.,* 2006)
	Chitosan films	Differentiation of C2C12 cell line	(Lopez-Lacomba *et al.*, 2006a)
Chitosan-alginate	Gels	Trabecular bone formation in mice	(Park *et al.*, 2005a)
Chitosan-gelatin	Composites	Differentiation of osteoblasts/myoblasts	(Liang *et al.,* 2005)
Chitosan-PGA	Composites	*	(Hsieh *et al.,* 2006)
Dextran	Hydrogels	Rat ectopic model	(Maire *et al.,* 2005)
Fibrin	Sealant	Dental pulp of dogs	(Ren *et al.,* 2000)
	Gels	Rats, rabbits, dogs and cats; different types of bone defects	(Schmoekel *et al.*, 2004; Schmoekel *et al.*, 2005a; Schmoekel *et al.*, 2005b)
	Sealant	Rat calvarial defects	(Han *et al.,* 2005)
	Sealant in PCL scaffolds	*	(Rai *et al.,* 2005)
	Sealant	Ectopic bone formation in mice	(Zhu *et al.*, 2006a; Zhu *et al.*, 2006b)
	-	Humans, frontal bone defect	(Arnander *et al.,* 2006)
	Sealant	Differentiation of rabbit bone marrow cells	(Cui *et al.,* 2007)

Fibrin-CaP	Sealant	Rat calvarial defects	(Hong *et al.,* 2006)
Fibrin-collagen	Sealant in collagen sponge	Rat spinal model	(Patel *et al.*, 2006b)
Gelatin	Hydrogels	Rabbit skull defects	(Hong *et al.,* 1998)
	Hydrogels	Ectopic bone formation in mice	(Yamamoto *et al.*, 2001; Yamamoto *et al.*, 2003b)
	Hydrogels	Critical size defects in rabbit ulnas	(Yamamoto *et al.,* 2006)
	Hydrogels	Skull; non-human primates	(Takahashi *et al.,* 2007)
Gelatin/dextran	Hydrogels	Differentiation oh human periodontal ligament cells	(Chen *et al.*, 2007a; Chen *et al.*, 2007b)
Hyaluronic acid	Hydrogels	Ectopic bone formation in rats	(Bulpitt and Aeschlimann, 1999)
	Sponges	Alveolar ridge defects in dogs	(Hunt *et al.,* 2001)
	Scaffolds	Differentiation of CH3H10T1/2 cells	(Kim and Valentini, 2002)
	-	Periodontal repair in dogs	(Wikesjo *et al.,* 2003)
	Gels	Osteotomy in non-human primates	(Seeherman *et al.,* 2004)
	Gels	Non-union tibial defects in rabbits	(Eckardt *et al.,* 2005)
	Sponges	Rat mandibular defects	(Arosarena and Collins, 2005a; Arosarena and Collins, 2005b)
Hyaluronan acrylated	Hydrogels	Rat calvarial defects	(Kim *et al.,* 2007)
Hyaluronic acid- Ti	Composites	Cranial defects in rats	(Itoh *et al.,* 2001)
Hyaluronic acid- HA	Scaffolds	Osteointegration in cancellous bone in sheeps	(Aebli *et al.,* 2005)
Hyaluronic acid- PLA	Composites	Critical size defect in rat femurs	(Vogelin *et al.,* 2005)
Silk Fibroin	Films	Cranial defects in mice	(Karageorgiou *et al.,* 2004)
	Scaffolds, loaded with human stem cells	Cranial defects in mice	(Karageorgiou *et al.,* 2006)

Electrospun nanofibers	Differentiation of human bone marrow cells	(Li *et al.,* 2006)
Scaffolds, loaded with human stem cells	Critical size femur defects in rats	(Kirker-Head *et al.*, 2007)

* These studies involved solely material testing and delivery kinetics, with no *in vitro* or *in vivo* bioactivity models

3.4. Ceramics

Many studies dedicated to the understanding of the processes of bone mineralization and it was concluded that ceramic materials such as hydroxyapatite (HA) and other types of calcium phosphates can promote, when implanted, the formation of a bone-like mineral surface layer that leads to increased interface between the materials and the surrounding bone. Calcium phosphate for tissue engineering of bone include use of calcium phosphate layers, films or coatings to promote bone ingrowth, and use of calcium phosphate fillers to replace fractured or damaged bone. Hydroxyapatite (HA) is a form of calcium phosphate mineral that comprises seventy percent of bone and can be formulated as powder, granule, disk or block (Tsuruga *et al.,* 1997). However, for bone tissue engineering applications, specific formulations work better than others, dependant on the geometric structure of the carrier (Kuboki *et al.*, 1998). Hydroxyapatite is a fairly osteoconductive material, and has been used for BMP delivery alone (Noshi *et al.*, 2001) or in composites with natural or with synthetic polymers as previously detailed. Hydroxyapatite has been used in combination with collagen for rabbit spinal fusion (Kraiwattanapong *et al.*, 2005), with natural origin polymers (Aebli *et al.*, 2005), with tricalcium phosphate in a rabbit calvarial model delivering rhBMP-2 (Schopper *et al.*, 2007), for differentiating mesenchymal stem cells with BMP-14/GDF-5 (Shimaoka *et al.*, 2004), or for lumbar spinal fusion in non-human primates (Boden *et al.,* 1999). Based on these and other works, hydroxyapatite has proven to be a suitable carrier for BMP delivery, not only enhancing the delivery of the growth factor but also in aiding its retention to the carrier and the osteoconductivity of the scaffold (Uludag *et al.*, 1999a).

Calcium phosphates for delivery of BMPs include calcium phosphates cements and ceramics and calcium phosphate coatings. Calcium phosphate (Ca-P) cements have been extensively investigated as these are osteoconductive, biocompatible and show fast deposition of new bone at the cement surface (Driessens *et al.,* 1998). The BMP may be incorporated into low temperature Ca-P cements by adding the protein in lyophilized form or in aqueous phase

prior to formation of cement without any risk of denaturation of the growth factor. In high temperature cements, the BMP is generally only adsorbed onto the surface. Porous structure can be fabricated to mimic the structure of trabecular bone (Dutta Roy *et al.,* 2003). Trials for rhBMP-2 delivery have included studies in rabbit ulnas (He *et al.*, 2003) and femurs (Cao *et al.,* 2006), and a canine tibial defect model (Edwards *et al.,* 2004). These studies have demonstrated that the use of Ca-P cements accelerates bone healing. Trials are have also demonstrated the efficacy of calcium phosphate matrices in some non-human primates trials, such as in alveolar ridge surgery using a composite of Ca-P, hydroxyapatite and a collagen sponge (Miranda *et al.,* 2005), in osteotomy sites with a single percutaneous injection of rhBMP-2 loaded into Ca-P cements (Seeherman *et al.*, 2006a), and in posterolateral fusion where Ca-P functioned as a bulking agent to improve osteogenic potential of rhBMP-2 loaded on an absorbable collagen sponge (Barnes *et al.,* 2005). Seeherman also reported achieving bridging of critical size defects in rabbits using the same minimally invasive injectable Ca-P cements (Seeherman *et al.*, 2006b). Ruhé and colleagues also reported several *in vivo* studies with the use calcium phosphate cements, loaded with rhBMP-2 (Ruhé *et al.,* 2005; Ruhé *et al.,* 2006). A main advantage of the use of calcium phosphates compared to other carriers is that, in general, high doses of rhBMPs are not required (Yuan *et al.*, 2001).

Calcium phosphate coatings are another elegant approach for delivering BMPs by incorporating these growth factors into the latticework of these mineral layers that may serve to coat specific scaffold materials. The BMP is biomimetically deposited during the formation of the calcium phosphate film which is form when the material is immersed on a solution of simulated body fluid that mimics the human blood plasma (Liu *et al.,* 2004). The group of de Groot has used calcium phosphate coated titanium disks for delivery of rhBMP-2 in a rat model, showing that much lower concentrations of BMP are required in comparison with collagen matrices (Liu *et al.,* 2004; Liu *et al.,* 2005). Alternatively, bioactive glass (45S5 - Bioglass), a synthetic surface reactive glass that is commonly used as a filler for damaged or fractured bone, may be also used to form biomimetic calcium phosphate coated scaffolds (Leonor *et al.,* 2003). The biomimetic layers, similar to bone apatite, may be used in combination with BMPs to guide the attachment and differentiation of bone precursor cells, given that the coatings have been shown to promote osteointegration and osteoinduction. Silva and colleagues proposed using blends of starch with polylactic acid and bioglass microspheres for the delivery of BMPs (Silva *et al.*, 2004a). Promising potential arises from the fact that bioglass is osteoconductive and osteoinductive, stimulating the recruitment and differentiation of osteoblasts which produce new bone and completely resorb the material.

Table *3*. Micro and nanoscale drug delivery systems based on synthetic and natural-origin polymers. The average size or size range of the particles is noted on the formulation.

Carrier	Formulation/ size	Biological models	References
PLGA	Microparticles	Rat calvarial bone defects	(Kenley *et al.,* 1994)
	Microparticles (247-430 µm)	Rat femur defects	(Lee *et al.,* 1994)
	Microparticles	*In vitro* differentiation of osteoblasts	(Oldham *et al.,* 2000)
	Microparticles	Rabbit calvarial bone defects	(Schrier *et al.,* 2001)
	Microparticles	Sheep vertebrae	(Phillips *et al.,* 2006)
	Nanoparticles (300 nm)	Rat ectopic model	(Wei *et al.,* 2007)
PLGA/Ca-P	Microparticles (66 µm)	Rat ectopic model/ cranial model	(Ruhe *et al.,* 2005)
PLA	Microparticles	Rat ectopic bone formation	(Saitoh *et al.,* 1994)
Collagen/HA	Microparticles	Rabbit femoral bone defects	(Wang *et al.,* 2003)
	Nanocrystals/fibbers	Dogs, spinal fusion/ tibia fractures	(Itoh *et al.,* 2004)
Chitosan/Alginate	Microparticles	*In vitro* differentiation of rabbit bone marrow stem cells	(Qin *et al.,* 2003)
Dextran	Nanoparticles (20 nm)	*In vitro* differentiation of rabbit bone marrow stem cells	(Chen *et al.*, 2005b)
Dextran/PEG	Microparticles (20-40 µm)	*In vitro* differentiation of human periodontal ligament cells	(Chen *et al.,* 2006)
Dextran/Gelatin	Microparticles (20-40 µm)	Canine defects	(Chen *et al.*, 2005a)
	Microparticles (0.5-1.5 µm)	Periodontal regeneration in dogs	(Chen *et al.*, 2007b)

3.5. Microparticles and nanoparticles for BMP delivery

The search for efficient, simple and cheap delivery systems for drug targeting has lead to a great investment on the area of nanoparticles and microparticles for drug delivery. Most common materials for the design of nanodevices to deliver BMPs include synthetic materials,

natural polymers and hydroxyapatite-based particles. Both in the scale of nano (up to 100 nm) and microspheres are reported (**Table 3**).

Polylactic acid and polylactic-co-glycolic acid have been used as materials for nanoparticles-based delivery system for BMPs. PLA was initially studied as a carrier for BMPs in a rat ectopic bone formation model (Saitoh *et al.,* 1994), showing formation of new bone at 4 weeks after implantation and mature bone after 24 weeks. However, by blending PLA with polyglycolic acid in copolymer polylactic-co-glycolic acid (PLGA), biodegradation is controlled by changing the proportions of each of the two materials, since PLA degrades much slower than PGA. Microspheres of PLGA have been since then evaluated in diverse animal models such as on rat calvarial bone defects (Kenley *et al.,* 1994), rat femur defects (Lee *et al.,* 1994), and in calvarial defects in rabbits (Schrier *et al.,* 2001), forming much more bone when BMPs were delivered via the PLGA particles. Interesting work has been developed by Ruhé *et al.*, using microspheres of PLGA in combination with Ca-P cement, as carriers for rhBMP-2 delivery (Ruhé *et al.,* 2005). The release of rhBMP-2 was observed to be dependent in the composite composition and the nanostructure, as well as of the pH of the release medium. Sustained slow release was observed possibly due to interaction of rhBMP-2 with the calcium phosphate cement. Delivery of rhBMP-7 was evaluated in PLGA nanospheres encapsulated in PLA scaffolds, with interconnected macroporous and nano-fibrous architectures (Wei *et al.,* 2007). The group concluded that the carrier delivered rhBMP-7 in a time-controlled manner and induced significant bone formation.

Diverse natural origin materials were also proposed as carriers at a nano and micro scale for delivering BMPs. Collagen-hydroxyapatite microspheres were evaluated for rhBMP-4 delivery in femoral defects of rabbits (Wang *et al.,* 2003). Regeneration occurred in the animal group treated with BMP-4 particles while with the carrier alone the defects were filled with fibrous tissue and inflammatory cells. Microspheres based in blends of chitosan with sodium alginate were reported *in vitro* in bone marrow derived cells, showing an increased on the levels of ALP (Qin *et al.,* 2003). During the last years, dextran-based microspheres and nanospheres were extensively evaluated by Chen *et al.* for the delivery of BMPs. In 2005, the group reported delivering BMP-2 with dextran-based microparticles (20-40 μm) in canine defects (Chen *et al.*, 2005a) and nanoparticles (20 nm) in the differentiation of rabbit bone marrow cells (Chen *et al.*, 2005b) One year later, the authors studied a novel class of methacrylate dextran/PEG microspheres in periodontal ligament cells (Chen *et al.,* 2006). Recently, the group reported dextran-gelatin microspheres loaded into thermomechanical dextran/gelatin hydrogels to deliver rhBMP-2 for periodontal regeneration in dogs (Chen *et al.*, 2007b). The group studied the kinetics of release and demonstrated that by changing the ratio

of components, the rhBMP release could be varied from 18 to more than 28 days (Chen *et al.*, 2007a).

Nanoparticle technology seems definitely one of the most promising approaches for the future of bone tissue engineering, by overcoming some fundamental issues in the methods applied for tissue regeneration such as the insufficient mechanical strength of scaffolds and the lack of stability or bioactivity of growth factors such as BMPs at the defect site (Kim and Fisher, 2007). Major nanotechnology areas of research such as the fabrication of scaffold-nanoparticle composites and the design of nano-patterned materials are some of the areas we found with greatest potential for the delivery of BMP in orthopedic regenerative science.

4. Human clinics and the future of bone tissue engineering

In the western world, an estimated 5-10% of all bone fractures show deficient healing, leading to delayed union or non-union, causing significant morbidity and psychological stress to the patients and bringing elevated costs to society (Westerhuis *et al.*, 2005b). Fortunately, the current advances in bone tissue engineering have led researchers to find new strategies and devices with use of BMPs for accelerate healing of bone tissues on orthopedic field. In fact, by the end of 2007, nearly one million patients worldwide will have been treated with BMPs for diverse bone related problems and diseases (Pecina and Vukicevic, 2007). The clinical uses of BMPs include spinal fusion, treatment of long bone defects and non-unions, dental and periodontal tissue engineering, craniofacial defects and diseases, fracture repair, the improvement of osteointegration with metallic implants, musculoskeletal reconstructive surgery and tendon and ligament reconstruction. There are currently two main collagen-based products containing BMP-2 or BMP-7 that were approved by the Food and Drug Administration (FDA) in the last years for human clinical use: Infuse™ Bone Graft (Medtronic, US; Wyeth, UK) containing rhBMP-2 and Osigraft™ (Stryker Biotech) containing rhBMP-7, known by the designation of OP-1 (osteogenic protein-1). BMP-2 Infuse™ bone graft was approved for certain intervertebral body fusion procedures in 2002, for open tibial fractures in 2004, and for alveolar ridge and sinus augmentations in 2007 (McKay *et al.,* 2007). BMP-7 Osigraft™ was approved for long bone fractures and as alternative to autografts in patients requiring posterolateral lumbar spinal fusion. There has been also an increasing number of trials that provide supporting evidence for the use of rhBMP-7/OP-1 in treatment of open tibial fractures, distal tibial fractures, tibial nonunions, scaphoid nonunions and atrophic long bone nonunions (White *et al.,* 2007).

4.1. Spinal fusion

Spine fusion applications are an important part of clinical trials currently ongoing (Carlisle and Fischgrund, 2005). Spinal fusions consist of nearly half of all grafting surgery. Furthermore, failure rates up to 35% have been reported. The interest is in the use of rhBMPs to accelerate healing in patients with disk degenerative disease, removing the need for autograft harvesting and reducing morbidity. Degenerative disc disease is defined as back pain caused by degeneration of the disc as confirmed by clinical data and symptoms. The common approach is to use a collagen or other carriers soaked with rhBMP and place these within titanium spacers called cages which will be implanted in the spine. There are two types of fusion approaches: posterolateral fusion involving placing the bone graft between the transverse processes in the back of spine and intervertebral body fusion which involves placing the bone graft between the vertebrae in the area occupied by the intervertebral disk. In intervertebral body fusion of lumbar vertebrae, based in the success of previous trials, a prospective study for rhBMP-2 was then performed by McKay and Sandhu involving 279 patients with disk degenerative disease, from which 143 patients received lumbar tapered cages filled with rhBMP-2 and 136 patients received the device filled with autologous bone from iliac crest (McKay and Sandhu, 2002). Since at the conclusion of the study, higher rates of spinal fusion were observed for the rhBMP-2 group and less operative time and morbidity were reported, FDA granted approval for use of rhBMP-2 in treatment of single-level lumbar degenerative disc disease. Posterolateral spinal fusions are common for treating spondylolisthesis but require distinct mechanic and biological properties of the carrier. Boden *et al.* using rhBMP-2 delivered via a biphasic carrier of tricalcium phosphate and hydroxyapatite, reported achieving complete fusion in all patients treated with rhBMP-2 as compared with the control group (Boden *et al.*, 2002). Although the carrier did not obtained approval from FDA, there are several other trials currently ongoing in humans, such as with collagen sponges (Glassman *et al.*, 2007).

The efficacy of use of rhBMP-7/OP-1 as a replacement for iliac crest autograft was first evaluated by Johnsson *et al.* showing higher rates of fusion in posterolateral spinal fusions with application of rhBMP-7 (Johnsson *et al.,* 2002), which were confirmed by subsequent work (Vaccaro *et al.,* 2004; Kanayama *et al.,* 2006). With no adverse effects, OP-1 was considered as a viable alternative to autograft and, as a result, FDA gave approval of rhBMP-7 for patients who have failed a posterolateral fusion and are at risk for repeated pseudarthrosis. At the present, there is little focus on human trials involving either the use of other BMPs or with the use of natural polymers as delivery carriers, but one is to expect that these options would be soon evaluated clinically, in the next years, considering the current state of biomaterials research.

4.2. Long bone fractures

In the most cases where rhBMPs are applied to fractures, these consist in non-unions of long bones. It is estimated as an example that in the UK, 42% of these fractures are of tibias, 20% are femurs and the rest are of other bones (Giannoudis and Tzioupis, 2005). RhBMP-2 has received approval of FDA for use in treating open tibial fractures. Initially, Govender *et al.* performed a randomized trial with 450 patients having open tibial fractures. Patients were randomized to receive different doses of rhBMP-2: 0.75 mg/ml (total dose of 6 mg), 1.50 mg/ml (total dose of 12 mg) or no rhBMP-2, in collagen sponges. After 12 months, analysis showed accelerated healing and reduced infection with increasing dosing of rhBMP-2 (Govender *et al.,* 2002). There are numerous studies in the literature suggesting that rhBMP-7/OP-1 is also a safe and effective alternative for treatment of diverse long-bone fractures and non-unions. In tibial non-unions, a trial that led to multiple regulatory approvals worldwide, concluded that OP-1 delivered in a collagen sponge, was a safe and effective alternative to bone grafting (Friedlaender *et al.,* 2001). In scaphoid nonunions, a study led to conclude that OP-1 could allow successful use of allograft, eliminating the donor site morbidity of an iliac crest autograft (Bilic *et al.,* 2006). In another curious trial, McKee and colleagues assessed the efficacy of OP-1 on treating diverse long bone non-unions on 62 patients that failed previous autograft operations. The involved bones included 16 tibiae, 18 claviculae, 11 humeri, 10 femora, 4 ulnae and 3 radii. At the end of the study, 54 of 61 non-unions (89%) had healed, pointing that rhBMP-7 was an effective treatment (White *et al.,* 2007).

4.3. Dental Tissue Engineering

In periodontal and dental tissue engineering, rhBMPs find their place in inducing pulp stem cells to differentiate into odontoblasts and promoting regeneration of pulp and teeth. Since the pulp, is an organ known to have tremendous regenerative abilities, during the last years tissue engineering has been considered as a promising approach for diverse clinical cases such as caris, pulpitis, and apical periodontitis (Nakashima and Akamine, 2005). Particularly interesting is the fact that human pulp stem cells have self-renewal ability and that tubular dentil is formed after the transplantation of these stem cells with hydroxyapatite power in mice (Gronthos *et al.,* 2002). Recombinant BMPs have been noted to induce dentin formation *in vivo* when delivered with a collagen scaffold (Nakashima, 1994). The ultimate goal in dental tissue engineering using BMPs is in achieving a complete restoration of physiological, structural and mechanical integrity of the native dentil-pulp complex, including nerve and vascular regeneration (Nakashima and Akamine, 2005).

4.4. Future challenges, a global perspective

Bone repair and regeneration with BMPs are ushering in a new era in orthopedics. The past 10 years have seen practical demonstration of bone repair in a series of animal studies and subsequently in clinical trials. The expected value of BMPs in the treatment of bone defects, spinal fusion applications and other types of related applications is enormous. Extensive research in preclinical models has led to the approval of restricted use for human trials. However, despite the significant evidence of potential for bone healing demonstrated in animal models, future clinical investigations will be needed to better define variables such as dose, scaffold and route of administration. The impressive results of animal models are difficult to replicate in humans. It is unclear why these differences occur. Some insight is provided by the clear species-specific dose response ranging from 25 μg/ml in rodents, to 50 μg/ml in dogs, 100 μg/ml in non-human primates and 800 μg/ml in humans (Luginbuehl *et al.*, 2004), in the case of BMP-2. The recruitment of bone precursor cells and bone turnover may occur differently in rodents, small animals and large mammals. Likewise, the dosing may not be optimal yet. In fact, the concentrations of BMP in use are supraphysiological and of a million times factor higher (milligrams in assays as compared to nanogram range *in vivo*). BMP inhibitors such as noggin or sclerotin which are upregulated by BMP presence may be interfering and providing a negative feedback effect on the body healing mechanisms (Westerhuis *et al.*, 2005a). Understanding of the regulation between BMPs and BMP-inhibitors might be a key issue. Moreover, different fractures may require different dosage (Schmitt *et al.,* 1999). Critical issues to consider include the potential risk of BMPs inducing heterotopic bone formation, especially when implanted adjacent to neural tissues (Paramore *et al.,* 1999), and the serious issue of reported antibody formation noted in up to 38% of patients in some trials with BMPs (Walker and Wright, 2002).

Clearly the use of BMPs in orthopedics is still in its early days, but the latest trials in humans suggest that an exciting and promising future will unfold in the development of novel tissue engineering products for a wide range of clinical situations, with the use of BMPs. To date, clinical trials have focused mostly in rhBMP-2 and -7 and with the use of collagen as delivery materials. However, given the intricate network of molecules interplaying during bone regeneration, it is possible that a "cocktail" of different BMPs with simultaneous or sequential release, would be the most desirable approach to clinical uses instead of a single stimulus or molecule (Hadjiargyrou *et al.,* 2002). Raiche and Puleo have already explored the sequential release of rhBMP-2 in combination with insulin-like growth factor-1 (IGF-1) (Raiche and Puleo, 2004a, b). However, the development of such cocktail for clinical cases may come across with difficulties since the commercial rights of the two currently approved rhBMPs are for restricted

use and owned by different companies (Westerhuis *et al.*, 2005b). Nevertheless, in near future, the emergent advances with recombinant production of BMPs (Klösch *et al.*, 2005; Schmoekel *et al.*, 2005b; Bessa *et al.*, 2008) will aid researchers in obtaining larger amounts of bioactive rhBMPs which could be used for tissue engineering research and development of novel products.

With the excitement over the potential of other natural origin polymers as novel delivery systems for BMPs, there is little doubt that these will also find relevant places in regenerative medicine of bone and traumatology and may be soon approaching clinical trials in humans. Diverse natural origin polymers have shown promising success for bone tissue engineering such as fibrin, hyaluronic acid, chitosan, silk fibroin and starch-based composites. Furthermore, these overcome limitations and disadvantages from the use of synthetic polymers and the risks of disease transmission inherent to the use of collagen from bovine sources. The recent advances in biomaterials science will certainly boost the number of tissue engineering approaches for the healing of bone with the use of BMPs. Novel strategies will possibly involve the specific targeting of BMPs, in injectable systems and stimulus-responsible hydrogels, the use of nano-scale patterning or encapsulated particles or with the use of molecules combined with the BMP mimicking the extracellular matrix, all of which allow restricted and site-specific delivery of these growth factors. Additionally, the design of 3D specific-architecture scaffolds by methods such as rapid prototyping or design of bilayered scaffolds surely ensures that the carrier for delivering the BMP will mimic closely the bone structure. Guided-tissue engineering delivery systems, which would not only deliver BMPs but angiogenic factors, would, for instance, prompt the recruitment and distribution of blood-vessels precursor cells which is necessary for formation of mature bone. Finally, the use of Ca-P cements and biomimetic coatings is a very promising approach since it furthers mimics the bone mineral makeup and aids in retaining the BMP and improving the tissue-material integration. The expanding variety of options for biomedical usage of BMPs, gives the promise that the future of clinical regenerative medicine and that of BMPs, particularly for bone applications, will be certainly be a bright one in the coming decades for millions of people.

References

Aebli N, Stich H, Schawalder P, *et al.* 2005, Effects of bone morphogenetic protein-2 and hyaluronic acid on the osseointegration of hydroxyapatite-coated implants: an experimental study in sheep, J Biomed Mater Res A, 73: 295-302.

Arnander C, Westermark A, Veltheim R, *et al.* 2006, Three-dimensional technology and bone morphogenetic protein in frontal bone reconstruction, J Craniofac Surg, 17: 275-9.

Arosarena O and Collins W. 2005a, Comparison of BMP-2 and -4 for rat mandibular bone regeneration at various doses, Orthod Craniofac Res, 8: 267-76.

Arosarena OA and Collins WL. 2005b, Bone regeneration in the rat mandible with bone morphogenetic protein-2: a comparison of two carriers, Otolaryngol Head Neck Surg, 132: 592-7.

Baran ET, Mano JF and Reis RL. 2004, Starch-chitosan hydrogels prepared by reductive alkylation cross-linking, J Mater Sci Mater Med, 15: 759-65.

Barnes B, Boden SD, Louis-Ugbo J, *et al.* 2005, Lower dose of rhBMP-2 achieves spine fusion when combined with an osteoconductive bulking agent in non-human primates, Spine, 30: 1127-33.

Bessa PC, Pedro AJ, Klösch B, *et al.* 2008, Osteoinduction in human fat-derived stem cells by recombinant human bone morphogenetic protein-2 produced in *Escherichia coli*, Biotechnol Lett, 30: 15-21.

Bilic R, Simic P, Jelic M, *et al.* 2006, Osteogenic protein-1 (BMP-7) accelerates healing of scaphoid non-union with proximal pole sclerosis, International Orthopaedics, 30: 128-134.

Blanquaert F, Barritault D and Caruelle JP. 1999, Effects of heparan-like polymers associated with growth factors on osteoblast proliferation and phenotype expression, J Biomed Mater Res, 44: 63-72.

Blunk T, Sieminski AL, Appel B, *et al.* 2003, Bone morphogenetic protein 9: a potent modulator of cartilage development *in vitro*, Growth Factors, 21: 71-7.

Boden SD, Kang J, Sandhu H, *et al.* 2002, Use of recombinant human bone morphogenetic protein-2 to achieve posterolateral lumbar spine fusion in humans: a prospective, randomized clinical pilot trial: 2002 Volvo Award in clinical studies, Spine, 27: 2662-73.

Boden SD, Martin GJ, Jr., Morone MA, *et al.* 1999, Posterolateral lumbar intertransverse process spine arthrodesis with recombinant human bone morphogenetic protein 2/hydroxyapatite-tricalcium phosphate after laminectomy in the nonhuman primate, Spine, 24: 1179-85.

Bulpitt P and Aeschlimann D. 1999, New strategy for chemical modification of hyaluronic acid: preparation of functionalized derivatives and their use in the formation of novel biocompatible hydrogels, J Biomed Mater Res, 47: 152-69.

Cao X, Liu C and Chen J. 2006, [Experimental studies on the porous calcium phosphate cement combined with recombinant human bone morphogenetic protein 2 for bone defects repair], Zhongguo Xiu Fu Chong Jian Wai Ke Za Zhi, 20: 916-9.

Carlisle E and Fischgrund JS. 2005, Bone morphogenetic proteins for spinal fusion, Spine J, 5: 240S-249S.

Chang PC, Liu BY, Liu CM, *et al.* 2007, Bone tissue engineering with novel rhBMP2-PLLA composite scaffolds, J Biomed Mater Res A, 81: 771-80.

Chen F, Wu Z, Wang Q, *et al.* 2005a, Preparation and biological characteristics of recombinant human bone morphogenetic protein-2-loaded dextran-co-gelatin hydrogel microspheres, *in vitro* and *in vivo* studies, Pharmacology, 75: 133-44.

Chen FM, Wu ZF, Jin Y, *et al.* 2005b, [Preparation and property of recombinant human bone morphogenetic protein-2 loaded hydrogel nanospheres and their biological effects on the proliferation and differentiation of bone mesenchymal stem cells], Shanghai Kou Qiang Yi Xue, 14: 485-9.

Chen FM, Wu ZF, Sun HH, *et al.* 2006, Release of bioactive BMP from dextran-derived microspheres: a novel delivery concept, Int J Pharm, 307: 23-32.

Chen FM, Zhao YM, Sun HH, *et al.* 2007a, Novel glycidyl methacrylated dextran (Dex-GMA)/gelatin hydrogel scaffolds containing microspheres loaded with bone morphogenetic proteins: formulation and characteristics, J Control Release, 118: 65-77.

Chen FM, Zhao YM, Zhang R, *et al.* 2007b, Periodontal regeneration using novel glycidyl methacrylated dextran (Dex-GMA)/gelatin scaffolds containing microspheres loaded with bone morphogenetic proteins, J Control Release, 121: 81-90.

Cui G, Li J and Lei W. 2007, [Effect of injectable fibrin sealant compounded with bone morphogenetic protein on proliferation and differentiation of marrow stromal cells towards osteoblasts in rabbits], Zhongguo Xiu Fu Chong Jian Wai Ke Za Zhi, 21: 70-5.

Driessens FC, Planell JA, Boltong MG, *et al.* 1998, Osteotransductive bone cements, Proc Inst Mech Eng [H], 212: 427-35.

Dutta Roy T, Simon JL, Ricci JL, *et al.* 2003, Performance of hydroxyapatite bone repair scaffolds created via three-dimensional fabrication techniques, J Biomed Mater Res A, 67: 1228-37.

Eckardt H, Christensen KS, Lind M, *et al.* 2005, Recombinant human bone morphogenetic protein 2 enhances bone healing in an experimental model of fractures at risk of non-union, Injury, 36: 489-94.

Edwards RB, 3rd, Seeherman HJ, Bogdanske JJ, *et al.* 2004, Percutaneous injection of recombinant human bone morphogenetic protein-2 in a calcium phosphate paste accelerates healing of a canine tibial osteotomy, J Bone Joint Surg Am, 86-A: 1425-38.

Elvira C, Mano JF, San Roman J, *et al.* 2002, Starch-based biodegradable hydrogels with potential biomedical applications as drug delivery systems, Biomaterials, 23: 1955-66.

Fisher JP, Jo S, Mikos AG, *et al.* 2004, Thermoreversible hydrogel scaffolds for articular cartilage engineering, J Biomed Mater Res A, 71: 268-74.

Friedlaender GE, Perry CR, Cole JD, *et al.* 2001, Osteogenic protein-1 (bone morphogenetic protein-7) in the treatment of tibial nonunions, J Bone Joint Surg Am, 83-A Suppl 1: S151-8.

Gao T and Uludag H. 2001, Effect of molecular weight of thermoreversible polymer on *in vivo* retention of rhBMP-2, J Biomed Mater Res, 57: 92-100.

Gautschi OP, Frey SP and Zellweger R. 2007, Bone morphogenetic proteins in clinical applications, ANZ J Surg, 77: 626-31.

Geiger M, Li RH and Friess W. 2003, Collagen sponges for bone regeneration with rhBMP-2, Adv Drug Deliv Rev, 55: 1613-29.

Giannoudis PV and Tzioupis C. 2005, Clinical applications of BMP-7: the UK perspective, Injury, 36 Suppl 3: S47-50.

Glassman SD, Carreon L, Djurasovic M, *et al.* 2007, Posterolateral lumbar spine fusion with INFUSE bone graft, Spine J, 7: 44-9.

Gomes ME, Godinho JS, Tchalamov D, *et al.* 2002, Alternative tissue engineering scaffolds based on starch: processing methodologies, morphology, degradation and mechanical properties, Materials Science & Engineering C-Biomimetic and Supramolecular Systems, 20: 19-26.

Gomes ME, Malafaya PB and Reis RL. 2004, Methodologies for processing biodegradable and natural origin scaffolds for bone and cartilage tissue-engineering applications, Methods Mol Biol, 238: 65-76.

Govender S, Csimma C, Genant HK, *et al.* 2002, Recombinant human bone morphogenetic protein-2 for treatment of open tibial fractures: a prospective, controlled, randomized study of four hundred and fifty patients, J Bone Joint Surg Am, 84-A: 2123-34.

Grayson AC, Voskerician G, Lynn A, *et al.* 2004, Differential degradation rates *in vivo* and *in vitro* of biocompatible poly(lactic acid) and poly(glycolic acid) homo- and co-polymers for a polymeric drug-delivery microchip, J Biomater Sci Polym Ed, 15: 1281-304.

Gronthos S, Brahim J, Li W, *et al.* 2002, Stem cell properties of human dental pulp stem cells, Journal of Dental Research, 81: 531-535.

Hadjiargyrou M, Lombardo F, Zhao S, *et al.* 2002, Transcriptional profiling of bone regeneration. Insight into the molecular complexity of wound repair, J Biol Chem, 277: 30177-82.

Han DK, Kim CS, Jung UW, *et al.* 2005, Effect of a fibrin-fibronectin sealing system as a carrier for recombinant human bone morphogenetic protein-4 on bone formation in rat calvarial defects, J Periodontol, 76: 2216-22.

Hattori T. 1990, [Experimental investigations of osteogenesis and chondrogenesis by implant of BMP-fibrin glue mixture], Nippon Seikeigeka Gakkai Zasshi, 64: 824-34.

He XB, Lu WZ, Tang KL, *et al.* 2003, [Effects of bone morphogenetic protein and transforming growth fractor-beta on biomechanical property for fracture healing in rabbit ulna], Zhongguo Xiu Fu Chong Jian Wai Ke Za Zhi, 17: 185-8.

Hong L, Tabata Y, Yamamoto M, *et al.* 1998, Comparison of bone regeneration in a rabbit skull defect by recombinant human BMP-2 incorporated in biodegradable hydrogel and in solution, Journal of Biomaterials Science-Polymer Edition, 9: 1001-1014.

Hong SJ, Kim CS, Han DK, *et al.* 2006, The effect of a fibrin-fibronectin/beta-tricalcium phosphate/recombinant human bone morphogenetic protein-2 system on bone formation in rat calvarial defects, Biomaterials, 27: 3810-6.

Hsieh CY, Hsieh HJ, Liu HC, *et al.* 2006, Fabrication and release behavior of a novel freeze-gelled chitosan/gamma-PGA scaffold as a carrier for rhBMP-2, Dent Mater, 22: 622-9.

Hu JJ, Jin D, Quan DP, *et al.* 2005, [Bone defect repair with a new tissue-engineered bone carrying bone morphogenetic protein in rabbits], Di Yi Jun Yi Da Xue Xue Bao, 25: 1369-74.

Hu YY, Zhang C, Lu R, *et al.* 2003, Repair of radius defect with bone-morphogenetic-protein loaded hydroxyapatite/collagen-poly(L-lactic acid) composite, Chin J Traumatol, 6: 67-74.

Hubbell J. 2006, Matrix-bound growth factors in tissue repair, Swiss Med Wkly, 136: 387-91.

Hunt DR, Jovanovic SA, Wikesjo UM, *et al.* 2001, Hyaluronan supports recombinant human bone morphogenetic protein-2 induced bone reconstruction of advanced alveolar ridge defects in dogs. A pilot study, J Periodontol, 72: 651-8.

Itoh S, Kikuchi M, Koyama Y, *et al.* 2004, Development of a hydroxyapatite/collagen nanocomposite as a medical device, Cell Transplant, 13: 451-61.

Itoh S, Matubara M, Kawauchi T, *et al.* 2001, Enhancement of bone ingrowth in a titanium fiber mesh implant by rhBMP-2 and hyaluronic acid, J Mater Sci Mater Med, 12: 575-81.

Jen A, Madorin K, Vosbeck K, *et al.* 2002, Transforming growth factor beta-3 crystals as reservoirs for slow release of active TGF-beta3, J Control Release, 78: 25-34.

Jeon O, Song SJ, Kang SW, *et al.* 2007, Enhancement of ectopic bone formation by bone morphogenetic protein-2 released from a heparin-conjugated poly(L-lactic-co-glycolic acid) scaffold, Biomaterials, 28: 2763-71.

Jin QM, Takita H, Kohgo T, *et al.* 2000, Effects of geometry of hydroxyapatite as a cell substratum in BMP-induced ectopic bone formation, J Biomed Mater Res, 51: 491-9.

Johnsson R, Stromqvist B and Aspenberg P. 2002, Randomized radiostereometric study comparing osteogenic protein-1 (BMP-7) and autograft bone in human noninstrumented posterolateral lumbar fusion: 2002 Volvo Award in clinical studies, Spine, 27: 2654-61.

Jones AA, Buser D, Schenk R, *et al.* 2006, The effect of rhBMP-2 around endosseous implants with and without membranes in the canine model, J Periodontol, 77: 1184-93.

Kaito T, Myoui A, Takaoka K, *et al.* 2005, Potentiation of the activity of bone morphogenetic protein-2 in bone regeneration by a PLA-PEG/hydroxyapatite composite, Biomaterials, 26: 73-9.

Kanayama M, Hashimoto T, Shigenobu K, *et al.* 2006, A prospective randomized study of posterolateral lumbar fusion using osteogenic protein-1 (OP-1) versus local autograft with ceramic bone substitute: emphasis of surgical exploration and histologic assessment, Spine, 31: 1067-74.

Karageorgiou V, Meinel L, Hofmann S, *et al.* 2004, Bone morphogenetic protein-2 decorated silk fibroin films induce osteogenic differentiation of human bone marrow stromal cells, J Biomed Mater Res A, 71: 528-37.

Karageorgiou V, Tomkins M, Fajardo R, *et al.* 2006, Porous silk fibroin 3-D scaffolds for delivery of bone morphogenetic protein-2 *in vitro* and *in vivo*, J Biomed Mater Res A, 78: 324-34.

Kato M, Namikawa T, Terai H, *et al.* 2006, Ectopic bone formation in mice associated with a lactic acid/dioxanone/ethylene glycol copolymer-tricalcium phosphate composite with added recombinant human bone morphogenetic protein-2, Biomaterials, 27: 3927-33.

Kawamoto T, Motohashi N, Kitamura A, *et al.* 2003, Experimental tooth movement into bone induced by recombinant human bone morphogenetic protein-2, Cleft Palate Craniofac J, 40: 538-43.

Kenley R, Marden L, Turek T, *et al.* 1994, Osseous regeneration in the rat calvarium using novel delivery systems for recombinant human bone morphogenetic protein-2 (rhBMP-2), J Biomed Mater Res, 28: 1139-47.

Kim HD and Valentini RF. 2002, Retention and activity of BMP-2 in hyaluronic acid-based scaffolds *in vitro*, J Biomed Mater Res, 59: 573-84.

Kim J, Kim IS, Cho TH, *et al.* 2007, Bone regeneration using hyaluronic acid-based hydrogel with bone morphogenic protein-2 and human mesenchymal stem cells, Biomaterials, 28: 1830-7.

Kim K and Fisher JP. 2007, Nanoparticle technology in bone tissue engineering, J Drug Target, 15: 241-52.

Kirker-Head C, Karageorgiou V, Hofmann S, *et al.* 2007, BMP-silk composite matrices heal critically sized femoral defects, Bone, 41: 247-55.

Kirker-Head CA. 2000, Potential applications and delivery strategies for bone morphogenetic proteins, Adv Drug Deliv Rev, 43: 65-92.

Klösch B, Furst W, Kneidinger R, *et al.* 2005, Expression and purification of biologically active rat bone morphogenetic protein-4 produced as inclusion bodies in recombinant *Escherichia coli*, Biotechnol Lett, 27: 1559-64.

Kokubo S, Fujimoto R, Yokota S, *et al.* 2003, Bone regeneration by recombinant human bone morphogenetic protein-2 and a novel biodegradable carrier in a rabbit ulnar defect model, Biomaterials, 24: 1643-51.

Kokubo S, Mochizuki M, Fukushima S, *et al.* 2004, Long-term stability of bone tissues induced by an osteoinductive biomaterial, recombinant human bone morphogenetic protein-2 and a biodegradable carrier, Biomaterials, 25: 1795-803.

Kraiwattanapong C, Boden SD, Louis-Ugbo J, *et al.* 2005, Comparison of Healos/bone marrow to INFUSE(rhBMP-2/ACS) with a collagen-ceramic sponge bulking agent as graft substitutes for lumbar spine fusion, Spine, 30: 1001-7; discussion 1007.

Kuboki Y, Takita H, Kobayashi D, *et al.* 1998, BMP-induced osteogenesis on the surface of hydroxyapatite with geometrically feasible and nonfeasible structures: topology of osteogenesis, J Biomed Mater Res, 39: 190-9.

Langer R and Folkman J. 1976, Polymers for the sustained release of proteins and other macromolecules, Nature, 263: 797-800.

Lee SC, Shea M, Battle MA, *et al.* 1994, Healing of large segmental defects in rat femurs is aided by RhBMP-2 in PLGA matrix, J Biomed Mater Res, 28: 1149-56.

Leonor IB, Ito A, Onuma K, *et al.* 2003, *In vitro* bioactivity of starch thermoplastic/hydroxyapatite composite biomaterials: an in situ study using atomic force microscopy, Biomaterials, 24: 579-85.

Li C, Vepari C, Jin HJ, *et al.* 2006, Electrospun silk-BMP-2 scaffolds for bone tissue engineering, Biomaterials, 27: 3115-24.

Li RH and Wozney JM. 2001, Delivering on the promise of bone morphogenetic proteins, Trends Biotechnol, 19: 255-65.

Liang D, Zuo A, Wang B, *et al.* 2005, *In vitro* osteogenesis of the compound of chitosan and recombinant human bone morphogenetic protein 2, Zhongguo Xiu Fu Chong Jian Wai Ke Za Zhi, 19: 721-4.

Lippman CR, Hajjar M, Abshire B, *et al.* 2004, Cervical spine fusion with bioabsorbable cages, Neurosurg Focus, 16: E4.

Liu Y, de Groot K and Hunziker EB. 2005, BMP-2 liberated from biomimetic implant coatings induces and sustains direct ossification in an ectopic rat model, Bone, 36: 745-57.

Liu Y, Hunziker EB, Layrolle P, *et al.* 2004, Bone morphogenetic protein 2 incorporated into biomimetic coatings retains its biological activity, Tissue Eng, 10: 101-8.

Lopez-Lacomba JL, Garcia-Cantalejo JM, Casado JVS, *et al.* 2006a, Use of rhBMP-2 activated chitosan films to improve osseointegration, Biomacromolecules, 7: 792-798.

Lopez-Lacomba JL, Garcia-Cantalejo JM, Sanz Casado JV, *et al.* 2006b, Use of rhBMP-2 activated chitosan films to improve osseointegration, Biomacromolecules, 7: 792-8.

Luginbuehl V, Meinel L, Merkle HP, *et al.* 2004, Localized delivery of growth factors for bone repair, European Journal of Pharmaceutics and Biopharmaceutics, 58: 197-208.

Lutolf MP, Lauer-Fields JL, Schmoekel HG, *et al.* 2003a, Synthetic matrix metalloproteinase-sensitive hydrogels for the conduction of tissue regeneration: engineering cell-invasion characteristics, Proc Natl Acad Sci U S A, 100: 5413-8.

Lutolf MP, Weber FE, Schmoekel HG, *et al.* 2003b, Repair of bone defects using synthetic mimetics of collagenous extracellular matrices, Nat Biotechnol, 21: 513-8.

Maire M, Chaubet F, Mary P, *et al.* 2005, Bovine BMP osteoinductive potential enhanced by functionalized dextran-derived hydrogels, Biomaterials, 26: 5085-92.

Malafaya PB, Elvira C, Gallardo A, *et al.* 2001, Porous starch-based drug delivery systems processed by a microwave route, J Biomater Sci Polym Ed, 12: 1227-41.

Malafaya PB, Gomes ME, Salgado AJ, *et al.* 2003, Polymer based scaffolds and carriers for bioactive agents from different natural origin materials, Adv Exp Med Biol, 534: 201-33.

Mano J and Reis RL. 2007, Osteochondral defects: present situation and tissue engineering approaches, J Tissue Eng Regen Med 1: 261–273.

Mano JF, Silva GA, Azevedo HS, *et al.* 2007, Natural origin biodegradable systems in tissue engineering and regenerative medicine: present status and some moving trends, J R Soc Interface, 4: 999-1030.

Matsushita N, Terai H, Okada T, *et al.* 2004, A new bone-inducing biodegradable porous beta-tricalcium phosphate, J Biomed Mater Res A, 70: 450-8.

Matsushita N, Terai H, Okada T, *et al.* 2006, Accelerated repair of a bone defect with a synthetic biodegradable bone-inducing implant, J Orthop Sci, 11: 505-11.

Mattioli-Belmonte M, Gigante A, Muzzarelli RA, *et al.* 1999a, N,N-dicarboxymethyl chitosan as delivery agent for bone morphogenetic protein in the repair of articular cartilage, Med Biol Eng Comput, 37: 130-4.

Mattioli-Belmonte M, Gigante A, Muzzarelli RAA, *et al.* 1999b, N,N-dicarboxymethyl chitosan as delivery agent for bone morphogenetic protein in the repair of articular cartilage, Medical & Biological Engineering & Computing, 37: 130-134.

Mayer M, Hollinger J, Ron E, *et al.* 1996, Maxillary alveolar cleft repair in dogs using recombinant human bone morphogenetic protein-2 and a polymer carrier, Plast Reconstr Surg, 98: 247-59.

McKay B and Sandhu HS. 2002, Use of recombinant human bone morphogenetic protein-2 in spinal fusion applications, Spine, 27: S66-85.

McKay WF, Peckham SM and Badura JM. 2007, A comprehensive clinical review of recombinant human bone morphogenetic protein-2 (INFUSE((R)) Bone Graft), Int Orthop.

Meinel L, Fajardo R, Hofmann S, *et al.* 2005, Silk implants for the healing of critical size bone defects, Bone, 37: 688-98.

Meinel L, Hofmann S, Betz O, *et al.* 2006, Osteogenesis by human mesenchymal stem cells cultured on silk biomaterials: comparison of adenovirus mediated gene transfer and protein delivery of BMP-2, Biomaterials, 27: 4993-5002.

Meinel L, Karageorgiou V, Hofmann S, *et al.* 2004, Engineering bone-like tissue *in vitro* using human bone marrow stem cells and silk scaffolds, J Biomed Mater Res A, 71: 25-34.

Miller RA, Brady JM and Cutright DE. 1977, Degradation rates of oral resorbable implants (polylactates and polyglycolates): rate modification with changes in PLA/PGA copolymer ratios, J Biomed Mater Res, 11: 711-9.

Miranda DA, Blumenthal NM, Sorensen RG, *et al.* 2005, Evaluation of recombinant human bone morphogenetic protein-2 on the repair of alveolar ridge defects in baboons, J Periodontol, 76: 210-20.

Miyamoto S, Takaoka K, Okada T, *et al.* 1992, Evaluation of polylactic acid homopolymers as carriers for bone morphogenetic protein, Clin Orthop Relat Res, 278: 274-85.

Murakami N, Saito N, Takahashi J, *et al.* 2003, Repair of a proximal femoral bone defect in dogs using a porous surfaced prosthesis in combination with recombinant BMP-2 and a synthetic polymer carrier, Biomaterials, 24: 2153-9.

Nakashima M. 1994, Induction of Dentin Formation on Canine Amputated Pulp by Recombinant Human Bone Morphogenetic Proteins (Bmp)-2 and (Bmp)-4, Journal of Dental Research, 73: 1515-1522.

Nakashima M and Akamine A. 2005, The application of tissue engineering to regeneration of pulp and dentin in endodontics, J Endod, 31: 711-8.

Namikawa T, Terai H, Suzuki E, *et al.* 2005, Experimental spinal fusion with recombinant human bone morphogenetic protein-2 delivered by a synthetic polymer and beta-tricalcium phosphate in a rabbit model, Spine, 30: 1717-22.

Noshi T, Yoshikawa T, Dohi Y, *et al.* 2001, Recombinant human bone morphogenetic protein-2 potentiates the *in vivo* osteogenic ability of marrow/hydroxyapatite composites, Artif Organs, 25: 201-8.

Oldham JB, Lu L, Zhu X, *et al.* 2000, Biological activity of rhBMP-2 released from PLGA microspheres, J Biomech Eng, 122: 289-92.

Paramore CG, Lauryssen C, Rauzzino MJ, *et al.* 1999, The safety of OP-1 for lumbar fusion with decompression-- a canine study, Neurosurgery, 44: 1151-5; discussion 1155-6.

Park DJ, Choi BH, Zhu SJ, *et al.* 2005a, Injectable bone using chitosan-alginate gel/mesenchymal stem cells/BMP-2 composites, J Craniomaxillofac Surg, 33: 50-4.

Park Y, Sugimoto M, Watrin A, *et al.* 2005b, BMP-2 induces the expression of chondrocyte-specific genes in bovine synovium-derived progenitor cells cultured in three-dimensional alginate hydrogel, Osteoarthritis Cartilage, 13: 527-36.

Park YJ, Kim KH, Lee JY, *et al.* 2006, Immobilization of bone morphogenetic protein-2 on a nanofibrous chitosan membrane for enhanced guided bone regeneration, Biotechnol Appl Biochem, 43: 17-24.

Patel VV, Zhao L, Wong P, *et al.* 2006a, Controlling bone morphogenetic protein diffusion and bone morphogenetic protein-stimulated bone growth using fibrin glue, Spine, 31: 1201-1206.

Patel VV, Zhao L, Wong P, *et al.* 2006b, Controlling bone morphogenetic protein diffusion and bone morphogenetic protein-stimulated bone growth using fibrin glue, Spine, 31: 1201-6.

Pecina M and Vukicevic S. 2007, Biological aspects of bone, cartilage and tendon regeneration, Int Orthop.

Pereira CS, Cunha AM, Reis RL, *et al.* 1998, New starch-based thermoplastic hydrogels for use as bone cements or drug-delivery carriers, Journal of Materials Science-Materials in Medicine, 9: 825-833.

Phillips FM, Turner AS, Seim HB, 3rd, *et al.* 2006, *In vivo* BMP-7 (OP-1) enhancement of osteoporotic vertebral bodies in an ovine model, Spine J, 6: 500-6.

Prabaharan M and Mano JF. 2005, Chitosan-based particles as controlled drug delivery systems, Drug Deliv, 12: 41-57.

Pratt AB, Weber FE, Schmoekel HG, *et al.* 2004, Synthetic extracellular matrices for in situ tissue engineering, Biotechnol Bioeng, 86: 27-36.

Qin Y, Pei GX, Xie DM, *et al.* 2003, [Effect of bone morphogenetic protein microspheres on biological behavior of rabbit bone marrow stem cells], Di Yi Jun Yi Da Xue Xue Bao, 23: 1021-4.

Rai B, Teoh SH, Hutmacher DW, *et al.* 2005, Novel PCL-based honeycomb scaffolds as drug delivery systems for rhBMP-2, Biomaterials, 26: 3739-48.

Raiche AT and Puleo DA. 2004a, Cell responses to BMP-2 and IGF-I released with different time-dependent profiles, J Biomed Mater Res A, 69: 342-50.

Raiche AT and Puleo DA. 2004b, *In vitro* effects of combined and sequential delivery of two bone growth factors, Biomaterials, 25: 677-85.

Reddi AH. 1998, Role of morphogenetic proteins in skeletal tissue engineering and regeneration, Nat Biotechnol, 16: 247-52.

Reddi AH. 2005, BMPs: from bone morphogenetic proteins to body morphogenetic proteins, Cytokine Growth Factor Rev, 16: 249-50.

Ren W, Yang L and Dong S. 2000, [The effects of the complex of rhBMP2 and fibrin sealant on dental pulp], Zhonghua Kou Qiang Yi Xue Za Zhi, 35: 18-20.

Rizzi SC, Ehrbar M, Halstenberg S, *et al.* 2006, Recombinant protein-co-PEG networks as cell-adhesive and proteolytically degradable hydrogel matrixes. Part II: biofunctional characteristics, Biomacromolecules, 7: 3019-29.

Ruhe PQ, Boerman OC, Russel FG, *et al.* 2006, *In vivo* release of rhBMP-2 loaded porous calcium phosphate cement pretreated with albumin, J Mater Sci Mater Med, 17: 919-27.

Ruhe PQ, Boerman OC, Russel FG, *et al.* 2005, Controlled release of rhBMP-2 loaded poly(dl-lactic-co-glycolic acid)/calcium phosphate cement composites *in vivo*, J Control Release, 106: 162-71.

Saito A, Suzuki Y, Kitamura M, *et al.* 2006, Repair of 20-mm long rabbit radial bone defects using BMP-derived peptide combined with an alpha-tricalcium phosphate scaffold, J Biomed Mater Res A, 77: 700-6.

Saito A, Suzuki Y, Ogata S, *et al.* 2003a, Activation of osteo-progenitor cells by a novel synthetic peptide derived from the bone morphogenetic protein-2 knuckle epitope, Biochim Biophys Acta, 1651: 60-7.

Saito A, Suzuki Y, Ogata S, *et al.* 2004, Prolonged ectopic calcification induced by BMP-2-derived synthetic peptide, J Biomed Mater Res A, 70: 115-21.

Saito A, Suzuki Y, Ogata S, *et al.* 2005a, Accelerated bone repair with the use of a synthetic BMP-2-derived peptide and bone-marrow stromal cells, J Biomed Mater Res A, 72: 77-82.

Saito N, Murakami N, Takahashi J, *et al.* 2005b, Synthetic biodegradable polymers as drug delivery systems for bone morphogenetic proteins, Adv Drug Deliv Rev, 57: 1037-48.

Saito N, Okada T, Horiuchi H, *et al.* 2001, Biodegradable poly-D,L-lactic acid-polyethylene glycol block copolymers as a BMP delivery system for inducing bone, J Bone Joint Surg Am, 83-A Suppl 1: S92-8.

Saito N, Okada T, Horiuchi H, *et al.* 2003b, Local bone formation by injection of recombinant human bone morphogenetic protein-2 contained in polymer carriers, Bone, 32: 381-6.

Saito N and Takaoka K. 2003, New synthetic biodegradable polymers as BMP carriers for bone tissue engineering, Biomaterials, 24: 2287-93.

Saitoh H, Takata T, Nikai H, *et al.* 1994, Effect of polylactic acid on osteoinduction of demineralized bone: preliminary study of the usefulness of polylactic acid as a carrier of bone morphogenetic protein, J Oral Rehabil, 21: 431-8.

Schmitt JM, Hwang K, Winn SR, *et al.* 1999, Bone morphogenetic proteins: an update on basic biology and clinical relevance, J Orthop Res, 17: 269-78.

Schmoekel H, Schense JC, Weber FE, *et al.* 2004, Bone healing in the rat and dog with nonglycosylated BMP-2 demonstrating low solubility in fibrin matrices, J Orthop Res, 22: 376-81.

Schmoekel HG, Weber FE, Hurter K, *et al.* 2005a, Enhancement of bone healing using non-glycosylated rhBMP-2 released from a fibrin matrix in dogs and cats, J Small Anim Pract, 46: 17-21.

Schmoekel HG, Weber FE, Schense JC, *et al.* 2005b, Bone repair with a form of BMP-2 engineered for incorporation into fibrin cell ingrowth matrices, Biotechnol Bioeng, 89: 253-62.

Schopper C, Moser D, Spassova E, *et al.* 2007, Bone regeneration using a naturally grown HA/TCP carrier loaded with rh BMP-2 is independent of barrier-membrane effects, J Biomed Mater Res A.

Schrier JA, Fink BF, Rodgers JB, *et al.* 2001, Effect of a freeze-dried CMC/PLGA microsphere matrix of rhBMP-2 on bone healing, AAPS PharmSciTech, 2: E18.

Schwarz N, Redl H, Zeng L, *et al.* 1993, Early osteoinduction in rats is not altered by fibrin sealant, Clin Orthop Relat Res, 293: 353-9.

Seeherman H, Li R, Bouxsein M, *et al.* 2006a, rhBMP-2/calcium phosphate matrix accelerates osteotomy-site healing in a nonhuman primate model at multiple treatment times and concentrations, J Bone Joint Surg Am, 88: 144-60.

Seeherman H and Wozney JM. 2005, Delivery of bone morphogenetic proteins for orthopedic tissue regeneration, Cytokine Growth Factor Rev, 16: 329-45.

Seeherman HJ, Azari K, Bidic S, *et al.* 2006b, rhBMP-2 delivered in a calcium phosphate cement accelerates bridging of critical-sized defects in rabbit radii, J Bone Joint Surg Am, 88: 1553-65.

Seeherman HJ, Bouxsein M, Kim H, *et al.* 2004, Recombinant human bone morphogenetic protein-2 delivered in an injectable calcium phosphate paste accelerates osteotomy-site healing in a nonhuman primate model, J Bone Joint Surg Am, 86-A: 1961-72.

Shimaoka H, Dohi Y, Ohgushi H, *et al.* 2004, Recombinant growth/differentiation factor-5 (GDF-5) stimulates osteogenic differentiation of marrow mesenchymal stem cells in porous hydroxyapatite ceramic, J Biomed Mater Res A, 68: 168-76.

Shimazu C, Hara T, Kinuta Y, *et al.* 2006, Enhanced vertical alveolar bone augmentation by recombinant human bone morphogenetic protein-2 with a carrier in rats, J Oral Rehabil, 33: 609-18.

Silva GA, Costa FJ, Coutinho OP, *et al.* 2004a, Synthesis and evaluation of novel bioactive composite starch/bioactive glass microparticles, J Biomed Mater Res A, 70: 442-9.

Silva GA, Costa FJ, Coutinho OP, *et al.* 2004b, Synthesis and evaluation of novel bioactive composite starch/bioactive glass microparticles, Journal of Biomedical Materials Research Part A, 70A: 442-449.

Simmons CA, Alsberg E, Hsiong S, *et al.* 2004, Dual growth factor delivery and controlled scaffold degradation enhance *in vivo* bone formation by transplanted bone marrow stromal cells, Bone, 35: 562-9.

Smith JD, Melhem ME, Magge KT, *et al.* 2007, Improved growth factor directed vascularization into fibrin constructs through inclusion of additional extracellular molecules, Microvasc Res, 73: 84-94.

Suzuki A, Terai H, Toyoda H, *et al.* 2006, A biodegradable delivery system for antibiotics and recombinant human bone morphogenetic protein-2: A potential treatment for infected bone defects, J Orthop Res, 24: 327-32.

Suzuki Y, Tanihara M, Suzuki K, *et al.* 2000, Alginate hydrogel linked with synthetic oligopeptide derived from BMP-2 allows ectopic osteoinduction *in vivo*, J Biomed Mater Res, 50: 405-9.

Takahashi Y, Yamamoto M, Yamada K, *et al.* 2007, Skull bone regeneration in nonhuman primates by controlled release of bone morphogenetic protein-2 from a biodegradable hydrogel, Tissue Eng, 13: 293-300.

Tamai N, Myoui A, Hirao M, *et al.* 2005, A new biotechnology for articular cartilage repair: subchondral implantation of a composite of interconnected porous hydroxyapatite, synthetic polymer (PLA-PEG), and bone morphogenetic protein-2 (rhBMP-2), Osteoarthritis Cartilage, 13: 405-17.

Tian W, Bao C, Liu L, *et al.* 2004, [Experimental study on the fabrication of bioactive membrane for inducing bone regeneration], Sheng Wu Yi Xue Gong Cheng Xue Za Zhi, 21: 844-7.

Tsuruga E, Takita H, Itoh H, *et al.* 1997, Pore size of porous hydroxyapatite as the cell-substratum controls BMP-induced osteogenesis, J Biochem (Tokyo), 121: 317-24.

Tuzlakoglu K, Alves CM, Mano JF, *et al.* 2004, Production and characterization of chitosan fibers and 3-D fiber mesh scaffolds for tissue engineering applications, Macromol Biosci, 4: 811-9.

Tuzlakoglu K, Bolgen N, Salgado AJ, *et al.* 2005, Nano- and micro-fiber combined scaffolds: A new architecture for bone tissue engineering, Journal of Materials Science-Materials in Medicine, 16: 1099-1104.

Uludag H, D'Augusta D, Palmer R, *et al.* 1999a, Characterization of rhBMP-2 pharmacokinetics implanted with biomaterial carriers in the rat ectopic model, J Biomed Mater Res, 46: 193-202.

Uludag H, Friess W, Williams D, *et al.* 1999b, rhBMP-collagen sponges as osteoinductive devices: effects of *in vitro* sponge characteristics and protein pI on *in vivo* rhBMP pharmacokinetics, Ann N Y Acad Sci, 875: 369-78.

Vaccaro AR, Patel T, Fischgrund J, *et al.* 2004, A pilot study evaluating the safety and efficacy of OP-1 Putty (rhBMP-7) as a replacement for iliac crest autograft in posterolateral lumbar arthrodesis for degenerative spondylolisthesis, Spine, 29: 1885-92.

Vogelin E, Jones NF, Huang JI, *et al.* 2005, Healing of a critical-sized defect in the rat femur with use of a vascularized periosteal flap, a biodegradable matrix, and bone morphogenetic protein, J Bone Joint Surg Am, 87: 1323-31.

Walker DH and Wright NM. 2002, Bone morphogenetic proteins and spinal fusion, Neurosurg Focus, 13: e3.

Wang YJ, Lin FH, Sun JS, *et al.* 2003, Collagen-hydroxyapatite microspheres as carriers for bone morphogenic protein-4, Artif Organs, 27: 162-8.

Wei G, Jin Q, Giannobile WV, *et al.* 2007, The enhancement of osteogenesis by nano-fibrous scaffolds incorporating rhBMP-7 nanospheres, Biomaterials, 28: 2087-96.

Westerhuis RJ, van Bezooijen RL and Kloen P. 2005a, Use of bone morphogenetic proteins in traumatology, Injury-International Journal of the Care of the Injured, 36: 1405-1412.

Westerhuis RJ, van Bezooijen RL and Kloen P. 2005b, Use of bone morphogenetic proteins in traumatology, Injury, 36: 1405-12.

White AP, Vaccaro AR, Hall JA, *et al.* 2007, Clinical applications of BMP-7/OP-1 in fractures, nonunions and spinal fusion, Int Orthop.

Wikesjo UM, Lim WH, Thomson RC, *et al.* 2003, Periodontal repair in dogs: evaluation of a bioabsorbable space-providing macroporous membrane with recombinant human bone morphogenetic protein-2, J Periodontol, 74: 635-47.

Winet H and Hollinger JO. 1993, Incorporation of polylactide-polyglycolide in a cortical defect: neoosteogenesis in a bone chamber, J Biomed Mater Res, 27: 667-76.

Yamamoto M, Ikada Y and Tabata Y. 2001, Controlled release of growth factors based on biodegradation of gelatin hydrogel, Journal of Biomaterials Science-Polymer Edition, 12: 77-88.

Yamamoto M, Tabata Y and Ikada Y. 1998, Ectopic bone formation induced by biodegradable hydrogels incorporating bone morphogenetic protein, J Biomater Sci Polym Ed, 9: 439-58.

Yamamoto M, Takahashi Y and Tabata Y. 2003a, Controlled release by biodegradable hydrogels enhances the ectopic bone formation of bone morphogenetic protein, Biomaterials, 24: 4375-83.

Yamamoto M, Takahashi Y and Tabata Y. 2003b, Controlled release by biodegradable hydrogyels enhances the ectopic bone formation of bone morphogenetic protein, Biomaterials, 24: 4375-4383.

Yamamoto M, Takahashi Y and Tabata Y. 2006, Enhanced bone regeneration at a segmental bone defect by controlled release of bone morphogenetic protein-2 from a biodegradable hydrogel, Tissue Engineering, 12: 1305-1311.

Yang C, Hillas PJ, Baez JA, *et al.* 2004, The application of recombinant human collagen in tissue engineering, BioDrugs, 18: 103-19.

Yang W, Gomes RR, Brown AJ, *et al.* 2006, Chondrogenic differentiation on perlecan domain I, collagen II, and bone morphogenetic protein-2-based matrices, Tissue Eng, 12: 2009-24.

Yoneda M, Terai H, Imai Y, *et al.* 2005, Repair of an intercalated long bone defect with a synthetic biodegradable bone-inducing implant, Biomaterials, 26: 5145-52.

Yuan H, De Bruijn JD, Zhang X, *et al.* 2001, Use of an osteoinductive biomaterial as a bone morphogenetic protein carrier, J Mater Sci Mater Med, 12: 761-6.

Zhang C, Hu Y, Xiong Z, *et al.* 2005, [Tissue engineered bone regeneration of periosteal cells using recombinant human bone morphogenetic protein 2 induce], Zhongguo Xiu Fu Chong Jian Wai Ke Za Zhi, 19: 100-4.

Zheng YX, Zhao HY, Jing XB, *et al.* 2006, [Reconstruction of orbital floor defect with polylacticglycolide acid/recombinant human bone morphogenetic protein 2 compound implanted material in sheep], Zhonghua Yan Ke Za Zhi, 42: 535-9.

Zhu SJ, Choi BH, Huh JY, *et al.* 2006a, A comparative qualitative histological analysis of tissue-engineered bone using bone marrow mesenchymal stem cells, alveolar bone cells, and periosteal cells, Oral Surgery Oral Medicine Oral Pathology Oral Radiology and Endodontics, 101: 166-171.

Zhu SJ, Choi BH, Jung JH, *et al.* 2006b, A comparative histologic analysis of tissue-engineered bone using platelet-rich plasma and platelet-enriched fibrin glue, Oral Surgery Oral Medicine Oral Pathology Oral Radiology and Endodontics, 102: 175-179.

Zou X, Li H, Chen L, *et al.* 2004, Stimulation of porcine bone marrow stromal cells by hyaluronan, dexamethasone and rhBMP-2, Biomaterials, 25: 5375-85.

SECTION 2

Chapter III

Materials and Methods

Chapter III

Materials and Methods

This chapter intends to give an overview on the experimental work behind the studies presented in this dissertation. All the ground work that support the achieved results (presented in Sections 3 and 4) will be herein described in detail. This is expected to leave the reader with a more clear vision of the purpose of each studied subject and of the way that these can be correlated.

1. Recombinant technology for cloning and expression of proteins

1.1. BL21 DE3 strain *Escherichia coli* expression system

Because of its long history of laboratory culture and ease of manipulation, *Escherichia coli* plays nowadays an important role in modern biological engineering and industrial microbiology. There are other expression systems for recombinant production of proteins such as mammalian cells or insect cells but these involved more sophisticated culturing conditions and significantly lower yields of expression of the recombinant protein. Using the recent advances in protein production in bacteria, it is possible to express proteins in large amounts and refold these into their native and bioactive structure.

BL21(DE3) strain is the most widely used host background for protein expression and has the advantage of being deficient in both *lon* and *ompT* proteases which could degrade protein during purification (Studier 1991). The BL21(DE3) strain has a high expression level of recombinant proteins, induced upon the addition of isopropyl-1-thio-β-galactopyranoside (IPTG). IPTG activates the T7 RNA polymerase *lac* promoter and consequently upregulates the expression of the cloned gene.

1.2. pET-25b expression system

The pET System is a powerful expression vector developed for the cloning and expression of recombinant proteins in *Escherichia coli*, based on the T7 promoter-driven system originally developed by Studier and colleagues (Studier and Moffatt 1986; Studier *et al.* 1990). The pET-25b vector carries an N-terminal pelB signal sequence for potential secretion of protein into the periplasm space, plus an optional C-terminal HSV-Tag and the 6x-histidine-Tag (**Figure 1**). The use of pET-25b vector provides a suitable strategy to express recombinant proteins that require disulfide-bond formation for full bioactivity, such in the case of BMPs.

The recombinant proteins are induced for export into the periplasm space, which is an environment favorable for disulfide bond formation, critical for the folding of dimeric BMPs.

In addition, pET-25b vector allows the purification of protein by affinity chromatography, due to the presence of a C-terminal polyhistidine-tag. The polyhistidine-tags are an amino acid motif in proteins that consists of at least six histidine (His) residues, often at the N- or the C-terminus of the protein, and commonly used for affinity purification of the recombinant protein. Please refer to section 3.3.1. of the present chapter for more information on the histidine-tag affinity purification.

2. Cloning of bone morphogenetic proteins

2.1 Obtaining bone morphogenetic cDNA (BMP mature domain)

Different cDNA sources were researched for cloning of bioactive domains of the different human BMPs. A common source is to clone the BMP corresponding DNA from an human cDNA library from cells or tissues that express BMPs. However, since it is an expensive approach, we opt to clone the DNA corresponding to the bioactive domain of BMPs directly from the human genome, since for the different BMPs used in this thesis, all their bioactive domains are located solely in one exon. Bacteria clones were acquired from Sanger Institute (Cambridge, US), which contained human DNA encoding the different human BMP genes. From this template, PCR was performed, as a way of cloning the DNA corresponding to the bioactive domain of the BMPs into the pET-25b vector and expressing the different recombinant proteins.

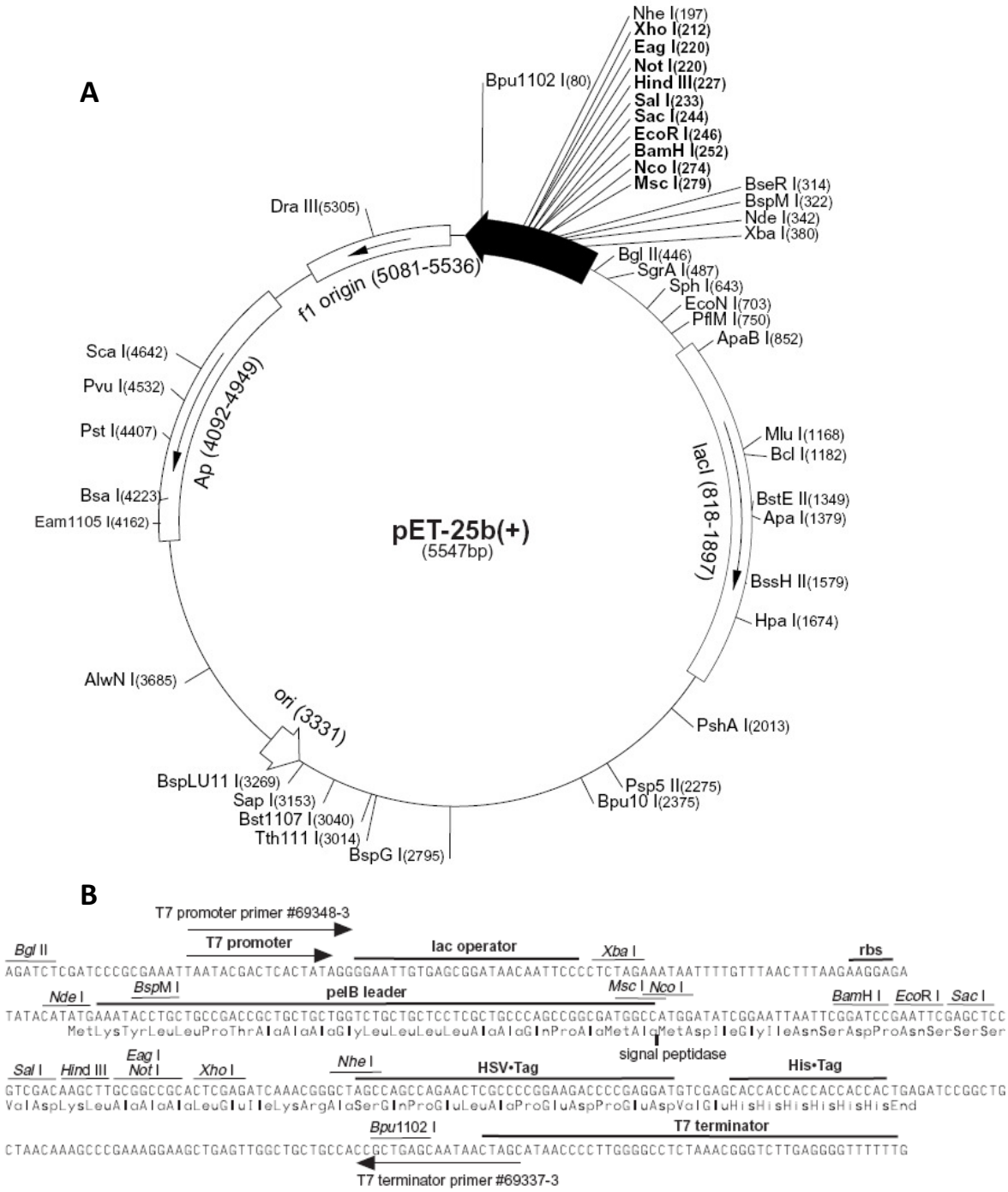

Figure 1. Vector pET-25b was used for the expression of different human BMPs in *E. coli*. In the representation above, the vector restriction sites (A) and multiple cloning site (coding strand transcribed by T7 RNA polymerase) (B), are shown.

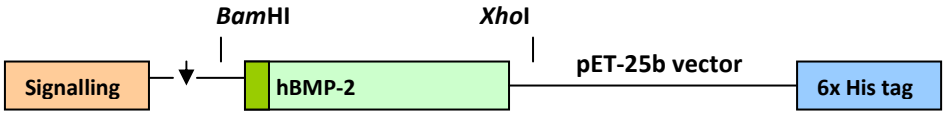

Figure 2. Schematic representation of cloning of human BMP-2 in pET-25b vector, showing the N-terminal histidine tag of vector, and peIB signal sequence for secretion into periplasm. The signalling sequence is proteolytically cleaved in periplasm of *Escherichia coli*. The (natural-occurring) heparin binding domain of BMP-2 is indicated in dark green color. The same methodology was performed for cloning of human BMP-4, BMP-9, BMP-10, BMP-11/GDF-11 and BMP-14/GDF-5. *Bam*HI and *Xho*I restriction sites, used for cloning, are indicated.

2.2. Molecular biology tools used for cloning of BMPs

2.2.1. Designing primers for bone morphogenetic protein cloning

Primers were designed for amplifying the gene sequence coding for the mature part of the BMPs and flanked with restriction sites (*BamH*I and *Xho*I) allowing for insertion into the cloning and expression vectors (**Figure 2**). Primers were designed accordingly to a set of parameters well defined on the literature (such as nucleotide length, GC nucleotide percentage, and several other rules). Primer efficiency was first investigated by performing *in silico* PCR with Amplify and Primer 3 software tools.

2.2.2. Cloning of BMP cDNA by polymerase chain reaction (PCR)

Amplification by PCR of rhBMPs was performed upon the aforementioned cDNA, in section 2.1. In a PCR tube, 1 µg DNA was mixed with 0.5 µl dNTPs 10 mM, 2 µl $MgCl_2$ 50 mM, 1 µl of each primer (detailed information in chapters IV and V) of a 10 µM stock, 1 µl of proofreading accuzyme polymerase enzyme, 2.5 µl enzyme buffer (10x) and rest of ultrapure water for a total 25 µl.

Conditions regarding the (PCR) amplification cycles, were the following.

1) 94ºC – 2 min

2) 30 cycles (94ºC – 30 sec, Ta – 45 sec, 72ºC – 1 min)

3) 72ºC – 5min

4) 4ºC – *ad infinitium*

The primer annealing temperature (Ta) was calculated in primer manufacturer instructions. After the PCR, a volume of 1-2 µl was run in agarose gel electrophoresis for confirmation of DNA integrity and size (1% agarose gel stained with ethidium bromide, 6 µl per 100 TAE buffer). Amplified BMP DNA was then purified with GenElute PCR DNA Purification Kit (Sigma), which is a critical step for efficient ligation to cloning/expression plasmids.

2.2.3. Restriction of DNA and ligation into expression vector

Restrictions of both amplified DNA and of vector are required for insertion of the gene of interest to the cloning vector. They allow the complementary between insert and plasmid, for ligation. The restrictions sites of *Bam*HI and *Xho*I were selected for ligation, to discard the maximum of amino acids residues, upstream and downstream of BMP gene sequence, that could cause any interference in the folding and bioactivity of the protein. The restriction reaction was performed by incubating 10 µl purified DNA, 6 µl ultrapure water, 2 µl enzyme buffer and 1 µl of each restriction enzyme, at 37ºC (as indicated by the manufacturer) for 5 h. Following the restriction, the pET-25b-BMP2 vector was diphosphorylated to prevent the re-cycling of plasmid, by incubating the mixture with 1µl of SAP enzyme (30 min at 37ºC) and stopping the reaction (15 min, 65ºC). Before ligation, the DNA integrity was verified on gel electrophoresis, and DNA isolated using QIAquick Gel Extraction Kit (Qiagen). Ligation was performed by incubating 1 µl of plasmid, 7 µl of BMP DNA, 1 µl enzyme buffer and 1 µl ligation enzyme (Roche), overnight at 4ºC.

2.2.4. Transformation of XL1BLUE and BL21DE3 *Escherichia coli* strains

For cloning of plasmid, XL1BLUE or TOP10 *Escherichia coli* strains were used. For expression of protein, BL21DE3 *E. coli* strain was generally used (although Origami, Tuner and BLR strains were also investigated, data not shown). For transformation of XL1BLUE, bacteria stocks were thawed in ice (competent cells) and 10 µl ligation product were added and incubated for 30 min.

Then, cells were incubated for 30 sec at 42ºC with agitation and immediately returned to ice, for more 10 min. After this, 0.8 ml of SOC medium (Super Optimal broth with Catabolite repression) was added and cells grown at 37ºC with vigorous agitation for 1h. Cells were then centrifuged, resuspended in a small volume (50 µl) and plated into LB culture plates which contained 50 µg/ ml ampicillin. Negative controls included bacteria transformed with a plasmid with no BMP gene and cells having no resistance to the antibiotic. *E. coli* was grown at 37ºC overnight. The following day, colonies were selected, grown overnight in new plates and

plasmids were isolated with use of GenElute Plasmid Minipreps Kit (Sigma, US) (according to manufacturer instructions).

The extracted plasmid was then digested with specific restriction enzymes and run in agarose gel electrophoresis for screening which colonies had the correct insertion of the BMP genes. The integrity of the gene sequences was verified by DNA sequencing (Sanger *et al.* 1977) using ABI PRISM 310 Genetic Analyzer. The pET-25b and pET-25b/BMP vectors were then used for transformation of BL21DE3 *E. coli* strain, for expressing the recombinant BMPs. Cryotubes were prepared using collected biomass in 1.5 ml 30% glycerol for long-term storage of bacteria at -80ºC. Plasmids were stored at -20ºC. All work was performed under sterile conditions.

3. Expression, folding and purification of bone morphogenetic proteins

3.1 Expression of rhBMPs

3.1.1. Expression of protein in BL21DE3 *Escherichia coli* strain

Expression of recombinant BMPs was performed by using BL21DE3 cells which are indicated for the expression of recombinant proteins from pET vectors. Transformed BL21DE3 bacteria with pET-25b/rhBMP and pET-25b were inoculated in 50-200 ml Luria Bertani (LB) medium with 50 µg ampicillin/ml and incubated at 37 ºC (180 rpm), until an OD_{600} of 0.6-1.0 was obtained. To induce the recombinant protein expression IPTG 1 mM was then added to the culture media, and the temperature lowered to 25 ºC during 24 h. Biomass was collected by centrifugation (4000 g, 20 min, 4 ºC), washed once with PBS and stored at -20 ºC.

3.1.2. Analysis of protein expression using SDS-PAGE

Protein was isolated by resuspending frozen bacteria in phosphate buffer saline (or other lyses buffer), with addition of a proteases inhibitor (Complete Mini EDTA-free, Roche), and performing cell lyses by incubating ultrasonication of samples for 4 times for 15 s with intervals of 1 min, in ice. Supernatant and pellet fractions were collected by centrifugation (4000 g, 30 min, 4ºC), for SDS-PAGE analysis. SDS-PAGE was applied for a qualitative and semi-quantitative analysis of the protein, at different stages of BMP production: protein expression, solubilization and folding, purification and storage.

For SDS-PAGE, protein concentrations of 0.1-1 mg/ml were used. Protein samples were mixed with SDS-PAGE loading buffer and heated at 95ºC for 5 min. Samples were separated by using hand-cast 10–12% acrylamide/bisacrylamide SDS-PAGE gels, at 15 mA, for 1 h, in

reducing or non-reducing conditions. Reducing conditions included the use of loading buffer with 5% (v/v) β-mercaptoethanol as a reducing agent. Coomassie Blue-R or silver staining were used for the visualization and staining of gels. Gels were analyzed with Gel Pro Analyzer software (Media Cybernetics), for the estimation of protein molecular weight and concentration.

3.1.3. Analysis of protein expression using Western-blot

For Western-blot, protein concentrations of 1-10 µg/ml were used. Protein samples were mixed with SDS-PAGE loading buffer and heated at 95 °C for 5 min. Samples were separated by using hand-cast 10-12 % SDS–PAGE at constant 15 mA, for 1 h. Gels were then fixed for 5 min in transfer buffer (20mM Tris-HCl, 20mM glycine, 20% ethanol) and samples were electro-transferred to a nitrocellulose membrane at 100 V for 60 min (wet Western-blot transfer) or 10V, 400 mA, for 30min (semi-dry Western-blot transfer). The membrane was washed once with PBS for 10 min and blocked with 2% (w/v) BSA in PBS-T buffer (PBS, 0.05% Tween 20) for 2h at room temperature. After this, the membrane was washed once with PBS-T buffer and incubated with peroxidase conjugated anti-His antibody (Sigma) diluted 1:2000 or rabbit anti-human BMP-2 polyclonal primary antibody (AbD Serotec) diluted 1:5000 followed by mouse anti-rabbit peroxidase conjugated secondary antibody (Amersham) diluted 1:30000. Prior to colorimetric development, the membrane was washed 3x with PBS and image detection was performed with ChemiDoc XRS and Quantity One software (BioRad).

3.1.4 Optimization of protein expression levels

Protein expression was optimized for different variables that affected the amounts of produced protein: temperature of induction and expression, time length of expression and the influence of codon usage. First, the expression of rhBMP-2 was performed for 24h at 25ºC, 18ºC and 4ºC. By analyzing crude lysates (pellet fraction) using SDS-PAGE, rhBMP-2 expression was found to be higher at 25ºC (**Figure 3**). Following this, the amount of expressed BMP-2 was tested along different times of production, and optimal recovery of protein was found after a period of 24-48 h of expression (**Figure 4**). Finally, the cloning of a codon-usage optimized BMP-2 gene sequence did not affected significantly the expression of protein, compared to the native sequence derived from the BMP-2 cDNA (**Figure 5**).

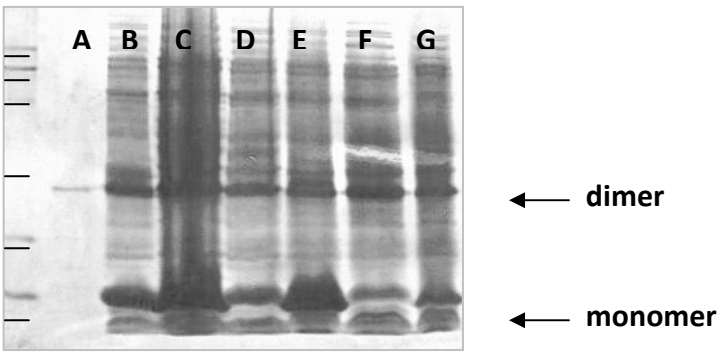

Figure 3. SDS-PAGE of samples of crude lysates (pellet fraction) with different temperature used for expression of rhBMP-2. Respectively, A-G correspond to the negative control, BMP-2 variant I (25ºC), BMP-2 variant II (25ºC), BMP-2 variant I (18ºC), BMP-2 variant II (18ºC), BMP-2 variant I (4ºC), BMP-2 variant II (4ºC). BMP-2 monomer and dimer are marked (18 kDa, 36 kDa). Marker: 116 kDa, 97 kDa, 66 kDa, 45 kDa, 22 kDa and 14 kDa. Expression of BMP-2 was significantly higher at 25ºC. Expression was performed for 24 h. Please refer to section 3.2.5. for rhBMP-2 variants.

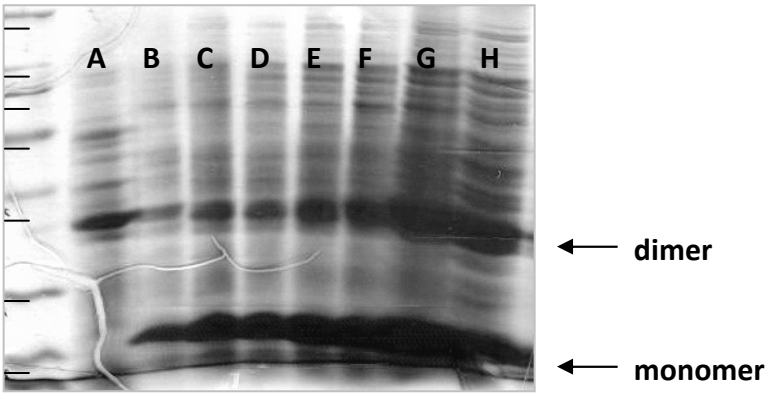

Figure 4. SDS-PAGE of samples of crude lysates (pellet fraction) with different time periods for expression of rhBMP-2. Respectively, A-H correspond to the following times of production: A (0h), B (4h), C (8h), D (16h), E (22h), F (24h), G (2 days) and H (4 days). Temperature of expression was 25ºC. BMP-2 monomer and dimer are marked (18 kDa, 36 kDa). Marker: 200 kDa, 116 kDa, 97 kDa, 66 kDa, 45 kDa, 22 kDa and 14 kDa. Expression of BMP-2 peaked after 24 -48 h.

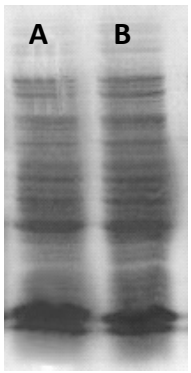

Figure 5. SDS-PAGE of samples of crude lysates (pellet fraction) with rhBMP-2 produced with native gene sequence (1), and a codon usage optimized sequence (2). The use of optimized codon use does not result in significant changes in the expression of rhBMP-2.

3.1.5. Bioreactor scale-up protein production

Scale-up expression of BMPs was performed using a 2 l Bioflo110 bioreactor (New Brunswick Scientific, USA) (**Figure 6**). Pre-cultures were transferred to the pre-autoclaved bioreactor which contained LB media with 50 µg ampicillin/ml. *E. coli* were grown at 37ºC until an OD_{600} of 0.6-1.0. At this time point, 1 mM IPTG was added and temperature lowered to 25ºC to induce the expression of the recombinant BMPs. During the entire process of fermentation, aeration was kept at 2 l/min and an agitation cascade of 300-1000 rpm was selected in order to maintain minimum dissolved oxygen levels at 30% of saturation. The pH 7.4 was kept constant using NH_4OH (30%, v/v) and H_3PO_4 (5 M) which were automatically pumped into the bioreactor vessel. In the end, the biomass was collected by centrifugation (4000 g, 20 min, 4ºC), washed once with PBS and stored at -20ºC.

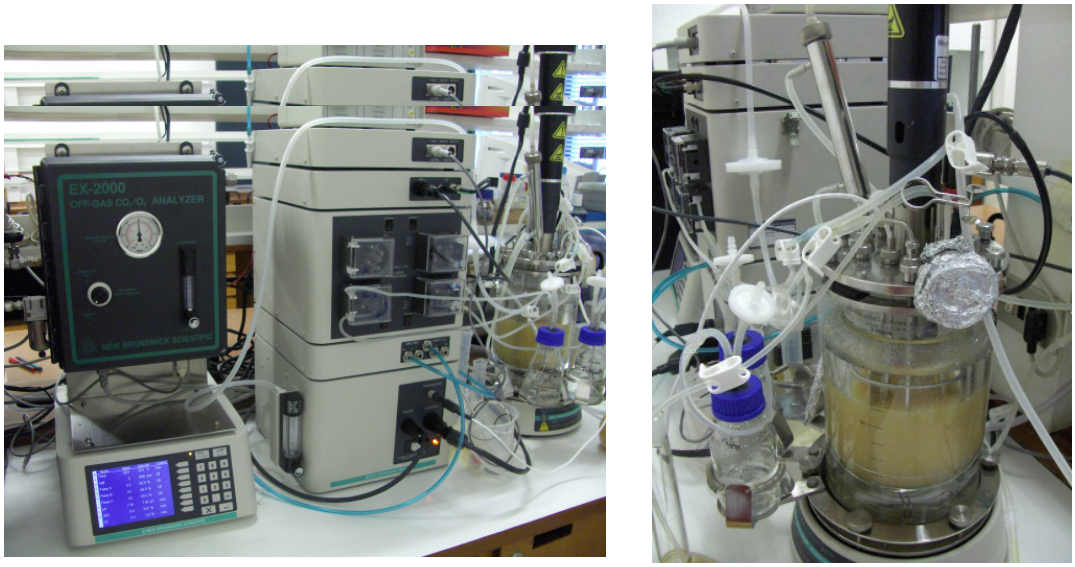

Figure 6. Use of a bioreactor allowed producing large-scale amounts of recombinant BMPs.

3.2. Recovery of rhBMPs

3.2.1. Protein folding and solubilization

The folding of proteins is dependent on several conditions, such as buffer composition, ionic strength, denaturant and protein concentration, pH and temperature (Vallejo and Rinas 2004). Since the recombinant protein was initially obtained in the pellet fraction of bacteria cell lysate, the protein solubilization was first analyzed in the presence of varied buffers and conditions (e.g. Triton, Tween, sodium lauryl sulphate, L-arginine, and urea, and different pH). The BMP-2 was found to be recovered best with phosphate buffer saline containing L-arginine (data not shown), a common aggregation-suppressor that enhances the solubilization and the refolding of proteins (Vallejo and Rinas 2004). Different concentrations of L-arginine were used,

with different pH, for optimizing the solubilization and folding of BMP-2 (**Table 1, Table 2**). A concentration of 0.5-0.7M and a pH 8.0-11.0 was found to be optimal and was generally used for this step.

Table 1. Effect of different L-arginine concentrations on the recovery of total protein of crude extracts, from which rhBMP-2 is a main fraction. Similar conditions of dilution of protein and pH 8.5 were used for these recovery assays. Protein was quantified using the Bradford method. The underlined conditions were selected.

[L-Arginine] (M)	Recovery of total protein
0	32%
0.3	44%
0.5	**57%**
0.7	63%
1.0	58%

Table 2. Effect of different pH on the recovery of total protein of crude extracts, from which rhBMP-2 is a main fraction. Similar conditions of dilution of protein and a fixed concentration of 0.5 M L-arginine were used for these recovery assays. Protein was quantified using the Bradford method. The underlined conditions were selected.

pH	Recovery of total protein
3	5%
5	6%
7	35%
8	48%
8.5	**57%**
9	68%
12	91%

3.2.2. Recovery of rhBMP-2 from periplasm

Recombinant proteins expressed with pET-25, are expected to be secreted to the periplasmatic space of bacteria where cellular environment allows for the formation of dimers (Messens and Collet 2006). Therefore, as a way of establishing an easier method for the recovery of BMPs, extraction of protein from the periplasm was performed by osmotic shock:

1) Unfrozen cells from bacteria fermentations were collected and washed with PBS.
2) Osmotic solution I (2mM $CaCl_2$, 20mM Tris-HCl, 20% sucrose w/v) was added and cells incubated 10min in ice.
3) The solution was centrifuged (10min, 4ºC, 5000 g) and supernatant discarded.
4) Add slowly osmotic solution II (2mM $CaCl_2$, 20mM Tris-HCl) and cells incubated 10min in ice.
5) The solution was centrifuged (10min, 4ºC, 5000 g) and supernatant containing the periplasm protein was collected and analyzed by SDS-PAGE.

However, no protein was recovered from the periplasm in significant amounts (data not shown), even when different conditions of expression were attempted (different temperatures, different time periods, or induction with different IPTG concentrations). As a consequence, the recovery of the recombinant BMPs was solely performed with the use of L-arginine as stated in 3.2.1.

3.3 Purification of rhBMPs

3.3.1. Purification by nickel affinity chromatography

Recombinant human BMPs were purified by nickel affinity chromatography. Briefly, up to 40 mg of filtered protein were loaded into a pre-equilibrated nickel HisTrap column (Amersham) (**Figure 7**), with phosphate buffer (40mM sodium phosphate, 0.5 M NaCl) containing 20 mM imidazole. Binding of protein to the column was optimal at pH 9.0 (data not shown). The column was then washed extensively with phosphate buffer containing 80 mM imidazole, with 60-100 ml. The recombinant BMPs were eluted with 15-20 ml of sodium phosphate buffer containing 400 mM imidazole, and stored at 4ºC for short-term use, or desalted and lyophilized.

Figure 7. Nickel affinity chromatography was used for the purification of histidine-tagged recombinant human BMPs.

3.3.2. Buffer exchange and storage

Desalting is an important step prior to bioactivity assays to remove buffer salts used during the folding and purification of recombinant proteins. The removal of salts or buffer exchange was first investigated using three different methods: dialysis tubing, ultracentrifugation columns or chromatographic desalting columns. The efficacy of each method was determined by assessing the amount of salts in solution using salt conductivity, and by measuring the loss of protein during buffer exchange (data not shown). It was found that with desalting columns (Amersham, UK), the recovery of BMP-2 was much higher than with ultracentrifugation columns (Vivascience, Germany) or dialysis cassettes (Pierce, US), while providing efficient salt removal. Therefore, this method was used for the desalting of rhBMPs.

For short-term storage, the BMPs were buffer exchanged to sodium phosphate buffer with no imidazole, prior to the bioactivity assays. These solutions of protein were stored at 4ºC for up to one month. For long-term storage, lyophilization or freeze storage were used. For lyophilization, the samples were desalted, quickly frozen in liquid N_2 and freeze dried. Lyophilized protein was resuspended in PBS, at concentrations up to 0.5 mg/ml. Optionally, bovine serum albumin (1%) was added to prevent degradation and L-arginine (0.5 M) was added to aid in the solubilization. Freeze-dried protein was stored at 4ºC or at room temperature, in dry conditions.

3.4 Stability of rhBMPs

The stability of rhBMP-2 during storage was studied in different conditions. Samples of purified BMP-2 were incubated in different buffers, concentrations and pH and analyzed after a period of two weeks, 4ºC. Silver stained SDS-PAGE revealed that the protein was stable when stored in phosphate buffer, at pH 7.0-9.0 (**Figure 8**). At more acidic pH, the BMP-2 tended to precipitate, while at higher pH the protein showed degradation. In addition, the protein was also more stable when stored at concentration of 0.01-0.5 mg/ml (data not shown).

For additional information, please refer to Attach I – supplementary data.

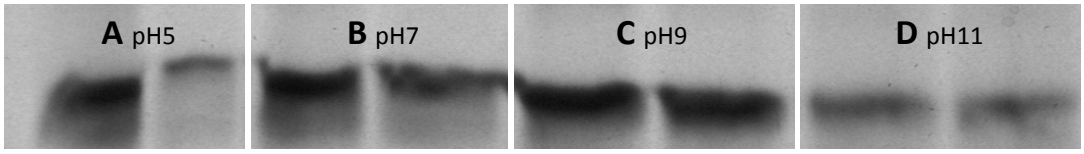

Figure 8. Silver stained SDS-PAGE showing the stability of BMP-2 in phosphate buffer, at different pH. The protein was stored for a period of two weeks at 4°C. Figure shows protein before and after centrifugation to remove precipitates. Lanes: A) protein stored in pH 5.0; B) protein stored in pH 7.0; C) protein stored in pH 9.0; D) protein stored in pH 11.0.. BMP-2 seems to be more stable and soluble when stored at pH 7.0-9.0, in phosphate buffer (B and C).

4. Assessing the bioactivity of BMPs

4.1. Bone differentiation and BMPs

During bone differentiation, bone morphogenetic proteins bind to serine-threonine cell receptors (Bessa *et al.* 2008), triggering the expression of genes involved in osteogenic differentiation.

One common assay to determine the biological activity of BMPs is to determine the enzymatic activity of alkaline phosphatase, which is a non-specific but highly upregulated gene during the differentiation to osteogenic phenotype, prior to bone mineralization (Gundberg 2000). Another method is to measure the induction of the expression of mRNA of BMP-target genes by semi-quantitative RT-PCR, having the advantage of providing more information about the extent and detail of osteogenic differentiation, at a genetic level. Different genes were assessed, including early markers such as transcriptional factors Osterix and Runx2, signaling molecules Smad-1, -5 or -3, and mineralization-related proteins such as Bone sialoprotein, Osteopontin, ALP and Osteocalcin. Finally, by performing mineralization calcium-specific

stainings such as Alizarin red or *Von Kossa*, it is possible to observe the the extent by which BMPs induce the formation of extracellular matrix of calcium phosphate, which is typical of bone formation. The morphological observation of cells was performed using a Axiovert10 (Zeiss) optical microscope with a coupled Coolpix950 (Nikon) camera.

4.2. Human adult stem cells

These cells have been shown to differentiate into osteoblasts *in vitro* when cultured with the appropriate supplements and factors such as BMPs (Skillington *et al.* 2002) To evaluate if this same behavior could still be observed when cultured with the recombinant BMPs, these cells were isolated and cultured according to the method described by Zuk *et al.* (2001). Human subcutaneous adipose tissue samples were obtained from lipoaspiration procedure. The tissue was firstly washed with PBS, 5 mg / 500 ml Ciprobay 200 (Bayer) and 10% Antibiotic-Antimycotic (Gibco, UK), and then digested with 0.2 % collagenase type I A (Sigma Aldrich, Germany) in PBS for 60 min at 37°C, in gentle stirring. The digested tissue was filtered using a 100 μm filter mesh (Sigma Aldrich, Germany) and centrifuged at 800 g for 7 min at 20°C and the supernatant eliminated. After performing the enzymatic digestion as above described, the cells were seeded in 75 cm^2 culture flasks with Basal Medium composed by DMEM (Sigma Aldrich, Germany), 10% FBS (Gibco, UK) and 1% Antibiotic-Antimycotic (Gibco, UK).

4.3. C2C12 cell line

C2C12 is a mice myoblast precursor cell line that differentiates into osteoblasts when cultured in presence of BMPs (Katagiri *et al.* 1994). C2C12 cells were originally obtained by Yaffe and Saxel (1977) through selective serial passage of myoblasts cultured from the thigh muscle of C3H mice 70 h after a crush injury. Due to its constant reliability, rapid growth and ease of manipulation, this was our standard choice for assessing the bioactivity of BMPs. In the present thesis, C2C12 were cultured in Dulbecco's modified Eagle's medium (DMEM) with 1% (v/v) fetal calf serum and 2mM L-glutamine, at 37ºC with 5% CO_2 in a humidified environment. Low serum concentration was used (1 %) to inhibit cellular proliferation. Since C2C12 cells became rapidly confluent, while differentiating into myoblasts, this occurrence was avoided, during expansion of the cell cultures. Thus, cells were generally seeded at lower densities, between 10^4 to 10^5 cells per ml, in a 24-well plate. Culture medium and BMPs were replaced every three to five days.

4.4. MTS cell viability assay

Short term cell viability screening, in response to purified BMPs was performed with the use of MTS test. The MTS test is a biochemical test widely used to assess cytotoxicity by measuring cell viability and proliferation in a qualitative way (Slater *et al.* 1963; Zeltinger *et al.* 2001). This biochemical test is based in the reduction of MTS salt (3-(4,5-dimethylthiazol-2-yl)-5-(3-carboxymethoxyphenyl)-2-(4-sulfophenyl)-2H-tetrazolium), by cell dehydrogenase mitochondrial enzymes, into a formazan product that is soluble in tissue culture medium. The salt absorbs at a wavelength of 490 nm and since only living cells have the capability of metabolize the MTS, it gives a measurement of the viable cells, and an inverse relationship of toxicity to the cells can be assumed (Mosmann 1983). Briefly, cells were incubated with a tetrazolium salt solution for 2h at 37 ºC and then absorbance read at 490 nm (Salgado *et al.* 2002). All the samples were tested in triplicate for at least two independent experiments. The results are expressed as a percentage of the control (scored as 100% viability) as mean ± standard deviation.

4.5. Alkaline phosphatase enzymatic activity

Alkaline phosphatase (ALP) hydrolyses phosphate esters and is involved in the initial processes of bone extracellular matrix mineralization. Consequently, it is widely regarded as an indicator of osteoblastic differentiation and analyzed by tests based on the hydrolysis of substrates containing phosphate. The enzymatic activity of ALP was measured by the conversion of p-nitrophenyl phosphate (pNPP) into p-nitrophenol (pNP) (Salgado *et al.* 2002). Cells were collected at each time point (n = 3) and frozen in 50 µl phosphate buffer saline at -80 ºC until further analysis. Then, cells were lysed by mixing the sample with 50 µl of PBS with 0.2 % Triton, for 1h at room temperature. The enzyme reaction was set up by mixing the sample with 50 µl of ALP-buffer containing 0.5 M 2-amino-2-methyl-1-propanol and 2 mM $MgCl_2$ (pH 10.3) and 7 mg/ml of pNPP. The solution was incubated at room temperature for 20 min and the reaction was then stopped by a solution containing 2 M NaOH and 0.2 mM EDTA in distilled water. The optical density was determined at 405 nm, with a reference filter at 620 nm. A standard curve was made using pNP solutions. The results were expressed in nmol of pNP/min/mg total protein. All samples were tested in triplicate, from at least two independent experiments. Assaying the membrane-bound ALP is much more accurate since it only quantifies the enzyme present in cells viable at the moment of the test and not the secreted enzyme which accumulates in the culture medium.

4.6. RNA extraction and RT-PCR analysis of osteoblastic markers

For RT-PCR, mRNA of cells was extracted after a specific time point in culture with TriReagent RNA Isolation Reagent (Sigma-Aldrich) from triplicate 24-well assays following the supplier instructions. Briefly, 500 µl of TriZol were added to each sample containing approx. 10^5 cells per ml. After an incubation of 5 minutes, additional 160 µl of chloroform (Sigma Aldrich, Germany) were added; the samples were then incubated for 15 min at 4 °C and centrifuged at the same temperature and 10000 g for 15 min. After the centrifugation, the aqueous part was collected and an equal part of isopropanol (Sigma Aldrich, Germany) was added. After an incubation of 2 hours at -20 °C the samples were washed in ethanol, centrifuged at 4 °C and 7000 g for 5 min and resuspended in 12 µl of water RNase/DNase free (Gibco, UK). The samples were then quantified using a NanoDrop ND-1000 Spectrophotometer (NanoDrop Technologies, USA) and cDNA was synthesized from 4 µg total RNA (A_{260nm} / A_{280nm} ratio between 1.7-2.0) with oligo dT primer (MWG Biotech AG) and AMV reverse transcriptase (Promega). The polymerase chain reaction (PCR) was performed with specific primers for osteogenic markers and with the use of HotStar Taq Polymerase (Qiagen). Agarose gels were imaged with MultiImage Light Cabinet (Alpha Innotech, USA) and gene expression analyzed with ChemiImage 4400 AlphaEase FC Image Analysis Software (Alpha Innotech, USA) and using polymerase II for normalizing gene expression, as housekeeping marker.

4.7. Mineralization assay: Alizarin Red staining

For both mineralization assays, cell cultures were seeded at low seeding density (3 x 10^4 cells/ ml) and grown for a period of two weeks in the presence of BMPs and with 1% serum DMEM culture media, supplemented with 10 mM β-glycerophosphate and 100 µM ascorbic acid (Sigma, USA). The Alizarin Red mineralization test was performed using the method described by Bodine *et al.* (1996), with modifications. Cells were washed for three times with PBS (with no Ca^{2+}, Mg^{2+}), and subjected to a fixative 4% v/v solution of formaldehyde in PBS for 30 min. After removal of fixative, cells were washed twice with distilled water and covered with Alizarin Red (AR) 1% solution, followed by gentle agitation in an orbital shaker for 10 min. The AR solution was then removed and the cells washed four times with distilled water. The cells were observed in a Axiovert10 (Zeiss) optical microscope with a coupled Coolpix950 (Nikon) camera.

The mineralization staining was quantified by the method proposed by Gregory *et al*. (2004). Briefly, the calcium from cells was extracted by incubation of 800 µl acetic acid (10% v/v) to each well, for 30 min in a orbital shaker. Then, the suspensions were transferred to a clean 1.5 ml eppendorf and vortexed for 30 sec; 500 µl of mineral oil was added and the

suspensions heated at 85 ºC for 10 min and then cooled in ice for 5 min. The suspensions were centrifuged (20 min, 10000 g), the supernatant carefully removed, and 200 µl ammonium hydroxide (10%) added (until pH ~4.1). The solutions were read for absorbance at 405 nm, in a Spectra III spectrophotometer (SLT, Austria).

5. Production of silk fibroin and elastin particles for BMP delivery

5.1. Development of fibroin microparticles

5.1.1. Isolation of silk fibroin

Silk fibroin was first isolated from *Bombyx mori* cocoons after a standard degumming protocol, with modifications (Zhang *et al.* 2007), for the removal of silk sericin. The cocoon shells of silkworm *Bombyx mori* were degummed twice in boiling solution of 0.5 % Na_2CO_3 for 0.5 h, at 90 ºC, and the resulting degummed fiber was subsequently dissolved in a ternary system, i.e. a mixed solution of calcium chloride, ethanol and water ($CaCl_2$ / C_2H_5OH / H_2O: 1:2:8 mole ratio) at 90ºC for 6 h. The solution was then filtered (0.22 µm, Rotilab, Germany), and the solution was extensively dialyzed, using a cellulose semi-permeable (molecular weight cut-off = 12,000 kDa) membrane, against distilled water to remove $CaCl_2$, smaller molecules and impurities. The silk fibroin was lyophilized and used for the preparation of microparticles.

5.1.2. Microparticle preparation and loading of BMPs

Silk fibroin microparticles were prepared by ethanol precipitation according to the method described by Cao and colleagues (2007), with modifications. A solution of approximately 1% (w/v) fibroin in phosphate buffer saline (PBS, pH 7.4) was prepared (5 ml) and filtered with a 0.22 µm PVDF membrane filter (Rotilab, Germany). Then, 5 µg/ml or 50 µg/ml BMP-2, BMP-9 or BMP-14 were added (approximately 5 or 0.5 µg BMP per mg of fibroin). The solution was incubated at room temperature with stirring (600 rpm). Absolute ethanol was added dropwise to a ratio of 1:2 to the initial volume of silk fibroin, and the solution incubated overnight at -20 ºC. Different ratios were also tested for a comparative study of the particles size. The resulting microparticles (**Figure 9**) were collected by centrifugation at 4000 g, 4ºC, for 5 min, washed, and stored at 4ºC or lyophilized, after quick-freezing in liquid nitrogen, in a Christ Alpha 1-4 (Linder, Austria) lyophilizer. Sterile conditions were used during the entire procedure.

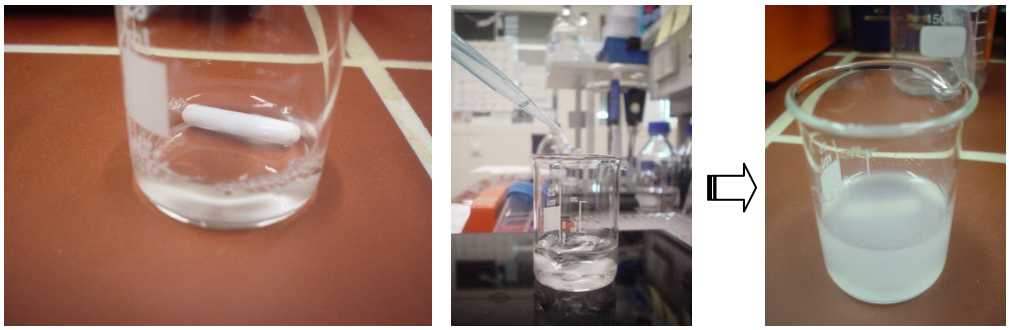

Figure 9. Silk fibroin microparticles, for loading and delivery of rhBMPs, were formed after dropwise addition of ethanol and overnight incubation at - 20 ºC.

5.2. Development of elastin-like nanoparticles

5.2.1. Nanoparticle preparation

The elastin-like polymer, $(VPAVG)_{220}$ consists of 220 repeats of the main monomer VPAVG and was produced by recombinant technology and purified as reported elsewhere (Machado *et al.* 2009). Particles were produced by resuspending lyophilized polymer in ice-cold phosphate buffer saline (PBS) to a final solution of 0.1%. The solution was then incubated at 37 ºC for 30 min. Particles were collected by centrifugation (10000 g, 37 ºC, 10 min), and washed once with pre-warmed PBS. Due to its hysteresis behavior, the particles are stable at room temperature and only solubilize when a strong undercooling is achieved (of about 6 to 8 ºC). The particles were prepared under sterile conditions, and stored at room temperature.

5.2.2. BMP loading

Elastin nanoparticles were loaded with a mix or single BMP-2 and BMP-14, during the formation of the particles. Growth factor was added at a concentration of 20 µg/ml to the elastin solution. The nanoparticles were produced with the different combinations of the two growth factors:

I) Unloaded particles (no growth factor)

II) BMP-2 encapsulated

III) BMP-14 encapsulated

IV) BMP-2 and BMP-14 encapsulated

5.3. Characterization of the developed particles

5.3.1. Morphological characterization

The particles were morphologically characterized by scanning electron microscopy (SEM). SEM analysis was performed on gold-coated air-dried samples (Agar Sputercoater 108, Essex, UK) and using a Philips XL20 microscope (Philips, Eidhoven, NL). Particle size measurements were obtained from different micrographs acquired in the SEM.

5.3.2. Size distribution

Measurements of particle size were performed on freshly prepared microparticle solution by dynamic light scattering (DLS), using a Zetasizer NanoZS (Malvern, UK). Each sample was diluted to an appropriate concentration with filtered (0.2 µm filters Millex-GN, Millipore) ultrapure water. Each analysis lasted 60 s and was performed at 25 ºC.

5.3.3. Water uptake

The hydration degree of silk fibroin and elastin particles was evaluated after immersion into PBS, pH 7.4. All experiments were conducted at 37 ºC, in triplicate. Percentage of water uptake (WU) after each time period of immersion (t) was calculated using the following equation:

WU (%)=(Ww-Wd) / Wd x 100

'Wd' and 'Ww' correspond to the weight of the particles in dry and wet state, respectively.

5.4. Release of BMPs

5.4.1. Determination of loading capacity and encapsulation efficiency

The particle encapsulation efficiency was determined upon their separation from the aqueous preparation medium containing the non-associated protein by centrifugation (10000 g, 10 min). The amount of free BMP-2 was determined in the supernatant by using a BMP-2 sandwich-type ELISA development kit (Eubio, Austria). The amount of free BMP-9 and BMP-14 was estimated by dot blot. The blot intensities were compared with standards of known concentration, using image software analysis (ChemiImage 4400, Alpha Innotech, US). Each sample was assayed in triplicate (n = 3). The particle encapsulation efficiency (E.E.) and BMP loading capacity (L.C) were calculated using the following equations:

$$E.E.(\%) = \frac{\text{Total BMP amount (µg)} - \text{Free BMP amount (µg)}}{\text{Total BMP amount}} \times 100$$

$$L.C.(\mu g\ BMP\ /\ mg\ particles) = \frac{\text{Total BMP amount (µg)} - \text{Free BMP amount (µg)}}{\text{Microparticles weight (mg)}}$$

5.4.2. *In vitro* release

In vitro release studies were conducted in phosphate buffer saline (PBS), pH 7.4. Particles were incubated in PBS, at 37 ºC, with 200 rpm agitation. At pre-determined time points, a sample from the solution was removed, centrifuged and stored at -20 ºC until measurement. The solution was replaced with a similar volume of fresh buffer. Sterile conditions were used to prevent any contamination of samples.

5.4.3. Quantification of released BMPs

For measurement of BMP-2 concentration, a BMP-2 sandwich-type ELISA kit (Eubio, Austria) was used, following the manufacturer's instructions. A calibration curve was obtained using standard preparations of BMP-2 of known concentration. For detection of the concentration of BMP-9 and BMP-14, the samples were estimated by dot blot as described before. Each sample was assayed in triplicate (n = 3) and mean ± SD values reported.

5.4.4. Release kinetics models

To study the release kinetics, the data obtained from the *in vitro* release was treated accordingly to zero order as cumulative amount of drug released *vs*. time (equation 1), first order as log cumulative percent drug remaining *vs*. time (equation 2), Higuchi kinetics as cumulative percent drug released *vs*. square root of time (equation 3) and Korsmeyer kinetics as log cumulative percent drug released *vs*. log time (equation 4) (Huguchi 1963, Chowdary and Ramesh 1993, Hadjiioannou *et al*. 1993, Bourne 2002):

$R = k_1 t$ (1)

$\text{Log } UR = k_2 t\ 2.303$ (2)

$R = k_3 t\ 0.5$ (3)

$\text{Log } R = \log k_4 + n \log t$ (4)

where R and UR are released and unreleased percentages, respectively, at time (t); k_1, k_2, k_3 and k_4 are the rate constants of zero-order, first order, Higuchi and Korsmeyer models, respectively; n is a exponent that characterizes the mechanism of release.

5.5. *In vitro* bioactivity

When a molecule is incorporated inside a release system, it is vital that its biological activity is maintained throughout loading, incorporation and release. For released BMPs, the maintenance of its bioactivity was measured by the induction of ALP activity in C2C12 cell line. C2C12 cells were incubated with the fibroin or elastin particles containing specific amounts of loaded BMPs. Growth factor was used to the culture media, as a positive control. Alkaline phosphatase (ALP) activity was measured accordingly to described in section 4.5, after 5 days of cell culture. Cell viability was evaluated, as described in section 4.4, by incubating specific amounts of particles into the cell cultures.

5.6. *In vivo* bioactivity (silk fibroin particles)

5.6.1. Rat ectopic bone formation model

The bioactivity of delivered BMP-2 in fibroin particles was assessed *in vivo* using a rat ectopic bone formation model. Male Sprague-Dawley rats (weighting 340-360 g), were purchased from the Institut für Labortiertechnik und -genetik (Himberg, Austria). They were housed in light and temperature-controlled facilities and given food and water *ad libitum*. In three animals, surgery was performed after general anesthesia with an intramuscular injection of 60 mg/kg of body weight (BW) ketamine (Ketavet®, Pharmacia, Erlangen, Germany) and 7.5 mg/kg BW xylazine (Rompun®, Bayer, Leverkusen, Germany). After shaving and disinfecting the dorsum of the animals, four midsagittal incisions were made dorsally in the proximal area of each limb and subcutaneous pockets were created by blunt dissection. The fibroin particles were implanted subcutaneously into each pocket. Three groups were defined: group I (unloaded particles), group II (particles + 5 µg BMP-2) and group III (particles + 12.5 µg BMP-2). The animals were randomized and were implanted with four samples (n = 4) per each group. Only one group was assigned to each animal to avoid the potential interference of released BMP by blood circulation. After placement of the particles, the incisions were closed with sutures, and the wound covered with vapor-permeable spray dressing (Opsite®, Smith & Nephew, London, UK). Analgesia treatment was given post operation, of 0.01 mg/kg BW Buprenorphin. At the end of each implantation period (4 weeks), the animals were sacrificed

and samples from the tissues surrounding the implantation site were harvested. The animal protocol was approved by the authority of the city government of Vienna.

5.6.2. *In vivo* microCT

Live microCT (vivaCT 75, Scanco Medical AG, Switzerland) was used to examine bone formation in individual rats. MicroCT imaging was performed at weeks 2 and 4 respectively. Rats were anesthetized for 5 min with 2 % isoflurane during measurement. No X-ray contrast media was used in this study. Image reconstruction was performed using the built-in 3D visualization software (Scanco Medical AG, Switzerland). The evaluation of newly formed bone and bone density were performed using IPL version v5.06b (Scanco Medical AG, Switzerland).

5.6.3. Histological analysis

Harvested samples were fixed in neutral buffered 10 % formalin and embedded in paraffin. Three-micrometer or four-micrometer sections were cut and stained with hematoxylin and eosin (H & E) or Alizarin Red S, respectively, for light microscopy observation. For a detailed analysis of the tissue differentiation, immunohistochemical staining was performed in selected samples. Briefly, paraffin sections were dewaxed with xylene and rehydrated in a graded ethanol series. After enzymatic antigen retrieval with 0.1 % Proteinase (Sigma Aldrich, USA) sections were incubated with an Osteocalcin antibody (Santa Cruz Biotechnology, USA) in a humidified chamber at 4 ºC overnight. After rinsing, sections were incubated with the EnVision™ system (Dako, Denmark) at room temperature for 30 min. and immunoreactivity was visualized with AEC solution (Thermo Fisher Scientific, USA). Slides known to express Osteocalcin were used as positive controls, omitting of the primary antibody served as negative control.

6. Statistical analysis

In the scope of this thesis, experiments were performed at least in triplicate and expressed as means ± standard deviations. Student's t test was used for statistical analysis. Statistical significance was defined as $p < 0.01$ or $p < 0.05$ for a 99% or a 95% confidence.

References

Bessa PC, Casal M and Reis RL. Bone morphogenetic proteins in tissue engineering: the road from laboratory to the clinic, part I (basic concepts). J Tissue Eng Regen Med. 2, 1-13, 2008.

Bodine PV, Trailsmith M, Komm BS. Development and characterization of a conditionally transformed adult human osteoblastic cell line. Journal of Bone Mineral Research 11, 806-819, 1996.

Bourne DW. Pharmacokinetics. In: Banker GS, Rhodes C, eds Modern Pharmaceutics. 4th ed. New York, NY, Marcel Dekker Inc. 67-92, 2002.

Cao Z, Chen X, Yao J, *et al.* The preparation of regenerated silk fibroin microspheres. Soft Matter 3, 910-915, 2007.

Chowdary KP and Ramesh KV. Studies on microencapsulation of diltiazem. J Pharm Sci 55, 52-4, 1993.

Gregory CA, Gunn WG, Peister A, *et al.* An Alizarin red-based assay of mineralization by adherent cells in culture: comparison with cetylpyridinium chloride extraction. Anal Biochem. 329, 77-84, 2004.

Gundberg CM, Biochemical markers of bone formation. Clin Lab Med. 20, 489-501, 2000.

Hadjiioannou TP, Christian GD, Koupparism MA. Quantitative calculations in pharmaceutical practice and research. New York, NY, VCH Publishers Inc. 345-348, 1993.

Higuchi T. Mechanism of sustained action medication. Theorical analysis of rate of release of solid drugs dispersed in solid matrices. J. Pharm Sci. 52, 1145-1149, 1963.

Katagiri T, Yamaguchi A, Komaki M, *et al.* Bone morphogenetic protein-2 converts the differentiation pathway of C2C12 myoblasts into the osteoblast lineage. J Cell Biol. 127, 1755-66, 1994.

Machado R, Ribeiro AJ, Padrão J *et al.* Exploiting the sequence of naturally occuring elastin: construction, production and characterization of a recombinant thermoplastic protein-based polymer. Journal of NanoResearch 6, 133-145, 2009.

Messens J and Collet JF. Pathways of disulfide bond formation in *Escherichia coli*. Int J Biochem Cell Biol. 38, 1050-62, 2006.

Mosmann T. Rapid colorimetric assay for cellular growth and survival: application to proliferation and cytotoxicity assays. J Immunol Methods 65, 55-63, 1983.

Salgado AJ, Gomes ME, Chou A, *et al.* Preliminary study on the adhesion and proliferation of human osteoblasts on starch-based scaffolds. Materials Science & Engineering C-Biomimetic and Supramolecular Systems 20, 27-33, 2002.

Sanger F, Nicklen S and Coulson AR DNA sequencing with chain-terminating inhibitors. Proc. Natl. Acad. Sci. USA 74, 5463-5467, 1977.

Skillington J, Choy L, Derynck R. Bone morphogenetic protein and retinoic acid signaling cooperate to induce osteoblast differentiation of preadipocytes. Journal of Cell Biology, 159, 135-146, 2002.

Slater TF, Sawyer B, Strauli U. Studies on succinate-tetrazolium reductase systems. III. Points of coupling of four different tetrazolium salts. Biochim Biophys Acta 77, 383-393, 1963.

Studier FW, Moffatt BA. Use of bacteriophage T7 RNA polymerase to direct selective high-level expression of cloned genes. J. Mol Biol. 189, 113-30, 1986.

Studier FW, Rosenberg AH, Dunn JJ, *et al.* Use of T7 RNA polymerase to direct expression of cloned genes. Methods Enzymol. 185, 60-89, 1990.

Studier FW. Use of bacteriophage T7 lysozyme to improve an inducible T7 expression system. J. Mol Biol. 219, 37-44, 1991.

Vallejo LF and Rinas U. Strategies for the recovery of active proteins through refolding of bacterial inclusion body proteins. Microb. Cell Fact. 3, 11, 2004.

Yaffe D and Saxel O. Serial passaging and differentiation of myogenic cells isolated from dystrophic mouse muscle. Nature 270, 725-7, 1977.

Zeltinger J, Sherwood JK, Graham DA, *et al.* Effect of pore size and void fraction on cellular adhesion, proliferation and matrix deposition. Tissue Eng 7, 557-572, 2001.

Zhang YQ, Shen WD, Xiang RL *et al.* Formation of silk fibroin nanoparticles in water miscible organic solvent and their characterization. Journal of Nanoparticle Research 9, 885-900, 2007.

Zuk PA, Zhu M, Mizuno H, *et al.* Multilineage cells from human adipose tissue: implications for cell-based therapies. Tissue Eng 7, 211, 2001.

SECTION 3

Chapter IV

Osteoinduction in human fat derived stem cells by recombinant human bone morphogenetic protein-2 produced in *Escherichia coli*

This Chapter is based on the following publication:

Bessa PC, Pedro AJ, Klösch B, Nobre A, van Griensven M, Reis RL and Casal M, 2008, Osteoinduction in human fat derived stem cells by recombinant human bone morphogenetic protein-2 produced in *Escherichia coli*, Biotechnology Letters **30**, 15-21

Chapter IV

Osteoinduction in human fat derived stem cells by recombinant human bone morphogenetic protein-2 produced in *Escherichia coli*

Abstract

Bioactive recombinant human bone morphogenetic protein-2 (rhBMP-2) creating an alternative to the time-consuming methods of inclusion bodies preparation was obtained using *Escherichia coli* pET-25b expression system. 55 mg purified rhBMP-2 were achieved per gram cell dry weight, with up to 95% purity. In murine C2C12 cell line, rhBMP-2 induced an increase in the transcription of Smads and of osteogenic markers Runx2/Cbfa1 and Osterix, measured by semi-quantitative RT-PCR. Bioassays performed in human fat derived stem cells showed increase activity of early osteogenic marker alkaline phosphatase and absence of cytotoxicity.

1. Introduction

Bone morphogenetic proteins (BMPs) are a group of cytokines from the TGF-β superfamily (Wozney *et al.* 1988) with strong ability to induce bone and cartilage formation (Urist 1965, Reddi 1998). BMPs have been used as powerful osteoinductive components in several late-stage tissue engineering products for bone grafting (Westerhuis *et al.* 2005).

During the process of bone healing, signals from BMPs trigger the differentiation of stem cells into bone forming cells that are recruited to the site of injury (Reddi 1981). BMPs bind to serine-threonine kinase cell receptors and mediate their signals through Smad related cascades and Smad-independent pathways (Derynck 2001, Shi & Massague 2003). Signal is regulated by different factors such as binding to cell surface receptors (Kirsch *et al.* 2000, Sebald *et al.* 2004), formation of BMP-heterodimers (Israel *et al.* 1996), presence of antagonists such as Noggin (Groppe *et al.* 2002), cross-talk with other pathways (Miyazono *et al.* 2005) and the presence of a heparin binding domain in the N-terminal region of BMP-2 which provides anchorage of the cytokine to the extracellular matrix (Ruppert *et al.* 1996, Kubler *et al.* 1999, Wurzler *et al.* 2004).

Currently, most BMPs are obtained from mammalian cell cultures in low yields (Wang *et al.* 1990, Israel *et al.* 1992) or from bacteria inclusion bodies after time-consuming refolding procedures (Kubler *et al.* 1998, Vallejo *et al.* 2002, Long *et al.* 2006). Aiming to circumvent the

disadvantages of the previously reported methods, we have developed a novel approach for the production of high amounts of soluble and pure rhBMP-2, with bioactivity verified in murine myoblast C2C12 cell line as well as in human fat derived adult stem cells.

2. Materials and methods

2.1. Cloning of rhBMP-2

The sequence coding for the mature (bioactive) domain of human BMP-2 was obtained from a bacterial clone (Sanger Institute, UK), containing locus 20p12.1-13 of chromosome 20 of human genome, which includes the entire gene for human BMP-2 (clone ref. RP5-859D4). According to the data in Human Genome Project (http://www.ensembl.org/homo_sapiens), the entire human BMP-2 gene (Ensembl gene OTTHUMG00000031833) includes three exons and two introns with the open reading frame located on exons 2 and 3. By consulting UniProtKB/Swiss-Prot, human BMP-2 protein (P12643) mature domain consists of amino acids 283-396, which is obtained after cleavage from propeptide (Hillger *et al.* 2005). The region corresponding to the mature domain is located solely in exon 3 and, for this reason, we have cloned directly by PCR this sequence from the above mentioned clone (**Figure 1A**). Mature domain was amplified by PCR using primers 5' CGG GAT CCA **CAA** GCC AAA CAC AAA CAG C 3' (forward primer) and 5' CCC TCG AG**G CG**A CAC CCA CAA CCC TC 3' (reverse primer). The nucleotides for cleavage by *BamH*I and *Xho*I in forward primer and reverse primers are underlined, respectively; the codons corresponding to amino acids 283 and 396 are represented in bold. PCR-product was first cloned into pGEM T-Easy vector (Promega, USA) and then subcloned in a pET-25b vector (Novagen, USA) via the two restriction sites, *BamH*I and *Xho*I (plasmid pET-25b/rhBMP-2), that was used to transform *E .coli* BL21(DE3) strain (Invitrogen, UK). DNA cloning and manipulation were performed according to standard protocols (Sambrook et al 1989). The integrity of cloned PCR products was verified by DNA sequencing (Sanger *et al.* 1977) using ABI PRISM310 Genetic Analyzer.

2.2. Expression of rhBMP-2 in bioreactor

Transformed *E. coli* BL21(DE3) strain with pET-25b/rhBMP-2 or pET-25b vectors were picked and transferred into 50 ml Luria Bertani (LB) media with 50 µg ampicillin/ml and incubated at 37 ºC for 1-2h. Pre-cultures were then transferred to a pre-autoclaved 2 L Bioflo110 bioreactor (New Brunswick Scientific, USA) containing LB media with 50 µg ampicillin/ml and cultured at 37 ºC until an OD_{600} of 1.0. 1 mM IPTG was then added and temperature lowered to 25 ºC. During the entire process, aeration was kept at 2 L/min and an

agitation cascade between 300 and 1000 rpm was selected in order to maintain minimum dissolved oxygen levels at 30% of saturation. The pH 7.4 was kept constant using solutions of ammonium hydroxide (30%, v/v) and phosphoric acid (5 M) pumped into the bioreactor vessel. Biomass was collected by centrifugation (4000 g, 20 min, 4 ºC), washed once with PBS and stored at -20 ºC.

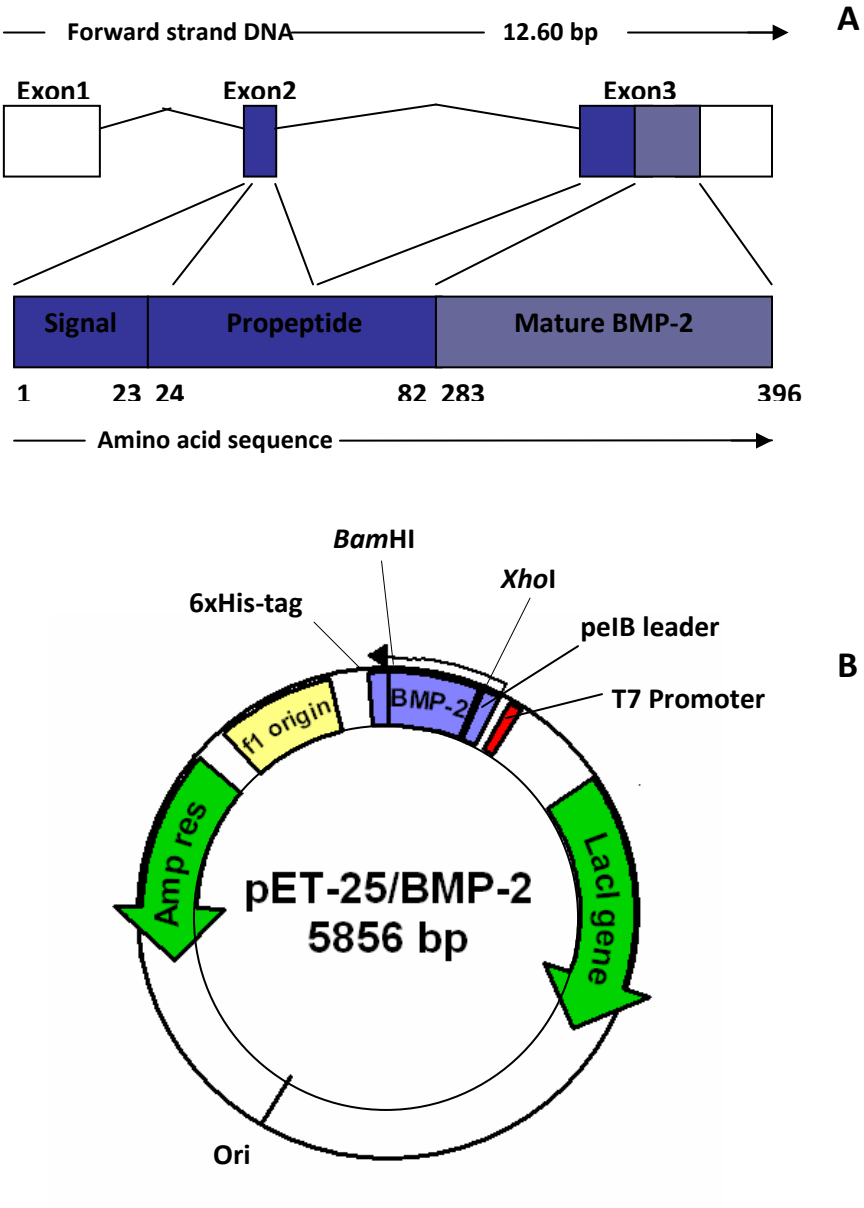

Figure 1. Strategy used for cloning the mature domain of human bone morphogenetic protein-2. A) BMP-2 gene contains three exons represented by boxes and two introns corresponding to the lines. Coding region is represented by black boxes located in exon 2 and 3. The mature domain of human BMP-2 protein is entirely located on exons 3 correspondent to amino acids 283 to 396. B) Construction of vector pET-25b/rhBMP-2 for expression of human BMP-2 in *E. coli*. The mature BMP-2 was cloned into the vector pET-25b together with its own leader sequence and 6-histidine tag for purification.

2.3. Purification of rhBMP-2

Frozen bacteria were resuspended in lyses buffer (20 mM sodium phosphate buffer, 0.5 M NaCl, 1 mg/ml lysozyme), with inhibitor of proteases (Complete Mini EDTA-free, Roche). Bacteria were ultrasonicated 4 times for 15 s with intervals of 1 min on ice and supernatant and pellet fractions collected by centrifugation (4000 g, 30 min, 4 ºC). The pellet was then incubated overnight in solubilization buffer (phosphate saline buffer, 40 mM imidazole, 0.7 M L-arginine, pH 11.0) at 18 ºC with gentle stirring and the supernatant containing soluble rhBMP-2 collected after centrifugation (4000 g, 4 ºC, and 30 min). The supernatant was adjusted to pH 8.5 with 0.1M HCl and applied to a pre-equilibrated HisTrap chromatography column (Amersham). Briefly, column was equilibrated with 5 column volumes of sodium phosphate buffer containing 40 mM imidazole. The column was washed extensively with 60-80 ml of sodium phosphate buffer containing 80 mM imidazole and sample eluted in 15 ml of sodium phosphate buffer containing 500 mM imidazole. A flow rate of 5 ml/min was kept during the whole procedure by the use of a peristaltic pump. Samples were analyzed by SDS-PAGE and Western-blot. Imidazole was removed by buffer exchange to phosphate buffer saline with use of a HiTrap desalting column (Amersham) prior to bioactivity tests.

2.4. Analytical detection of rhBMP-2 by reducing and non-reducing SDS-PAGE and Western-blot

Protein samples were mixed with SDS-PAGE loading buffer and heated at 95 °C for 5 min. Samples were separated by using hand-cast 10-12 % SDS–PAGE gels in reducing or non- reducing conditions. Reducing conditions included the use of SDS-PAGE loading buffer with 5 % β-mercaptoethanol as reducing agent. Coomassie blue-R or silver staining was used for visualization and staining of gels. Samples were then electro-transferred (semi-dry Western-blot transfer) to a nitrocellulose membrane at 400 mA, 10 V for 30 min. The membranes were blocked with 2 % BSA in PBS-T buffer (PBS, 0.05 % Tween 20) and incubated either with peroxidase conjugated anti-His antibody (Sigma) diluted 1:5000 or rabbit anti-human BMP-2 polyclonal primary antibody (AbD Serotec) diluted 1:5000 followed by mouse anti-rabbit peroxidase conjugated secondary antibody (Amersham) diluted 1:30000. Image detection was performed with ChemiDoc XRS and Quantity One software (BioRad).

2.5. Bioactivity tests

C2C12 cells were seeded at 10^5 cells/ml per well in a 24-well plate, attached overnight in Dulbecco's modified Eagle's medium (DMEM) with 1 % fetal calf serum and no antibiotics, at 37 ºC with 5 % CO_2 in a humidified environment. Cells were incubated for 5 days with rhBMP-2

purified by the method described above and a commercial rhBMP-2 (Wyeth, USA) used as control. Primary cultures of human fat tissue derived stem cells (Malafaya *et al.* 2005, Zuk *et al.* 2002) were seeded at 10^5 cells/ml per well in a 24-well plate and attached overnight in DMEM with 50 µg/ml ascorbic acid, 10 mM β-glycerophosphate, 100 U/ml penicillin, 100 µg/ml streptomycin and 10 % fetal bovine serum at 37 ºC in 10 % CO_2. Cells were incubated for 14 days with rhBMP-2 purified by our method, with media replacement every two days. Alkaline phosphatase (ALP) enzymatic activity was determined accordingly to standard procedures (Salgado *et al.* 2002) after 5 days on C2C12 cell line cultures and after 3, 7 and 14 days on cell cultures of mesenchymal stem cells. MTS cell viability assay was determined after 3, 7 and 14 days of cell culture in human stem cells (Salgado *et al.* 2002). For RT-PCR, mRNA of C2C12 cells was extracted after 5 days of cell culture with TriReagent RNA Isolation Reagent (Sigma-Aldrich) and cDNA was synthesized from 4 µg total RNA with oligo dT primer (MWG Biotech AG) and AMV reverse transcriptase (Promega). The polymerase chain reaction (PCR) was performed with specific primers for osteogenic markers (**Table 1**) and with use of a Hot Star Taq Polymerase (Qiagen). Agarose gels were imaged with MultiImage Light Cabinet (Alpha Innotech, USA) and gene expression analyzed with ChemiImage 4400 AlphaEase FC Image Analysis Software (Alpha Innotech, USA) and using polymerase II for normalizing expression.

Table 1. Oligonucleotide primers for semi-quantitative RT-PCR analysis in murine C2C12 cells.

Gene marker	Primer sequence: Sense/ Antisense
Runx2/Cbfa1	5’ GCC GCA GTG CCC CGA TTG AGG 3’
	5’ AGG GAG GGC CTG GGG TTC TGA GG 3’
Smad-1	5’ CCC ACC TGC TTA CCT GCC TCC TGA 3’
	5’ TGG GGT GAA AGC CGT GGT GGT AGT 3’
Smad-5	5’ AAT GGG CAG AAA AGG CAG TGG ATG 3’
	5’ AGC GTT GTT GGG TTG GTG GAA AGA 3’
Osterix	5’ GCA GTG GGG CAG GGC GTT CTA CC 3’
	5’ GGG GCG GCT GAT TGG CTT CTT CTT 3’
Osteocalcin	5’ ATT CAT ATG AGG ACC CTC TCT CTG 3’
	5’ ATT AGA TCT CTA ATG ATG ATG ATG ATG ATG AAT AGT GAT ACC GTA GAT 3’
ALP	5’ CAC GCG ATG CAA CAC CAC TCA GG 3’
	5’ GCA TGT CCC CGG GCT CAA AGA 3’
Polymerase II	5’ TAC ACC CCA GCT TCT CCC AAA TAC 3’
	5’ AGC TCT TCG CCC TGT TCG 3’

3. Results

3.1. Cloning, expression and purification of rhBMP-2

The PCR gave a single product of the coding region of human BMP-2, with expected size of 359 bp (data not shown). DNA sequencing revealed a total correspondence to the encoded amino acids (Ensembl gene OTTHUMG00000031833). **Figure 1B** shows the map of the expression vector pET-25b/rhBMP-2 used for transformation of bacteria. *E. coli* BL21 (DE3) strain transformants were grown and collected in conditions described in Material and Methods section. After bacteria lyses, rhBMP-2 was found mainly in the pellet (fraction corresponding to bacterial debris) (**Figure 2A**). Soluble protein was then recovered with phosphate buffer containing 0.7M L-arginine, pH 11.0. Purification procedures revealed that rhBMP-2 was expressed in monomer, dimer and polymer forms visible in Western-blot using antibodies anti-histidine tag and anti-BMP-2. Silver stained SDS-PAGE revealed up to 95 % purity (**Figure 2B**). RhBMP-2 stored in 20mM phosphate sodium, 0.5M NaCl was found to be stable over two months at pH range of 7-9 (data not shown).

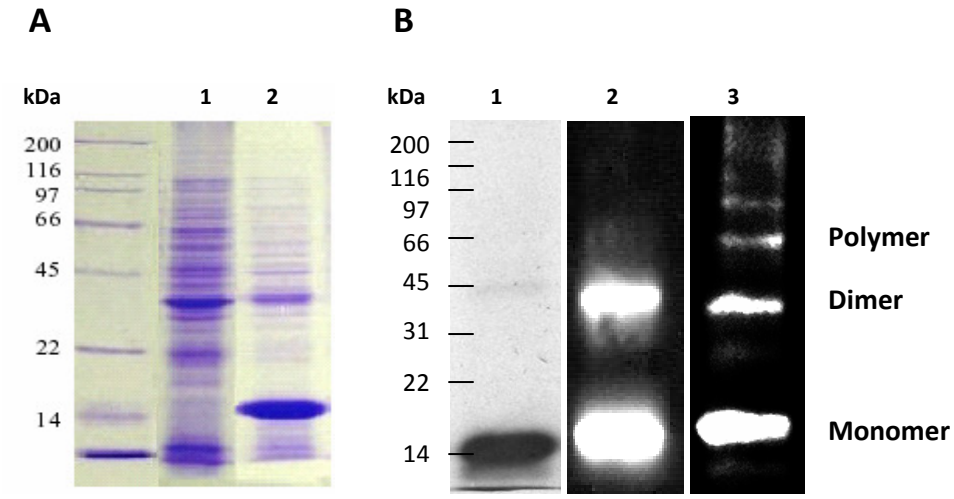

Figure 2. A) Coomassie-blue stained SDS-PAGE of crude lysates, pellet fraction, from batch cultivation of transformed *E. coli*. Lanes 1) pET-25b clone; 2) rhBMP-2/pET-25b clone. Monomer appears as a well-defined band around 17 kDa. Molecular weight is in kDa (Broad Range, BioRad). B) rhBMP-2 purified by affinity chromatography: 1) Silver stained reduced SDS-PAGE, showing the monomer of BMP-2 with significant purity; 2) Western-blot using anti-his tag antibody; 3) Western-blot using anti-BMP-2 antibody. BMP-2 is visible in monomer, dimer and polymer.

3.2. Biological activity in C2C12 cells

Bioassays were performed in murine myoblast C2C12 cell line, by the administration of purified rhBMP-2. Semi-quantitative RT-PCR revealed an increase of expression of early osteoblast differentiation markers after 5 days of cell culture, such as the osteochondral transcription factor Runx2/Cbfa1 (by 2-3 fold), Smad-1 and -5 (up to 1.5 fold) and osteoblast transcription factor Osterix (up to 1.5 fold). In these tests, the levels of ALP mRNA did not changed significantly. Commercial mammalian rhBMP-2 induced markedly Runx2/Cbfa1 by 3-7 fold, Smad-1 and Smad-5 by 2-5 fold, Osterix by 2-4 fold, Osteocalcin by 2-9 fold and high levels of ALP expression were detected (**Figure 3**).

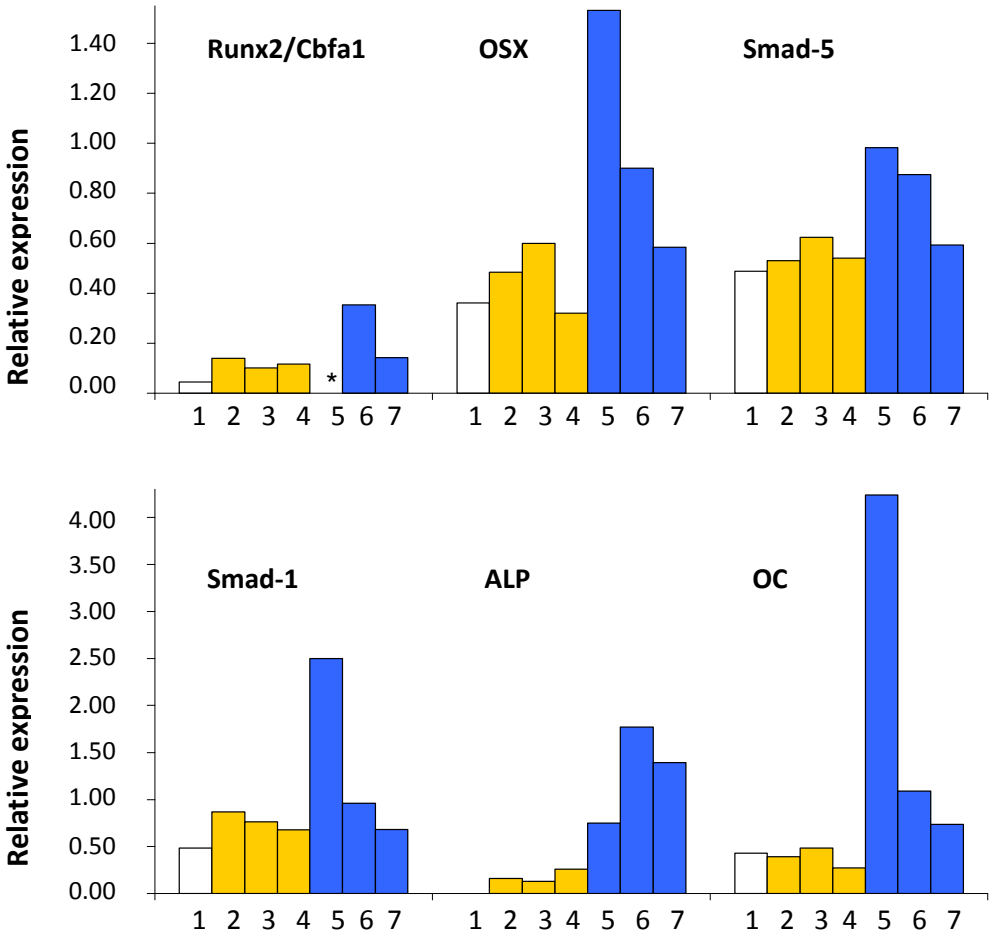

Figure. 3. RT-PCR for genes involved during osteoblast differentiation of C2C12 cells after 5 days of culture with purified rhBMP-2 and commercial mammalian rhBMP-2 as control. Gene expression was analyzed with ChemiImage 4400 AlphaEase FC Image Analysis Software (Alpha Innotech) and standardized with Polymerase II expression. OSX: osterix; OC: osteocalcin; ALP: alkaline phosphatase. Conditions used: 1) No rhBMP-2; 2) 250 ng/ml; 3) 500 ng/ml; 4) 1000 ng/ml; 5) 250 ng/ml commercial preparation; 6) 500 ng/ml commercial preparation; 7) 1000 ng/ml commercial preparation. Data presented are mean values of two independent experiments. (* bioassay was not performed)

3.3. Biological activity in mesenchymal stem cells

RhBMP-2 did not show any significant evidence of cytotoxicity in human mesenchymal stem cells after two weeks of cell culture (**Figure 4A**). MTS is a viability/proliferation test and an inverse relationship of toxicity to cells can be assumed. In human primary cultures of fat derived stem cells, there was an increase in levels of ALP enzymatic activity (**Figure 4B**). Data correlates with morphological observations of the cells with optical microscopy (**Figure 5**).

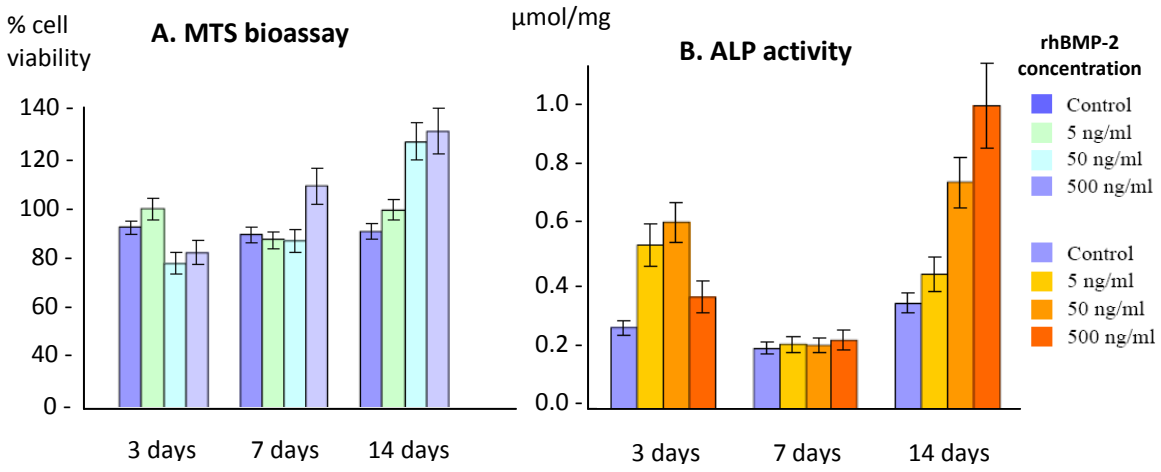

Figure 4. A) Tetrazolium salt (MTS) test performed in fat tissue derived human stem cells as a function of rhBMP-2 concentration, after 3, 7 and 14 days of cell culture. Cell viability is expressed in percentage. B) Bioactivity of rhBMP-2 as measured by the induction of alkaline phosphatase activity in fat tissue derived human stem cells. ALP activity levels are expressed in µmol ALP per mg of total protein.

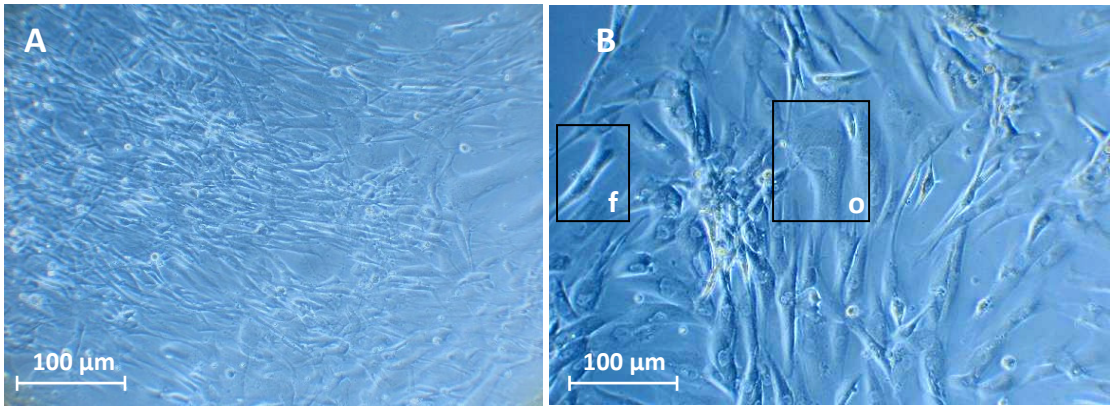

Figure 5. Cell morphology of fat derived human stem cells after 10 days of cell culture with A) no growth factor (control) and B) with 500 ng/ml purified rhBMP-2 (replacement of growth factor and culture media every two days). x400. Fibroblast-like (f) and osteoblast-like (o) morphologies were observed when rhBMP-2 was used on the mesenchymal stem cell primary culture.

4. Discussion

A novel and more simple approach for the production of readily soluble rhBMP-2 using *E. coli* that, for the first time, is bioactive in human cell cultures. In previous reports, recombinant BMP-2 production was achieved in bacterial inclusion bodies in fairly large amounts (Li *et al.* 1998, Vallejo *et al.* 2002, Long *et al.* 2005). However, inclusion bodies require time-consuming steps for solubilization and refolding. In our approach, we have achieved expression of rhBMP-2 directly folded in dimer by use of pET-25 expression system which directs production of soluble recombinant protein into periplasmatic space of *E. coli*, thus allowing the formation of disulfide bridges.

Recovery with 0.7 M L-arginine buffer resulted in monomer, dimer and polymer forms adding value to what has been reported by Klösch *et al.* (2005) and Long *et al.* (2006). In fact, the formation of cysteine bridges is known to be favored at slightly alkaline pH, thus increasing amounts of dimeric rhBMP-2 (Vallejo & Rinas 2004). However, this contribution seems to be the first one to show this method to obtain soluble and dimeric BMP-2 directly upon production. The amount of purified rhBMP-2 was about 55 mg per gram cell dry weight, corresponding to 110 mg purified rhBMP-2 per litter of culture broth.

In previous studies, recombinant BMPs obtained from *E. coli* were reported to be tested in murine cells lines C2C12 (Vallejo *et al.* 2002, Long *et al.* 2006), MC3T3-E1 (Klösch *et al.* 2005) and CH310T1/2 (Yang *et al.* 2003) or *in vivo* rodent models (Kubler *et al.* 1998, Bessho *et al.* 2000, Hillger *et al.* 2005). In our case, we report bioactivity on primary cultures of human stem cells. Binding of active BMP-2 to cell receptors results in an increase of early markers activated during osteogenic differentiation (i.e. Runx2, Osterix). In human stem cells, rhBMP-2 increased ALP enzymatic activity and differentiated cells into osteoblast-like morphology. In conclusion, the novel approach described herein shows steps for improving the production of high amounts of readily soluble rhBMP-2 that shows bioactivity in primary human adult stem cells, and can be use for diverse bone tissue engineering research applications.

References

Bessho K, Konishi Y, Kaihara S, Fujimura K, Okubo Y and Iizuka T (2000) Bone induction by *Escherichia coli* -derived recombinant human bone morphogenetic protein-2 compared with Chinese hamster ovary cell-derived recombinant human bone morphogenetic protein-2. Br J. Oral Maxillofac. Surg. 38: 645-649

Derynck R, Akhurst RJ and Balmain, A (2001) TGF-beta signaling in tumor suppression and cancer progression. Nat. Genet. 29: 117–29.

Groppe J, Greenwald J, Wiater E, Rodriguez-Leon J, Economides AN, Kwiatkowski W, Affolter M, Vale WW, Belmonte JC and Choe S (2002), Structural basis of BMP signalling inhibition by the cystine knot protein Noggin. Nature, 420: 636-42.

Hillger F, Herr G, Rudolph R, Schwarz E (2005) Biophysical comparison of BMP-2, ProBMP-2, and the free pro-peptide reveals stabilization of the pro-peptide by the mature growth factor. J. Biol. Chem. 280: 14974-80.

Israel DI, Nove J, Kerns KM, Moutsatsos IK and Kaufman RJ (1992) Expression and characterization of bone morphogenetic protein-2 in Chinese hamster ovary cells. Growth Factors 7: 139– 150.

Israel DI, Nove J, Kerns KM, Kaufman RJ, Rosen V, Cox KA and Wozney JM (1996) Heterodimeric bone morphogenetic proteins show enhanced activity *in vitro* and *in vivo*. Growth Factors 13: 291–300.

Kirsch T, Nickel J and Sebald W (2000) BMP-2 antagonists emerge from alterations in the low-affinity binding epitope for receptor BMPR-II. EMBO J., 19: 3314-24.

Klösch B, Fürst W, Kneidinger R, Schuller M, Rupp B, Banerjee A and Redl H (2005) Expression and purification of biologically active rat bone morphogenetic protein-4 produced as inclusion bodies in recombinant *Escherichia coli*. Biotechnol. Lett. 27: 1559-64.

Kubler NR, Reuther JF, Faller G, Kirchner T, Ruppert R and Sebald W (1998) Inductive properties of recombinant human BMP-2 produced in a bacterial expression system. International Journal of Oral and Maxillofacial Surgery 27: 305-309.

Kubler NR, Wurzler K, Reuther JF, Faller G, Sieber E, Kirchner T and Sebald W (1999) EHBMP-2. Initial BMP analog with osteoinductive properties. Mund Kiefer Gesichtschir 3 Suppl 1: 134-9

Li M, Chen C, Pu Q and Chen S (1998) Production of human recombinant bone morphogenetic protein-2A by high density culture of *Escherichia coli* with stationary dissolved oxygen fed-batch condition. Chin. J. Biotechnol. 14: 157-63.

Long S, Truong L, Bennett K, Phillips A, Wong-Staal F and Ma H (2006) Expression, purification, and renaturation of bone morphogenetic protein-2 from *Escherichia coli*. Protein. Expr. Purif. 46: 374-8.

Malafaya PP, Pedro AJ, Peterbauer A, Gabriel C, Redl H and Reis RL (2005) Chitosan particles agglomerated scaffolds for cartilage and osteochondral tissue engineering approaches with adipose tissue derived stem cells. J. Mater. Sci. Mater. Med. 16: 1077-85.

Miyazono K, Maeda S and Imamura T (2005) BMP receptor signalling: transcriptional targets, regulation of signal and signalling cross-talk. Cytokine and Growth Factor Rev. 16: 251-263

Reddi AH (1981) Cell biology and biochemistry of endochondral bone development. Coll. Relat. Res. 1: 209-26.

Reddi AH (1998) Role of morphogenetic proteins in skeletal tissue engineering and regeneration. Nature Biotechnology 16: 247-252.

Ruppert R, Hoffmann E and Sebald W (1996) Human bone morphogenetic protein 2 contains a heparin-binding site which modifies its biological activity. Eur. J. Biochem. 237: 295–302.

Salgado AJ, Gomes ME, Chou A, Coutinho OP, Reis RL and Hutmacher DW (2002) Preliminary study on the adhesion and proliferation of human osteoblasts on starch-based scaffolds. Mater. Sci. Eng. 20: 27-33

Sambroock J, Fritsch EF and Maniatis T (1989), Molecular Cloning: A Laboratory Manual, second ed., Cold Spring Harbor Laboratory, New York.

Sanger F, Nicklen S and Coulson AR (1977) DNA sequencing with chain-terminating inhibitors. Proc. Natl. Acad. Sci. USA 74: 5463-5467

Sebald W, Nickel J, Zhang JL and Mueller TD (2004) Molecular recognition in bone morphogenetic protein (BMP)/receptor interaction. Biol. Chem. 385: 697-710.

Shi Y and Massague J (2003) Mechanisms of TGF-b signaling from cell membrane to the nucleus. Cell 113: 685–700.

Urist MR (1965) Bone: formation by autoinduction. Science 150: 893-9

Vallejo LF, Brokelmann M, Marten S, Trappe S, Cabrera-Crespo J, Hoffmann A, Gross G, Weich HA and Rinas U (2002) Renaturation and purification of bone morphogenetic protein-2 produced as inclusion bodies in high-cell-density cultures of recombinant *Escherichia coli*. J. Biotechnol. 94: 185–194.

Vallejo LF and Rinas U (2004) Strategies for the recovery of active proteins through refolding of bacterial inclusion body proteins. Microb. Cell Fact. 3: 11

Wang EA, Rosen V, D'Alessandro JS, Bauduy M, Cordes P, Harada T, Israel DI, Hewick RM, Kerns KM, LaPan P *et al* (1990) Recombinant human bone morphogenetic protein induces bone formation, Proc. Natl. Acad. Sci. USA, 87: 2220–2224.

Westerhuis RJ, van Bezooijen RL and Kloen P (2005) Use of bone morphogenetic proteins in Traumatology. Injury. 36: 1405-12.

Wozney JM, Rosen V, Celeste AJ, Mitsock LM, Whitters MJ, Kriz RW, Hewick RM and Wang EA (1988) Novel Regulators of Bone-Formation - Molecular Clones and Activities. Science 242: 1528-1534.

Wurzler KK, Emmert J, Eichelsbacher F, Kubler NR, Sebald W and Reuther JF (2004) Evaluation of the osteoinductive potential of genetically modified BMP-2 variants. Mund Kiefer Gesichtschir. 8: 83-92.

Yang JH, Zhao L, Yang S, Wu SQ, Zhang J and Zhu TH (2003) Expression of recombinant human BMP-6 in *Escherichia coli* and its purification and bioassay *in vitro*. Sheng Wu Gong Cheng Xue Bao. 19: 556-60.

Zuk PA, Zhu M, Ashjian P, De Ugarte DA, Huang JI, Mizuno H, Alfonso ZC, Fraser JK, Benhaim P and Hedrick MH (2002) Human adipose tissue is a source of multipotent stem cells. Mol. Cell Biol. 13: 4279-95.

Chapter V

Expression, purification and osteogenic bioactivity of recombinant human BMP-4, -9, -10, -11 and -14

This Chapter is based on the following publication:

Bessa PC, Cerqueira MT, Rada T, Gomes ME, Neves NM, Nobre A, Reis RL and Casal M, 2009, Expression, purification and osteogenic bioactivity of recombinant human BMP-4, -9, -10, -11 and -14, Protein Expression and Purification **63**, 89-94.

Chapter V

Expression, purification and osteogenic bioactivity of recombinant human BMP-4, -9, -10, -11 and -14

Abstract

Bone morphogenetic proteins (BMPs) are cytokines from the TGF-β superfamily, with important roles during embryonic development and in the induction of bone and cartilage tissue differentiation in the adult body. In this contribution, we report the expression of recombinant human BMP-4, BMP-9, BMP-10, BMP-11 (or growth differentiation factor-11, GDF-11) and BMP-14 (GDF-5), using *Escherichia coli* pET-25b vector. BMPs were overexpressed, purified by affinity his-tag chromatography and shown to induce the expression of early markers of bone differentiation (e.g. smad-1, smad-5, runx2/cbfa1, dlx5, osterix, osteopontin, bone sialoprotein and alkaline phosphatase) in C2C12 cells and in human adipose stem cells. The described approach is a promising method for producing large amounts of different recombinant BMPs that show potential for novel biomedical applications.

1. Introduction

Discovered in 1965, bone morphogenetic proteins (BMPs) are a group of several cytokines belonging to the transforming growth factor-β (TGF-β) superfamily. These proteins have strong inducing activity in bone and cartilage formation, and also have important roles during embryonic patterning and early skeletal development (Bessa *et al.* 2008a). During the last decades, BMPs have been used as powerful osteoinductive components in several late-stage tissue engineering products for bone grafting (Westerhuis *et al.* 2005). Since 2002, BMP-2 and BMP-7 received approval for specific clinical uses (Bessa *et al.* 2008b).

Despite being extensively investigated, to date, most research has been focused only in a few BMPs, particularly in BMP-2 and BMP-7, whilst little is known about the physiological roles and the biomedical relevance for the remaining BMPs. Both, BMP-4 and BMP-9 have been shown clearly bone-inducing roles, as shown by their ability to induce osteogenic differentiation in C2C12 cell line (Cheng *et al.,* 2003) and orthotopic ossification in mice (Kang *et al.,* 2004). BMP-4 is also implicated in diverse roles during embryonic development, and as a differentiation factor to haematopoietic and nerve cells (Li *et al.* 2001, Giacomini *et al.* 2006,

Reissmann *et al.* 1996). BMP-14 (or growth and differentiation factor-5) induces mainly tendon and cartilage formation (Aspenberg and Forslund 1999; Dines *et al.* 2007) and has been also studied in healing of periodontal ligament (Nakamura *et al.* 2003). BMP-11 and BMP-10 have not been identified for any bone-inducing potential. BMP-10 has expression restricted solely to the heart tissue and is essential to cardiac morphogenesis (Neuhaus *et al.* 1999; Chen *et al.* 2004), while BMP-11 (or growth and differentiation factor-11) has roles in the establishment of axial patterning (Andersson *et al.* 2006). In former reports, human BMP-4 and BMP-14 have been expressed in *E. coli* and reported to induce alkaline phosphatase marker in murine cells but these were not tested in human cells (Kubler *et al.* 1998, Sieber *et al.* 2006). In addition, the expression of human BMP-9, -10 and -11 in *Escherichia coli* is not yet reported. In this work, we described the production, purification and bioactivity of recombinant human BMP-4, -9, -10, -11 and -14 by a novel method that was previously reported for the overexpression of human BMP-2 (Bessa *et al.* 2008c). The different BMPs were analyzed by their ability to induce the mRNA expression of several markers of bone differentiation in C2C12 cells and in human adult stem cells from adipose tissue. Our results suggest a promising and straightforward way for the production of different BMPs, all capable of inducing cell differentiation in the aforementioned models.

2. Materials and methods

2.1. Cloning and expression of rhBMP-4, -9, -10, -11 and -14

The sequences coding the mature (bioactive) domains of human BMP-4, BMP-9, BMP-10, BMP-11/GDF-11 and BMP-14/GDF-5 were obtained from different bacterial clones (Sanger Institute, UK), which contained the full genes encoding the human BMPs: clone reference RP11-808F04 for BMP-4, RP11-463P17 for BMP-9, RP11-88N13 for BMP-10, RP11-55N12 for BMP-11, and RP11-173P06 for BMP-14. According to the data from the UniProtKB/Swiss-Prot database (http://www.expasy.org) and from the Human Genome Project public database (http://www.ensembl.org/homo_sapiens), the sequences coding for the bioactive domains of these BMPs, are located in one sole exon, thus allowing direct PCR cloning of these BMPs from the above mentioned clones, as was previously described (Bessa *et al.* 2008c).

DNA coding for the mature/bioactive protein domains was amplified by PCR using the primers indicated in **Table 1**. PCR-products were cloned in a pET-25b vector (Novagen, USA) via the two restriction sites, *BamH*I and *Xho*I, that were used to transform *E. coli* BL21(DE3) strain (Invitrogen, UK). The restriction sites for these enzymes were specific.

Table 1. Oligonucleotide primers for cloning of human BMP-4, -9, -10, -11 and -14. The nucleotides for restriction by *BamH*I and *Xho*I are underlined in the forward and reverse primers, respectively. The codons representing the beginning and the end of BMP sequences are represented in bold.

Gene	Primer sequence: Forward / Reverse
BMP-4	5' CGG GAT CCA **AGC** CCT AAG CAT CAC TCA C 3'
	5' CCC TCG AG**G CG**G CAC CCA CAT CC 3'
BMP-9	5' CGG GAT CCA **AGC** GCC GGG GCT GGC AG 3'
	5' CCC TCG AG**C CT**G CAC CCA CAC TCT GCC AC 3'
BMP-10	5' CGG GAT CCA **AAC** GCC AAA GGA AAC TAC 3'
	5' CCC TCG AG**T CT**A CAG CCA CAT TCG GAG 3'
BMP-11	5' CGG GAT CCA **AAC** CTG GGT CTG GAC TG 3'
	5' CCC TCG AG**A GA**G CAG CCA CAG CGA TC 3'
BMP-14	5' CGG GAT CCA **GCC** CCA CTG GCC ACT C 3'
	5' CCC TCG AG**C CT**G CAG CCA CAC GAC TC 3'

DNA cloning and manipulation were performed according to standard protocols (Sambrook *et al.* 1989). The integrity of the cloned PCR products was verified by DNA sequencing (Sanger *et al.* 1977) using a ABI PRISM310 Genetic Analyzer. Transformed *E. coli* BL21(DE3) strain with pET-25b/rhBMP were inoculated in 50 ml Luria-Bertani (LB) medium with 50 µg ampicillin/ml and incubated at 37 ºC, until an OD_{600} of 0.8 was obtained. To induce recombinant protein expression IPTG 1 mM was then added to the culture media, and the temperature lowered to 25 ºC during 24 h. Biomass was collected by centrifugation (4000 g, 20 min, 4 ºC), washed once with PBS and stored at -20 ºC.

2.2. Purification of rhBMPs

Frozen bacteria were resuspended in lyses buffer (20 mM sodium phosphate buffer, 0.5 M NaCl, 1 mg/ml lysozyme), with a protease inhibitors (Complete Mini EDTA-free, Roche). Bacteria cells were ultrasonicated 6 times for 30 s with intervals of 5 min on ice and supernatant and pellet fractions collected by centrifugation (4000 g, 30 min, 4 ºC). The pellet was then incubated overnight in solubilization buffer (phosphate saline buffer, 30 mM imidazole, 0.7 M L-arginine, pH 10.0) at 18 ºC with gentle stirring and the supernatant containing soluble rhBMP collected after centrifugation (4000 g, 20 min, 4 ºC). The pH of supernatant was adjusted to 7.5 with 0.5M HCl and applied to a pre-equilibrated HisTrap

chromatography column (Amersham). Briefly, the column was equilibrated with 5 column volumes of sodium phosphate buffer containing 30 mM imidazole, washed extensively with 100-120 ml of sodium phosphate buffer containing 60 mM imidazole and the sample eluted in 20 ml of phosphate buffer supplemented with 400 mM imidazole. A flow rate of 5 ml/min was kept during the whole procedure by the use of a peristaltic pump. Purified protein was desalted with the use of a HiTrap desalting column (Amersham) and freeze-dried. BMPs were resuspended in sterile phosphate buffer saline, prior to bioactivity tests. Protein concentration was measured by Bradford method (Bradford *et al.* 1996) using bovine serum albumin (BSA) standards of known concentration. Protein purity was estimated using SDS-PAGE image analysis (GelPro Analyzer 4.0, Media Cybernetics).

2.3. Western-blot detection of rhBMPs

Protein samples were mixed with SDS-PAGE loading buffer and heated at 95 °C for 5 min. Samples were separated by using hand-cast 10-12 % reduced SDS–PAGE gels and Coomassie blue-R was employed for visualization and staining of gels. Samples were then electro-transferred (wet Western-blot transfer) to a nitrocellulose membrane at 100 V for 60 min. The membrane was blocked with 2% (w/v) BSA in PBS-T buffer (PBS, 0.05% Tween 20) and incubated with peroxidase conjugated anti-His antibody (Sigma) diluted 1:2000. Image detection was performed with ChemiDoc XRS and Quantity One software (BioRad).

2.4. Bioactivity tests

C2C12 cells were seeded at 2.5 x 10^4 cells/ml per well in a 24-well plate, attached in Dulbecco's modified Eagle's medium (DMEM) with 1% (v/v) fetal bovine serum, 100 U/ml penicillin and 100 µg/ml streptomycin, at 37 ºC with 5% CO_2 in a humidified environment. Cells were incubated for 5 days with BMP-4, -9, -10, -11 and -14, purified by the method described above (500 ng/ml) and a control with no cytokine. MTS cell viability assay was performed in C2C12 cells after 3 days of culture (Salgado *et al.* 2002). Primary cultures of human adult stem cells isolated from adipose tissue (Malafaya *et al.* 2005) were cultured under similar conditions and incubated with BMP-4, -9 and -14 (500 ng/ml) for 3 days of cell culture. For RT-PCR, the mRNA of cells was extracted with TriZol Reagent (Invitrogen, USA) from triplicate 24-well assays following the procedure provide by the supplier. Samples were quantified using a NanoDrop ND-1000 Spectrophotometer (NanoDrop Technologies, USA) and cDNA synthesis performed with iScript cDNA synthesis Kit (BioRad, USA). PCR was performed with specific primers for osteogenic markers. Agarose gels were visualized using Eagle Eye imaging system

(Stratagene) and gene expression was analyzed with Gel-Pro Analyzer (Media Cybernetics), using polymerase II expression as a housekeeping marker.

2.5. Statistical analysis

Experiments were performed at least in triplicate and expressed as means ± standard deviations. Student's t test was used for statistical analysis using a two-tailed paired test and analyzed by a paired analysis of variance. Statistical significance was defined as $p < 0.05$ for a 95% confidence.

3. Results

3.1. Cloning, expression and purification of rhBMPs

The PCR originated single products for the coding regions of human BMP-4, -9, -10, -11 and -14 (data not shown). DNA sequencing revealed a total correspondence to encoded nucleotides and corresponding amino acids. *Escherichia coli* BL21(DE3) strain transformants were then cultivated and collected as described in the Material and methods section. After cell lyses, rhBMPs were found mainly in the pellet (fraction corresponding to cell debris) (data not shown). Soluble protein was recovered using phosphate buffer containing 0.7M L-arginine, pH 10.0, as indicated in Materials and Methods. After purification by affinity chromatography, the rhBMPs were visible as monomer, dimer and polymer, with Western-blot, using a antibody against the six-histidine tag (**Figure 1**). Estimating from Coomassie blue-stained SDS-PAGE, the BMPs were pure up to 95% (**Table 2**).

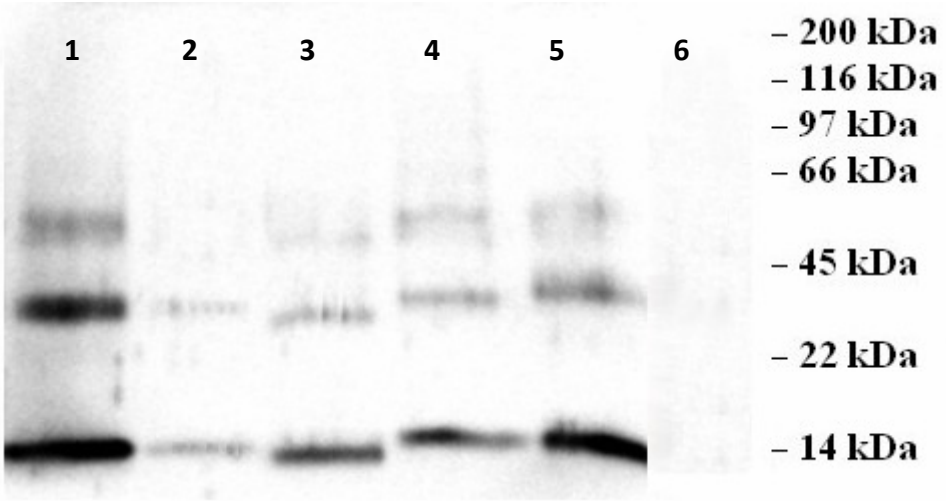

Figure 1. Western-blot of purified rhBMP-4, -9, -10, -11 and -14 and a negative control (respectively 1-6) using an anti 6-His tag antibody. The BMPs are visible in monomer, dimer and polymer.

Table 2. Purification of recombinant human BMP-4, BMP-9, BMP-10, BMP-11 (GDF-11) and BMP-14 (GDF-5).

Steps	**Crude lysate** [a]		**L-arginine solubilization**		**Ni-NTA chromatography**	
Protein	Total protein (mg)[b]	Purity (%)[c]	Total protein (mg)	Purity (%)	Total protein (mg)	Purity (%)
hBMP-4	497.5	24.4	203.6	42.3	53.6	91.0
	Yield 100 %		Yield 70.5 %		Yield 40.0 %	
hBMP-9	531.5	17.2	220.9	27.5	45.9	88.7
	Yield 100 %		Yield 66.5 %		Yield 44.5 %	
hBMP-10	533.3	14.9	261.3	23.7	22.7	92.4
	Yield 100 %		Yield 77.4 %		Yield 25.5 %	
hBMP-11	506.4	13.5	278.5	19.7	23.4	87.7
	Yield 100 %		Yield 80.1 %		Yield 30.1 %	
hBMP-14	569.1	19.7	252.5	32.5	35.0	95.1
	Yield 100 %		Yield 73.4 %		Yield 29.5 %	

[a] The recombinant hBMPs were purified from 1 L *E. coli* culture.

[b] Total protein quantification was determined using Bradford method

[c] Estimated from SDS-PAGE image analysis

3.2. Cytotoxicity of rhBMPs

Bioassays were performed in murine myoblast C2C12 cell line, by the administration of purified rhBMP-2. The different proteins did not show cytotoxicity in C2C12 cells after three days of cell culture at 50 and 500 ng/ml (**Figure 2**). MTS is a viability/proliferation test and an inverse relationship of toxicity to cells can be assumed. BMP-4 (50 ng/ml), BMP-9 (50 ng/ml) and BMP-10 (500 ng/ml) significantly stimulated cell proliferation by approximately 10 to 25 % ($p < 0.05$).

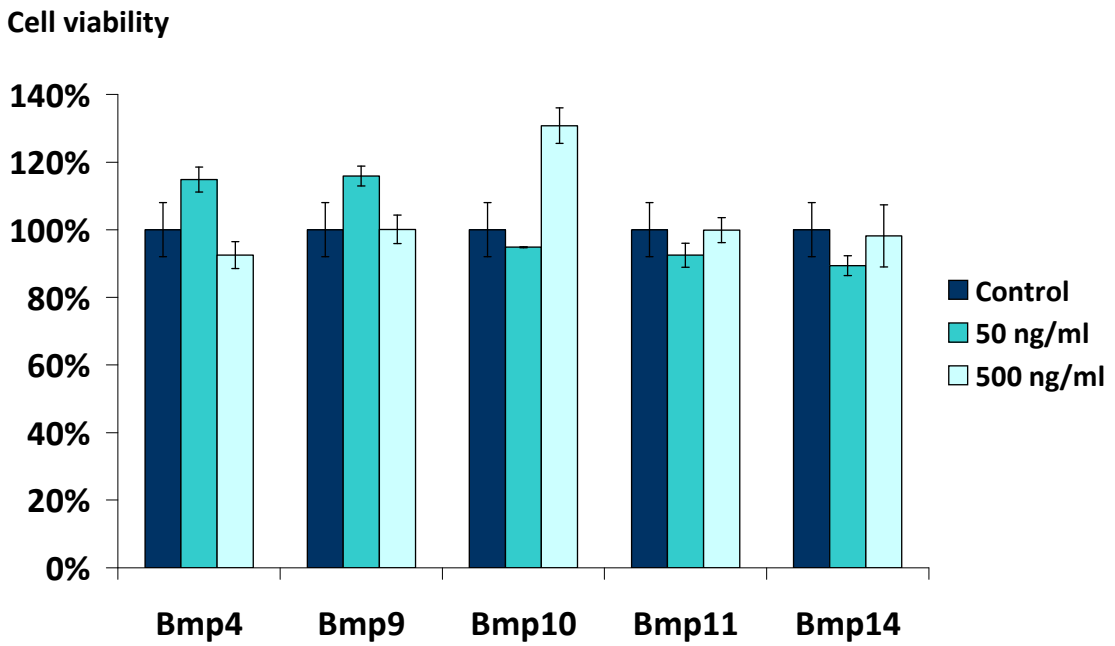

Figure 2. Tetrazolium salt (MTS) test performed in C2C12 cells as a function of the concentration of the different rhBMPs, after 3 days of cell culture. Cell viability is expressed in percentage (mean ± S.D., *n*=3, * $p < 0.05$).

3.3. Expression of osteogenic markers induced by rhBMPs

Semi-quantitative RT-PCR revealed an increase in expression of several early osteoblast differentiation markers in C2C12 cell line after five days of cell culture with the different BMPs (**Figure 3**). The increased mRNA levels were mean values of independent assays, and normalized against the expression of polymerase II. The expression of early osteochondral transcription factor runx2/cbfa1 was induced by 2 to 3-fold with BMP-4 and BMP-11, 4-fold with BMP-10 and BMP-14, and 6-fold with BMP-9 ($p < 0.05$ in all cases). Expression of smad-1 and smad-5, two signaling molecules for BMPs, were also induced but in a lower extent. The expression of smad-5 with induced 2-fold with BMP-4 and BMP-9 ($p < 0.05$). Expression of smad-1 was induced with BMP-9 (2-fold, $p < 0.05$). With BMP-10, BMP-11 and BMP-14, there was no significant increase in the expression of smad-1 or -5. Osterix, a transcription factor downstream of runx2/cbfa-1 and a marker of commitment to osteoblastic lineage, was induced both with BMP-4 (2-fold) and BMP-9 (2-fold, $p < 0.05$) and its expression maintained with the other BMPs. Osterix expression was slightly decreased by BMP-11 (not statistically significant). The expression of transcription factor dlx5 was nearly the same with all BMPs, with a slight increase with BMP-4 (1.5-fold) which is not significant. Alkaline phosphatase (ALP), bone sialoprotein and osteopontin, three markers of bone formation, were induced with some

of these BMPs. ALP was induced with BMP-4, BMP-9 (2-fold, $p < 0.05$) and BMP-10 and -14 (1.5-fold), and reduced by half (0.5-fold) with BMP-11 ($p < 0.05$). Bone sialoprotein expression was up-regulated with BMP-14 (3-fold) and with BMP-4 (5-fold, $p < 0.05$). Osteopontin expression was up-regulated mainly with BMP-9, BMP-14 and less with BMP-4 and BMP-10 ($p < 0.05$), compared with basal expression in the control and with BMP-11. Osteocalcin, a marker specific of late-stages of bone mineralization, was not detected in any assay. The observations on cell morphology correlated well with the induction of the several osteogenic markers (**Figure 4**). BMP-9, and to a less degree BMP-4 and BMP-14, induced an osteoblast-like morphology.

In the primary cultures of fat-derived human stem cells, BMP-4, BMP-9 and BMP-14 were also able to induce an increase in the expression of the different early markers of osteogenic differentiation (**Figure 5**). BMP-4 induced the highest levels of osteogenic markers, particularly runx2 (7-fold, $p < 0.05$), bone sialoprotein (7-fold, $p < 0.05$) and osteopontin (8-fold, $p < 0.05$). BMP-9 induced runx2 (2-fold) and alkaline phosphatase (2-fold), while BMP-14 induced the expression of alkaline phosphatase (5-fold, $p < 0.05$) and bone sialoprotein (3-fold, $p < 0.05$). Bacteria transformed with blank vector (e.g. no BMP) did not induce any expression of osteogenic genes (data not shown).

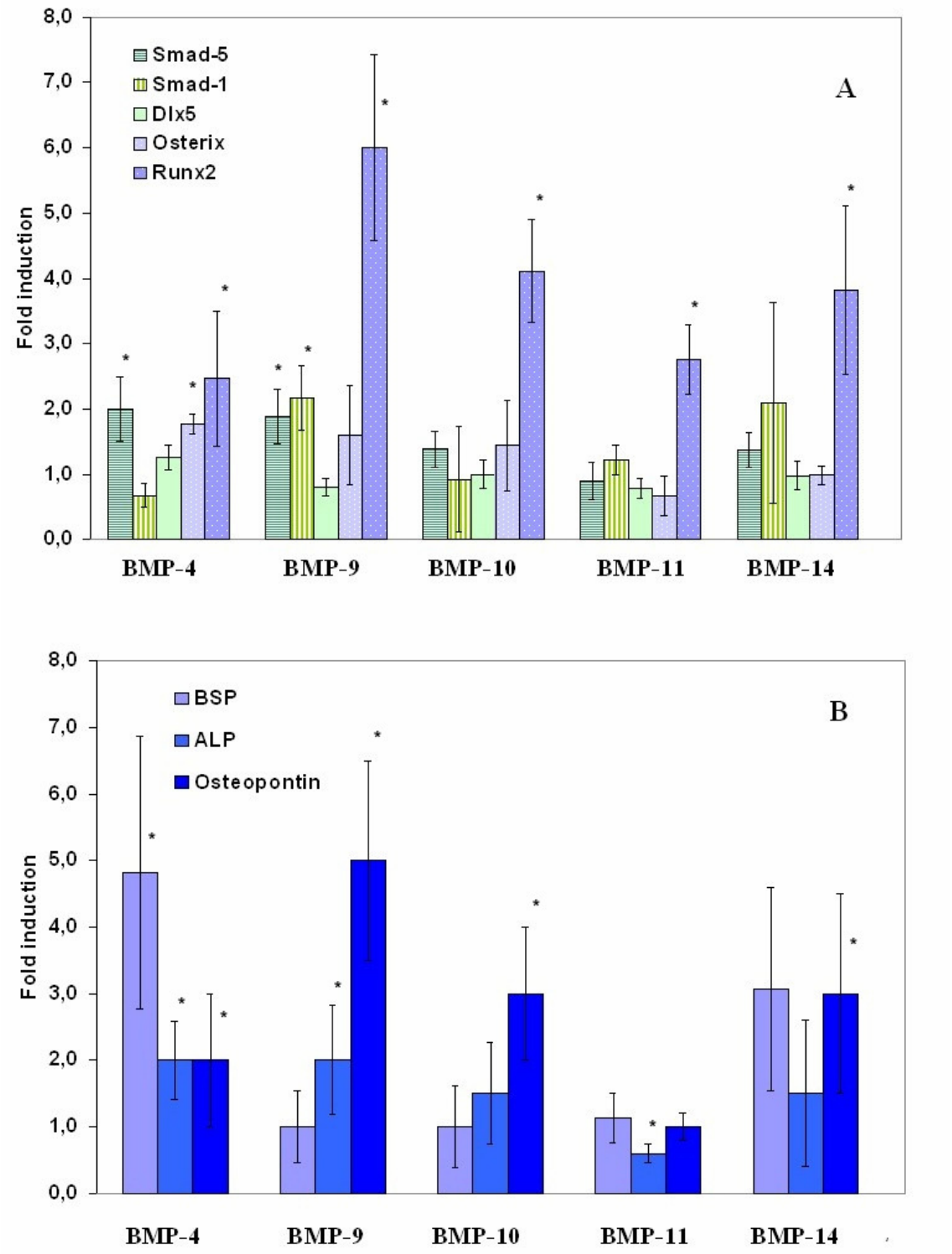

Figure 3. mRNA expression of signaling molecules and transcription factors (A) and osteogenic-specific markers (B) induced by BMPs, measured by semi-quantitative RT-PCR after 5 days of cell culture in C2C12 cell line. Bars represent mean values ± SD of gene expression fold variation of at least three independent determinations (* $p < 0.05$). Smad-1 and Smad-5 were induced mostly for BMP-4, -9 and -14, Osterix for BMP-4 and -9, Runx2 was induced for all BMPs but higher for BMP-9. Bone sialoprotein was induced mostly for BMP-4 and -11; ALP was induced 1.5 to 2-fold for all BMPs except BMP-11; osteopontin was induced mainly for BMP-9, BMP-10 and BMP-14.

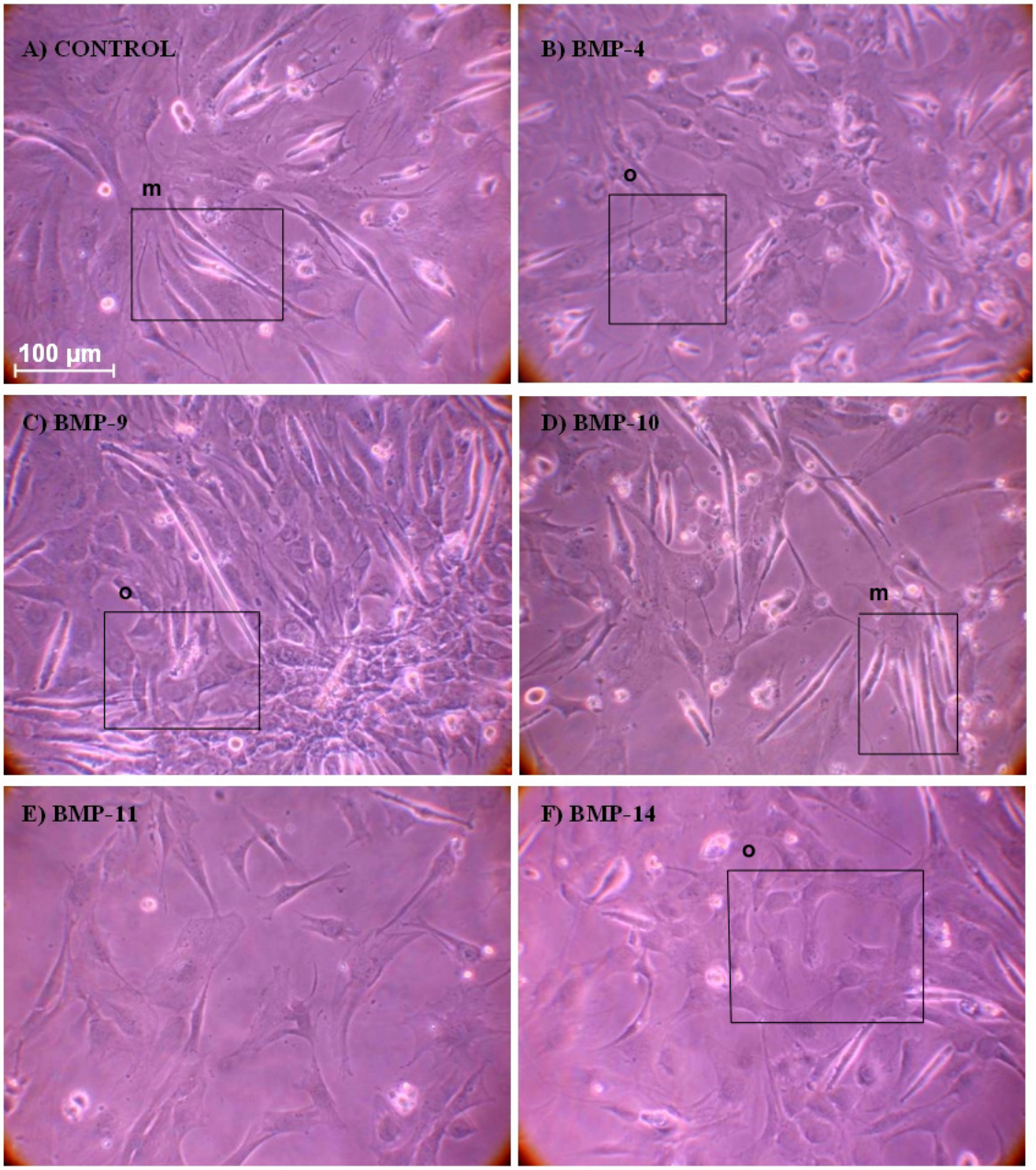

Figure 4. Cell morphology of C2C12 cells after 5 days of cell culture with A) no growth factor (control), B) 500 ng/ml rhBMP-4, C) 500 ng/ml rhBMP-9, D) 500 ng/ml rhBMP-10, E) 500 ng/ml rhBMP-11, and F) 500 ng/ml rhBMP-14. Purified BMP was used. x400. Osteoblast-like morphology (o) was observed in C2C12 cells stimulated with BMP-4, BMP-9 and BMP-14 and myoblast-like morphology (m) in control and cells stimulated with BMP-10.

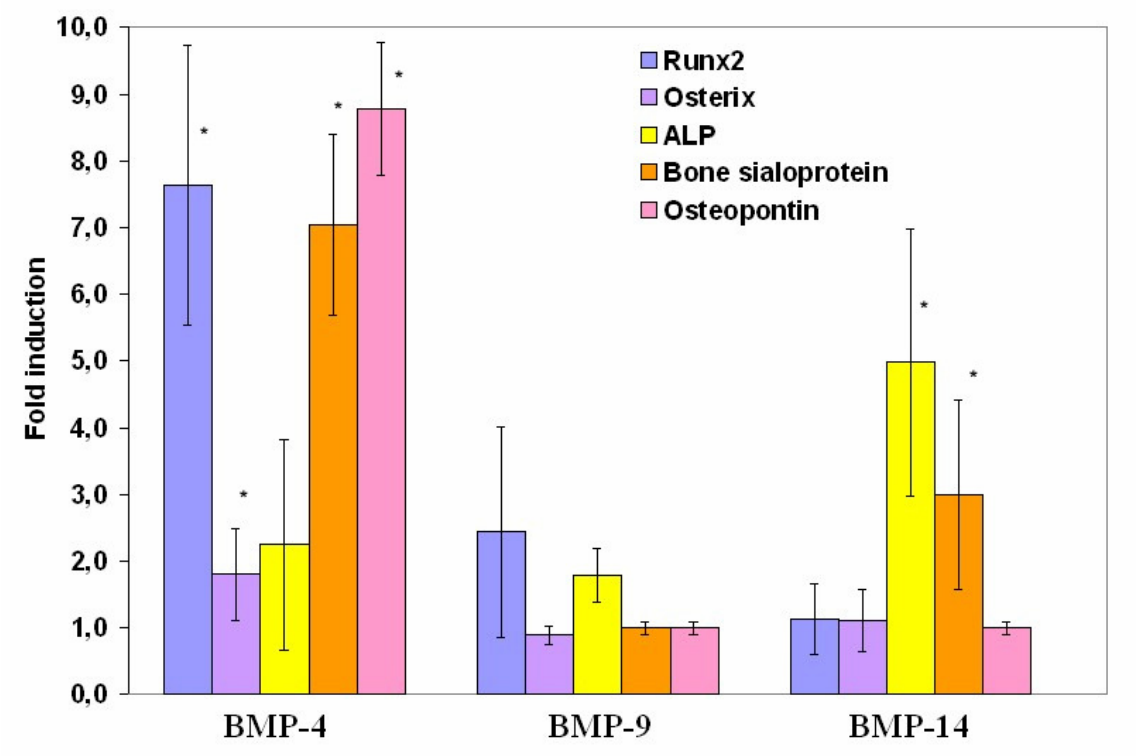

Figure 5. mRNA expression of early markers of osteogenic differentiation induced by BMPs, measured by semi-quantitative RT-PCR after 3 days of human adult stem cell cultures. Bars represent mean values ± SD of gene expression fold variation of at least three independent determinations (* $p < 0.05$). The expression of osteogenic markers was induced mainly with BMP-4. BMP-9 induced runx2 and ALP (2-fold) and BMP-14 induced solely ALP (5-fold) and bone sialoprotein (3-fold).

4. Discussion

In this work we report a straightforward methodology for the expression of recombinant human BMP-4, BMP-9, BMP-10, BMP-11/GDF-11 and BMP-14/GDF-5 in *Escherichia coli*, that showed bioactivity in both C2C12 cell line and human adult stem cells.

Although the concept of overexpressing BMPs in *E. coli* is not novel, we have shown, for the first time, the overexpression of functional BMP-9, -10 and -11 using *E. coli* and characterized the bioactivity of BMP-4, BMP-14 and BMP-9 using primary cultures of human adult stem cells, which has not been shown before. Using a single-step method, which was previously reported for the solubilization of rhBMP-2 (Bessa *et al.* 2008c), the recovery with 0.7 M L-arginine buffer resulted in monomer, dimer and polymer, in a similar way to former reports (Klösch *et al.* 2005; Long *et al.* 2006), with up to 50 mg purified BMPs per liter of culture broth.

All tested BMPs have shown evidence of bioactivity in C2C12 cells. C2C12 cell line is a well-known model for studying the osteogenic differentiation induced by BMPs as has been reported by several investigators (Vallejo *et al.* 2002; Long *et al.* 2006; Bessa *et al.* 2008a). The different BMPs induced several early markers of BMP signaling (smad-1/-5, runx2/cbfa-1 or osterix) and of bone mineralization (bone sialoprotein, osteopontin or ALP).

Semi-quantitative RT-PCR analysis of mRNA expression was selected since it is well established that upon binding of the BMPs to their cell receptors, the expression of these genes is highly induced, triggering osteogenic differentiation (Bessa *et al.* 2008a). In C2C12 cells, BMP-4, -9 and -14 appeared to have had the most significant effects in the markers of bone formation. BMP-11 solely induced significantly the BMP-activated transcription factor runx2, showing that probably this BMP does not have any important role in bone formation and healing, besides those described in the literature during embryonic development (Andersson *et al.* 2006). In human stem cells, BMP-4, -9 and -14 also demonstrated bioactivity, despite the fact that the osteogenic potential was higher for BMP-4 than BMP-9 or -14, which could point for the stronger bone-inducing potential of this cytokine.

Despite the fact that these recombinant BMPs show bioactivity, further studies will be performed to assess the detailed response of cells to BMPs, including the induction of the different markers by Real-Time RT-PCR, and immunostaining analysis.

In conclusion, the approach we detailed herein shows a promising route for producing large amounts of several different bioactive recombinant BMPs. The results in human adult stem cell cultures suggest that some of these BMPs could be used with success for future clinical applications.

References

Andersson, O., Reissmann, E. and Ibáñez, C.F. (2006) Growth differentiation factor 11 signals through the transforming growth factor-beta receptor ALK5 to regionalize the anterior-posterior axis. EMBO Rep. 7, 831-7.

Aspenberg, P. and Forslund C. (1999) Enhanced tendon healing with GDF 5 and 6. Acta Orthop Scand. 70, 51-4.

Bessa, P.C., Casal, M. and Reis, R.L. (2008a) Bone morphogenetic proteins in tissue engineering: the road from laboratory to the clinic, part I (basic concepts). J Tissue Eng Regen Med. 2, 1-13.

Bessa, P.C., Casal, M. and Reis, R.L. (2008b) Bone morphogenetic proteins in tissue engineering: the road from laboratory to the clinic, part II (BMP delivery). J Tissue Eng Regen Med. 2, 81,96.

Bessa, P.C., Pedro, A.J., Klösch, B., *et al.* (2008c) Osteoinduction in human fat-derived stem cells by recombinant human bone morphogenetic protein-2 produced in *Escherichia coli*. Biotechnol Lett. 30, 15-21.

Bradford, M.M. (1976) A Rapid and Sensitive Method for the Quantitation of Microgram Quantities of Protein Utilizing the Principle of Protein-Dye Binding. Anal. Biochem. 72, 248-254.

Chen, H., Shi, S., Acosta, *et al.* (2004) BMP10 is essential for maintaining cardiac growth during murine cardiogenesis. Development. 131, 2219-31.

Cheng, H., Jiang, W., Phillips, F.M., *et al.* (2003) Osteogenic activity of the fourteen types of human bone morphogenetic proteins (BMPs), J Bone Joint Surg Am. 85-A, 1544-52.

Dines, J.S., Weber, L., Razzano, P., Prajapati, R., Timmer, M., Bowman, S., Bonasser, L., Dines, D.M. and Grande, D.P. (2007) The effect of growth differentiation factor-5-coated sutures on tendon repair in a rat model. J Shoulder Elbow Surg. 16, S215-21.

Giacomini, D., Páez-Pereda, M., Theodoropoulou, M. *et al.* (2006) Bone morphogenetic protein-4 control of pituitary pathophysiology. Front. Horm. Res. 35, 22-31.

Kang, Q., Sun, M.H., Cheng, H., *et al.* (2004) Characterization of the distinct orthotopic bone-forming activity of 14 BMPs using recombinant adenovirus-mediated gene delivery. Gene Ther, 11, 1312-20.

Klösch, B., Fürst, W., Kneidinger, R., Schuller, M., Rupp, B., Banerjee, A. and Redl, H. (2005) Expression and purification of biologically active rat bone morphogenetic protein-4 produced as inclusion bodies in recombinant *Escherichia coli*. Biotechnol. Lett. 27, 1559-64.

Kübler N.R., M. Moser M., and Berr .K, (1998). Biological activity of *E. coli* expressed BMP-4. Mund Kiefer Gesichtschir 2(1), S149-52.

Li, F., Lu, S., Vida, I. *et al.* (2001) Bone morphogenetic protein 4 induces efficient hematopoietic differentiation of rhesus monkey embryonic stem cells *in vitro*. Blood. 98, 335-342.

Long, S., Truong, L., Bennett, K., Phillips, A., Wong-Staal, F. and Ma, H. (2006) Expression, purification, and renaturation of bone morphogenetic protein-2 from *Escherichia coli*. Protein. Expr. Purif. 46, 374-8.

Malafaya P.P., Pedro A.J., Peterbauer A., *et al.* (2005) Chitosan particles agglomerated scaffolds for cartilage and osteochondral tissue engineering approaches with adipose tissue derived stem cells. J. Mater. Sci. Mater. Med. 16 1077-85.

Nakamura, T., Yamamoto, M., Tamura, M., Izumi, Y. (2003) Effects of growth/differentiation factor-5 on human periodontal ligament cells. J Periodontal Res. 38, 597-605.

Neuhaus, H., Rosen, V., Thies, R.S. (1999) Heart specific expression of mouse BMP-10 a novel member of the TGF-beta superfamily. Mech Dev. 80, 181-4.

Reissmann, E., Ernsberger, U., Francis-West, P.H. *et al.* (1996) Involvement of bone morphogenetic protein-4 and bone morphogenetic protein-7 in the differentiation of the adrenergic phenotype in developing sympathetic neurons. Development 122, 2079-88.

Salgado, A.J., Gomes, M.E., Chou, A., Coutinho, O.P., Reis, R.L. and Hutmacher, D.W. (2002) Preliminary study on the adhesion and proliferation of human osteoblasts on starch-based scaffolds. Mater. Sci. Eng. 20, 27-33.

Sambroock, J., Fritsch, E.F. and Maniatis, T. (1989), Molecular Cloning: A Laboratory Manual, second ed., Cold Spring Harbor Laboratory, New York.

Sanger, F., Nicklen, S. and Coulson, A.R. (1977) DNA sequencing with chain-terminating inhibitors. Proc. Natl. Acad. Sci. USA 74, 5463-5467.

Sieber C., Plöger F., and Schwappacher R. (2006) Monomeric and dimeric GDF-5 show equal type I receptor binding and oligomerization capability and have the same biological activity. Biol Chem. 387, 451-60.

Vallejo, L.F., Brokelmann, M., Marten, S., Trappe, S., Cabrera-Crespo, J., Hoffmann, A., Gross, G., Weich, H.A. and Rinas, U. (2002) Renaturation and purification of bone morphogenetic protein-2 produced as inclusion bodies in high-cell-density cultures of recombinant *Escherichia coli*. J. Biotechnol. 94, 185–194.

Westerhuis, R.J., van Bezooijen, R.L. and Kloen, P. (2005) Use of bone morphogenetic proteins in Traumatology. Injury. 36, 1405-12.

SECTION 4

Chapter VI

Silk fibroin microparticles as carriers for delivery of human recombinant BMPs. Physical characterization and drug release

This Chapter is based on the following publication:

Bessa PC, Balmayor ER, Azevedo HS, Nürnberger S, Casal M, van Griensven M, Reis RL, Redl H, 2009, Silk fibroin microparticles as carriers for delivery of human recombinant BMPs. Physical characterization and drug release, Journal of Tissue Engineering and Regenerative Medicine, *submitted.*

Chapter VI

Silk fibroin microparticles as carriers for delivery of human recombinant BMPs. Physical characterization and drug release

Abstract

Bone morphogenetic proteins (BMPs) are cytokines with strong ability to promote new bone formation. Herein, we report the use of silk fibroin microparticles as carriers for the delivery of BMP-2, BMP-9 or BMP-14. BMP-containing fibroin microparticles were prepared by a mild methodology using dropwise addition of ethanol, exhibiting mean diameters of 2.7 ± 0.3 μm. Encapsulation efficiencies varied between 67.9 ± 6.1 % and 97.7 ± 2.0 % depending on the type and the amount of BMP loaded. Release kinetics showed that BMP-2, BMP-9 and BMP-14 were released in two phases profile, with a burst release in the first two days followed by a slower release, for a period of 14 days. The release data were best explained by Korsmeyer's model and the Fickian model of drug diffusion. Silk fibroin microparticles can offer a promising approach for the sustained delivery of different BMPs in tissue engineering applications.

1. Introduction

Bone morphogenetic proteins (BMPs) have recently sparked great interest in the tissue engineering field due to their strong ability to promote new bone and cartilage formation (Reddi, 2005; Bessa *et al*., 2008a). Different materials have been proposed as carriers for BMPs (Bessa *et al*., 2008b). Carriers are used to increase the lifetime, stability and bioactivity of the BMPs and release these growth factors in both timely and site-specific sustained ways. Microparticles as carriers can offer the advantages of a controlled release, protecting the protein from loss of bioactivity and targeting the delivery into the specific injury site, with no dispersion into surrounding tissues.

Several different microparticulated systems have been investigated for the delivery of BMPs, most based on polylactic-co-glycolic acid (PLGA) (Lee *et al*., 1994; Phillips *et al*., 2006; Wei *et al*., 2007), on collagen (Wang *et al*., 2003, Itoh *et al*., 2004) or on dextran (Chen *et al*., 2006, 2007). Silk is an attractive choice as a material for bone tissue engineering, due to being biocompatible, slowly biodegradable and possessing excellent mechanical properties such as tensile strength and rigidity which are highly desirable for a potential use as a scaffold for bone tissue engineering (Scheibel 2006). Silk fibroin has been investigated as a carrier for BMPs in

several contributions by Kaplan and colleagues, in form of membranes for healing cranial defects in mice (Karageorgiou *et al*., 2004), electrospun nanofibers (Li *et al*., 2006), and scaffolds used for critical size defects in rats (Kirker-Head *et al*., 2007) and mice (Karageorgiou *et al*., 2006).

Fibroin has been recently described to produce microparticles when precipitated with ethanol at specific fibroin concentrations and freeze temperature (Nam and Park, 2001; Cao *et al*., 2007; Zhang *et al*., 2007). Ethanol causes a shift in the random coil structure of fibroin to an insoluble beta-sheet configuration (Nam and Park, 2001). The addition of ethanol to the fibroin solution causes it to either precipitate to form a gel that can be used as a scaffold for tissue engineering (Nazarov *et al*., 2004; Tamada, 2005) or to form a gel consisting of micrometric particles (Nam and Park, 2001; Zhang *et al*., 2007). If these variables are controlled, a control of particle size is possible and could be adapted to specific clinical applications. Therefore, we were interested in using this system as a possible delivery micro-carrier for BMPs.

This study explores the use of silk fibroin microparticles as a potential delivery system for the release of different BMPs. Fibroin microparticles were produced under very mild conditions, with a concomitant loading of BMP-2, BMP-9 or BMP-14. Besides the fact that BMP-2 has been widely researched as a osteogenic factor (Bessa *et al*., 2008b), we also evaluated the potential of the fibroin particles to deliver BMP-9 and BMP-14 due to their potential in novel therapeutical applications. BMP-9 is reported to be one of the most osteogenic BMPs (Kang *et al*., 2004) and BMP-14 is used in tendon and ligament regeneration (Nakamura *et al*., 2003; Dines *et al*., 2007), in spinal fusion (Spiro *et al*., 2001), bone formation (Simank *et al*., 2004; Kadamatsu *et al*., 2008) and is critical for digit and limb development (Merino *et al*., 1999). The particles were characterized for morphology, size distribution, water uptake, encapsulation efficiency and the release kinetics of the three BMPs, with different amounts of loaded growth factor.

2. Materials and methods

2.1. Materials

Silk containing *Bombyx mori* cocoons were purchased from Halcyon Yarn, US. Human BMP-2, expressed in Chinese Hamster Ovary (CHO) cells, was purchased from Wyeth, UK. Human BMP-9 and BMP-14 were cloned and expressed in *Escherichia coli*, purified by histidine-tag affinity chromatography and freeze-dried, as described elsewhere (Bessa *et al*., 2009). All chemicals were of analytical grade and used as received.

2.2. Methods

2.2.1. Preparation of BMP-loaded silk fibroin microparticles

Isolation of silk fibroin from Bombyx mori cocoons

Silk fibroin was isolated from *Bombyx mori* cocoons following a degumming protocol with modifications (Zhang *et al*., 2007). Briefly, the cocoon shells of silkworm *Bombyx mori* were degummed twice in a boiling solution of 0.5 % Na_2CO_3 for 0.5 h, at 90 ºC, and the resulting degummed fibers were subsequently dissolved, in a ternary system, i.e. a mixed solution of calcium chloride, ethanol and water ($CaCl_2$ / C_2H_5OH / H_2O: 1:2:8 mole ratio) at 90ºC for 6 h. The solution was then filtered (0.22 µm, Rotilab, Germany), and the solution was extensively dialyzed, using a cellulose semi-permeable (molecular weight cut-off = 12 000 kDa) membrane, against distilled water to remove $CaCl_2$, smaller molecules and impurities. The fibroin was lyophilized and used for the preparation of microparticles.

Microparticle preparation

Silk fibroin microparticles were prepared by ethanol precipitation according to the method described by Cao *et al*. (2007), with modifications. A solution of 1% (w/v) silk fibroin in phosphate buffer saline (PBS, pH 7.4) was prepared (5 ml) and filtered with a 0.22 µm PVDF membrane (Rotilab, Germany). For preparation of BMP loaded particles, 5 or 50 µg/ml of growth factor (either BMP-2, BMP-9 or BMP-14) were added to the fibroin suspension, corresponding to a smaller or a larger dose of loaded BMP (0.5 or 5 µg of BMP per mg of fibroin, respectively). The solution was incubated at room temperature with stirring (600 rpm) for 20 min. Absolute ethanol was added dropwise to a ratio of 1:2 to the initial volume of silk fibroin, and the solution incubated overnight at -20 ºC. Different ratios (ethanol to initial volume of fibroin suspension) were also tested to investigate the change in particle size. The resulting microparticles were collected by centrifugation at 4000 g, 4ºC, for 5 min, washed twice with distilled water and lyophilized, after snap-freezing in liquid nitrogen, in a Christ Alpha 1-4 (Linder, Austria) lyophilizer. Sterile conditions were used during the entire procedure.

2.2.2. Physical characterization

Scanning electron microscopy (SEM)

Fibroin particles were morphologically characterized by scanning electron microscopy (SEM). SEM analysis was performed on gold-coated air-dried samples (Agar Sputercoater 108,

Essex, UK) and using a Philips XL20 microscope (Philips, Eidhoven, The Netherlands). Particle size measurements were obtained from different micrographs acquired in the SEM.

Size distribution

Measurements of particle size were performed on freshly prepared samples by dynamic light scattering (DLS), using a Zetasizer NanoZS (Malvern, UK). For the analysis, each sample was diluted to an appropriate concentration with ultrapure (filtered) water. Each analysis lasted 60 s and was performed at 25 ºC.

Water uptake and degradation studies

The hydration degree of unloaded fibroin microparticles was evaluated after immersion into PBS, at 37 ºC, for periods up to 30 days (30 min, 4 h, 24 h, 2 d, 5 d, 8d, 14 d, 21 d and 30 d). The weight loss of unloaded fibroin particles was assessed after immersion into PBS, at 37 ºC, for periods up to 30 days (1 d, 2 d, 5 d, 8 d, 14 d and 30 d). All experiments were performed in triplicate. Percentage of water uptake (WU) after each time period of immersion (t) was calculated using the following equation:

$WU\ (\%)=(W_w-W_i) / W_i \times 100$

The percentage of mass remaining (MR) after each time period (t) was calculated using the following equation: $WL\ (\%)=W_d/ W_i \times 100$

'W_w' and 'W_d' correspond, respectively, to the weight of fibroin particles in wet state (after removal from solution, washing with distilled water and soft-blotting with filter paper) and dry state (after removal of solution, washing after distilled water and freeze-drying); 'Wi' correspond to the initial dry weight of particles, before immersion.

2.2.3. *In vitro* release studies

Quantification of protein

For measurement of BMP-2 concentration, a BMP-2 sandwich-type ELISA kit (Eubio, Austria) was used, following the manufacturer's instructions. A calibration curve was obtained using standard preparations of BMP-2 of known concentration. For detection of BMP-9 and BMP-14, the sample concentrations were estimated by dot blot with the use of an anti-histidine tag antibody (Sigma, US). The blot intensities were compared with standards of known concentration, using image analysis (ChemiImage 4400, Alpha Innotech, US).

Determination of loading capacity and encapsulation efficiency

The microparticle encapsulation efficiency was determined upon their separation from the aqueous preparation medium containing the non-associated protein (free BMP) by centrifugation (10 000 g, 10 min). Theoretical drug content (total BMP) was calculated assuming that the entire amount of drug added to the fibroin solution was encapsulated and no drug loss occurred at any stage of the particle preparation. All experiments were performed in triplicate. The microparticle encapsulation efficiency (E.E.) and BMP loading capacity (L.C) were calculated using the following equations:

$$\text{E.E.}(\%) = \frac{\text{Total BMP amount } (\mu g) - \text{Free BMP amount } (\mu g)}{\text{Total BMP amount}} \times 100$$

$$\text{L.C.}(\mu g \text{ BMP / mg particles}) = \frac{\text{Total BMP amount } (\mu g) - \text{Free BMP amount } (\mu g)}{\text{Microparticles weight (mg)}}$$

In vitro release

Silk fibroin particles loaded with BMP-2, BMP-9 or BMP-14 (initial loading of 0.5 or 5 µg /mg) were suspended in 5 ml PBS (pH 7.4), at 37 ºC, with 200 rpm agitation, to a concentration of 2 mg/ml of microparticles. At pre-determined time points (1 h, 4 h, 1 d, 2 d, 4 d, 8 d and 14 d), 250 µl of solution was removed, centrifuged (10 000 g, 10 min) and filtered in 0.22 µm membranes and stored at -20 ºC until quantification. The volume of solution removed was replaced with fresh buffer. Sterile conditions were applied to prevent any contamination of samples. All experiments were performed in triplicate. Percentage of release was obtained by comparing the measured growth factor content with the actual loading capacity.

Release kinetics models

To study the release kinetics, the data obtained from the *in vitro* release was treated accordingly to zero order as cumulative amount of drug released *vs*. time (equation 1), first order as log cumulative percent drug remaining *vs*. time (equation 2), Higuchi kinetics as cumulative percent drug released *vs*. square root of time (equation 3) and Korsmeyer kinetics as log cumulative percent drug released *vs*. log time (equation 4) (Huguchi, 1963; Chowdary and Ramesh, 1993; Hadjiioannou *et al*., 1993; Bourne, 2002):

$R = k_1 t$ (1)

$\text{Log UR} = k_2 t\ 2.303$ (2)

$R = k_3 t\ 0.5$ (3)

$\text{Log } R = \log k_4 + n \log t$ (4)

where R and UR are released and unreleased percentages, respectively, at time (t); k_1, k_2, k_3 and k_4 are the rate constants of zero-order, first order, Higuchi and Korsmeyer models, respectively; n is a exponent that characterizes the mechanism of release.

2.2.4. Statistical analysis

Experiments were performed in triplicate (n = 3) and mean ± standard deviations were reported. Student's t test was used for statistical analysis using a two-tailed paired test. Statistical significance was defined as $p < 0.01$ for a 99% confidence.

3. Results

3.1. Morphology, size distribution and encapsulation efficiency

The morphology of fibroin particles observed by SEM is shown in **Figure 1**. Fibroin formed spherical microparticles with diameters increasing when the ratio of ethanol to silk solution (used during the preparation of particles) increased. The particles had mean sizes of 580.0 ± 120.6 nm using a 1:2 ratio of ethanol and silk, increasing up to 1.1 ± 0.3 μm with a 1:3 ratio ($p < 0.01$), and to 1.2 ± 0.4 μm with 1:4 ratio (not significant). Using size distribution, the particles, using a 1:2 ratio, showed an average size of 2.7 ± 0.3 μm, in wet state (**Figure 2**). The largest part of microspheres (88.5 %) had sizes ranging from 1.5 to 3.0 μm in diameter. The encapsulation efficiency of BMP-2 into the fibroin particles was 97.7 ± 2.0 % per total amount of growth factor added during the preparation of the particles, when 0.5 μg BMP-2 (per mg fibroin) was loaded, and 76.8 ± 3.5 %, when 5.0 μg of BMP-2 were loaded (**Table 1**). The loading capacity was 0.69 ± 0.06 μg of BMP-2 per mg of fibroin particles, and 5.4 ± 0.5 μg of BMP-2 per mg of particles, when the different amounts were loaded. For BMP-9, the encapsulation efficiency was 90.2 ± 5.9 % and 72.4 ± 4.4 %, and the loading capacity was 0.63 ± 0.17 and 5.1 ± 0.5 μg/mg of particles, when 0.5 or 5.0 μg BMP-9 were loaded, respectively. For BMP-14, the encapsulation efficiency was 82.5 ± 6.0 % and 67.9 ± 6.1 %, and the loading capacity was 0.60 ± 0.17 and 4.8 ± 0.6 μg of BMP-14 per mg of particle weight, when 0.5 or 5.0 μg BMP-14 were loaded, respectively.

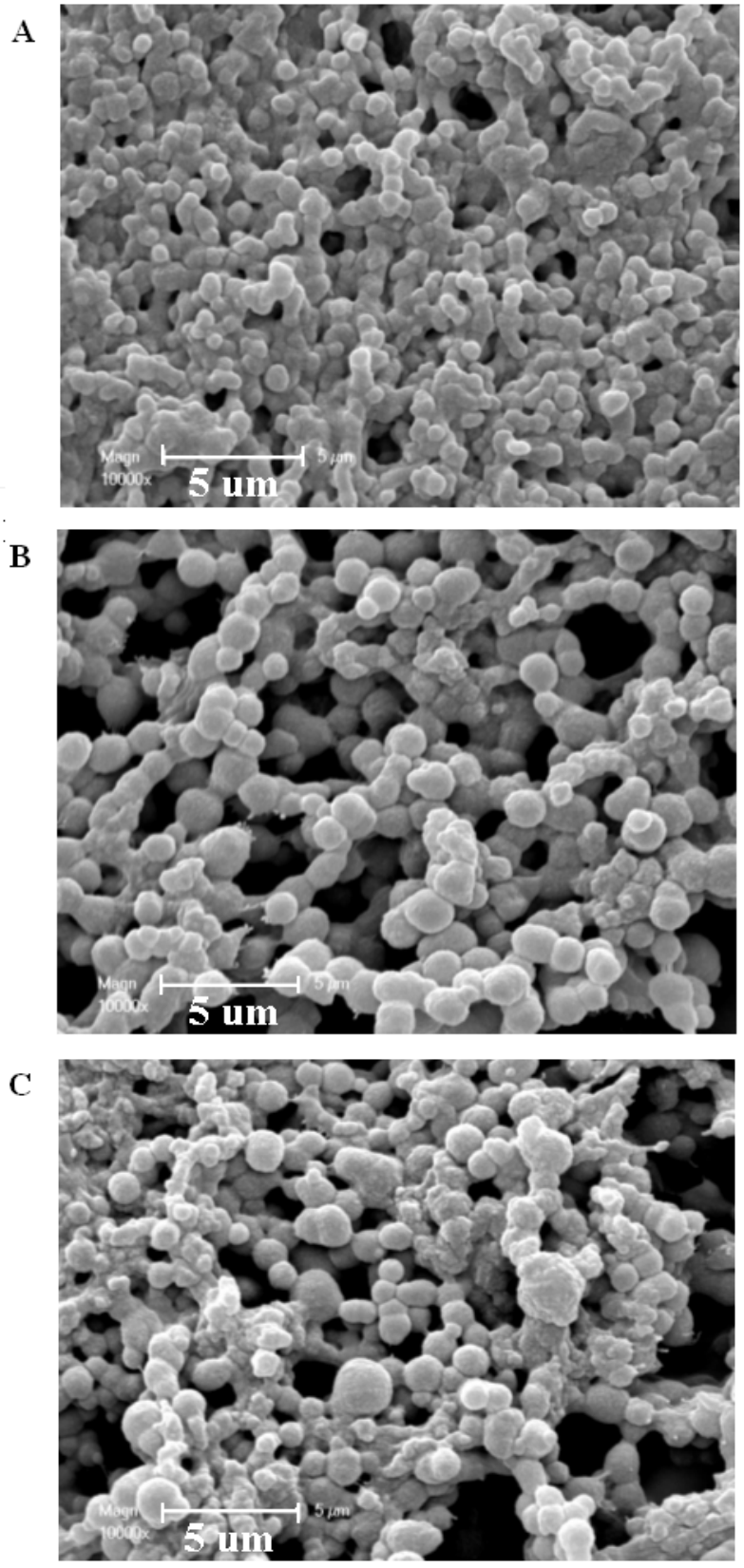

Figure 1. SEM micrographs of unloaded fibroin microparticles, produced with different ethanol : fibroin solution ratios: A) 1:2 ratio, B) 1:3 ratio, and C) 1:4 ratio. Magnification 10.000 x.

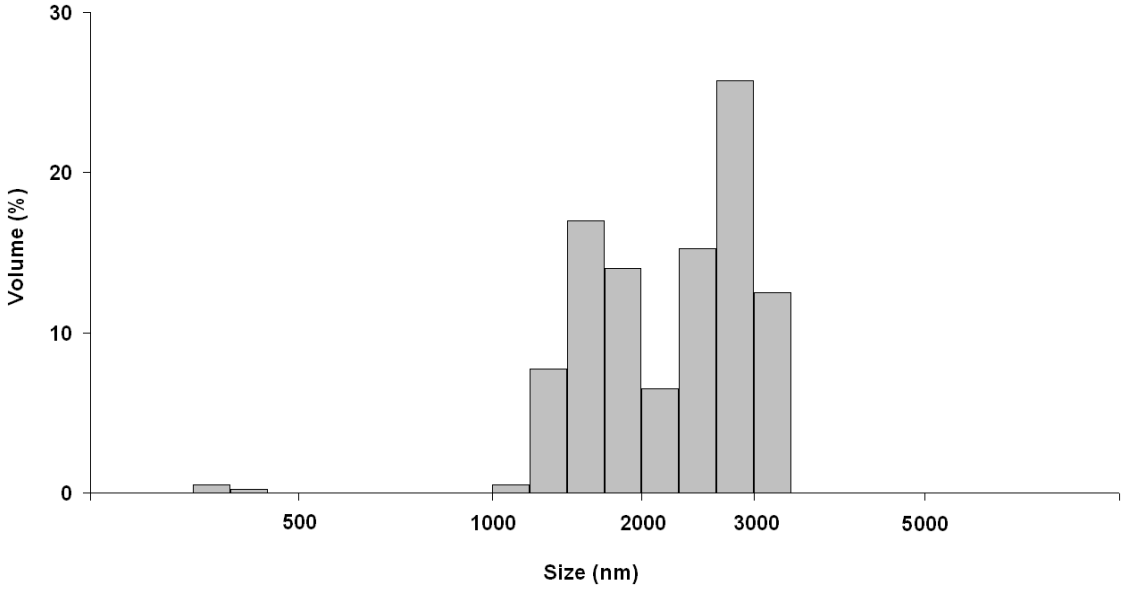

Figure 2. Size distribution of unloaded silk fibroin particles. Almost all particles showed sizes ranging between 1.5 and 3.0 µm, with a mean diameter of 2.7 ± 0.3 µm. Size refers to particle diameter (nanometers).

Table 1. Loading and encapsulation efficiencies of BMP loaded fibroin microparticles (mean ± SD, *n* = 3).

Growth factor	Amount of growth factor per mg of fibroin, prior to loading	Encapsulation efficiency (%)	Loading capacity (µg BMP / mg particles)
BMP-2	0.5 µg	97.7 ± 2.0	0.69 ± 0.06
BMP-9	0.5 µg	90.2 ± 5.9	0.63 ± 0.17
BMP-14	0.5 µg	85.8 ± 6.0	0.60 ± 0.17
BMP-2	5.0 µg	76.8 ± 3.5	5.4 ± 0.5
BMP-9	5.0 µg	72.4 ± 4.4	5.1 ± 0.5
BMP-14	5.0 µg	67.9 ± 6.1	4.8 ± 0.6

Encapsulation efficiency (%) = [(Total BMP amount (µg) −Free BMP (µg)) / Total BMP (µg)] x 100.
Loading capacity (µg BMP / mg particles) = [(Total BMP amount (µg)−Free BMP (µg)) / Microparticles weight (mg)].

3.2. Water uptake and degradation studies

The swelling occurred rapidly during the first two days of immersion, up to 48.5 ± 6.7 % after 30 min and up to 167.7 ± 14.1 % after day 2 ($p < 0.01$), with water uptake reaching a peak at day 8 with 227.7 ± 26.6 % ($p < 0.01$) (**Figure 3**). This was followed by a slow and gradual decline in wet weight, with a swelling value of 203.4 ± 25.0 % (non-significant) after day 30, possibly due to weight loss. The remaining mass was 97.1 ± 1.5 % after day 5, 95.4 ± 2.5 % after day 14, and 93.5 ± 3.3 % after day 30 (**Figure 4**).

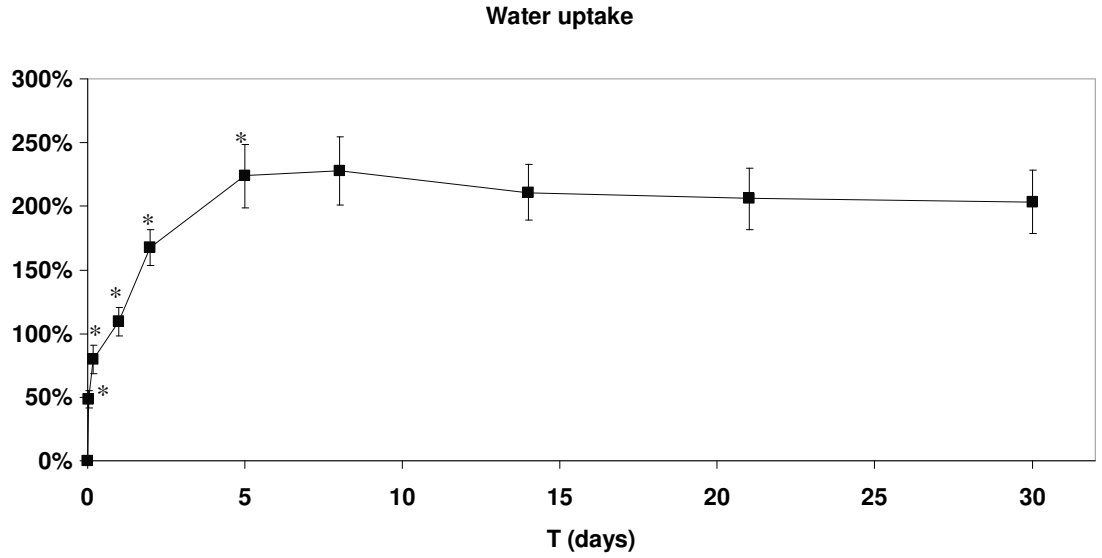

Figure 3. Evolution of water uptake behavior of unloaded silk fibroin microparticles in phosphate buffer saline as a function of immersion time (t). (mean ± SD, $n = 3$). Water uptake increased significantly up to 5 days, peaked after 8 days, and then slightly declined (non-significantly). * $p < 0.01$ related to the difference between consecutive time measurements.

3.3. *In vitro* release studies

Drug release studies were evaluated when fibroin particles loaded with BMP-2, BMP-9 and BMP-14 were immersed in PBS, at 37ºC, with agitation. The microparticles loaded with 0.5 µg of BMPs /mg fibroin, showed an initial burst release with more than half of protein being released during the first two days (64.1 ± 5.1 % for BMP-2, 78.4 ± 7.9 % for BMP-9 and 62.5 ± 7.3 % for BMP-14), followed by a second phase of a slower and more sustained release with 90.1 ± 6.9 % of BMP-2, 90.9 ± 5.2 % of BMP-9, and 80.4 ± 5.6% of BMP-14, released after 14 days (**Figure 5A**). This corresponds to a release rate, of 15 ng/day, 7 ng/day and 8 ng/day

(per mg of fibroin), between day 2 and 14, for each BMP, after a burst release of 442 ng, 499 ng and 377 ng of each BMP (in 2 days).

The particles loaded with 5 μg/mg of BMPs showed an initial release of about 28.6 ± 5.5 % of BMP-2, 22.7 ± 6.3 % of BMP-9 and 14.1 ± 6.7 % of BMP-14 being released after two days (**Figure 5B**), which corresponds to 1.5 μg, 1.1 μg and 0.7 μg of each growth factor. After 14 days, 47.3 ± 7.0 % BMP-2, 38.9 ± 8.9 % BMP-9, and 33.2 ± 8.8 % BMP-14 were released, corresponding to a release rate of 86 ng/day, 72 ng/day and 76 ng/day, for each BMP. At the end of this period, 2.5 μg, 2.0 μg and 1.5 μg of each growth factor were (cumulatively) released from the particles (per mg of fibroin).

The release data of the BMPs were treated accordingly to first order, Higuchi and Korsmeyer equations (**Table 2**) and zero order equation (data not shown). The release data of BMP-2, BMP-9 and BMP-14 were best explained by Korsmeyer's equation (r^2 varying between 0.92 and 0.98), followed by Higuchi's equation (r^2 varying between 0.75 and 0.95) and by first order kinetics (r^2 varying between 0.71 and 0.91). The release exponent "n" of Korsmeyer's model, varied in the different experimental conditions between 0.30 and 0.42. Since $n < 0.43$ the release data fitted a Fickian mode of diffusion (Ritger and Peppas, 1987). The zero order modeling showed low linearity (data not shown).

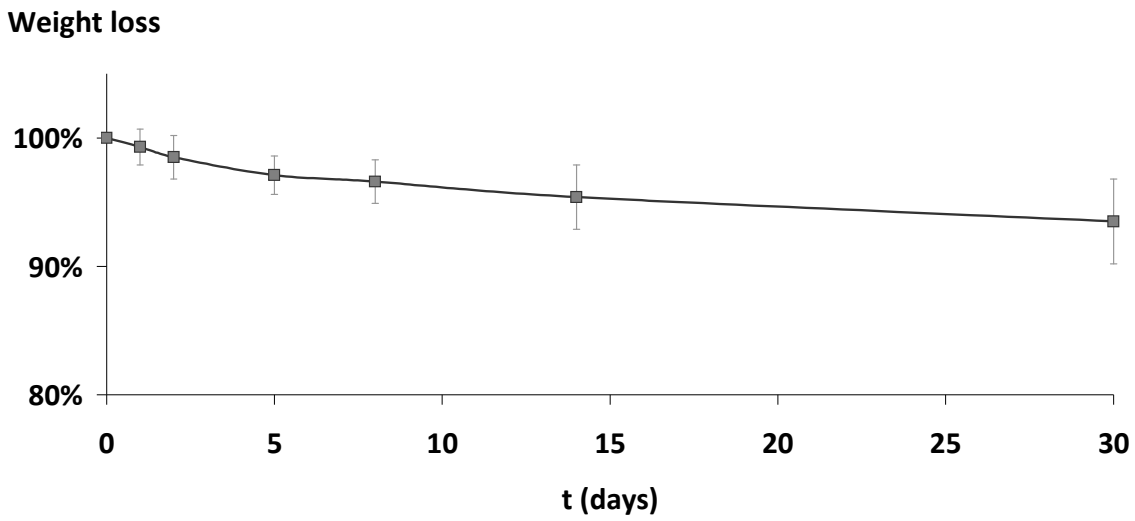

Figure 4. Evolution of weight loss of unloaded fibroin particles in phosphate buffer saline as a function of immersion time (t). (mean ± SD, n = 3). The remaining mass decreased to 97.1 ± 1.5 % after day 5, 95.4 ± 2.5 % after day 14, and 93.5 ± 3.3 % after day 30.

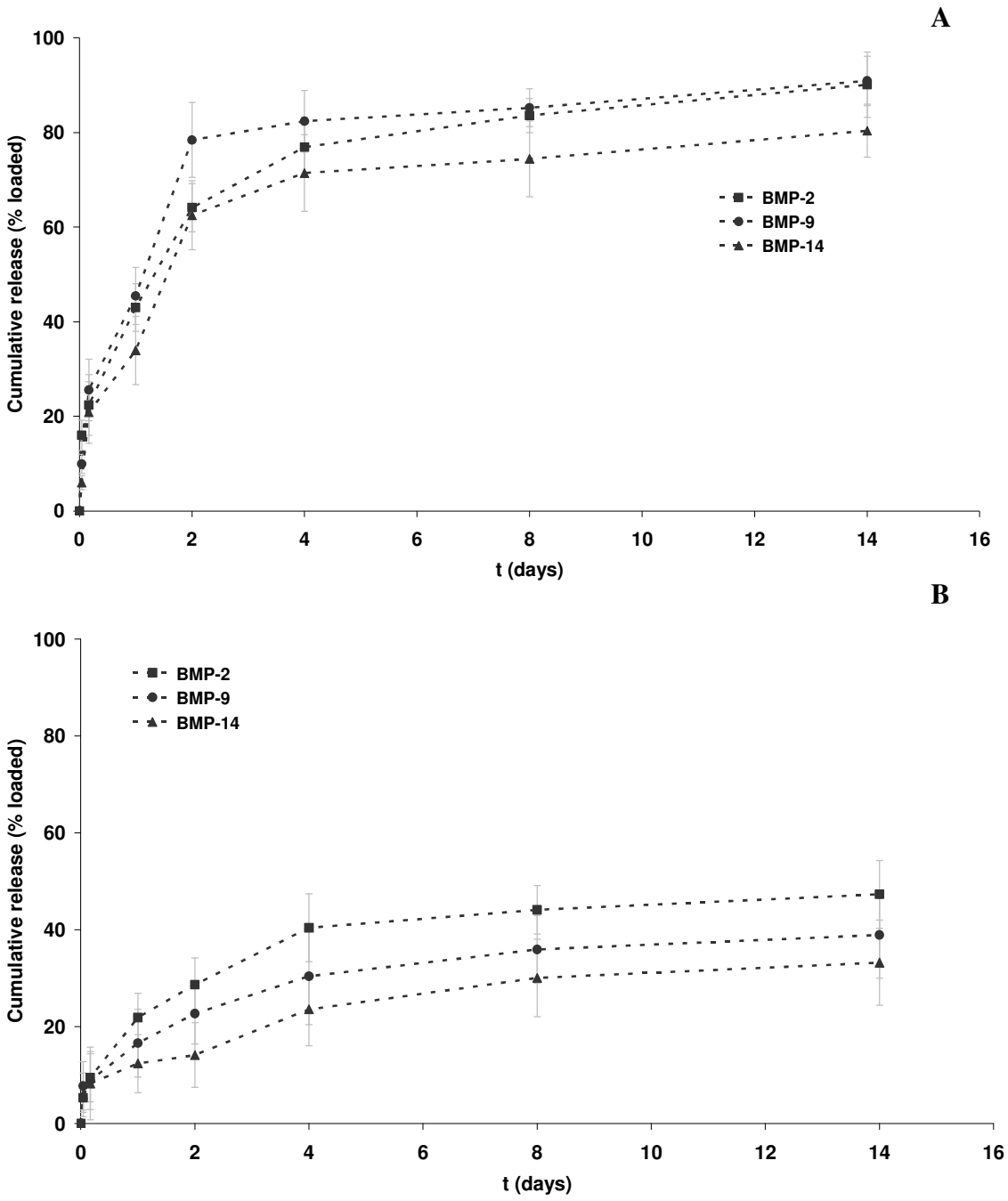

Figure 5. Release kinetics of BMP-2, BMP-9 and BMP-14 immobilized in fibroin particles. ELISA was used for BMP-2 quantification and dot-blot for BMP-9 and BMP-14 quantification (Mean ± SD, *n* = 3). A) Release from particles containing 0.5 µg of BMP per mg of fibroin; B) release from particles containing 5.0 µg of BMP per mg of fibroin. Cumulative release is expressed in percentage of loaded protein.

Table 2. Release kinetics of BMPs immobilized in fibroin particles. First order (log cumulative percent drug remaining *vs*. time), Higuchi kinetics (cumulative percent drug released *vs*. square root of time) and Korsmeyer kinetics (log cumulative percent drug released *vs*. log time), with correlation values (r^2).

Growth factor	**Amount of growth factor per mg of fibroin, prior to loading**	**Equation modeling (First order [a], Higushi [b], Korsmeyer [c])**
BMP-2	0.5 µg	$y = -0.057x + 1.7547$; $r^2 = 0.91$ [a] $y = 17.926x + 26.183$; $r^2 = 0.85$ [b] $y = 0.3029x + 1.6459$; $r^2 = 0.97$, $n = 0.30$ [c]
BMP-9	0.5 µg	$y = -14.148x + 25.648$; $r^2 = 0.71$ [a] $y = 19.509x + 25.325$; $r^2 = 0.75$ [b] $y = 0.3674x + 1.6277$; $r^2 = 0.92$, $n = 0.37$ [c]
BMP-14	0.5 µg	$y = -0.0344x + 1.8002$; $r^2 = 0.70$ [a] $y = 18.232x + 17.785$; $r^2 = 0.80$ [b] $y = 0.4195x + 1.519$; $r^2 = 0.92$, $n = 0.42$ [c]
BMP-2	5.0 µg	$y = -0.0133x + 1.9131$; $r^2 = 0.71$ [a] $y = 11.018x + 8.4402$; $r^2 = 0.88$ [b] $y = 0.385x + 1.2845$; $r^2 = 0.98$, $n = 0.39$ [c]
BMP-9	5.0 µg	$y = -77.226x + 150.34$; $r^2 = 0.77$ [a] $y = 8.5682x + 7.496$; $r^2 = 0.92$ [b] $y = 0.301x + 1.2361$; $r^2 = 0.96$, $n = 0.30$ [c]
BMP-14	5.0 µg	$y = -0.0083x + 1.9499$; $r^2 = 0.83$ [a] $y = 7.2919x + 5.3548$; $r^2 = 0.95$ [b] $y = 0.2978x + 1.1429$; $r^2 = 0.97$, $n = 0.30$ [c]

4. Discussion

Microparticles as drug carriers have the advantages of sustained or controlled release, the possibility of drug targeting to specific tissues, thus reducing side effects of drugs and improving their bioavailability. Therefore, microparticles as delivery systems have drawn much attention in the pharmaceutical field and have been successfully applied in several clinical trials. The goal of this study was to assess the possibility of the use of silk-derived fibroin as a microparticle carrier for the release of different BMPs.

Fibroin microspheres were manufactured in a semi-aqueous system, avoiding the use of toxic organic solvents, harsh conditions, cross-linking agents or surfactants, as a way of minimizing the risk of a loss of BMP activity during the particle preparation. The group of Kaplan and colleagues have recently reported that fibroin could form either particles or films with methanol and conserving the activity of incorporated drugs (Hofmann *et al*., 2006; Wang *et al*., 2007). When compared with other methods of processing, such as spray drying (Hino *et al*., 2003), this approach not only avoids conditions unfavorable for the growth factor activity such as high temperature, but it also allows generating particles with smaller size.

The microparticles were easily prepared under sterile conditions and had a small size in a rather narrow size distribution. The size of particles was significantly smaller in the SEM counterpart images, probably due to the large swelling of the particles in the wet state. This was reported also in a former work (Cao *et al*., 2007). The small particle size presented a double advantage, first by potentially enhancing the drug availability in the particle surface, and also by providing a surgical material that may be suitable for injectable implantation in bone defects in a slurry form. The BMPs were successfully encapsulated with a rather high efficiency, which is comparable to other works (Patel *et al*., 2008; Wenk *et al*., 2008). The lower encapsulation efficiencies observed for BMP-14 could be due to the differences in the BMP charge and its interaction with the fibroin material. Interestingly, this BMP has a lower isoelectric point when compared to BMP-2 (calculated using Expasy Proteomics tool Compute pI/Mw, at www.expasy.org ; pI = 6.3 for BMP-2, pI = 5.9 for BMP-9 and pI = 5.8 for BMP-14). It is possible that this growth factor interacted to a weaker extent with the fibroin carrier since fibroin has an acidic isoelectric point (pI = 5.5).

During the initial stages of swelling, the fibroin microspheres showed substantial water uptake, mostly during the first two days of immersion, which also corresponded to the initial burst release, as the drug was rapidly released from the particles. Then, as swelling became gradually counterbalanced, the BMP was released slower and the release was mainly determined by the diffusion of the growth factor from the particle to the medium. It is possible

that the erosion of the carrier contributed little to this, since we have found both that the release data best fitted with the Korsmeyer's equations and slope values between 0.30 and 0.42, thus indicating that the release was of a Fickian type of diffusion, controlled by only one mechanism and thus not dependent on carrier erosion (this applies when $n < 0.43$, in the case of spherical particles) (Ritger and Peppas, 1987). In fact, as we have observed the silk fibroin microparticles exhibited a slow rate of degradation. The release amounts during this phase were such that they could meet the concentrations of growth factor required in most *in vitro* and *in vivo* applications (in the range of few hundreds of nanograms to a few micrograms), by choosing a specific amount of BMP during the loading process (Kenley *et al*., 1994; Hosseinkhani *et al*., 2007; Wei *et al*., 2007; Bessa *et al*., 2009).

The silk fibroin microspheres have shown to work as a microcarrier that provides a sustained release of the different BMPs in a timewise manner that could be used in bone regenerative applications. The bioactivity of the BMPs released from the silk fibroin microparticles will be explored in future works.

References

Bessa PC, Cerqueira MT, Rada T, Gomes ME, Neves NM, Nobre A, Reis RL *et al.* 2009, Expression, purification and osteogenic bioactivity of recombinant human BMP-4, -9, -10, -11 and -14, Protein Expr and Purif , 63; 89-94.

Bessa PC., Casal M and Reis RL. 2008a, Bone morphogenetic proteins in tissue engineering: the road from laboratory to the clinic, part I (basic concepts). J Tissue Eng Regen Med , 2; 1-13.

Bessa PC., Casal M and Reis RL. 2008b, Bone morphogenetic proteins in tissue engineering: the road from laboratory to the clinic, part II (BMP delivery). J Tissue Eng Regen Med , 2; 81-96.

Bourne DW. 2002, 'Pharmacokinetics' in Modern Pharmaceutics eds. Banker GS, Rhodes C, Marcel Dekker Inc, NY, USA, 67-92.

Cao Z, Chen X, Yao J, Huang L, Shao Z. 2007, The preparation of regenerated silk fibroin microspheres. Soft Matter , 3; 910-915.

Chen FM, Wu ZF, Sun HH, Wu H, Xin SN, Wang QT, Dong GY. 2006, Release of bioactive BMP from dextran-derived microspheres: a novel delivery concept. Int J Pharm , 307; 23–32.

Chen FM, Zhao YM, Sun HH, Jun T, Wang QT, Zhou W, Wu ZF. 2007, Novel glycidyl methacrylated dextran (Dex-GMA)/gelatin hydrogel scaffolds containing microspheres loaded with bone morphogenetic proteins: formulation and characteristics. J Control Release , 118; 65–77.

Chowdary KP and Ramesh KV. 1993, Studies on microencapsulation of diltiazem. J Pharm Sci , 55; 52-4.

Dines JS, Weber L, Razzano P, Prajapati R, Timmer M, Bowman S, Bonasser L *et al.* 2007, The effect of growth differentiation factor-5-coated sutures on tendon repair in a rat model. J Shoulder Elbow Surg , 16; S215-21.

Hadjiioannou TP, Christian GD, Koupparism MA. 1993, Quantitative calculations in pharmaceutical practice and research. VCH Publishers Inc, NY, USA, 345-348.

Higuchi T. 1963, Mechanism of sustained action medication. Theorical analysis of rate of release of solid drugs dispersed in solid matrices. J Pharm Sci , 52; 1145-1149.

Hino T, Tanimoto M and Shimabayashi S, 2003, Change in secondary structure of silk fibroin during preparation of its microspheres by spray-drying and exposure to humid atmosphere, J. Colloid Interface Sci , 266; 68–73.

Hofmann S, Foo CT, Rossetti F, Textor M, Vunjak-Novakovic G, Kaplan DL, Merkle HP *et al.* 2006, Silk fibroin as an organic polymer for controlled drug delivery. J Control Release , 111; 219-27.

Hosseinkhani H, Hosseinkhani M, Khademhosseini A, *et al.* 2007, Bone regeneration through controlled release of bone morphogenetic protein-2 from 3-D tissue engineered nano-scaffold. J Control Release , 117; 380-6.

Itoh S, Kikuchi M, Koyama Y, Takakuda K, Shinomiya K, Tanaka J. 2004, Development of a hydroxyapatite/collagen nanocomposite as a medical device. Cell Transpl , 13; 451–461.

Kadomatsu H, Matsuyama T, Yoshimoto T, Negishi Y, Sekiya H, Yamamoto M, Izumi Y. 2008, Injectable growth/differentiation factor-5-recombinant human collagen composite induces endochondral ossification via Sry-related HMG box 9 (Sox9) expression and angiogenesis in murine calvariae. J Periodont Res , 43; 483-489.

Kang Q, Sun MH, Cheng H, Peng Y, Montag AG, Deyrup AT, Jiang W *et al.* 2004, Characterization of the distinct orthotopic bone-forming activity of 14 BMPs using recombinant adenovirus-mediated gene delivery. Gene Ther , 11; 1312-20.

Karageorgiou V, Meinel L, Hofmann S, Malhotra A, Volloch V, Kaplan D. 2004, Bone morphogenetic protein-2 decorated silk fibroin films induce osteogenic differentiation of human bone marrow stromal cells. J Biomed Mater Res A , 71; 528–537.

Karageorgiou V, Tomkins M, Fajardo R, Meinel L, Snyder B, Wade K, Chen J *et al.* 2006, Porous silk fibroin 3D scaffolds for delivery of bone morphogenetic protein-2 *in vitro* and *in vivo*. J Biomed Mater Res A , 78; 324–334.

Kenley R., Marden L, Turek T *et al.* 1994, Osseous regeneration in the rat calvarium using novel delivery systems for recombinant human bone morphogenetic protein-2 (rhBMP-2), J Biomed Mater Res , 28; 1139-47.

Kirker-Head C, Karageorgiou V, Hofmann S, Fajardo R, Betz O, Merkle HP, Hilbe M *et al.* 2007, BMP–silk composite matrices heal critically sized femoral defects. Bone , 41; 247–255.

Lee SC, Shea M, Battle MA, Kozitza K, Ron E, Turek T, Schaub RG, *et al.* 1994, Healing of large segmental defects in rat femurs is aided by RhBMP-2 in PLGA matrix. J Biomed Mater Res , 28; 1149–1156.

Li C, Vepari C, Jin HJ, Kim HJ, Kaplan DL. 2006, Electrospun silk-BMP-2 scaffolds for bone tissue engineering. Biomaterials , 27; 3115–3124.

Merino R, Macias D, Gañan Y, Economides AN, Wang X, Wu Q, Stahl N *et al.* 1999, Expression and function of Gdf-5 during digit skeletogenesis in the embryonic chick leg bud. Dev Biol , 206; 33-45.

Nakamura T, Yamamoto M, Tamura M, Izumi Y. 2003, Effects of growth/differentiation factor-5 on human periodontal ligament cells. J Periodontal Res , 38; 597-605.

Nam J and Park YH. 2001, Morphology of Regenerated Silk Fibroin: Effects of Freezing Temperature, Alcohol Addition, and Molecular Weight. Journal of Applied Polymer Science , 81; 3008–3021.

Nazarov R, Jin HJ and Kaplan DL. 2004, Porous 3-D scaffolds from regenerated silk fibroin. Biomacromolecules , 5; 718-26.

Patel ZS, Yamamoto M, Ueda H, Tabata Y, Mykos AG. 2008, Biodegradable gelatin microspheres as delivery systems for the controlled release of bone morphogenetic protein-2. Acta Biomater , 4; 1126-38.

Phillips FM, Turner AS, Seim HB, MacLeay J, Toth CA, Pierce AR, Wheeler DL, *et al.* 2006, *In vivo* BMP-7 (OP-1) enhancement of osteoporotic vertebral bodies in an ovine model. Spine J , 6; 500–506.

Reddi AH. 2005, BMPs: from bone morphogenetic proteins to body morphogenetic proteins. Cytokine Growth Factor Rev, 16 : 249–250.

Ritger PL and Peppas NA. 1987, A simple equation for description of solute release. I. Fickian and non-Fickian release from non-swellable devices in the form of slabs, spheres, cylinders or discs. J Control Release , 5; 23-26.

Scheibel T. 2006, Silk: a biomaterial with several facets, Appl. Phys A , 82; 191-196.

Simank HG, Herold F, Schneider M, Maedler U, Ries R, Sergi C, 2004, Growth and differentiation factor 5 (GDF-5) composite improves the healing of necrosis of the femoral head in a sheep model. Analysis of an animal model, Orthopade , 33; 68-75.

Spiro RC, Thompson AY, Poser JW. 2001, Spinal fusion with recombinant human growth and differentiation factor-5 combined with a mineralized collagen matrix., Anat Rec , 263; 388-95.

Tamada Y. 2005, New process to form a silk fibroin porous 3-D structure. Biomacromolecules , 6; 3100-6.

Wang X, Wenk E, Matsumoto A, Meinel L, Li C and Kaplan DL. 2007, Silk microspheres for encapsulation and controlled release. J Control Release , 117; 360-370.

Wang YJ, Lin FH, Sun JS, Huang YC, Chuec SC, Hsu FY *et al.* 2003, Collagen–hydroxyapatite microspheres as carriers for bone morphogenic protein-4. Artif Organs , 27; 162–168.

Wei G, Jin Q, Giannobile WV and Ma PX. 2007, The enhancement of osteogenesis by nanofibrous scaffolds incorporating rhBMP-7 nanospheres. Biomaterials , 28; 2087–2096.

Wenk E, Wandrey AJ, Merkle HP, Meinel L. 2008, Silk fibroin spheres as a platform for controlled drug delivery. J Control Release , 132; 26-34.

Zhang YQ, Shen WD, Xiang RL, Zhuge LJ, Gao WJ and Wang WB. 2007, Formation of silk fibroin nanoparticles in water-miscible organic solvent and their characterization. Journal of Nanoparticle Research , 9; 885–900.

Chapter VII

Silk fibroin microparticles as carriers for delivery of human recombinant BMP-2. *In vitro* and *in vivo* bioactivity

This Chapter is based on the following publication:

Bessa PC, Balmayor ER, Hartinger J, Zanoni G, Dopler D, Meinl A, Banerjee A, Casal M, Redl H, Reis RL, van Griensven M, 2009, Silk fibroin microparticles as carriers for delivery of human recombinant BMP-2. *In vitro* and *in vivo* bioactivity, Tissue Engineering, Part C - Methods, *submitted.*

Chapter VII

Silk fibroin microparticles as carriers for delivery of human recombinant BMP-2. *In vitro* and *in vivo* bioactivity

Abstract

Bone morphogenetic proteins (BMPs) are growth factors with an important role in bone formation. In this study, we evaluated the use of silk fibroin microparticles as a novel delivery carrier for BMP-2, *in vitro* and *in vivo* in a rat model for ectopic bone formation. The particles did not exhibit significant cytotoxicity. In murine C2C12 cells, the fibroin particles with entrapped BMP-2 induced osteogenic mineralization and an increase in alkaline phosphatase activity. In the rat ectopic model, bone formation was observed by *in vivo* μCT after 2 and 4 weeks post-implantation, both with 5 and 12.5 μg BMP-2, with an increase in bone density over time. Histology revealed further evidence of ectopic bone formation, observed by strong Alizarin Red staining and osteocalcin immunostaining. Our findings showed that fibroin microparticles may be used for the sustained delivery of BMP-2, allowing the formation of new bone.

Introduction

Bone morphogenetic proteins (BMPs) are a group of cytokines from the transforming growth factor-beta (TGF-β) superfamily that have been used as powerful osteoinductive components in several late-stage tissue engineering products for bone grafting (Reddi *et al.* 2005, Bessa *et al.* 2008a, Bessa *et al.* 2008b). Currently, two devices using BMPs have been approved by the FDA for human clinical application based on the use of collagen sponges (Gautschi *et al.* 2007). However, as collagen poses several drawbacks such as sub-optimal handling conditions and the risk of disease transmission, there is still a need for an optimized BMP delivery system (Kirker-Head et al. 2007; Bessa et al. 2008).

The search for efficient, simple and cheap delivery systems for drug targeting has lead to a great investment in the area of nano and microparticles for drug delivery. In tissue engineering, these systems are excellent choices for growth factor delivery, since they can be easily prepared and sterilized. They can be processed into injectable systems allowing an easy and non-invasive implantation in the patient. Silk offers one versatile alternative as a natural biocompatible and biodegradable protein polymer that has been shown to efficiently deliver

BMPs in a variety of works (Karageorgiou *et al*. 2004, 2006, Li *et al*. 2006, Kirker-Head *et al*. 2007).

We have been studying a fibroin-based microparticle system as a potential new carrier for loading and release of BMPs (Bessa *et al.* 2008c). In the present study, we examined the bioactivity of BMP-2 loaded fibroin microparticles *in vitro* in C2C12 cells, by quantification of the alkaline phosphatase (ALP) activity and calcium mineralization, and in a rat ectopic bone formation model, using *in vivo* μCT and histological analysis.

2. Materials and Methods

2.1. Materials

Silk-containing *Bombyx mori* cocoons were purchased from Halcyon Yarn, US. The silk fibroin was isolated from the cocoons following an adapted degumming protocol (Zhang *et al.* 2007). Fibroin microparticles were prepared using the method of by Cao and Colleagues (2007), with modifications. Briefly, a solution 1% (w/v) fibroin in phosphate buffer saline was prepared, to which 0.5 μg BMP-2 (Wyeth, UK) was loaded. This solution was incubated at room temperature with stirring (600 rpm), while absolute ethanol was added dropwise to a ratio of 1:2 to the initial volume of fibroin. The solution was incubated overnight at -20 ºC, washed with distilled water, collected by centrifugation and freeze-dried. The characterization of the fibroin microparticles by scanning electron microscopy (SEM), dynamic light scattering (DLS), swelling behavior, and the release profile of BMP-2, was described elsewhere (Bessa *et al.* 2008c). All other chemicals were of analytical grade.

2.2 Methods

2.2.1. Bioactivity in C2C12 cells

C2C12 cells have been used for screening the osteogenic activity of BMPs in a variety of works (Klösch *et al.* 2004, Long *et al.* 2006, Bessa *et al.* 2008d, Bessa *et al.* 2009). These cells do not express significant amounts of endogenous BMPs, thus making them an effective model for testing the activity of the released BMP-2 (Katagiri *et al.* 1994). C2C12 cells were seeded at 10^5 cells/ml per well in a 24-well plate, attached in Dulbecco's modified Eagle's medium (DMEM), with 1% (v/v) fetal calf serum, at 37 ºC, with 5% CO_2 in a humidified environment. The cells were incubated with unloaded particles and with particles containing 0.5 and 2.5 μg loaded BMP-2 (Wyeth, UK). BMP-2 was added as a positive control, to the culture medium, at 0.1, 0.5 and 1.0 μg/ml. As another control, unloaded particles which were immersed for 30 min in 5 μg/ml BMP-2 and washed twice, were also added to the cells (adsorbed BMP control).

Alkaline phosphatase (ALP) enzymatic activity was measured accordingly to standard procedures (Salgado *et al.* 2002) after 5 days in C2C12 cultures. For the Alizarin Red mineralization assay, C2C12 cells were seeded at 3 x 10^4 cells /ml per well and cultured in DMEM supplemented with 100 µM ascorbic acid and 10 mM β-glycerophosphate, in the presence of both unloaded and BMP-2 loaded microparticles. Media and particles were replaced every 5 days. After 14 days of culture, the cells were washed for three times with PBS (without Ca^{2+}, Mg^{2+}) and fixed in 4% (v/v) formaldehyde, for 30 min. After removal of the fixative, cells were washed twice with distilled water and covered with Alizarin Red 1% solution, followed by gentle agitation in an orbital shaker for 10 min. The solution was then removed and the cells washed three more times with distilled water. The cells were observed using a Axiovert10 (Zeiss, Germany) optical microscope, and imaged with a coupled Coolpix950 (Nikon, Japan) camera.

2.2.2. MTS cell viability assay

Human osteosarcoma cells (SaOS-2 cell line; ECACC) were used for cell viability tests instead of murine C2C12 cell line, since these are a well-established human cell line of an osteoblast phenotype. Human osteosarcoma cells were seeded at 10^6 cells/ ml in a 24-well plate, attached overnight in Dulbecco's modified Eagle's medium (DMEM) with 1 % fetal calf serum and no antibiotics, at 37 ºC, 5 % CO_2, in a humidified environment, and cultured for 1, 3 and 5 days. Unloaded fibroin particles were added to the cell culture at 0.5 mg/ml. MTS cell viability assay was determined after these time periods using a standard procedure (Salgado *et al.* 2002). Latex rubber (Velos-Perforex, Manchester, UK) and standard culture medium were used as positive and negative controls, respectively. Latex rubber is known to have a strong cytotoxic effect leading to extensive cell death and lysis, and is commonly used as a positive control for cell death. All the samples were tested in triplicate for at least two independent experiments with reproducible results. The results are expressed as a percentage of the control (scored as 100% viability) as mean ± SD.

2.2.3. Rat ectopic bone formation model

Male Sprague-Dawley rats (weighting 340-360 g), were purchased from the Institut für Labortiertechnik und -genetik (Himberg, Austria). They were housed in light and temperature-controlled facilities and given food and water *ad libitum*. In three animals, surgery was performed after general anesthesia with an intramuscular injection of 60 mg/kg of body weight (BW) ketamine (Ketavet®, Pharmacia, Erlangen, Germany) and 7.5 mg/kg BW xylazine (Rompun®, Bayer, Leverkusen, Germany). After shaving and disinfecting the dorsum of the

animals, four midsagittal incisions were made dorsally in the proximal area of each limb and subcutaneous pockets were created by blunt dissection. The fibroin particles were implanted subcutaneously into each pocket. Three groups were defined: group I (unloaded particles), group II (particles + 5 µg BMP-2) and group III (particles + 12.5 µg BMP-2). The animals were randomized and were implanted with four samples (n = 4) per each group. Only one group was assigned to each animal to avoid the potential interference of released BMP by blood circulation. After placement of the particles, the incisions were closed with sutures, and the wound covered with vapor-permeable spray dressing (Opsite®, Smith & Nephew, London, UK). Analgesia treatment was given post operation, of 0.01 mg/kg BW Buprenorphin. At the end of each implantation period (4 weeks), the animals were sacrificed and samples from the tissues surrounding the implantation site were harvested. The animal protocol was approved by the authority of the city government of Vienna.

2.2.4. *In vivo* µCT

Live microCT (vivaCT 75, Scanco Medical AG, Switzerland) was used to examine bone formation in individual rats. MicroCT imaging was performed at weeks 2 and 4 respectively. Rats were anesthetized for 5 min with 2 % isoflurane during measurement. No X-ray contrast media was used in this study. Image reconstruction was performed using the built-in 3D visualization software (Scanco Medical AG, Switzerland). The evaluation of newly formed bone and bone density were performed using IPL version v5.06b (Scanco Medical AG, Switzerland).

2.2.5. Histology

Harvested samples were fixed in neutral buffered 10 % formalin and embedded in paraffin. Three-micrometer or four-micrometer sections were cut and stained with hematoxylin and eosin (H & E) or Alizarin Red S, respectively, for light microscopy observation. For a detailed analysis of the tissue differentiation, immunohistochemical staining was performed in selected samples. Briefly, paraffin sections were dewaxed with xylene and rehydrated in a graded ethanol series. After enzymatic antigen retrieval with 0.1 % Proteinase (Sigma Aldrich, USA) sections were incubated with an Osteocalcin antibody (Santa Cruz Biotechnology, USA) in a humidified chamber at 4 ºC overnight. After rinsing, sections were incubated with the EnVision™ system (Dako, Denmark) at room temperature for 30 min. and immunoreactivity was visualized with AEC solution (Thermo Fisher Scientific, USA). Slides known to express Osteocalcin were used as positive controls, omitting of the primary antibody served as negative control.

2.2.6. Statistical analysis

Experiments were performed at least in triplicate and expressed as means ± standard deviation. Student's t test was used for statistical analysis using a two-tailed non-paired test. Statistical significance was defined as $p < 0.01$ for a 99% confidence.

3. Results

3.1. Alkaline phosphatase in C2C12 cells

The bioactivity of BMP-2 released from the silk fibroin microparticles was studied by determining the ability to induce ALP enzymatic activity over basal levels in C2C12 cells (negative controls) after 5 days of culture, and by comparing the cell response to a BMP-2 dose-response effect directly added to the culture medium (positive control). The BMP-2 released from the fibroin particles was able to induce a significant increase in ALP activity over basal levels after 5 days ($p < 0.01$, **Figure 1**). Particles containing 2.5 μg of BMP-2 could induce high levels of ALP activity comparable to the positive control. Cells were observed to have differentiated into osteoblast morphology (data not shown). The fibroin particles with only adsorbed BMP-2 was able to induce solely a small increase in ALP activity. Unloaded particles did not induce any increase in ALP activity or osteoblast morphology. After two weeks of cell culture, the BMP-2-loaded fibroin particles were able to induce mineralization as observed by Alizarin red staining (**Figure 2**), identically to positive control (BMP-2 added to culture medium).

3.2. Cell viability

The silk fibroin microparticles did not show any significant evidence of cytotoxicity in human osteosarcoma cells, after 1, 3 or 5 days of cell culture (**Figure 3**). The cells were able to proliferate normally along this time period. MTS is a viability/proliferation test and an inverse relationship of toxicity to cells can be assumed (Salgado *et al.* 2002). Data correlates with morphological observations of the cells with optical microscopy (data not shown). Similar data was also obtained when particles were tested in primary cultures of human adult adipose derived stem cells (data not shown).

3.3. *In vivo* μCT

All animals showed no complications in wound healing, during the 4-week follow up. After 2 and 4 weeks, all sites of fibroin particle implantation were easily identified and retrieved for analysis by μCT. The μCT reconstructions showed clearly ectopic calcifications in all BMP-2

loaded implanted particles, which varied from 1 to 3 mm in width. The bone formed as a solid shell on part of the surface and as having a trabecular structure inside (**Figure 4 and 5**). We were not able to image the implantation site of group III (fibroin particles + 12.5 µg BMP-2) after 2 weeks follow-up, as the animal breathing interfered with the imaging process. Comparing the reconstructions of group II (fibroin particles + 5 µg BMP-2) between 2 and 4 weeks follow-up, large differences in amount of ectopic bone formed could be observed (**Table 1**). There was an increase in both the bone density and bone volume in group II (fibroin particles + 5 µg BMP-2) between 2 and 4 weeks (178.3 to 288.2 mg HA/mm^3 bone and 1.9 mm^3 to 2.5 mm^3) and an increase in the ratio between bone and tissue (0.025, after 2 weeks, to 0.050, after 4 weeks). The dimensions of the newly formed bone was nearly similar between the two time periods. Furthermore, the µCT imaging at the 2 weeks measurement had to be performed with a lower threshold, thereby adding evidence that a significant increase in bone formation occurred in the period between 2 and 4 weeks, in group II. At 4 weeks post-implantation, group III (fibroin particles + 12.5 µg BMP-2) revealed that ectopically formed bone an higher density (433.0 mg HA/mm^3 bone) compared to group II (fibroin particles + 5 µg BMP-2) (288.2 mm HA/mm^3 bone). No ectopic bone formation was detected in group I, where unloaded fibroin particles were implanted (data not shown).

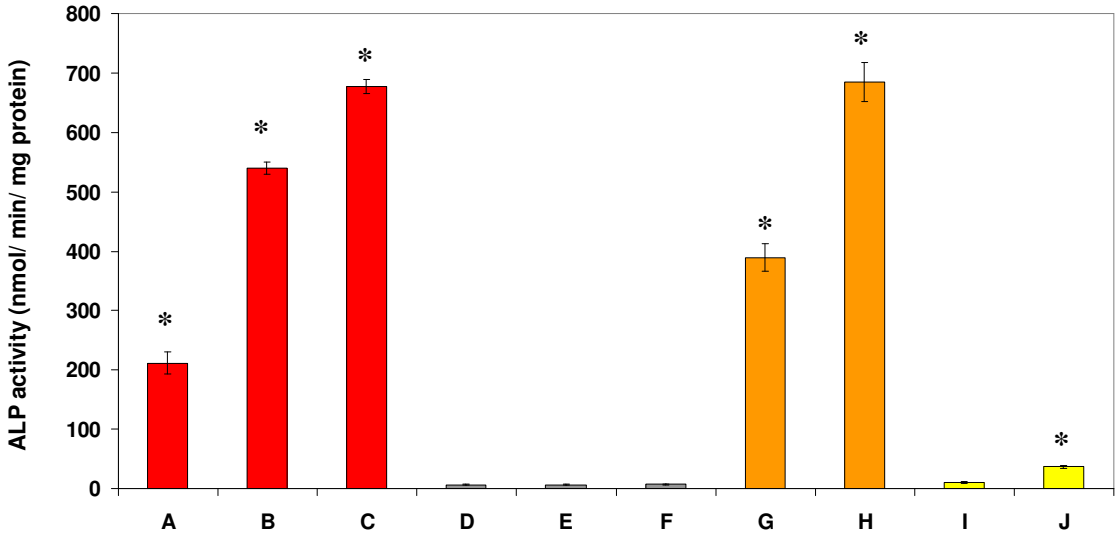

Figure 1. Alkaline phosphatase activity of C2C12 cell line after 5 days of culture. A-C) BMP-2 soluble protein, positive control, 0.1, 0.5 and 1.0 µg/ml; D) control cells (no growth factor or particles added); E and F) unloaded particles; G) particles with loaded BMP-2 (0.5 µg), H) fibroin particles with loaded BMP-2 (2.5 µg), I-J) fibroin particles with adsorbed BMP-2. ALP activity is reported in nmol /min /mg of total protein (Mean ± SD, n = 3), * $p < 0.01$ relative to negative control cells (D).

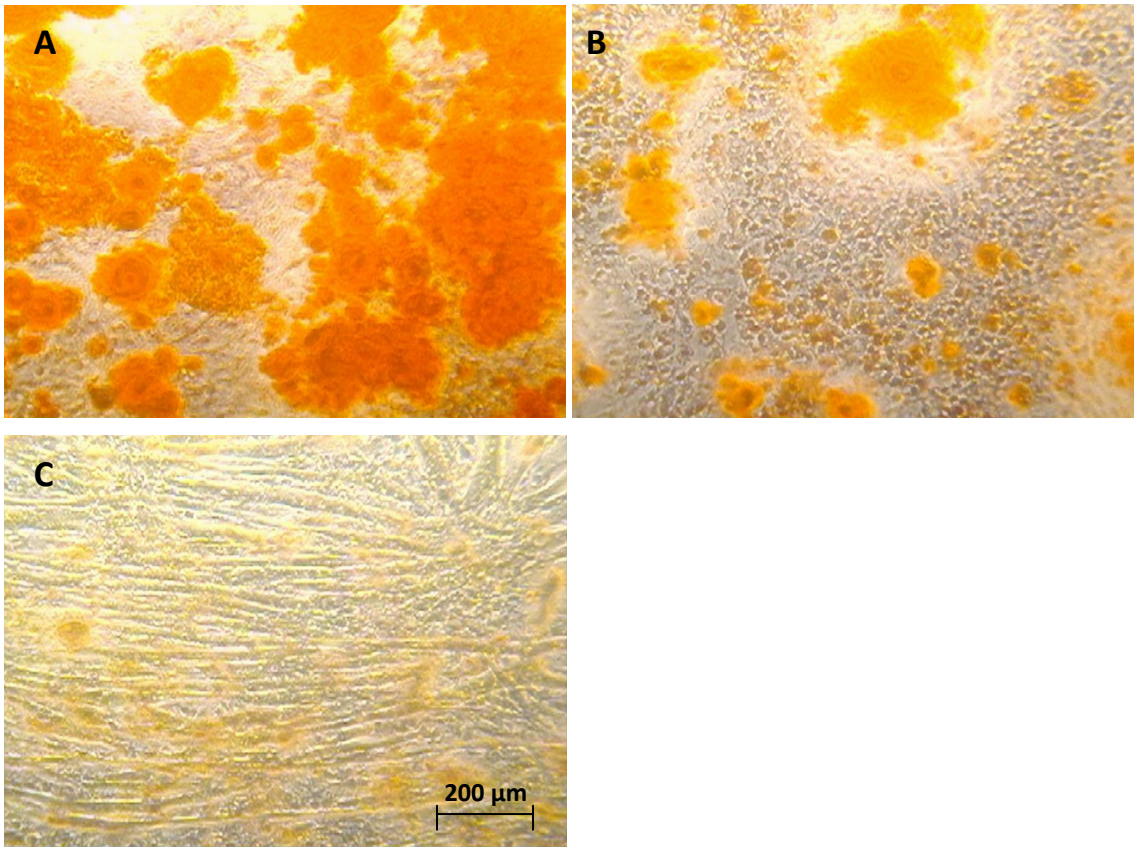

Figure 2. Alizarin red mineralization staining of showing sites of calcium-phosphate deposits (orange color) in C2C12 cell line differentiated into osteoblast after 14 days of culture with particles loaded with 0.5 µg BMP-2 (A), and 0.5 µg/ml BMP-2 added to culture medium (B). Unloaded fibroin particles did not show any mineralization (C).

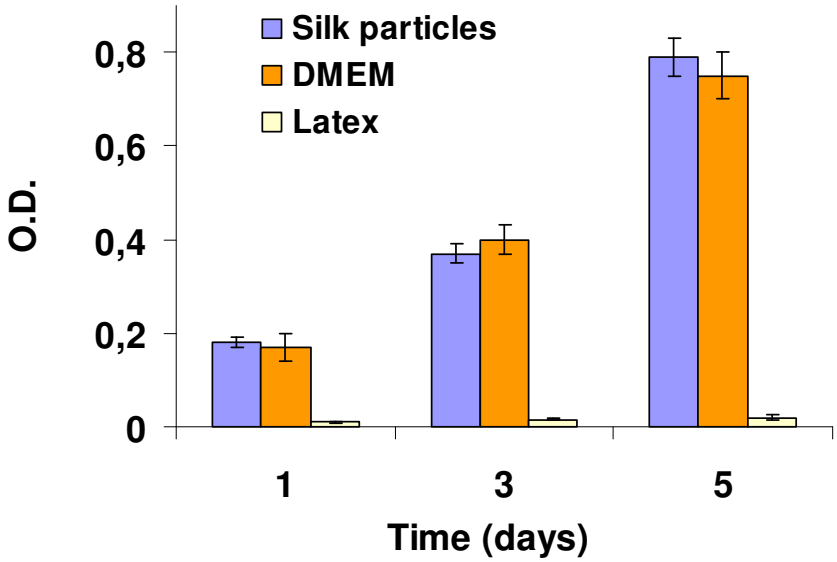

Figure 3. Cell viability tetrazolium salt (MTS) test performed in SaOS-2 cells as a function of the time of cells culture with 0.5 mg/ml silk fibroin microparticles. DMEM and Latex were used as a negative and a positive control for cell death, respectively. (mean ± SD, *n* = 3)

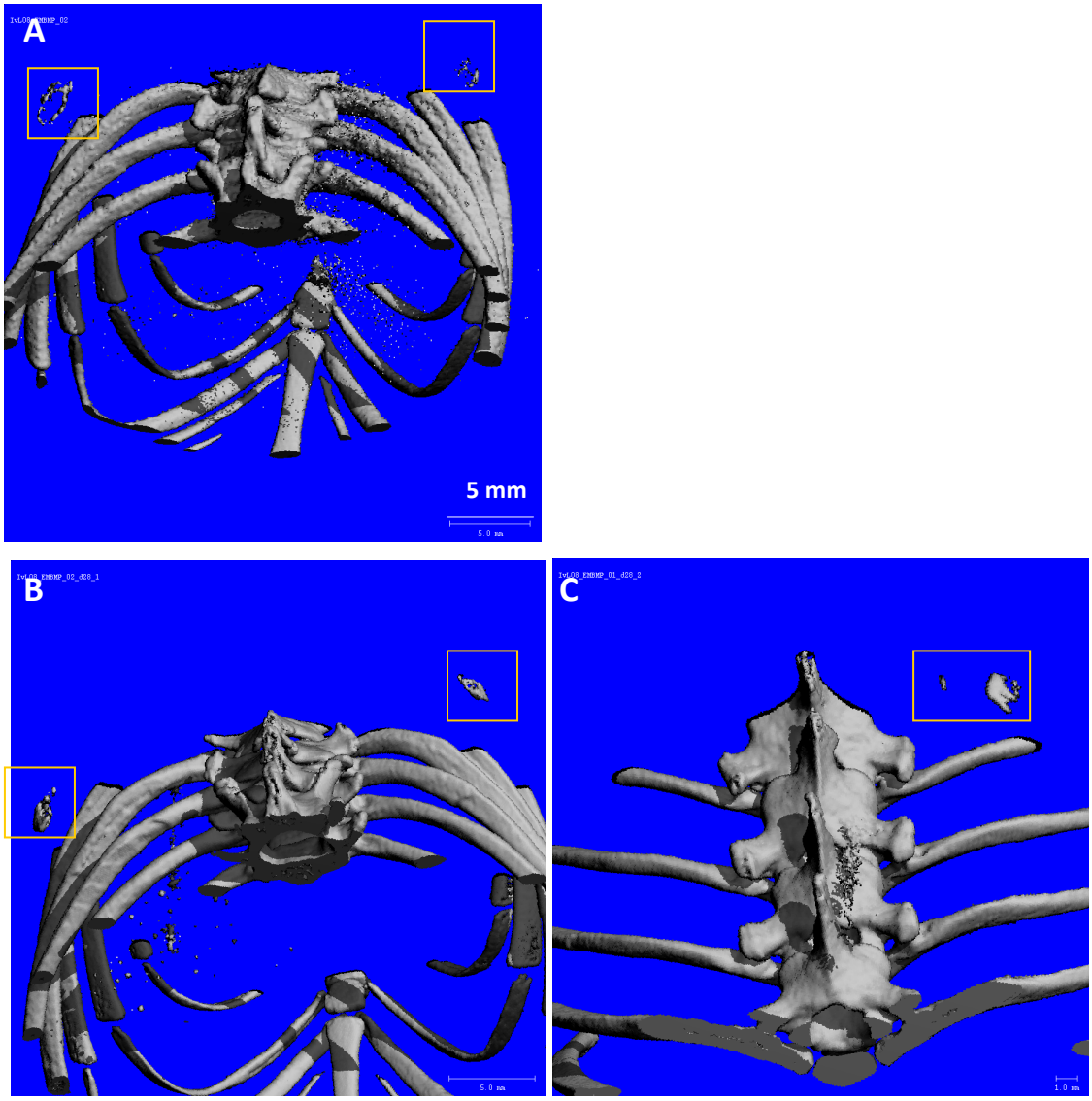

Figure 4. Live microCT analysis of ectopic bone formation induced by fibroin particles + 2.5 µg BMP-2 after 2 weeks (A) and 4 weeks (B), and fibroin particles + 12.5 µg BMP-2 after 4 weeks (C). Scale is 5 mm.

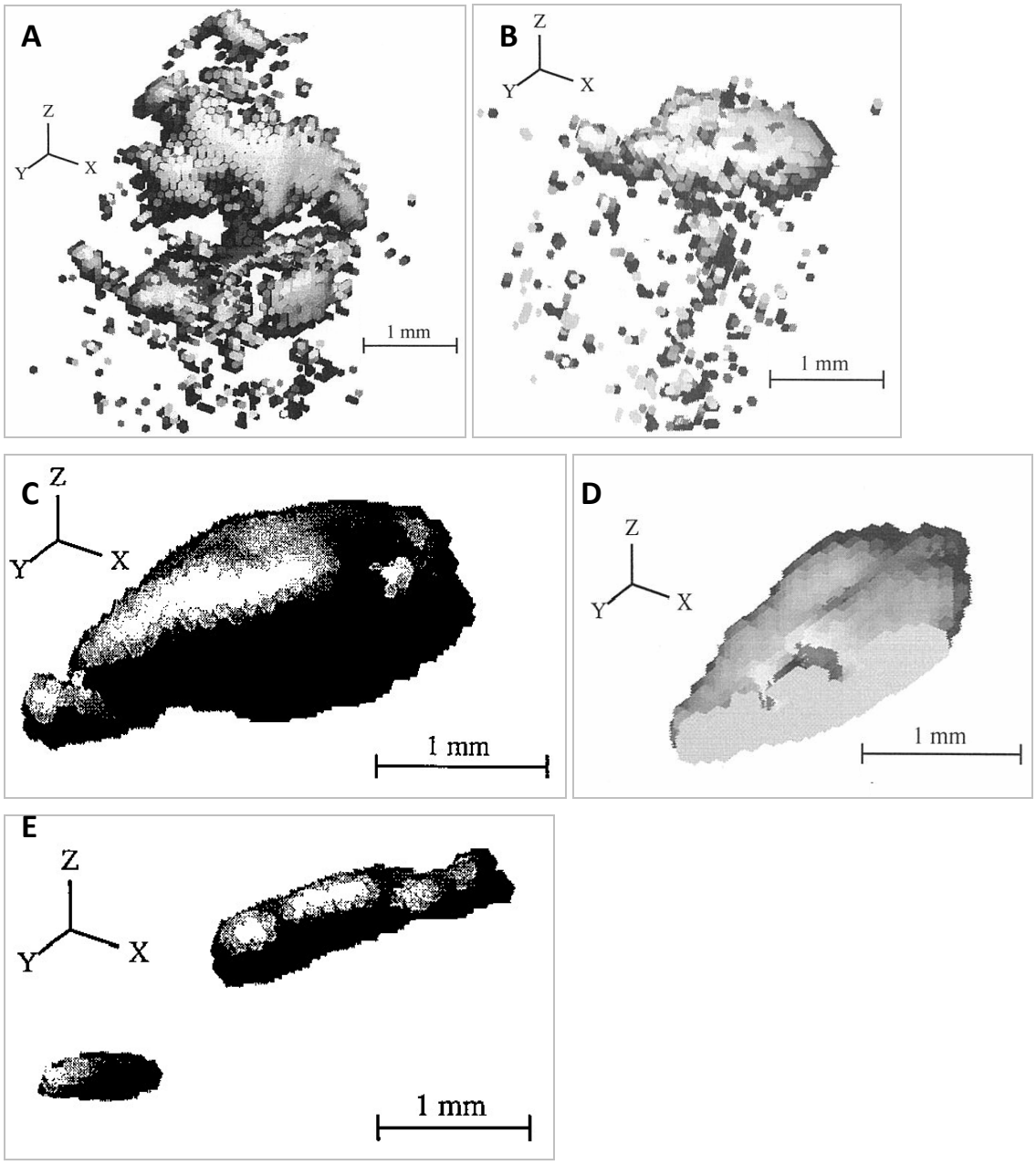

Figure 5. Detailed live microCT analysis of ectopic bone formation induced by fibroin particles + 2.5 µg BMP-2 after 2 weeks (A and B) and 4 weeks (C and D), and fibroin particles + 12.5 µg BMP-2 after 4 weeks (E). Background signal in A and B is due to a lower threshold used for bone visualization. Scale is 1 mm.

Table 1. Analysis of *in vivo* μCT data, showing bone size, surface area, volume and mean density. Group II (fibroin particles + 5 μg BMP-2), group III (fibroin particles + 12.5 μg BMP-2). (mean ± standard error, *n* = 2)

Group	Group III (4 weeks)	Group II (4 weeks)	Group II (2 weeks) *
Bone density (mg HA/mm^3)	433.0	288.2 ± 20.8	178.3 ± 11.3
Bone volume (BV) (mm^3)	1.2	2.5 ± 0.5	1.9 ± 0.6
Tissue volume (TV) (mm^3)	89.6	47.9 ± 18.3	76.6 ± 18.9
Bone volume ratio (BV/TV)	0.013	0.050 ± 0.001	0.025 ± 0.002

* the threshold used for bone detection in μCT was lower than that used for the measurements at 4 weeks

3.4. Histology

H&E staining revealed no signs of vascularization, but in group II some parts showed calcified tissue. In this group, H&E staining revealed abundant presence of osteoblasts and osteocytes surrounded by an extracellular matrix (**Figure 6A**). These tissues showed intense Alizarin Red staining (**Figure 6B**). In group III, no Alizarin Red positive areas could be observed, despite the fact that in the μCT ectopic bone formation was observed. At the time of harvest it was not possible to localize where the new bone formation was occurring. No staining was detected in the control group as expected (data not shown). Immunohistological evaluation with an osteocalcin-specific antibody revealed moderate staining in sections of group II (**Figure 6C**), in the site where osteoblasts surrounding a mineralized matrix were detected. Staining was not detected in a negative control with no incubation with the osteocalcin antibody (data not shown).

4. Discussion

It is well recognized the need for an efficient delivery system for BMPs as a way of providing effective and sustained stimulation of bone formation, as shown in several experimental models (Seeherman and Wozney 2005). The main role of a carrier is to retain these growth factors at the site of injury for a prolonged time frame, protecting the

immobilized drugs from degradation and maintaining its bioactivity, whilst releasing the protein in a time and site-controlled way to promote the formation of new bone at the treatment site.

Currently, diverse synthetic and natural origin polymers have been investigated for the delivery of BMPs in bone tissue engineering. The most common includes collagen, polylactic-co-glycolic acid (PLGA), polyethylene glycol (PEG), hydroxyapatite, gelatin, chitosan, fibrin, hyaluronic acic, and silk fibroin, generally in hydrogels, scaffolds or microparticles form (Bessa *et al.* 2008b). Fibroin-based biomaterials have been explored as novel alternatives for drug delivery and in tissue engineering as a result of their biocompatibility, biodegradability, mechanical strength, and versatility of formats into which the material could be processed (Lammel *et al.* 2008). In the present study we examined the *in vitro* and *in vivo* delivery of BMP-2 from fibroin microparticles.

The basis for evaluating the activity of the BMP released by the fibroin particles was to test initially particles loaded with the growth factor in C2C12 cell line and then using a rat ectopic bone formation model. C2C12 murine pre-myoblast cells are well-defined by their ability to rapidly differentiate into osteoblasts when cultured in presence of BMPs (Vallejo *et al.* 2002, Klösch *et al.* 2004, Long *et al.* 2006). In these cells, fibroin particles loaded with BMP-2 (0.5 and 2.5 μg) were able to induce a significant increase in ALP activity (after 5 days of culture), osteoblast-like morphology and the formation of a mineralized matrix (after two weeks of culture), thereby confirming that the protein was loaded into the particles remaining in bioactive state. This adds value to the method formerly developed to produce fibroin particles by ethanol precipitation (Nam and Park 2001, Cao *et al.* 2007, Zhang *et al*. 2007), confirming that is retains the activity of loaded drugs. A similar case was reported for fibroin particles and films, obtained by methanol precipitation, that retained the activity of immobilized horseradish peroxidase and lysozyme (Hofmann *et al*. 2006, Wang *et al*. 2007). In addition, the levels of ALP activity obtained with BMP-2 loaded particles were similar to those of induced by BMP-2 added to culture medium, indicating that most of the growth factor was released over the timeframe of 5 days. Since particles with surface-adsorbed BMP-2 induced low levels of ALP, it is likely that most of the growth factor accountable for the significant increase in ALP levels is BMP-2 loaded into the particles during their fabrication. No cytotoxicity was detected by the use of fibroin particles *in vitro*, as inferred by the MTS cell viability assay. In general, silk fibroin has been regarded as a good biocompatible material, effecting low immune responses *in vivo*, and with an historical use as sutures in clinical applications (Altman *et al.* 2003, Meinel *et al.* 2005, Wang *et al*. 2008).

Ectopic bone formation models in rodents have been used to test the activity of BMPs in a wide variety of studies (Bulpitt and Aeschlimann, 1999, Maire *et al*. 2005, Zhang *et al.* 2005, Kato *et al.* 2006, Jeon *et al.* 2007). The microparticles could form a slurry that was easily implanted ectopically in rats. After two and four weeks, bone formation was observed in all sites of implantation of BMP-2 loaded particles and the extent of ectopically formed bone was measured by microCT. Mineralized areas of bone were found as early as after two weeks post-implantation, and increased both in bone volume and hydroxyapatite density, after four weeks. MicroCT is a reliable and non-invasive method for scan and evaluation along time of bone mass, structure, geometric and density parameters (Hangartner 2007). The use of microCT imaging maximizes the results from single animals, offering sequential data within the same animal, reducing this way the required number of animals per study (Cowan *et al.* 2007). Ectopic bone formation was also confirmed by histological analysis, performed at four weeks post-implantation. New bone formation was detected by the presence of a calcified extracellular matrix, which was stained by Alizarin Red, revealing only surface mineralization without quantitative data, as compared to the microCT data. In addition, osteocalcin, a calcium-binding protein and a marker of mature bone formation (Price 1989), was also detected in the cells surrounding the newly formed bone.

New bone formation occurs as released BMP-2 triggers the recruitment of stem cells that differentiate into osteoblasts and form a calcium-phosphate matrix (Cunningham *et al*. 1992). This can only occur if there is not only an initial stimulation of the site by BMP-2 but also a sustained released of the growth factor in the following weeks, that allows the formation of new bone to occur. In the lack of a sustained release the BMP-2 is usually cleared from the implant site within hours, supposedly terminating its local effect (Louis-Ugbo *et al.* 2002). This is demonstrated by studies where surface-adsorbed BMP-2 was used in the particles which failed to induce new bone formation probably due to either loss of the BMP bioactivity or insufficient duration of stimulus (Wei *et al*. 2007). Thus, it has been suggested that materials exhibiting an higher retention of BMPs yield increased osteoinductive activity (Uludag *et al.* 1999, 2000). In our contribution, the amounts of BMP-2 loaded into the fibroin microparticles (5 and 12.5 μg), are similar to the values reported in the literature to achieve ectopic bone formation in rats with BMP-2, using other delivery systems (Kenley *et al.* 1994, Hosseinkhani et al. 2007, Wei *et al.* 2007). The fibroin microparticles have clearly shown to be able to deliver BMP-2 in a sustained way, allowing therefore the formation of new bone.

In conclusion, the fibroin microparticles may constitute a promising delivery system of recombinant human BMPs, for future bone tissue engineering applications.

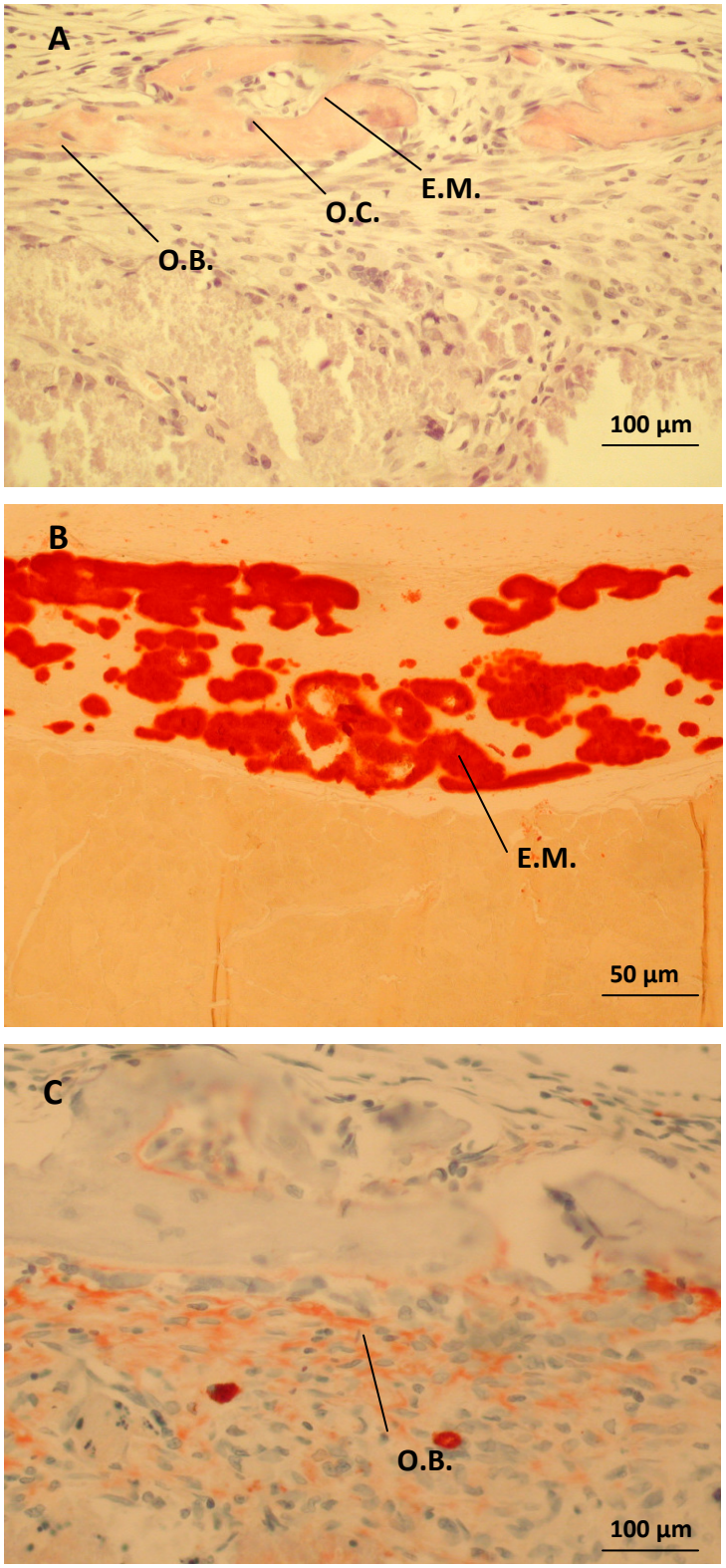

Figure 6. H&E staining for animals implanted with fibroin particles + 5 µg BMP-2 (group II) at 4 weeks post-implantation (A). Newly formed bone was indicated by the presence of a mineralized extracellular matrix (E.M.) which was stained with Alizarin Red (B), osteocytes (O.C.), and osteoblasts (O.B.) which were stained by osteocalcin immunostaining (C).

References

Altman GH, Diaz F, Jakuba C. *et al.*, Silk-based biomaterials. Biomaterials 24, 401–416, 2003.

Bessa PC, Casal M and Reis RL. Bone morphogenetic proteins in tissue engineering: the road from laboratory to the clinic, part I (basic concepts). J Tissue Eng Regen Med. 2, 1-13, 2008a.

Bessa PC, Casal M and Reis RL. Bone morphogenetic proteins in tissue engineering: the road from laboratory to the clinic, part II (BMP delivery). J Tissue Eng Regen Med. 2, 81-96, 2008b.

Bessa PC, Balmayor ER, Cerqueira MT *et al*. In 'Silk nanoparticles for delivery of human BMP-2 in bone regenerative medicine applications', TERMIS-EU Annual meeting, Portugal 2008, Tissue Engineering: Part A 14, 776-777, 2008c.

Bessa PC, Pedro AJ, Klösch B. *et al.* Osteoinduction in human fat-derived stem cells by recombinant human bone morphogenetic protein-2 produced in Escherichia coli. Biotechnol Lett. 30, 15-21, 2008d.

Bessa PC, Cerqueira MT, Rada T. *et al*. Expression, purification and osteogenic bioactivity of recombinant human BMP-4, -9, -10, -11 and -14, Protein Expr. and Purif. 63, 89-94, 2009.

Bulpitt P and Aeschlimann D. New strategy for chemical modification of hyaluronic acid: preparation of functionalized derivatives and their use in the formation of novel biocompatible hydrogels, J Biomed Mater Res, 47, 152-69, 1999.

Cao Z, Chen X, Yao J *et al.* The preparation of regenerated silk fibroin microspheres. Soft Matter 3, 910-915, 2007.

Cowan C, Aghaloo T, Chou YF. *et al.* MicroCT evaluation of three-dimensional mineralization in response to BMP-2 doses *in vitro* and in critical size rat calvarial defects. Tissue Eng 13, 501-512, 2007.

Cunningham NS, Paralkar V, Reddi AH. Osteogenin and recombinant bone morphogenetic protein 2B are chemotactic for human monocytes and stimulate transforming growth factor beta 1 mRNA expression. Proc Natl Acad Sci U S A. 89, 11740-4, 1992.

Gautschi OP, Frey SP, Zellweger R. Bone morphogenetic proteins in clinical applications. ANZ J Surg. 77, 626-3, 2007.

Hangartnen TN. Thresholding technique for accurate analysis of density and geometry in QCT, pQCT and microCT images. J Musculoskelet Neuronal Interact. 7, 9-16, 2007.

Hofmann S, Foo CT, Rossetti F. *et al*. Silk fibroin as an organic polymer for controlled drug delivery. J Control Release, 111, 219-27, 2006.

Hosseinkhani H, Hosseinkhani M, Khademhosseini A *et al.* Bone regeneration through controlled release of bone morphogenetic protein-2 from 3-D tissue engineered nano-scaffold. J Control Release. 117, 380-6, 2007.

Jeon O, Song SJ, Kang SW *et al.* Enhancement of ectopic bone formation by bone morphogenetic protein-2 released from a heparin-conjugated poly(L-lactic-co-glycolic acid) scaffold, Biomaterials, 28, 2763-71, 2007.

Karageorgiou V, Meinel L, Hofmann S *et al*. Bone morphogenetic protein-2 decorated silk fibroin films induce osteogenic differentiation of human bone marrow stromal cells. J Biomed Mater Res A 71, 528–537, 2004.

Karageorgiou V, Tomkins M, Fajardo R *et al*. Porous silk fibroin 3D scaffolds for delivery of bone morphogenetic protein-2 *in vitro* and *in vivo*. J Biomed Mater Res A 78, 324–334, 2006.

Katagiri T, Yamaguchi A, Komaki M *et al.* Bone morphogenetic protein-2 converts the differentiation pathway of C2C12 myoblasts into the osteogenic lineage. J. Cell Biol. 127, 1755-66, 1994.

Kato M, Namikawa T, Terai H *et al.* Ectopic bone formation in mice associated with a lactic acid/dioxanone/ethylene glycol copolymer-tricalcium phosphate composite with added rhBMP-2, Biomaterials 27, 3927-33, 2006.

Kenley R, Marden L, Turek T *et al.* Osseous regeneration in the rat calvarium using novel delivery systems for recombinant human bone morphogenetic protein-2 (rhBMP-2), J Biomed Mater Res, 28, 1139-47, 1994.

Kirker-Head C, Karageorgiou V, Hofmann S *et al*. 2007; BMP–silk composite matrices heal critically sized femoral defects. Bone 41, 247–255.

Klösch B, Fürst W, Kneidinger R *et al.* Expression and purification of biologically active rat bone morphogenetic protein-4 produced as inclusion bodies in recombinant *Escherichia coli*. Biotechnol. Lett. 27, 1559-64, 2005.

Lammel A, Schwab M, Slotta U *et al.* Processing conditions for the formation of spider silk microspheres. ChemSusChem. 1, 413-6, 2008.

Li C, Vepari C, Jin HJ *et al*. Electrospun silk-BMP-2 scaffolds for bone tissue engineering. Biomaterials 27, 3115–24, 2006.

Long S, Truong L, Bennett K *et al.* Expression, purification, and renaturation of bone morphogenetic protein-2 from *Escherichia coli*. Protein. Expr. Purif. 46, 374-8, 2006.

Louis-Ugbo J, Kim HS, Boden SD *et al.* Retention of 125I-labeled recombinant human bone morphogenetic protein-2 by biphasic calcium phosphate or a composite sponge in a rabbit posterolateral spine arthrodesis model. J Orthop Res. 20, 1050-9, 2002.

Maire M, Chaubet F, Mary P *et al.* Bovine BMP osteoinductive potential enhanced by functionalized dextran-derived hydrogels, Biomaterials 26, 5085-92, 2005.

Meinel L, Hofmann S, Karageorgiou V *et al.* The inflammatory responses to silk films *in vitro* and *in vivo*, Biomaterials 26, 147–155, 2005.

Nam J and Park YH. Morphology of Regenerated Silk Fibroin: Effects of Freezing Temperature, Alcohol Addition, and Molecular Weight. Journal of Applied Polymer Science 81, 3008–3021, 2001.

Price PA, Gla-containing proteins of bone, Connect Tissue Res. 21, 51-7, 1989.

Reddi AH. BMPs: from bone morphogenetic proteins to body morphogenetic proteins. Cytokine Growth Factor Rev 16, 249–250, 2005.

Salgado AJ, Gomes ME, Chou A *et al.* Preliminary study on the adhesion and proliferation of human osteoblasts on starch-based scaffolds. Mater. Sci. Eng. 20, 27-33, 2002.

Seeherman H and Wozney JM. Delivery of bone morphogenetic proteins for orthopedic tissue regeneration, Cytokine Growth Factor Rev, 16, 329-45, 2005.

Uludag H, D'Augusta D, Golden J *et al.* Implantation of recombinant human bone morphogenetic proteins with biomaterial carriers: A correlation between protein pharmacokinetics and osteoinduction in the rat ectopic model. J Biomed Mater Res. 50, 227-38, 2000.

Uludag H, D'Augusta D, Palmer R *et al.* Characterization of rhBMP-2 pharmacokinetics implanted with biomaterial carriers in the rat ectopic model, J Biomed Mater Res, 46, 193-202, 1999.

Vallejo LF, Brokelmann M, Marten S *et al.* Renaturation and purification of bone morphogenetic protein-2 produced as inclusion bodies in high-cell-density cultures of recombinant *Escherichia coli*. J. Biotechnol. 94, 185–194, 2002.

Wang X, Wenk E, Matsumoto A *et al.* Silk microspheres for encapsulation and controlled release. Journal of Controlled Release 117, 360-370, 2007.

Wang Y, Rudym DD, Walsh A. *et al. In vivo* degradation of three-dimensional silk fibroin scaffolds. Biomaterials 29, 3415-28, 2008.

Wei G, Jin Q, Giannobile WV *et al*. The enhancement of osteogenesis by nanofibrous scaffolds incorporating rhBMP-7 nanospheres. Biomaterials 28, 2087–2096, 2007.

Zhang C, Hu Y, Xiong Z *et al.* [Tissue engineered bone regeneration of periosteal cells using recombinant human bone morphogenetic protein 2 induce], Zhongguo Xiu Fu Chong Jian Wai Ke Za Zhi, 19, 100-4, 2005.

Zhang YQ, Shen WD, Xiang RL *et al.* Formation of silk fibroin nanoparticles in water-miscible organic solvent and their characterization. Journal of Nanoparticle Research 9, 885–900, 2007

Chapter VIII

Thermoresponsive self-assembled elastin-based nanoparticles for delivery of BMPs

This Chapter is based on the following publication:

Bessa PC, Machado R, Nürnberger S, Dopler D, Meinl A, Banerjee A, Cunha AM, Rodríguez-Cabello JC, Redl H, van Griensven M, Reis RL, Casal M, 2009, Thermoresponsive self-assembled elastin-based nanoparticles for delivery of BMPs, Journal of Controlled Release, *submitted.*

Chapter VIII

Thermoresponsive self-assembled elastin-based nanoparticles for delivery of BMPs

Abstract

Elastin-like polymers are a new type of protein-based polymers that display interesting properties in the biomaterial field. Bone morphogenetic proteins (BMPs) are cytokines with a strong ability to promote new bone formation. In this work, we explored the use of elastin-like nanoparticles (237.5 ± 3.0 nm), created by thermoresponsive self-assembly, for the combined release of bone morphogenetic protein-2 (BMP-2) and bone morphogenetic protein-14 (BMP-14). These BMPs could be encapsulated at high efficiency into the elastin-like particles and delivered in a sustained way for 14 days. The activity of the growth factors was retained, as shown by the induction of ALP activity and osteogenic mineralization in C2C12 cells. Increased bioactivity was observed with a combined release of BMP-2 and BMP-14. This approach shows a significant potential for future tissue engineering applications in bone.

1. Introduction

Bone morphogenetic proteins (BMPs) have recently sparked great interest in the tissue engineering field due to its strong ability to promote bone and cartilage formation (Reddi 2005, Bessa *et al*. 2008a). During the process of bone formation, signals from BMPs trigger the differentiation of stem cells, which are recruited to the site of injury, into bone forming cells (Reddi 1981). In recent years, BMP-2 has demonstrated a successful regenerative potential in a variety of works in spinal disk regeneration, healing of long bone fractures, and periodontal repair (McKay *et al*. 2007). As part of the conceptual tissue engineering perspective, different materials have been proposed and researched as delivery carriers for BMPs (Bessa *et al*. 2008b). The materials for tissue engineering applications should ideally mimic the natural environment of tissues and, in this regard, natural polymers can exert signals to guide cells at the various stages of their development, accelerating healing, thus presenting excellent properties for clinical uses (Mano an Reis 2007).

Elastin-like polymers (ELPs) are repetitive polypeptides inspired on the mammalian elastin structure which consists of a pentapeptide repeat, VPGXG, where X may be any natural amino acid except proline (Chilkoti *et al*. 2006, Simnikc *et al*. 2007). The most interesting feature of

the ELPs is their Inverse Temperature Transition (ITT) behavior (Urry *et al*. 1992). Below a certain critical temperature, the transition temperature (T_t), and in the presence of water, the polymer remains soluble, with the chains relatively extended in a disordered state. Above the T_t, the polymer chains hydrophobically fold and self-assemble into a more ordered structure (Herrero-Vanrell *et al*. 2005, Machado *et al*. 2009). Poly(VPAVG), where the central glycine is replaced by an alanine, had been chemically synthesized and showed to form above its T_t, spherical microparticles, that are able to entrap active substances (Herrero-Vanrell *et al*. 2005, Rincón *et al*. 2006). The polymer self-assembling process occurs above a T_t of ~ 30 ºC, but the self-assembled structures only solubilize again when a strong cooling of ~10 ºC is achieved, a phenomenon called hysteresis (Herrero-Vanrell *et al*. 2005). The particles, once formed, are stable and can be used for drug delivery. In addition, ELPs demonstrate excellent biocompatibility (Urry *et al*. 1991). Apparently, the immune system ignores these polymers because it does not distinguish them from the natural elastin, and the degradation products are only natural amino acids.

Poly(VPAVG) can be produced by recombinant technology, in alternative to the typical chemical synthesis route (Machado *et al*. 2009). This has several advantages such as resulting in polymer with a defined molecular weight and, thus, a strictly monodisperse material. Moreover, the recombinant route allows the polymers to be designed accordingly for specific uses, by having a superior and easy control in the selection of its sequence, and hence, their physical-chemical properties. The recombinant polymer can be easily purified to high degrees by taking advantage of its thermal responsiveness (Meyer and Chilkoti 1999, Machado *et al*. 2009).

Herein, we report the production of elastin-like nanoparticles, by thermoresponsive self-assembly and by exploiting the inverse temperature transition of the biologically produced $(VPAVG)_{220}$, for a sustained release of both BMP-2 and BMP-14. BMP-14 (also known as GDF-5, growth and differentiation factor) is involved in tendon, ligament, and bone regeneration (Nakamura *et al*. 2003, Simank *et al*. 2004, Dines *et al*. 2007), possessing significant angiogenic activity (Yamashita *et al*. 1997, Zeng *et al*. 2007, Kadomatsu *et al*. 2008). Thus, it makes an attractive choice as a therapeutical agent in addition to BMP-2, due to the highly vascularised nature of bone and the interest to promote angiogenesis during bone formation. BMP-14 is a key growth factor involved during fracture repair (Al-Aql *et al*. 2008). The elastin nanoparticles were characterized for swelling behavior, the release profile of BMP-2 and BMP-14, and biological activity of the released growth factors in C2C12 cells.

2. Materials and Methods

2.1. Materials

The elastin-like polymer, $(VPAVG)_{220}$ consists of 220 repeats of the main monomer VPAVG and was produced by recombinant technology and purified as reported elsewhere (Machado *et al*. 2009). The polymer has a molecular weight of 96 kDa and self-assembles at temperatures above 33 ºC. More details in mass spectra (Maldi MS) verifying its amino acid composition, and self-assembling behavior, can be found in Machado *et al*. (2009). Human BMP-2, expressed in Chinese Hamster Ovary (CHO) cells, was purchased from Wyeth, United Kingdom. BMP-14, expressed in *E. coli* was purchased from PeProTech, United Kingdom. All other chemicals were of analytical grade and used as received.

2.2. Methods

2.2.1. Production of elastin-like nanoparticles

Particles were produced by resuspending lyophilized polymer in ice-cold phosphate buffer saline (PBS) to a final solution of 0.1%. The solution was then incubated at 37 ºC for 30 min. The particles were collected by centrifugation (10000 g, 37 ºC, 10 min), and washed once with pre-warmed PBS. Due to its hysteresis behavior, the particles are stable at room temperature and only solubilize when a strong undercooling is achieved (of about 10 ºC). The particles were prepared under sterile conditions, and stored at room temperature.

2.2.2. Physical characterization

Scanning electron microscopy (SEM)

Non-loaded elastin particles were morphologically characterized by scanning electron microscopy (SEM). SEM analysis was performed on gold-coated samples (Agar Sputercoater 108, Essex, United Kingdom) and using a Philips XL20 microscope (Philips, Eindhoven, The Netherlands). Particle size measurements were obtained from several micrographs acquired in the SEM.

Size distribution

Measurements of particle size were performed on freshly prepared filtered samples by dynamic light scattering (DLS), using a Zetasizer Nano Series (Malvern, UK). The analysis was performed at 37 ºC and by performing 10 readings.

Water uptake and degradation studies

The hydration degree of unloaded elastin nanoparticles was evaluated after immersion into PBS, pH 7.4, for periods up to 72 hours (30 min, 4h, 24 h, 48 h and 72h). The weight loss of unloaded elastin particles was assessed after immersion into PBS, pH 7.4, for periods up to 30 days (1 d, 3 d, 7 d, 15 d and 30 d). All experiments were conducted at 37 ºC, in triplicate. Percentage of water uptake (WU) after each time period of immersion (t) was calculated using the following equation:

$WU\ (\%)=(W_w-W_d) / W_d \times 100$

The percentage of mass remaining (MR) after each time period (t) was calculated using the following equation:

$WL\ (\%)=W_d/ W_i \times 100$

'W_w' and 'W_d' correspond to the weight of elastin particles in wet and dry state, respectively. 'W_i' corresponds to the initial dry weight of particles, before immersion.

2.2.3. *In vitro* delivery studies

Loading of BMP-2 and BMP-14

Elastin nanoparticles were loaded with BMP-2 or BMP-14 or a mix of the two, during the formation of the particles. Growth factor was added at a concentration of 20 µg/ml to the elastin-like polymer solution. The nanoparticles were produced with the different combinations of the two growth factors:

I) Unloaded particles (no growth factor)

II) encapsulated BMP-2

III) encapsulated BMP-14

IV) encapsulated BMP-2 and BMP-14

Determination of encapsulation efficiency

The nanoparticle encapsulation efficiency was determined upon their separation from the aqueous preparation medium containing the non-associated BMP by centrifugation (10000 g, 37 ºC, 10 min). The amount of free BMP-2 was determined in the supernatant by using a BMP-2 sandwich-type ELISA development kit (Eubio, Austria). The amount of free BMP-14 was estimated by dot blot using a rabbit anti-human BMP-14 antibody (BioVision, Germany) followed by an HRP-conjugated goat anti-rabbit antibody (Sigma, United States). The blot intensities were compared against BMP-14 standards of known concentration, with the use of image analysis software (ChemiImage 4400, Alpha Innotech, United States). Each sample was

assayed in triplicate (*n* = 3). The nanoparticle encapsulation efficiency (E.E.) was calculated using the following equation:

$$E.E.(\%) = \frac{\text{Total BMP amount } (\mu g) - \text{Free BMP amount } (\mu g)}{\text{Total BMP amount}} \times 100$$

In vitro release

Pre-weighted particles (250 µg dry weight), corresponding to particles loaded with BMP-2 or BMP-14 (groups II and III), were incubated in 5 ml PBS (pH 7.4), at 37 ºC, with 200 rpm agitation. At pre-determined time points (1 h, 4 h, 1 d, 2 d, 3 d, 7 d and 14 d), 100 µl of solution were removed, centrifuged (10000 g, 37 ºC, 10 min) and stored at -20 ºC until quantification. The solution was replaced with a similar volume of fresh buffer. Sterile conditions were applied to prevent any contamination of samples.

Quantification of released protein

For measurement of BMP-2 concentration, a BMP-2 sandwich-type ELISA kit (Eubio, Austria) was used, following the manufacturer's instructions. A calibration curve was obtained using standard preparations of BMP-2 of known concentration. For detection of concentration of BMP-14, the samples were estimated by dot blot as described before. Each sample was assayed in triplicate (*n* = 3) and mean ± SD values reported.

Release kinetics models

To study the release kinetics, the data obtained from the *in vitro* release was treated accordingly to zero order as cumulative amount of drug released *vs*. time (equation 1), first order as log cumulative percent drug remaining *vs*. time (equation 2), Higuchi kinetics as cumulative percent drug released *vs*. square root of time (equation 3) and Korsmeyer kinetics as log cumulative percent drug released *vs*. log time (equation 4) (Huguchi 1963, Chowdary and Ramesh 1993, Hadjiioannou *et al*. 1993, Bourne 2002):

$R = k_1 t$ (1)

$\text{Log } UR = k_2 t\ 2.303$ (2)

$R = k_3 t\ 0.5$ (3)

$\text{Log } R = \log k_4 + n \log t$ (4)

where R and UR are released and unreleased percentages, respectively, at time (t); k_1, k_2, k_3 and k_4 are the rate constants of zero-order, first order, Higuchi and Korsmeyer models, respectively; n is a exponent that characterizes the mechanism of release.

2.2.4. Bioactivity of released BMP

MTT cell viability assay

C2C12 cells were seeded at 5 X 10^4 cells/ ml in a 24-well plate, attached overnight in Dulbecco's modified Eagle's medium (DMEM) with 1 % fetal calf serum and no antibiotics, at 37 ºC, 5 % CO_2, in a humidified environment. Unloaded elastin particles were then added to the cell culture at 10 and 100 µg/ml. The MTT assay was determined after the 5 days of culture using a standard procedure (Salgado *et al*. 2002). Standard culture media, with no particles, was used as positive control of cell viability. All samples were tested in triplicate. The results are expressed as percentage of control (scored as 100% viability) as mean ± SD.

Alkaline phosphatase (ALP) activity

The bioactivity of the BMPs released from the elastin nanoparticles was studied by determining their ability to induce ALP enzymatic activity over basal levels in C2C12 cells (negative controls) after 5 days of culture, and by comparing the cell response to a BMP dose response effect when directly added to the culture medium (positive control). C2C12 cells were seeded at 5 x 10^4 cells/ml per well in a 24-well plate, attached in Dulbecco's modified Eagle's medium (DMEM), with 1% (v/v) fetal calf serum, at 37 ºC, with 5% CO_2 in a humidified environment. The cells were incubated with either unloaded or loaded elastin nanoparticles, in the experimental groups described before (I to IV). Particles contained 0.1, 0.25, 0.5 and 2.5 µg of BMP-2, BMP-14 or a mix of both, in the particle preparation added to the cells. BMP-2 (Wyeth, UK) and BMP-14 (PeProTech, UK) were added as controls to the culture medium, at 0.1, 0.25, 0.5 and 2.5 µg/ml (corresponding to similar amounts of growth factor loaded in the particles). Alkaline phosphatase enzymatic activity was measured accordingly to standard procedures (Salgado *et al*. 2002) after 5 days in C2C12 cultures, and normalized to the total protein content. All samples were tested in triplicate, with two independent experiments, with reproducible results.

Calcium mineralization assay

For the Alizarin Red mineralization assay, C2C12 cells were seeded at 5 x 10^4 cells /ml per well, in a 24-well plate, and cultured in DMEM in the presence of both unloaded and loaded

BMP-2/ BMP-14 particles, in the experimental groups described before (I to IV). The particles contained 2.5 μg of single or of both of each BMPs in the particle preparation added to the cells. BMP-2 or BMP-14 were added as controls to the culture media, at 2.5 μg/ml. After 5 days of culture, the cells were washed three times with PBS (to ensure that few or no particles were retained in the cell monolayer), the culture media was replaced by DMEM supplemented with 100 μM ascorbic acid and 10 mM β-glycerophosphate, and fresh particles or BMPs were added. This was repeated after day 10. After 14 days of culture, the cells were washed three times with PBS (without Ca^{2+}, Mg^{2+}) and fixed in 4% (v/v) formaldehyde, for 30 min. After removal of the fixative, cells were washed twice with distilled water and covered with Alizarin Red 1% solution, followed by gentle agitation in an orbital shaker for 10 min. The solution was then removed and the cells washed four more times with distilled water. The cells were observed using an Axiovert10 (Zeiss, Germany) optical microscope, and imaged with a coupled Coolpix950 (Nikon, Japan) camera. The mineralization was quantified by the method proposed by Gregory *et al*. (2004). Briefly, the calcium from cells was extracted by incubation of 800 μl acetic acid (10% v/v) to each well, for 30 min in orbital shaker. Then, the suspensions were transferred to a clean 1.5 ml eppendorf tube and vortexed for 30 sec; 500 μl of mineral oil was added and the suspensions heated at 85 ºC for 10 min and then cooled in ice for 5 min. The suspensions were centrifuged (20 min, 10000 g), the supernatant was carefully removed, and 200 μl ammonium hydroxide (10%) were added (until pH ~4.1). The solutions were read for absorbance at 405 nm, in a Spectra III spectrophotometer (SLT, Austria).

2.2.5. Statistical analysis

Experiments were performed at least in triplicate and expressed as means ± standard deviation. Statistical analysis was performed using the Student *t*-test as well as one-way analysis of variance (ANOVA) followed by a Tukey HSD test for post-hoc comparison. Statistical significance was defined as $p < 0.05$ for a 95% confidence. $p < 0.01$ corresponds to a 99 % confidence, and $p < 0.001$ to a 99.9 % confidence.

3. Results

3.1. Physical characterization

The elastin-like polymer was able to form spherical to slightly elongated nanoparticles, with average diameters of 115.5 ± 28.2 nm (**Figure 1**). Using dynamic light scattering, the particles showed an average size of 237.5 ± 3.0 nm, in wet state (**Figure 2**). Nearly all the particles (91.8 %) had sizes ranging from 190 nm to 295 nm in diameter. When incubated in

PBS, at 37 ºC, the swelling of the particles occurred rapidly during the first hours of immersion, up to 261.9 ± 41.0 % after 30 min and up to 416.4 ± 37.1 % after 24h ($p < 0.05$), with water uptake stabilizing at 466.7 ± 33.0 % (**Figure 3**). The remaining mass of the particles was 97.1 ± 3.1 % after day 5, 88.9 ± 6.3 % after day 14, and 64.5 ± 12.5 % after day 30 (**Figure 4**).

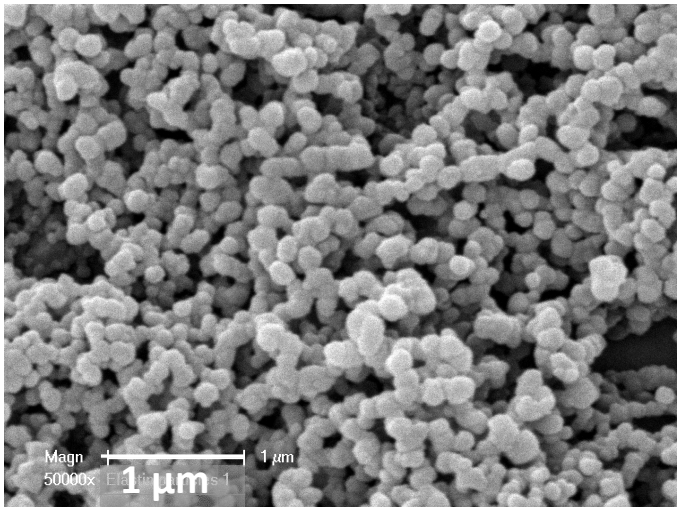

Figure 1. SEM micrographs of unloaded elastin nanoparticles. Magnification 50.000 x. Scale is 1 µm.

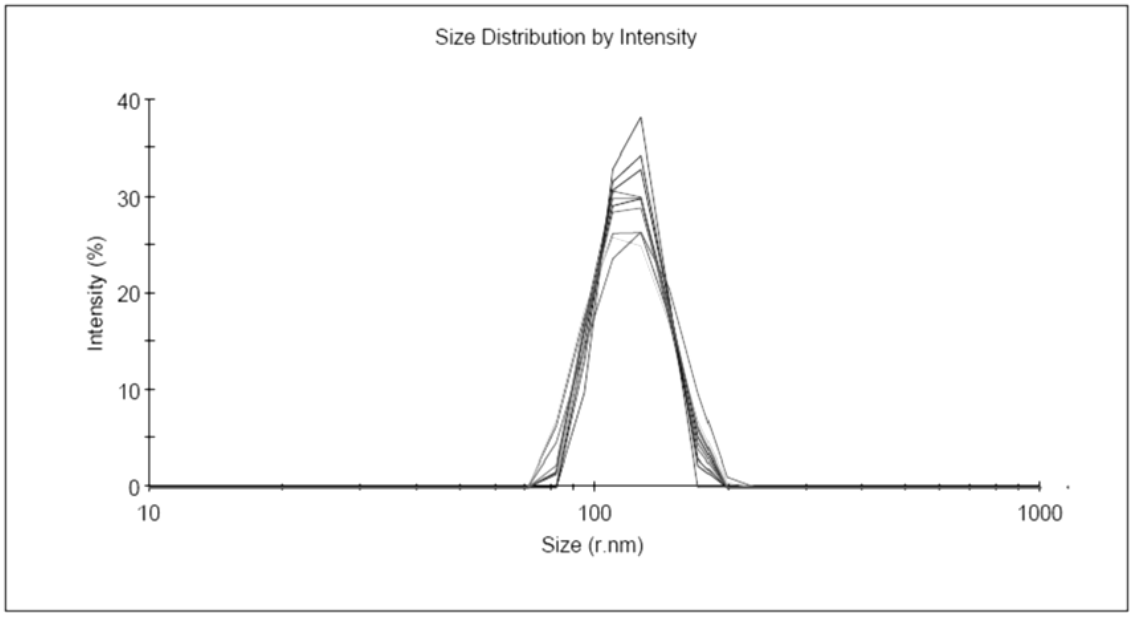

Figure 2. Size distribution of unloaded elastin-like particles, obtained by Dynamic Light Scattering (DLS). Almost all particles showed sizes ranging between 190 nm and 295 nm, with a mean diameter of 237.5 ± 3.0 nm. Size refers to particle diameter (nanometers).

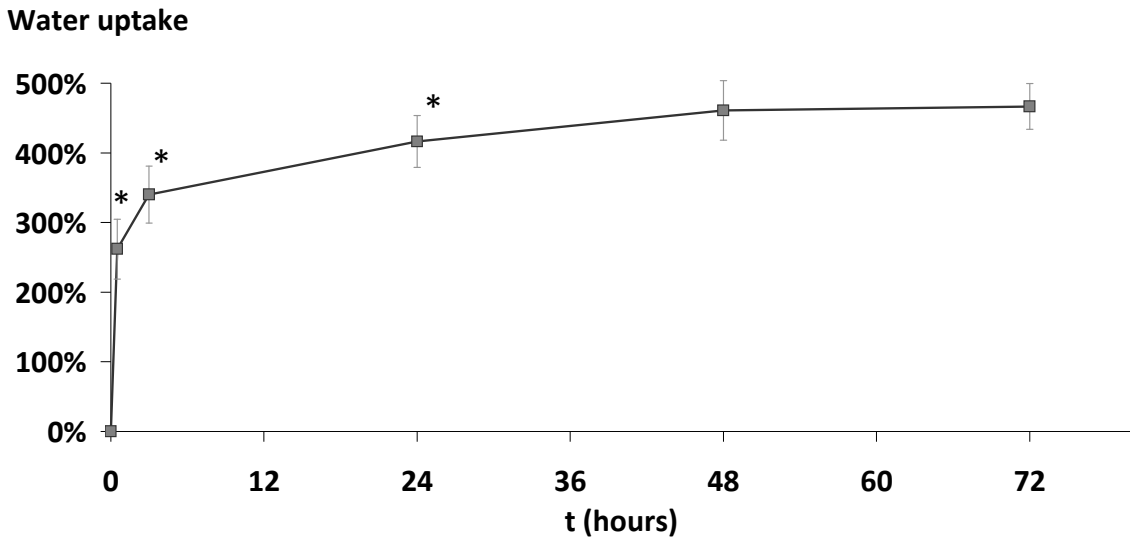

Figure 3. Evolution of water uptake behavior of unloaded elastin particles in phosphate buffer saline as a function of immersion time (t). (mean ± SD, *n* = 3). Water uptake increased significantly up to 24 hours, and then stabilized. * $p < 0.05$ is relative to the difference between consecutive time measurements.

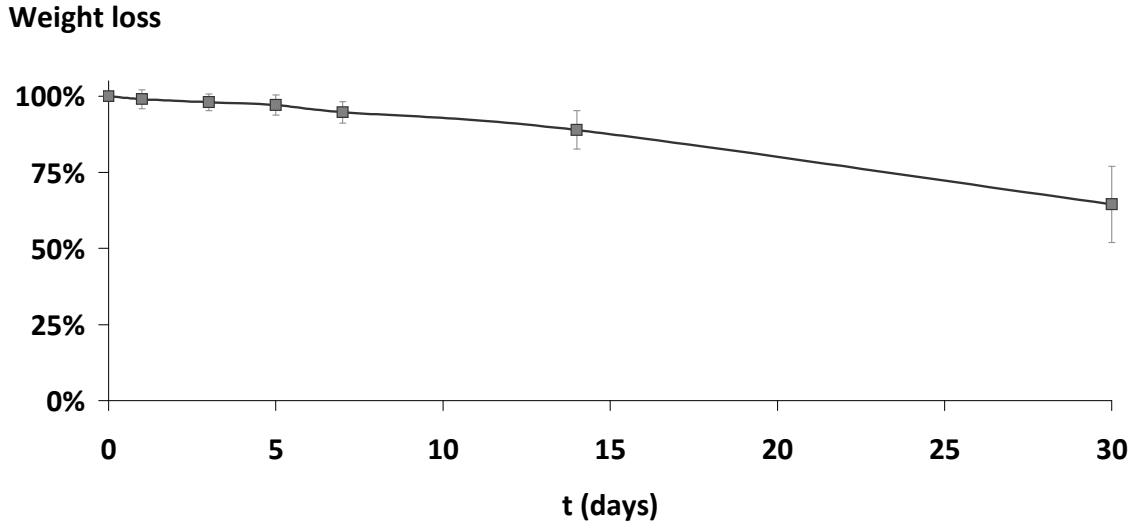

Figure 4. Evolution of weight loss of unloaded elastin particles in phosphate buffer saline as a function of immersion time (t). (mean ± SD, *n* = 3). The remaining mass decreased to 97.1 ± 3.1 % after day 5, 88.9 ± 6.3 % after day 14, and to 64.5 ± 12.5 % after day 30.

3.2. Loading and release of BMP-2 and BMP-14

Encapsulation efficiency

The encapsulation efficiency (E.E.) of BMP-2 and BMP-14 into the elastin-like particles was respectively 94.5 ± 1.8 % and 99.2 ± 0.4 %, per total amount of growth factor added during the preparation of the particles.

In vitro release

The nanoparticles loaded with BMP-2 showed an initial burst release during the first 24 hours, of 20.0 ± 2.3 % released growth factor (**Figure 5**). This was followed by a gradual release, with up to 30.7 ± 1.9 % (0.8 % per day, 151 ng/day per mg polymer) of released protein after day 14. In the case of BMP-14, there was a burst release during the first 24 hours, of 19.2 ± 3.2 %. After this, there was a gradual release, with up to 36.1 ± 1.7 % (1.3 % per day, 258 ng/day) after day 14.

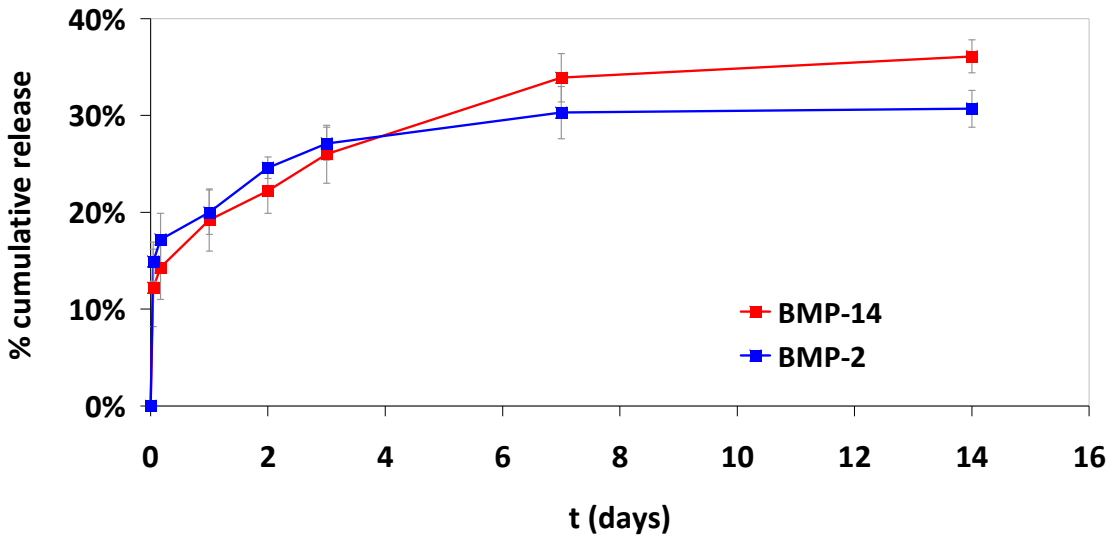

Figure 5. Release kinetics of BMP-2 and BMP-14 loaded in the elastin nanoparticles. ELISA was used for BMP-2 quantification and dot-blot for BMP-14 quantification (Mean ± SD, *n* = 3). Cumulative release is expressed in percentage of loaded protein.

Release kinetics models

The release profile fitted best the Korsmeyer model (r^2 of 0.97 for BMP-2 and r^2 of 0.96 for BMP-14) followed by Higuchi's model (r^2 of 0.96 for BMP-2 and r^2 of 0.88 for BMP-14), while first and zero order models showed low correlations (r^2 less than 0.85). The release exponent

"n" of Korsmeyer model had values of n = 0.20 for BMP-2 and n = 0.14 for BMP-14 (**Figure 6** and **Figure 7**). Since n < 0.43, in both cases, the release data fits a Fickian mode of diffusion (Ritger and Peppas 1987).

3.3. *In vitro* bioactivity

MTT cell viability

C2C12 incubated with unloaded elastin-like particles maintained their cell viability in a similar way to the positive control of cell viability (**Figure 8**). Unloaded particles have increased significantly cell viability to about 106.0 ± 0.3 % and 112.8 ± 1.2 % ($p < 0.05$ relative to control) when 10 or 100 µg/ml of elastin particles were added. Morphology observations corroborated the absence of cytotoxicity (data not shown).

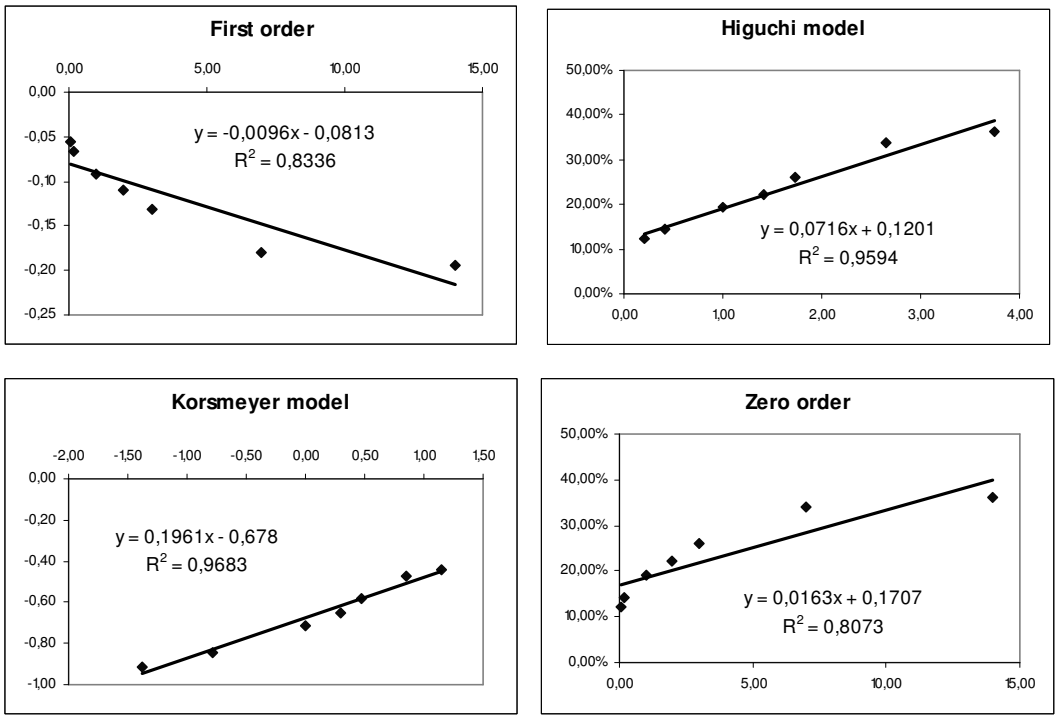

Figure 6. Release kinetics of encapsulated BMP-2. First order (log cumulative percent drug remaining *vs*. time), Higuchi kinetics (cumulative percent drug released *vs*. square root of time) and Korsmeyer kinetics (log cumulative percent drug released *vs*. log time), with correlation values (r^2).

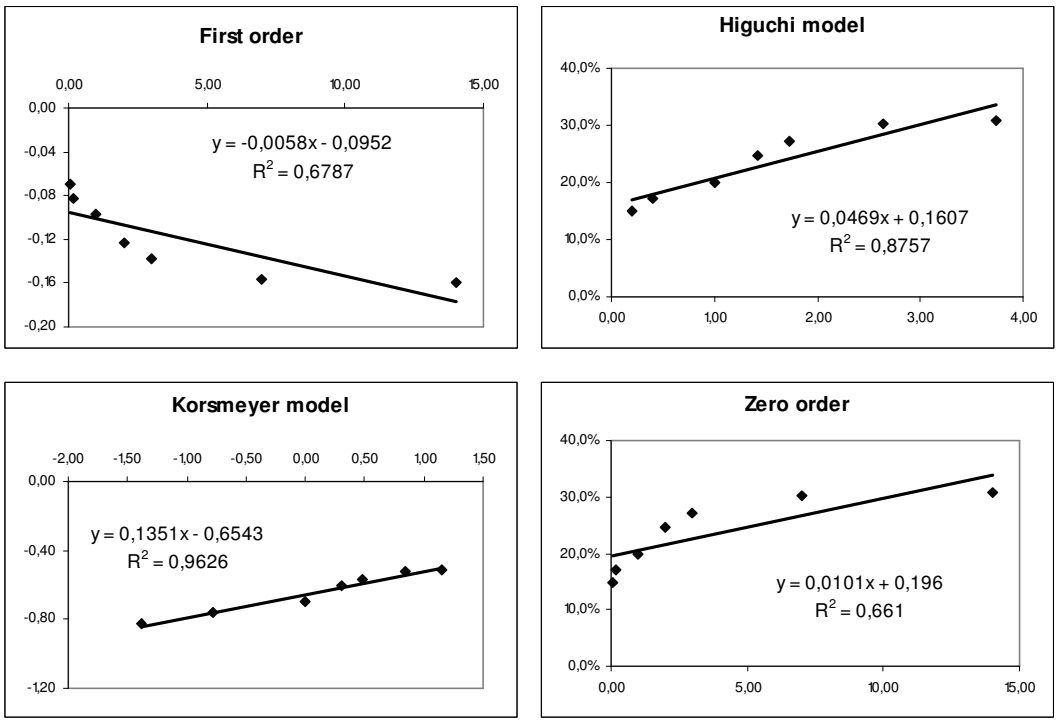

Figure 7. Release kinetics of encapsulated BMP-14. First order (log cumulative percent drug remaining *vs*. time), Higuchi kinetics (cumulative percent drug released *vs*. square root of time) and Korsmeyer kinetics (log cumulative percent drug released *vs*. log time), with correlation values (r^2).

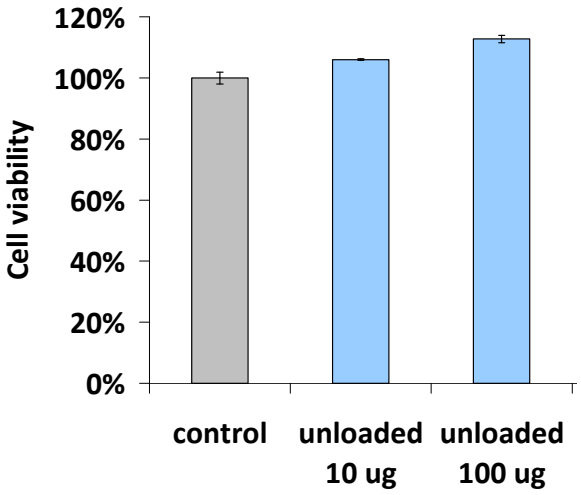

Figure 8. Cell viability tetrazolium salt (MTT) test performed in C2C12 cells, after 5 days of cell culture, with 10 or 100 µg/ml unloaded elastin-like nanoparticles. DMEM was used as a positive control for cell viability. Cell viability is expressed as a percentage of the control (scored as 100% viability) as mean ± SD (n = 3). * $p < 0.05$ is relative to differences to the control.

ALP activity

Cells incubated with BMP-2 loaded nanoparticles showed morphological changes into osteoblast-like shapes (data not shown) and a significant increase in ALP activity, after 5 days of culture (**Figure 9**). BMP-2 loaded particles induced 37-fold, 139-fold, 345-fold and 735-fold, corresponding to particles which contained 0.1, 0.25, 0.5 and 2.5 µg, respectively. The dose-wise increase in ALP activity was highly significant ($p < 0.001$). Particles loaded with the combination of BMP-14 and BMP-2, induced 40-fold, 296-fold, 369-fold and 783-fold, at the same respective amounts of loaded growth factor. Comparing particles with BMP-2 alone with BMP-2 and BMP-14, significant pairwise differences were found at specific doses (C with G and D with H, $p < 0.01$, E with I, $p < 0.05$). The overall additional effect of BMP-14 was significant ($p < 0.01$). Particles loaded with only BMP-14 induced ALP levels by 1.2-fold, 5-fold, 7-fold and 8-fold (not significant). Similar results were obtained with the control of BMP-14 added to medium. Differentiation into the osteoblast-like phenotype was also observed in these cases, although to a smaller extent as compared to BMP-2 loaded particles (data not shown).

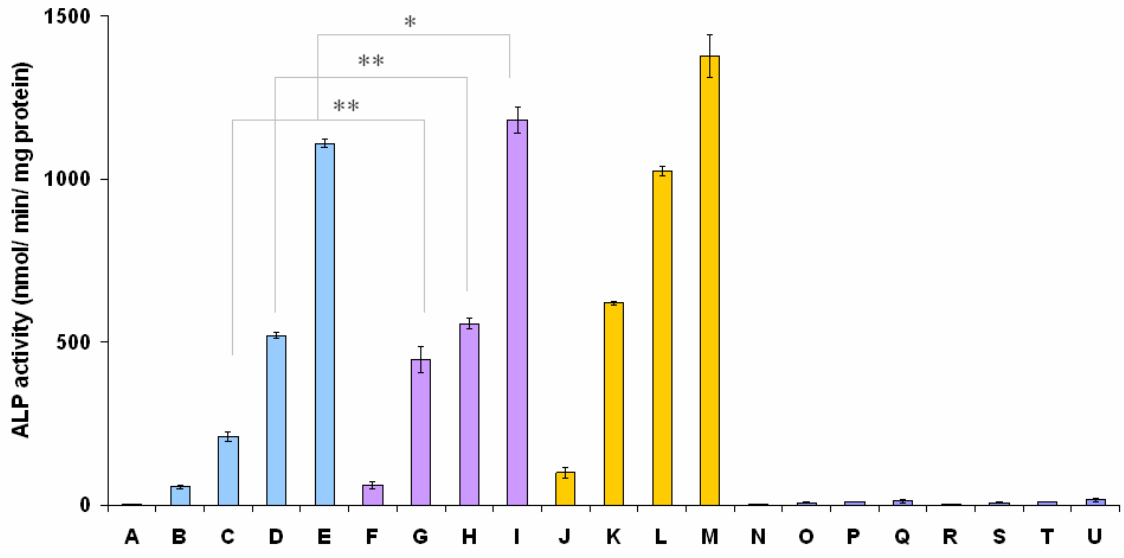

Figure 9. Alkaline phosphatase activity of C2C12 cell line after 5 days of culture, incubated with loaded and unloaded elastin nanoparticles: A) negative control with no added particles or growth factor; Elastin particles were loaded with: B-E) BMP-2 (0.1, 0.25, 0.5, 2.5 µg); F-I) BMP-2 and BMP-14 (0.1, 0.25, 0.5, 2.5 µg each); N-Q) BMP-14 (0.1, 0.25, 0.5, 2.5 µg); J-M) BMP-2 added to culture medium (0.1, 0.25, 0.5, 2.5 µg) as positive control; R-U) BMP-14 added to culture medium (0.1, 0.25, 0.5, 2.5 µg) as positive control. ALP activity is reported in nmol /min /mg of total protein (Mean ± SD, $n = 3$). * $p < 0.05$ and ** $p < 0.01$ are relative to the differences indicated.

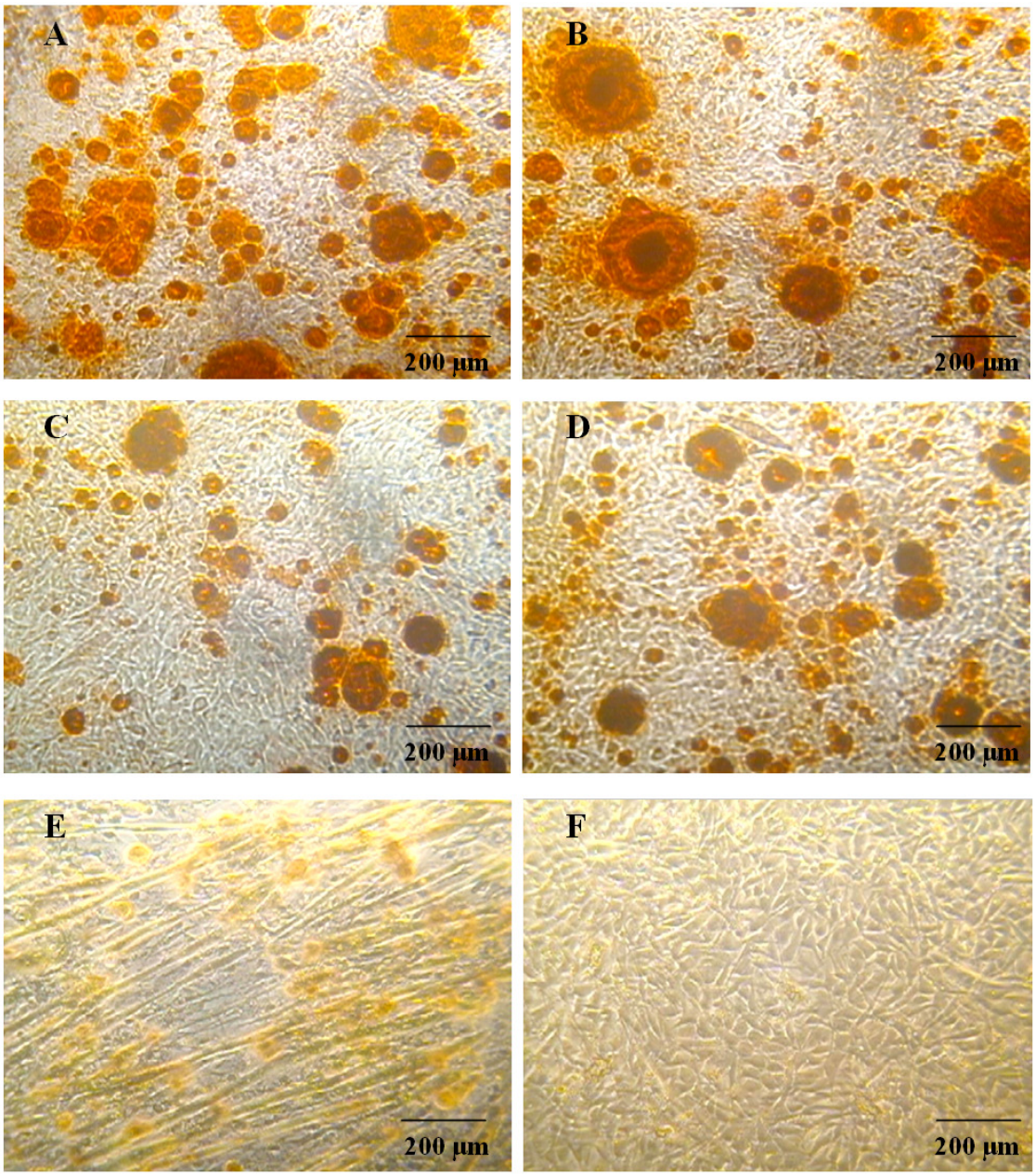

Figure 10. Alizarin Red mineralization staining of showing sites of calcium-phosphate deposits (orange color) in C2C12 cell line differentiated into osteoblast after 14 days of culture with particles loaded with BMP-2 (A), BMP-2 and BMP-14 (B), and the positive controls of BMP-2 (C) and BMP-2 + BMP-14 (D) added to culture media, at 2.5 µg/ml. Unloaded particles did not showed any mineralization (E). Unstained cells treated with particles loaded with BMP-2 + BMP-14 showed osteoblast morphology (F).

Alizarin Red mineralization

After two weeks of culture, BMP-loaded particles were able to induce osteogenic mineralization, as observed by Alizarin Red staining (**Figure 10**). Increased mineralization was observed in cells cultured with particles loaded with either BMP-2 or combined BMP-2 and BMP-14, than in cells cultured with corresponding doses of the growth factor added to culture media (at 2.5 μg/ml). No mineralization was observed for cells cultured with particles loaded with BMP-14 or with unloaded particles (data not shown). The amount of calcium was significantly higher ($p < 0.001$) for particles loaded with BMP-2 (1463.0 ± 11.2 %) or with combined BMP-2 and BMP-14 (1563.5 ± 15.0 %), compared to BMP-2 added to media (956.2 ± 29.3 %) or to combined BMP-2 and BMP-14 added to the media (1053.0 ± 3.5 %). In addition, the amount of calcium was also significantly higher ($p < 0.001$) with particles loaded with the combination BMP-2 and BMP-14 than with particles loaded only with BMP-2.

4. Discussion

Elastin-like polymers (ELPs) have been used in a wide variety of applications, ranging from protein purification to biosensors and surface-engineering, drug delivery and as biomaterials such as hydrogels (Chow *et al*. 2008). Recently, chemically synthesized poly(VPAVG) particles have been reported to deliver in a sustained way the model drug dexamethasone (Herrero-Vanrell *et al*. 2005). The self-assembly and smart behavior of ELPs make these a potential choice as a delivery system of growth factors in tissue engineering. Genetic engineering has been applied to obtain these polymers with a precise amino acid composition, sequence and length, resulting in the absolute control of its molecular weight, stereochemistry and thermoresponsive behavior (Chilkoti *et al*. 2006, Rodríguez-Cabello *et al*. 2007, Machado *et al*. 2009).

In this work, the self-assembly capacities of a recombinant ELP, $(VPAVG)_{220}$, has proven to be a potential way to obtain stable nanoparticle systems for delivery of BMPs. The repeat number of 220 was chosen to obtain a polypeptide considered as representative of an high molecular weight polymer (Machado *et al*. 2009). The particles showed average diameters of 237.5 nm, in DLS, which is of relevant interest for tissue engineering approaches, considering that the particles could be loaded into a specific scaffold or hydrogel. The size of the particles was smaller in the SEM counterpart images, mainly due to shrinkage of the particles caused by the dehydration process involved in SEM imaging, and also due to the initial high water content of the particles. The size in dynamic light scattering was significant smaller when

compared to that reported in a former work (Herrero-Vanrell *et al*. 2005). This is mainly due to the monodisperse nature of the $(VPAVG)_{220}$ polymer.

The particles were able to encapsulate significant amounts of BMP-2 or BMP-14, at high efficiencies. It is possible that hydrophobic interactions between the polymer and the growth factors could contribute to such efficiency. In fact, there is a significant difference in charge between the polymer and the loaded drugs; while $(VPAVG)_{220}$ has an isoelectric point of 5.5, BMP-2 and BMP-14 have isoelectric points around 9 and 8, respectively (Geiger *et al*. 2003, Plöger *et al*. 2008). Thus, this potential advantage could be applied for loading drugs that show low E.E. in other delivery systems due to low affinity to the material. Since the nanoparticles are manufactured in an aqueous-system, in mild conditions, with no harsh temperature, pH or organic solvents, this may also allow the incorporation of labile drugs; and may therefore be suitable for many therapeutical applications beyond those of bone tissue engineering by presenting an advantage due to its high E.E and easiness of preparation and handling. No cytotoxicity could be inferred by the cell viability assays, reinforcing the idea of the high biocompatibility of elastin-like polymers for clinical applications, observed before (Urry *et al*. 1991). The unloaded elastin particles had a small but significant stimulating effect in the cell proliferation. It is has been described that elastin peptides can induce the proliferation of diverse cell types, such as vascular smooth cells or fibroblasts, by interaction with specific cell signaling pathways (Tajima *et al*. 1997, Mochizuki *et al*. 2002).

The BMPs were successfully released over a sustained time period. The release of both BMP-2 and BMP-14 was associated with a two-phase delivery profile, consisting of an initial burst release during the first 24 h, followed by a slower and more gradual release for 14 days. During the initial stages of swelling, the elastin particles showed substantial water uptake (swelling ratio ~4) thus, the drug is rapidly released from the particle, correlating with the initial burst release observed during the first hours of immersion. The higher swelling ratio indicates the possibility that the system may be formulated also as a hydrogel-based material. It is probably that the diffusion is the only mechanism responsive for the release of the drugs in this second stage, since the release data matched Korsmeyer models of diffusion with Fickian correlation values, meaning that the release is mainly determined by the diffusion of the growth factor from the particle to medium and no degradation mechanisms. Since the temperature required for re-dissolution is well below the body or room temperature as observed previously (Herrero-Vanrell *et al*. 2005, Machado *et al*. 2009), due to the phenomena of hysteresis, the particles would remain in solid state in the body. This is also supported by the degradation data obtained. Stable particle formation is a peculiar behavior of the (VPAVG) pentapeptide. All ELPs based on the pentapeptide (VPGXG) (X representing any amino acid)

tend to form, upon heating above their *T*t, unstable particles that rapidly sediment and coalesce to form a viscous continuous phase called coacervate. However, the polymer based on (VPAVG) is a peculiar member of the ELP family. It is obtained by substitution of the first Gly by Ala in the representing pentapeptide (VPGVG). This position for amino acid substitution is particularly sensitive. In fact this Gly can be substituted only by Ala. Any other amino acid yields a polypeptide that does not show inverse temperature transition and, therefore, is not smart and self-assembling.

In this work, we have seen that the elastin-like particles were capable of delivering, in a bioactive way, both BMP-2 and BMP-14. The sustained release profile resulted in enhanced mineralization induced by particles containing the growth factors, when compared to the corresponding doses of BMPs added to the culture media. This shows that their slow release may present a potential for triggering bone formation *in vivo*. Despite the effort of recent tissue engineering advances to promote the combination of a release of two growth factors to enhance bone healing (Raiche and Puleo 2004, Basmanav *et al*. 2008, Patel *et al*. 2008, Chen *et al*. 2009, Wang *et al*. 2009), it is still unclear which combination may result in a better effect and this may well depend in the type of clinical application (e.g. long bone fractures, spinal fusion or tooth regeneration). In this study, we have found an increase in the bioactivity (both ALP and osteogenic mineralization) with the combined release of BMP-2 and BMP-14 compared to both growth factors alone. This shows that the combination of these growth factors might be an interesting one. Nevertheless, further studies are required, probably by screening the induction *in vivo* of neo-vascularization by BMP-14, to evaluate a potential synergistic impact in bone formation.

This work provides the first report on the potential use of an elastin-like, VPAVG polymer, as a new carrier for the delivery of BMPs, offering a range of exciting properties, such as the thermoresponsive behavior, high encapsulation efficiency, and sustained release.

References

Al-Aql ZS, Alagl AS, Graves DT *et al*. Molecular Mechanisms Controlling Bone Formation during fracture Healing and Distraction Osteogenesis. J. Dent. Res. 87 (2008) 107-118.

Basmanav FB, Kose GT, Hasirci V, Sequential growth factor delivery from complexed microspheres for bone tissue engineering. Biomaterials. 29 (2008) 4195-204.

Bessa PC, Casal M and Reis RL, Bone morphogenetic proteins in tissue engineering: the road from laboratory to the clinic, part I (basic concepts). J Tissue Eng Regen Med. 2 (2008a) 1-13.

Bessa PC, Casal M and Reis RL, Bone morphogenetic proteins in tissue engineering: the road from laboratory to the clinic, part II (BMP delivery). J Tissue Eng Regen Med. 2 (2008b) 81-96.

Bourne DW, Pharmacokinetics. In: G.S. Banker, C. Rhodes (Eds.) Modern Pharmaceutics. 4th ed., Marcel Dekker Inc,. New York, 2002, pp. 67-92.

Chen FM, Chen R, Wang XJ *et al. In vitro* responses to scaffolds containing two microencapsulated growth factors. Biomaterials [Epub ahead of time] (2009).

Chilkoti A, Christensen T, MacKay JA, Stimulus responsive elastin biopolymers: applications in medicine and biotechnology. Current Opinion in Chemical Biology 10 (2006) 652-657.

Chow D, Nunalae ML, Lim DW *et al.* Peptide-based biopolymers in biomedicine and biotechnology. Mater Sci Eng R Rep 62 (2008) 125-155.

Chowdary KP and Ramesh KV, Studies on microencapsulation of diltiazem. J Pharm Sci 55 (1993) 52-4.

Dines JS, Weber L, Razzano P *et al.* The effect of growth differentiation factor-5-coated sutures on tendon repair in a rat model. J Shoulder Elbow Surg. 16 (2007) S215-21.

Geiger M, Li RH and Friess W, Collagen sponges for bone regeneration with rhBMP-2. Advanced Drug Delivery Reviews 55, 12 (2003) 1613-1629.

Gregory CA, Gunn WG, Peister A *et al*. An Alizarin red-based assay of mineralization by adherent cells in culture: comparison with cetylpyridinium chloride extraction. Anal Biochem. 329 (2004) 77-84.

Hadjiioannou TP, Christian GD, Koupparism MA Quantitative calculations in pharmaceutical practice and research. VCH Publishers Inc , New York, 1993, pp. 345-348.

Herrero-Vanrell R, Rincón AC, Alonso M *et al*. Self-assembled particles of an elastin-like polymer as vehicles for controlled drug release. J. Control. Release 102 (2005) 113-122.

Higuchi T, Mechanism of sustained action medication. Theorical analysis of rate of release of solid drugs dispersed in solid matrices. J. Pharm Sci. 52 (1963) 1145-1149.

Kadomatsu H, Matsuyama T, Yoshimoto T *et al.* Injectable growth/differentiation factor-5-recombinant human collagen composite induces endochondral ossification via Sry-related HMG box 9 (Sox9) expression and angiogenesis in murine calvariae. J. Periodont Res 43 (2008) 483-489.

Machado R, Ribeiro AJ, Padrão J *et al.* Exploiting the sequence of naturally occurring elastin: construction, production and characterization of a recombinant thermoplastic protein-based polymer. Journal of NanoResearch 6 (2009) 133-145.

Mano J and Reis RL, Osteochondral defects: present situation and tissue engineering approaches, J Tissue Eng Regen Med 1 (2007) 261–273.

McKay WF, Peckham SM and Badura JM, A comprehensive clinical review of recombinant human bone morphogenetic protein-2 (INFUSE((R)) Bone Graft), Int Orthop. 31 (2007) 729-34.

Meyer DE, Chilkoti A, Purification of recombinant proteins by fusion with thermally-responsive polypeptides. Nat Biotechnol 17 (1999) 1112-1115.

Mochizuki S, Brassart B and Hinek A, Signalling pathways transduced through the elastin receptor facilitate proliferation of arterial smooth muscle cells, J. Biol. Chem. 227, 47 (2002) 44854-44863.

Nakamura T, Yamamoto M, Tamura M *et al.* Effects of growth/differentiation factor-5 on human periodontal ligament cells. J Periodontal Res. 38 (2003) 597-605.

Patel ZS, Young S, Tabata Y *et al.* Dual delivery of an angiogenic and an osteogenic growth factor for bone regeneration in a critical size defect model. Bone. 43 (2008) 931-40.

Plöger F, Seemann P, Kegler MS *et al.* Brachydactyly type A2 asociated with a defect in proGDF5 processing. Human Molecular Genetics 17, 9 (2008) 1222-1233.

Raiche AT and Puleo DA, *In vitro* effects of combined and sequential delivery of two bone growth factors, Biomaterials 25 (2004) 677-85.

Reddi AH, BMPs: from bone morphogenetic proteins to body morphogenetic proteins. Cytokine Growth Factor Rev 16 (2005) 249–250.

Reddi AH, Cell biology and biochemistry of endochondral bone development. Coll Relat Res 1 (1981) 209-226.

Rincón AC, Molina-Martinez IT, de las Heras B *et al.* Biocompatibility of elastin-like polymer poly(VPAVG) microparticles: *in vitro* and *in vivo* studies. J Biomed Mater Res A 78 (2006) 343–351.

Ritger PL and Peppas NA, A simple equation for description of solute release. I. Fickian and non-Fickian release from non-swellable devices in the form of slabs, spheres, cylinders or discs. J. Control. Release 5, (1987) 23-26.

Rodríguez-Cabello JC, Prieto S, Reguera J *et al.* Biofunctional design of elastin-like polymers for advanced applications in nanobiotechnology, J. Biomater. Sci. Polymer Edn. 18 (2007) 269-286.

Salgado AJ, Gomes ME, Chou A *et al.* Preliminary study on the adhesion and proliferation of human osteoblasts on starch-based scaffolds. Mater. Sci. Eng. 20 (2002) 27-33.

Simank HG, Herold F, Schneider M *et al.* [Growth and differentiation factor 5 (GDF-5) composite improves the healing of necrosis of the femoral head in a sheep model. Analysis of an animal model], Orthopade 33 (2004), 68-75.

Simnick A, Lim D, Chow D *et al.* Biomedical and Biotechnological Applications of Elastin-Like Polypeptides. Journal of Macromolecular Science, Part C: Polymer Reviews 47 (2007) 121-154.

Tajima S, Wachi H, Uemura Y *et al.* Modulation by elastin peptide VGVAPG of cell proliferation and elastin expression in human skin fibroblasts. Archives of Dermatological Research 289, 8 (1997) 489-492.

Urry DW, Hayes LC, Gowda DC *et al*. Reduction-driven polypeptide folding by the delta Tt mechanism. Biochem Biophys Res Commun. 188 (1992) 611-17.

Urry DW, T.M. Parker, M.C. Reid *et al.* Biocompatibility of the bioelastic materials, poly(Gvgvp) and its gamma-irradiation cross-linked matrix – summary of generic biological tests-results. J. Bioactive Comp Polym 6 (1991) 263-282.

Wang X, Wenk E, Zhang X *et al.* Growth factor gradients via microsphere delivery in biopolymer scaffolds for osteochondral tissue engineering. J Control Release. 4, 134 (2009) 81-90.

Yamashita H, Shimizu A, Mitsuyasu K *et al.* Growth/differentiation factor-5 induces angiogenesis *in vivo*. Experimental Cell Research 235 (1997) 218-226.

Zeng Q, Li X, Beck G *et al.* Growth and differentiation factor-5 (GDF-5) stimulates osteogenic differentiation and increases vascular endothelial growth factor (VEGF) levels in fat-derived stromal cells *in vitro*. Bone 40 (2007) 374-381.

SECTION 5

Chapter IX

General Conclusions and Final Remarks

Chapter IX

General Conclusions and Final Remarks

This chapter intends to give a brief outlook in the main goals and results achieved in the present thesis. General conclusions are indicated, with an overall review of the steps taken throughout the research process. The main challenges encountered are drawn to attention, as well as the solutions applied. The advantages and disadvantages of the methods used are stated, as well as the reasons why specific choices were made. The main findings and contributions from this thesis are identified, relating these to the context of the tissue engineering, clinical applications and the scientific community. Finally, a few recommendations are made on possible further studies to overcome specific challenges and future directions to broaden the horizons of the current field of investigation.

GENERAL CONCLUSIONS

The main goals of the present thesis were to clone, express, purify and characterize human recombinant BMPs, in primary cultures of human stem cells and in C2C12 cells, and investigate novel delivery systems for the sustained delivery of these BMPs.

The overall work was divided into the following parts:

- Cloning, expression, folding, purification and bioactivity characterization of different human recombinant BMPs (BMP-2, BMP-4, BMP-9, BMP-10, BMP-11 and BMP-14);
- Production of silk fibroin microparticles and elastin-like polypeptide thermoresponsive self-assembled nanoparticles for delivery of different human BMPs with physical characterization and *in vitro* or *in vivo* bioactivity characterization.

1. A METHOD FOR THE PRODUCTION OF RECOMBINANT BMPs

The production of growth factors by recombinant technology was originally proposed in order to meet the requirements of tissue engineering field to obtain large amounts of these molecules for research purposes. Bone morphogenetic proteins were specifically selected since these are the main signaling growth factors that promote the differentiation of progenitor cells to bone-forming cells, as described in section 1, chapter I.

Bone morphogenetic proteins were produced by recombinant technology in *Escherichia coli*, in an attempt to overcome the challenges of former methods, such as the low yields of native BMP extraction from bone, or from mammalian expression cells (as stated in Chapter I and IV).

This process involves a stepwise approach on which different issues had to be overcome:

- Source of genetic material for cloning of human BMPs. As detailed in chapter IV, the DNA was obtained from the Human Genome Project, due to the mature domain of these BMPs being located in only one exon. However, this method is not be applicable to every gene, which in those cases, cloning from a cDNA library would have to be used.
- Finding an ideal optimal plasmid as expression vector. The innovative approach is based on the pET25 vector, using *Escherichia coli* as a host for recombinant expression. This had main advantages: i) the fact that this vector facilitated the secretion of recombinant protein to the periplasm, promoting thus the formation of BMPs dimers, ii) allowing easy overexpression of the protein, and iii) allowing easy purification by affinity chromatography due to its integrated six-histidine-tag.
- Optimization of expression conditions. These steps were performed as detailed in chapter III. The overexpression was then scaled-up in a bioreactor, to achieve very large amounts of BMPs, after several fermentation variables were optimized (codon usage, temperature, expression period, induction method).
- Isolation of the recombinant growth factors and proper folding. Since initially the protein was detected in insoluble fraction, the protein was easily solubilized in a buffer containing L-arginine, which acts as a suppressor of protein aggregation and a facilitator of folding, i.e. a chaotrophic agent. The BMPs were present in monomer, dimer and polymer forms. Purification by affinity chromatography resulted in isolation of the BMPs, to purities up to 90-95%. The yields achieved were 25 to 45 % from total, or 23 to 54 mg

per Liter of fermentation batch, or 110 mg for BMP-2 in bioreactor (the only growth factor which had a scale-up).

- Stability and bioactivity of protein. BMP-2 was stable in physiological conditions such as phosphate saline buffer, pH 7.4. The purified BMPs were able to induce several markers of osteogenic differentiations and did not possess significant cell cytotoxicity, as observed by the cell viability assays. C2C12 cells were used as a standard and reproducible model for testing the *in vitro* bioactivity of the recombinant BMPs, while human fat-derived stem cells provides a human-based model to test the biological activities of the different BMPs.

Several main advantages were found with the overall methodology:

- The method developed is an easy way to obtain large amounts of recombinant BMPs of significantly purity, by a very straightforward, low-cost, and easy protocols.
- The proteins are stable in physiological conditions and easily stored.
- Recombinant BMPs are able to induce several markers of osteogenic differentiation.
- The expression and purification method can be easily adaptable to other growth factors.

And a few drawbacks:

- Bioactivity is lower when compared to commercial BMPs, produced in mammalian cells, requiring thus trial-and-error and time-consuming experimentation for the optimization of the protein folding and activity. Future studies are required to optimize the bioactivity to the levels obtained with BMPs expressed in mammalian cells.
- The protein is obtained in monomer, dimer and polymer forms, so further isolation of dimers is required.
- The protein, expressed in *E. coli*, does not have its natural glycosylation pattern, hence its bioactivity and stability may be reduced, compared to mammalian-derived BMPs.
- Further purification from residual endotoxins is also required.

As investigated in Chapter V, different recombinant BMPs were produced. This can provide a number of important contributions:

- To show that the novel strategy can be applied to several growth factors.
- Since different BMPs participate in a timely sequence of growth factors involved in the differentiation of osteoblast and new bone formation, these may be required for novel therapeutical applications, involving a combination of BMPs. In fact it is still poorly understood the entire sequential activation and physiological roles of the different BMPs in different clinical situations, such as spinal fusion, fracture healing or dental healing.

2. INNOVATIVE MICROPARTICULATE DELIVERY SYSTEMS FOR BMPs

The choice for the carrier was based on the assumption that materials for tissue engineering should ideally mimic the natural environment of tissues. We have chosen silk fibroin (chapter VI and VII) and elastin-like polymers (chapter VIII) due to a series of potential advantages for bone tissue engineering, which were demonstrated in this thesis:

- The ability to form nano- or microparticles, with a rather homogeneous distribution of size, by a very easy methodology.
- Both systems have very easy method of drug loading, with no use of harsh conditions, allowing the loading of more labile molecules
- Both systems have high efficiency of loading, applicable for the different BMPs
- Both systems did not show significant cytotoxicity as inferred by *in vitro* viability assays.
- Both systems showed the ability to deliver the BMPs, retaining their bioactivity *in vitro*. Fibroin particles loaded with BMP-2 have demonstrated to be able to trigger new bone formation *in vivo*, as demonstrated in the ectopic bone formation model, in chapter VII.
- Both particulate systems showed relatively small burst release, followed by gradual and sustained release of the BMPs for up to 14 days.
- Both systems possess slow degradability, having small weight loss over the short-term, which make these materials very suitable for bone regeneration. Silks have interesting mechanical properties, since by having slow degradation times, may allow adequate time for proper bone remodeling.

Elastin-like polypeptides presented further specific advantages:

- The thermoresponsive and hysteresis behavior allows the preparation of multi-loading particles for the release of combinations of different growth factors, with a very easy and fast method. The optimization of a system for a potential sequential release of growth factors requires further studies.

A few drawbacks may be noted for these particulate systems, namely:

- Particles alone disperse *in vivo*, and thus require a scaffold material as carrier.
- The significant swelling in both particle systems may be a disadvantage *in vivo*, with risk of increased inflammatory in the implantation site. This can be avoided by pre-soaking the carrier prior to implantation in PBS, or by incorporation into a scaffold material.

The rat ectopic bone formation model (Chapter VII) also proved an efficient model for accessing the activities of recombinant BMPs delivered via a carrier *in vivo*. The microCT and histological analysis provide two powerful techniques to analyze the formation of bone both on a histochemical level, by screening the expression of important mineralization proteins such as osteocalcin, but also a three-dimensional assessment of the quality of bone formed, its density and length, and how the doses of the BMP affect these parameters. However, one main drawback is that the ectopic model only provides an idea whether the carrier is delivering the BMP in a sufficiently bioactive and sustained way to trigger bone formation. Further *in vivo* orthotopic studies, from a clinical perspective, are required, using, for example, a long bone fracture model.

FUTURE DIRECTIONS

In this section, recommendations are made for further studies to improve the methodologies previously described. These include:

- Improvement of refolding methodologies to obtain recombinant BMPs, with increased bioactivity to levels similar to the ones induced by BMPs expressed in mammalian cells.
- Isolation of dimeric BMPs by using size exclusion chromatography or heparin affinity chromatography. Endotoxins should be also removed prior to clinical assays.
- Alternative expression systems may be explored, for instance in yeast, thereby avoiding the issues of protein misfolding due to overexpression.
- Novel delivery systems based in a combination of micro- or nanoparticles and a scaffold or hydrogel, for a sequential delivery of two or more growth factors. The scaffold would provide as carrier for the particles, while supporting also cells. Sequential delivery would be achieved by one growth factor being released first from this carrier, and a second growth factor released from the particles.

We also highlight other directions of future work that might be fruitful and interesting to exploit:

- Formation of heterodimeric recombinant BMPs, possibly yielding stronger bioactivity;
- Fusion proteins, between growth factors or BMPs and domains of interest, such as domains of binding to biomaterials, to possibly increase bioactivity. One example would be the cloning and expression of fusion proteins of BMPs to silk fibroin and elastin sequences, to achieve, in theory, a polypeptide that would simultaneous work as a carrier and as a growth factor, and exhibiting thermoresponsive behavior.
- Biomimetic coatings in the particulate systems since these were previously reported to increase the binding and retention of BMPs, and therefore increase their bioavailability.

A more attentive look at folding is required, as the folding structure of the recombinant BMPs is critical to its bioactivity. It is known, and detailed in chapter II, that BMPs bind to combinations of cell surface receptors, and these combinations can explain different bioactive effects. Mutations in one epitope affect ALP activity, and in another the triggering of Smads pathway. Therefore, the critical correct folding and subsequent bioactivity of recombinant BMPs has to be studied both with assays of the induction of ALP, induction of Smads pathway and transcription factors specific to osteogenic pathway, and the induction of mineralization proteins. Correct refolding of recombinant BMPs is achieved by finding the optimal conditions for a renaturation of monomer to dimer (e.g. protein concentration, ionic strength and buffer composition, the presence of chaotrophic agents and aggregation inhibitors (e.g. L-arginine, urea), temperature and duration of reaction).

Attach I

Supplementary data

Attach I

Supplementary data

This section intends to give additional methodologies and results obtained during the current thesis, which are of not of critical importance to the overall conclusions, but still of relevance.

REFOLDING STUDIES WITH RECOMBINANT BMPs

When the bioactivity of recombinant BMP-2 was compared to mammalian-derived BMP-2 (Wyeth, UK), the activity was significantly lower, with no induction of alkaline phosphatase (ALP) activity and no osteogenic mineralization in C2C12 cells. For this reason, we aimed at optimizing the refolding steps of the recombinant BMP, in order to achieve the full bioactivity. Below are briefly described these procedures, after extensive trial-and-error, which nevertheless failed in resulting in reproducible batches of fully bioactive recombinant BMPs.

A stepwise optimization of BMP refolding

The new method involves a stepwise methodology:

1. **Lyses of bacteria.** Briefly, cells are lysed by incubation with PBS supplemented with 1 mg/ml lysozyme at 37 ºC for 20 min, followed by extensive ultrasound treatment in ice. DNAse is added at a concentration of 20 mg/ml to promote the removal of nucleic acids and reduce the viscosity of the lysate. The lysate is resuspended at a concentration of 200 mg wet weight per ml.
2. **Wash and isolation of inclusion bodies.** The lysate is centrifuged and the pellet, where most BMP was found (chapter IV), is subsequently washed for several times with Tris buffer 0.1 M, 1 mM EDTA, and 2 % Triton, pH 8.0, to ensure the isolation of the inclusion bodies to high degree. Ultrasound treatment is used for the resuspending of inclusion bodies. These steps are performed at 4 ºC. The purification of inclusion bodies is important as the impurities in the lysate may trigger the precipitation of protein during the refolding.
3. **Solubilization of inclusion bodies.** The purified inclusion bodies are solubilized using 4 M guanidine-HCl, 0.1 M Tris, pH 8.5, 2 mM EDTA and 50 mM TCEP or DTT (reducing agent), to a concentration of 5 to 15 mg/ml. This step is performed at room

temperature for 1h, or overnight, at 4 ºC. The solubilized protein is centrifuged and the precipitate is discarded. Then, it is necessary to remove the reducing agent prior to refolding, by buffer exchange, since it can interfere with the oxidative folding pathway of the protein. The solution is buffer exchanged to an identical buffer, but with no reducing agent, and with the pH adjusted to 5.5, to prevent the formation of cysteine bridges. Solubilized inclusion bodies may be stored at -80 ºC.

4. **Refolding of inclusion bodies.** The inclusion bodies are refolded by rapid dilution into a specific buffer, with gentle mixing. A dilution into a final protein concentration of 50 to 100 µg/ml is recommended. The refolding buffer consists in Tris buffer 0.1 M, 1 M NaCl, 2 mM EDTA, 0.5 M L-arginine, 0.3 M guanidine-HCl, 5 mM oxidized glutathione and 2 mM reduced glutathione, pH 8.5, but a combination of different concentrations of each component may be experimented. Refolding is performed initially on ice, for 30 min., to avoid protein precipitation, followed by incubation for a specific period of time, at 4 ºC or room temperature, between 1h and 10 days, but mainly for 3 days. Prior to preparation, the refolding buffer is degassed and nitrogen-purged to ensure a buffer environment that protects the protein from amine alteration. Alternatively, the refolding is performed by stepwise dilution, by one-step dialysis or stepwise dialysis, involving a gradient of decreasing concentrations of guanidine-HCl, to test the influence of the removal rate of the protein denaturant from the solution. For a concentration of 0.4 M guanidine-HCl, a maximum of 200 µg/ml protein concentration is recommended; for 0.1 M guanidine-HCl, 50 µg/ml (as observed experimentally). Another option, involves the addition of pulses of denatured inclusion bodies into the refolding buffer, by slowly increasing the protein concentration over time.
5. **Purification of BMP dimer by heparin affinity chromatography.** The refolded protein is then dialysed against Tris 0.1 M, 4 M urea, pH 8.5 and applied to a pre-equilibrated heparin affinity chromatography column. The column is washed with Tris-urea buffer, with 0.3 M NaCl to remove the monomer. The dimer is eluted with Tris-urea buffer, with 0.8 M NaCl. The urea is used to avoid the protein precipitation in the column. The protein is temporarily unfolded during this step, refolding again after the removal of the urea. This purification step is optional as it does not interfere with the protein activity (as observed experimentally – data not shown).
6. **Buffer exchange to physiological buffer and storage.** The purified protein is then dialysed against 50 mM MES buffer, pH 5.0, to a maximum concentration of 50 µg/ml, and stored at -80 ºC until bioactivity tests, or at 4ºC for short-term use.

Bioactivity of BMPs refolded by the new method

The bioactivity of recombinant human BMPs, described in chapters IV and V, was much lower than commercial mammalian derived BMP-2 (Wyeth, UK) due its lack of induction of high levels of ALP activity after 5 days of culture, and bone mineralization after 21 days of culture in C2C12 cells (data not shown), despite the fact that it elevated significantly the expression of mRNA of several osteogenic markers in both C2C12 cells and human adipose derived stem cells.

For this reason, new variants of BMP-2 were cloned and expressed with N-terminal histidine tagged BMP-2, C-terminal histidine tagged BMP-2, non tagged BMP-2 and non-tagged BMP-2 with no heparin binding domain, which is postulated to reduce the BMP *in vitro* activity. These proteins were successfully overexpressed using pET-25 vector *E. coli* (data not shown) but still not showing full bioactivity, i.e. ability to induce high levels of ALP in C2C12 cells.

After successive experiments, fully bioactive protein was obtained in some refolding batches, but not in a reproducible way, despite the fact of the controlled experimental conditions. In these cases, BMP-2 and BMP-4 were able to trigger high levels of ALP enzymatic activity, in C2C12 cells, after 5 days of culture (**Figure 1**), with clear differentiation into osteoblast morphology, similar to that observed with the positive control of BMP-2 (**Figure 2**). The saturation levels of ALP activity were achieved at approximately 1000 ng/ml of BMP-4, 500 ng/ml of refolded BMP-2 and 250 ng/ml of positive BMP-2 control. Alizarin Red staining revealed that the refolded BMP-2 and BMP-4 could successfully induce calcium-phosphate bone-like mineralization after two weeks of cell culture (**Figure 3**). Mineralization was achieved using both 200 and 1000 ng/ml of BMP-2 and only with 1000 ng/ml of BMP-4.

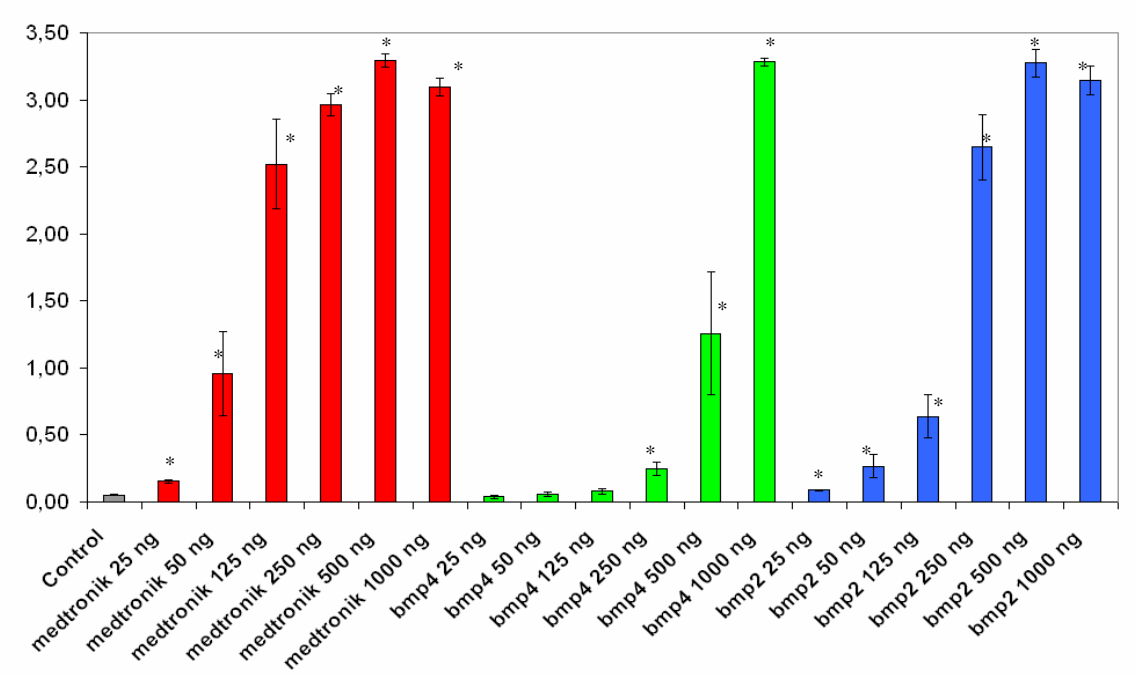

Figure 1. ALP activity in C2C12 cells after 5 days of culture with refolded BMP-2 (blue), BMP-4 (green) and positive BMP-2 control (red), at 25 to 1000 ng/ml. (mean ± S.D., n=3, * $p < 0.05$ relative to negative control)

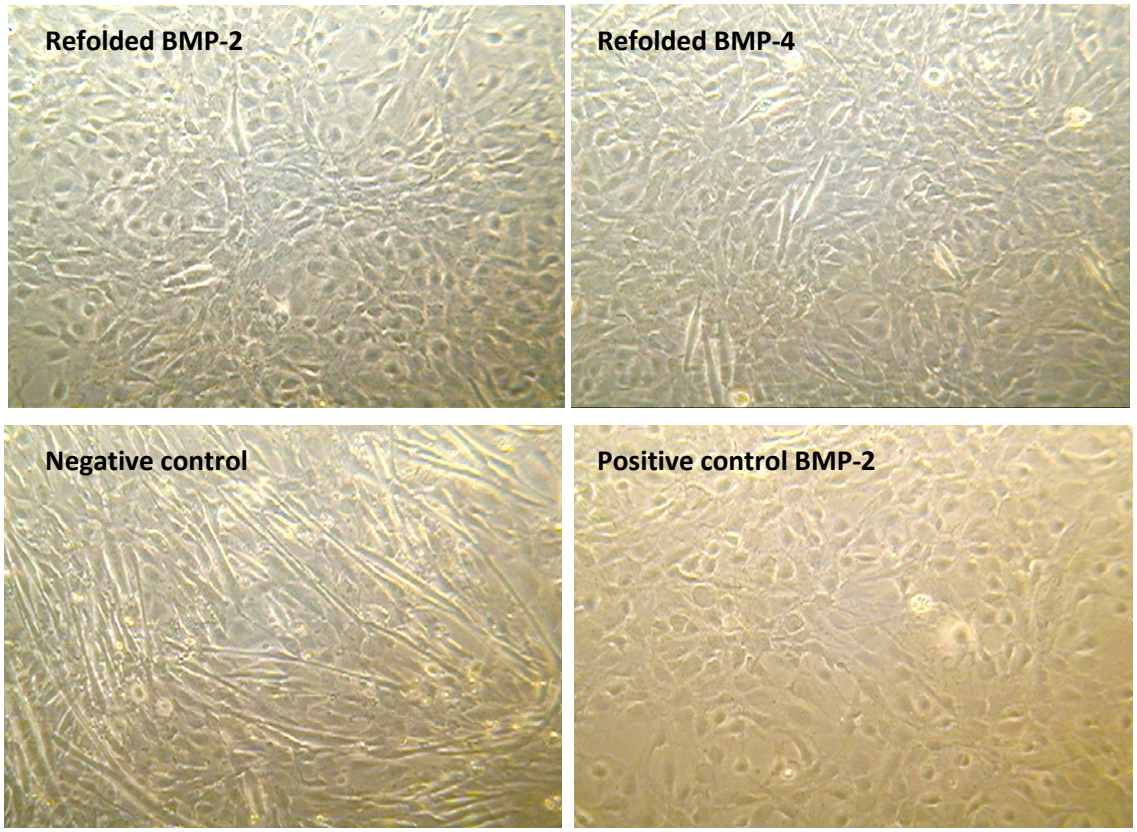

Figure 2. Morphology of C2C12 cells after 4 days of culture with refolded BMP-2 and BMP-4, positive BMP-2 control (mammalian-derived, Wyeth, UK), at 1000 ng/ml, and negative control (no growth factor). Osteoblast-like morphology is observed in all conditions except in negative control.

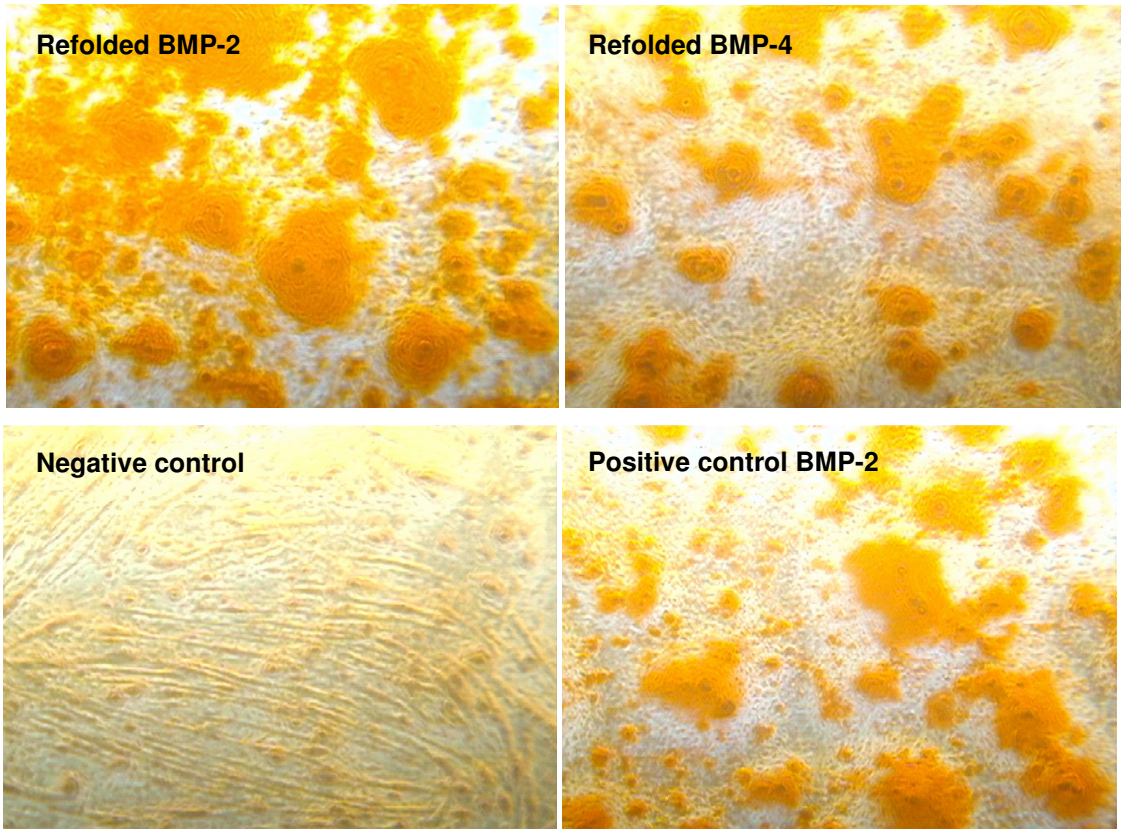

Figure 3. Alizarin Red staining of C2C12 cells treated with refolded BMP-2 and BMP-4, at 1000 ng/ml, in comparison with the positive control (mammalian-derived, Wyeth, UK), at 1000 ng/ml, and negative control (no growth factor), after 15 days of culture. Mineralized extracellular matrix is stained in cells treated with refolded BMP-2, BMP-4 and positive BMP-2 control.

Stability of bioactive BMP-2

The refolded BMP-2 showing activity was also studied for its stability in different conditions, such as pH and ionic strength, when incubated overnight. The protein retains the activity at pH between 4.5 and 9.0 (**Figure 4**), and at ionic strength above 10 mM phosphate buffer (**Figure 5**). This shows that physiological buffers, or slightly acidic conditions, are preferred for storage of the recombinant protein, which is of interest for tissue engineering and biomedical applications.

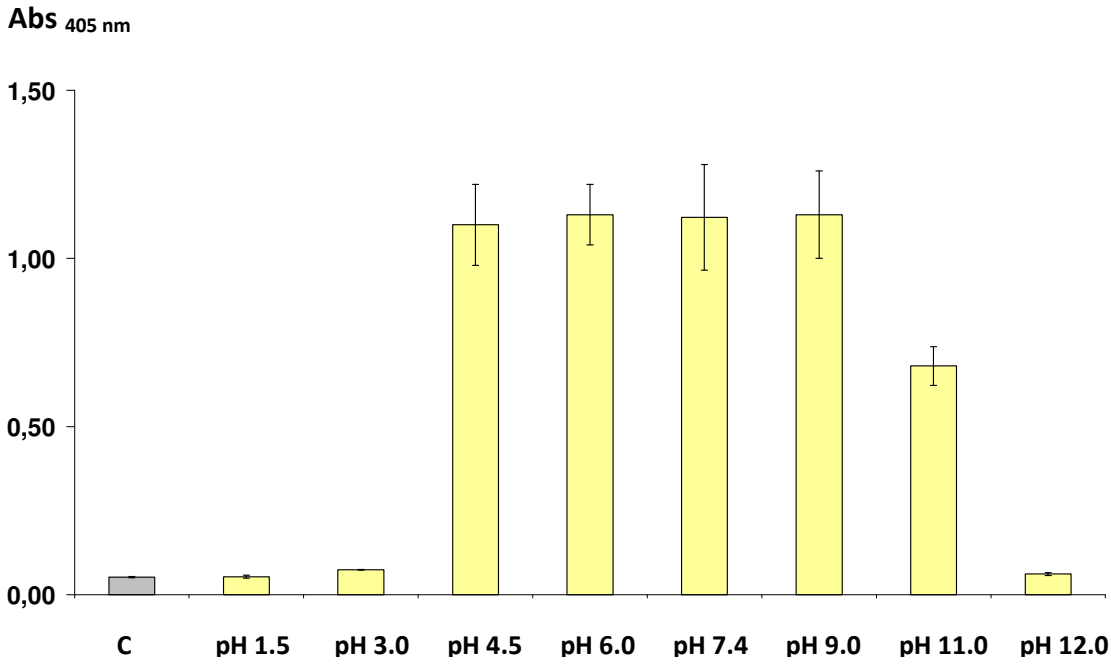

Figure 4. ALP activity in C2C12 cells after 5 days of culture of refolded BMP-2 stored at different pH conditions, added at 150 ng/ml, and a negative control with no growth factor (C). Loss of ALP activity is observed at pH 3.0 and pH 11.0. Activity is retained between pH 4.5 and pH 9.0.

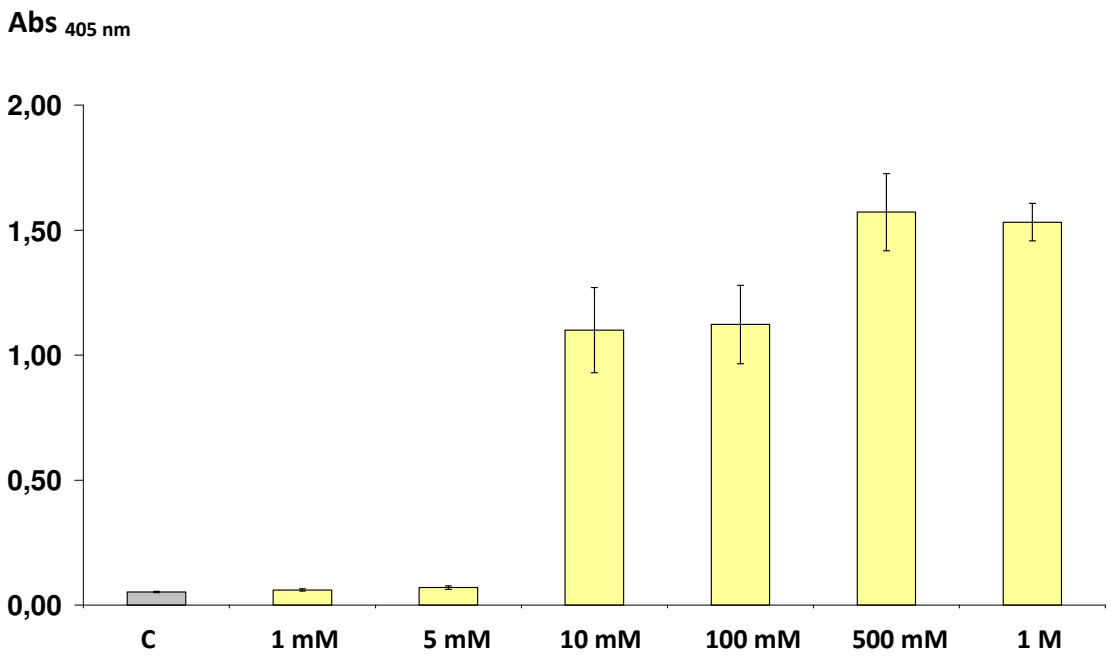

Figure 5. ALP activity in C2C12 cells after 5 days of culture of refolded BMP-2 stored at different ionic strength buffer conditions (phosphate buffer, pH 7.4), added at 150 ng/ml, and a negative control with no growth factor (C). Loss of ALP activity is observed at buffer conditions below 10 mM phosphate. Activity is retained in 10 mM to 1 M phosphate buffer.

Correct refolding *versus* misfolding

The protein is initially in the form of unfolded and reduced inclusion bodies, in the presence of a high concentration of chaotrophic salt (guanidine-HCl), before the refolding (**Figure 6A**). Then, as the concentration of the denaturant decreases during the refolding steps (e.g. dialysis or dilution), and oxidizing conditions are present, the protein gradually folds into its native structure, and forms dimers by cysteine bridge arrangements (Vallejo and Rinas 2004a). It was observed, by Western-blot, that the renaturation typically resulted in about 20 to 30 % of dimer formation (**Figure 6B**), as analysed by Gel Pro Analyzer image software (Media Cybernetics). However, as explained before, in several refolding batches, this did not correspond to bioactivity, when the protein was tested in the cells, even when the dimeric form was isolated by heparin affinity chromatography (**Figure 6C**) or by size exclusion chromatography (data not shown).

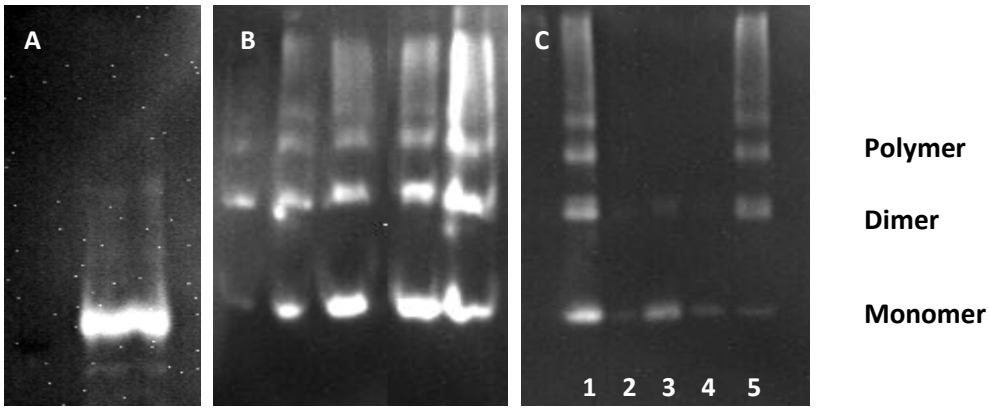

Figure 6. Western-blot showing unfolded and reduced inclusion bodies, prior to refolding (A); renaturation of BMP-2 inclusion bodies with formation of dimer, after 3 days of reaction at 4ºC (B); purification of refolded BMP-2 and isolation of dimer (C) by heparin affinity chromatography, with separation of monomer (2-4) and dimer (5).

As shown in **Figure 7**, the correct protein folding pathway (1) often competes with misfolding (2) and aggregation (3), depending in the several variables of the reaction mix (listed in next page). Disulfide-bond knot proteins, such as BMPs, can easily form misfolded products, due to the complicate nature of their intra- and intermolecular disulfide bonds (Arolas *et al.* 2006). The misfolded dimers would have the correct molecular weight but no bioactivity. If the percentage of correct refolding is low, below a certain threshold, no activity will be detected in the cell cultures; whether if the percentage of refolding is slightly increased, then bioactivity would be observed.

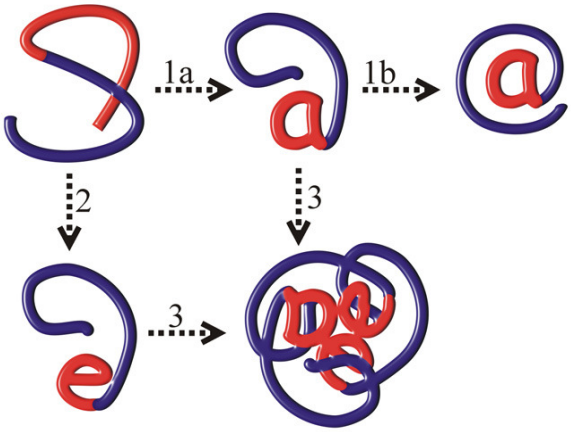

(Adapted from Vallejo and Rinas, 2004a)

Figure 7. Simplified model of correct folding versus misfolding and aggregation. The correct protein folding pathway (1) often competes with misfolding (2) and aggregation (3), depending in several variables. Disulfide knot proteins, such as BMPs, can easily form misfolded products, due to the complicate nature of intra- and intermolecular disulfide bridges. These misfolded dimers would have the correct molecular weight but no bioactivity.

Because the misfolded protein would appear with the same molecular weight, but not showing activity, it is therefore important to state that bioactivity assays are required to screen for the correct refolding of the protein and its full biological activity.

Different variables are known to affect refolding

Several factors are known to affect protein refolding (Rudolph and Lilie 1996, Singh and Panda 2005, Tsumoto *et al.* 2003, Vallejo and Rinas 2004a). The protein concentration, the removal rate of denaturant and the temperature are three key factors. pH is another critical factor, as it is the redox environment and the buffer composition (e.g. the addition of additives that prevent protein aggregation or enhance folding).

Thus, the following variables are known to affect protein refolding and were investigated:

- **Removal rate of denaturant**. Because of the competing processes of misfolding and aggregation, a key to refolding is in the intermediate concentration of the denaturant, where denaturant concentration is low enough to force protein molecules to collapse

into folded configuration, yet can allow them to stay in solution and be flexible to reorganize their structures**.** Such balance can be manipulated by two factors. One is the rate by which denaturant concentration is reduced, which depends in the method used (rapid dilution, one-step dialysis, stepwise dialysis or stepwise dilution). The other is to add additives that reduce protein aggregation or enhance folding. Another option that was evaluated was the slowly addition of pulses of denatured protein into the refolding buffer. Since completely folded proteins are usually not prone to precipitation, higher yields are theoretically possible, at higher protein concentrations.

- **Protein concentration**. In general, for the refolding of BMPs, concentrations between 30 μg/ml and 200 μg/ml. Higher concentrations, up to 500 μg/ml, were tested, but precipitation of the protein was frequently observed (data not shown). Since refolding is a first order reaction, and the competing misfolding and aggregation reactions are second-order processes, refolding is favoured by working at low protein concentration. One drawback of working with low concentrations, is that it may expose the protein to degradation or surface binding, resulting in lower recovery, and requires time-consuming concentrating steps, after refolding.
- **Temperature**. While increased temperature accelerates the rate of refolding, it also increases greatly the likehood of protein precipitation and misfolding. Therefore, as rule, refolding was mainly performed at 4 ºC. Whereas, other temperatures were evaluated, e.g. 10 ºC or room temperature, we have found that the incubation of protein on ice on the first stages of refolding (first 1-3 hours) was enough to avoid protein precipitation.
- **pH**. The formation of cysteine bridges in the BMPs is reported to occur mostly at a very narrow pH range, between 8.0 and 9.0, optimally at pH 8.5 (Vallejo and Rinas 2004b). In the context of this thesis, refolding experiments were conducted mainly at this pH, but a range of pH 5.0 to 9.0 was also tested. After refolding, buffer should be exchanged to acidic conditions, such as 50 mM MES, pH 5.0, since the solubility of the protein is best.
- **Buffer composition (e.g. ionic strength and presence of additives)**. The addition of additives that either reduce aggregation, enhance folding or protein interaction, is also recommended. Particularly, L-arginine is generally recommended (Tsumoto *et al.* 2004) as it suppresses protein aggregation during the early stages of refolding, therefore aiding in refolding. Routinely, concentrations of 0.5 to 1 M were used. Other additives include $MgCl_2$, glycine, ammonium buffers, sucrose, glycerol, PEG, CHES and EDTA.

General salt conditions include 0.1M Tris and 1 M NaCl, but other conditions were also studied.

- **Redox conditions**. The formation of intra and intermolecular cysteine bridges, required for correct folding and the formation of dimers, is achieved by adding a mix of oxidized and reduced thiol reagents such as glutathione, in both oxidized and reduced forms. In general, because thiol-disulfide exchange reactions are reversible, these reagents aid in increasing both the rate and the yield of correct disulfide bonds, by rapid reshuffling of improper disulfide bonds, that lead to wrong folding (Rudolph and Lilie, 1996). In the context of this thesis, we have experimented with different ratios of glutathione forms.
- **Preparation of inclusion bodies prior to refolding**. Other factors that can affect the efficiency of refolding are the purification degree of inclusion bodies prior to folding, the expression conditions during fermentation (lower rates of expression can correspond to increased yields of soluble and native protein), and the conditions used during inclusion body solubilization (milder solubilization, with lower concentrations of denaturant, may result in increased efficiency of refolding).

Future work will involve the optimization of the refolding conditions necessary to achieve the reproducibility of fully bioactive protein, under controlled conditions.

References

Arolas JL., Aviles FX, Chang JY *et al.* Folding of small disulfide-rich proteins: clarifying the puzzle. Trends Biochem. Sci. 31, 292-301, 2006.

Rudolph R and Lilie H. *In vitro* folding of inclusion body proteins. FASEB. J. 10, 49-56, 1996.

Singh SM and Panda AM. Solubilization and refolding of bacterial inclusion body proteins. Journal of Bioscience and Bioengineering 99, 303-310. 2005

Tsumoto K, Ejima D, Kumagai I. *et al.* Pratical considerations in refolding proteins from inclusion bodies. Protein Expression and Purification 28, 1-8, 2003.

Tsumoto K, Umetsu M, Kugamai I. Role of arginine in protein refolding, solubilization and purification. Biotechnol. Prog. 20, 1301-1308, 2004.

Vallejo L.F and Rinas U. Strategies for the recovery of active proteins through refolding of bacterial inclusion body proteins. Microb. Cell Fact. 3, 11, 2004a.

Vallejo L.F and Rinas U. Optimized procedure for renaturation of recombinant human bone morphogenetic protein-2 at high protein concentration. Biotechnol Bioeng 85: 601-609, 2004b.